The potential of the PARP-1 inhibitor, AG014699, in human cancers defective in Homologous Recombination DNA repair

Yvette Drew

Thesis submitted in part requirement for the degree of Doctor of Philosophy

Newcastle University

Northern Institute for Cancer Research

November 2011

Declaration

The work presented in this thesis was carried out at the Northern Institute for Cancer Research, Newcastle University and the Northern Centre for Cancer Treatment, Newcastle General Hospital between December 2006 and September 2010. These studies represent my own original work except where acknowledged by name or reference.

No part of this work is being, or has been submitted for another degree or other qualification in this or any other university

Abstract

The aims of this study were to undertake the first comprehensive *in vitro*, *in vivo* and clinical investigation into the effects of the PARP-1 inhibitor, AG014699, in human cancers defective in homologous recombination (HR) DNA double strand break (DSB) repair.

HR deficient cells were 9-fold more sensitive to AG014699 than HR proficient cells (mean LC_{50} = 3.26 μM *vs*. 29.68; $P < 0.0001$), confirming the theory of synthetic lethality. *BRCA*1 methylated UACC3199 breast cancer cells were also sensitive to AG014699 with mean LC_{50} significantly lower than the HR proficient cells (7.6 μM *vs*. 29.68; $P = 0.002$). AG014699 inhibited PARP activity by > 95% and induced DNA DSBs in *all* 11 cell lines studied. Evidence of HR (by Rad51 foci) was observed only in cells with functional BRCA1/2.

A prolonged schedule of AG014699 (10 mg/kg daily for five days of a seven-day cycle for six cycles) more effectively delayed the growth of *BRCA2* mutated xenografts than a ten day AG014699 schedule (tumour growth delay (TGD) = 27.5 *vs.* 12.5 days; $P = 0.02$). AG014699 significantly delayed UACC3199 tumour growth compared to untreated controls (mean time to relative tumour volume 5 = 35.8 *vs*. 25.2 days; $P = 0.05$); confirming *in vitro* findings that *BRCA*1 methylated cancer cells are sensitive to PARP inhibition.

Clinical trial data from 38 patients demonstrated that AG014699 is non-toxic and efficacious with a clinical benefit rate of 34%. Higher baseline PARP-1 activity was associated with response to AG014699.

The major findings of these studies are: the confirmation of the selective cytotoxicity of PARP inhibitors in *BRCA* mutated cancers; the results in UACC3199 cells which suggest that cancers with other HR defects could benefit from single agent PARP inhibitors, and finally the concept that length of exposure to (not just degree of) PARP inhibition is important for single agent anti-tumour activity. Furthermore, these data have formed the basis for a major amendment to the clinical trial; the result of which is eagerly awaited.

Acknowledgements

This is, of course, the bit that I have been really looking forward to writing.

Firstly, I would like to thank Cancer Research UK for funding this research fellowship and the patients who so willingly took part in the phase II PARP-BRCA clinical trial.

Thank you to my supervisors Professor Nicola Curtin and Professor Ruth Plummer for providing me with the opportunity to undertake these studies. For being an endless source of knowledge of all things DNA repair and PARP; for the hours of manuscript reading and critique and for encouraging me back then as a clinical fellow and now in my early career as a clinical academic. Special thanks to Nicola believing that, eventually, the JNCI would publish our paper.

I would also like to thank Professor Alan Boddy for supervising the pharmacokinetic and pharmacogenomic aspects of this work and for providing another listening ear for problems and ideas, and for reading sections of this manuscript.

Like most clinicians who undertake a period of laboratory based research, I have so many other individuals at the Northern Institute for Cancer Research to thank for giving me their time and advice when they themselves were busy and stretched. I apologise in advance if I have missed anyone out, but here goes…

Working to the standards of Good Clinical and Laboratory Practice is an arduous but necessary task when doing translational research and I thank Melanie Griffin, Julieann Sludden and Sally Davies for keeping me on the straight and narrow at all times. Special thanks to the members of lab 1.013 (as it was back in the days) for help with laboratory techniques and providing such a great and friendly working environment. In particular: Evan Mulligan, Tomasz Zaremba, Jill Hunter, Sarah Elliot, Suzanne Kyle, Huw Thomas and Elaine Wilmore. Thanks also to James Murray for so proficiently taking over the clinical trial sample analysis from me when I left and for the enduring nickname –'Dr Dre'. Thank you to Gordon Taylor and Phil Berry for help with the development and running of the AG014447 assay and the many, many, many hours spent puzzling over the API4000. Thanks to David Jamieson for the help and advice with all things pharmacogenomics and to all the research nurses at the Sir Bobby Robson Unit for the help with patient sample collection.

Now to my family, thank you to Gabriel and Dylan (now almost three years old), for helping me to keep things in perspective and for changing my life for the better when you arrived in 2009. I doubt that either of you two have any idea of the existence of this thesis as it was written whilst you were sleeping; **if only you had slept a little longer it might have been submitted earlier.**

Thank you to my parents (Peter and Polly) for all the love, encouragement and support I have received over the last thirty years (plus) and more recently, to my in-laws (Janet and David) for the same love and support

And finally, thank you to Simon for twelve years of friendship, laughter, love and support. A marriage that has almost survived the creation of not one but *two* PhDs….well, fingers crossed!!

Contents Page

List of abbreviations

3-AB	3-aminobenzamide
ADPRT	Adenosine diphosphate ribosyl transferase
AE	Adverse event
AIF	Apoptosis inducing factor
ANOVA	Analysis of variance
AP	Apurinc/apyrimidinic
ASCO	American Society of Clinical Oncology
AT	Doxorubicin and docetaxol
ATCC	American tissue type collection
ATM	Ataxia-telangiectasia mutated
ATP	Adenosine tri-phosphate
ATR	ATM Rad53-related
AZ	Astrazeneca
BASC	BRCA1- associated genome surveillance complex
BCA	bioinchoninic acid
BCLC	Breast cancer linkage consortium
BER	Base excision repair
BLBC	Basal-like breast cancer
BM	Bilateral mastectomy
BOCS	Breast Ovarian Cancer syndrome
BRCA	Breast cancer susceptibility
BRCT	BRCA1 carboxyl terminal
BSA	Bovine serum albumin
BSO	Bilateral salpingo-oophrectomy
C	Cycle
CA125	Cancer antigen 125
CBR	Clinical Benefit Rate
cm	Centimetre
C_{max}	Maximum or peak drug concentration achieved after administration
CMF	Cyclophosphamide, methotrexate and 5-fluorouracil
CRUK	Cancer Research UK
cs	Catalytic sub-unit
CT	Computerised Tomography
CTC	Circulating tumour cells
CTCAE	Common Terminology Criteria for Adverse Events
CV	Coefficient of variation
CY	Cytochrome
D	Day
DLT	Dose limiting toxicity
DMSO	Dimethyl sulfoxide
DNA-PK	DNA-protein kinase
DSB	Double strand break
E	Enhancement
EGTA	Ethylglyceroltetraacetic acid
EndoG	Endonuclease G
EOI	End of infusion

ER	Oestrogen receptor
ERα	Oestrogen receptor alpha
ES	Embryonic Stem
ETDA	Ethylenediaminetetraacetic acid
FEN1	Flap endonuclease 1
FFPE	Formalin fixed paraffin embedded
G	Gravitational
g	Gram
GCLP	Good Clinical and Laboratory practice
GCP	Good Clinical practice
GCR	Global genomic repair
Gy	Gray
H	Hour
HCQ	Highest QC concentration
HGSOC	High grade serous ovarian carcinoma
HR	Homologous Recombination
HRD	Homologous recombination deficiency
IC_{50}	Inhibitory concentration of an inhibitor where the response (or binding) is reduced by 50%
IHC	Immunohistochemistry
iNOS	Inducible nitric oxide synthase
IP	Intra-peritoneal
IR	Ionising Radiation
IS	Internal standard
kDa	KiloDaltons
kg	Kilogram
K_i	Dissociation constant of an inhibitor
L	Litres
LAU	Luminescent arbitrary units
LB-ME-BB	Laemelli Buffer minus mercaptoethanol and bromophenol blue
LCMSMS	Liquid chromatography/mass spectrometry/mass spectrometry
LQC	Lowest QC concentration
MBC	Metastatic breast cancer
mg	Milligram
Min	Minutes
ml	Millilitre
mm	Millimetre
mM	Millimolar
MMEJ	Micro-homology-mediated end joining
MMR	Mismatch repair
MQC	Medium QC concentration
MRI	Magnetic Resonance Imaging
MTD	Maximum tolerated dose
MTIC	5-(3-methyltriazeno)-imidazole-4-carboxamide
NAD	Nicotinamide adenine dinucleotide
NBS1	Nijmegen breakage syndrome
NBSP	National breast screening programme
NCI	National Cancer Institute
NER	Nucleotide Excision Repair

NF-κB	Nuclear factor-κB
ng	Nanogram
NHEJ	Non-homologous End Joining
NLS	Nuclear localisation signals
NO	Nitric oxide
NTC	No template controls
OCP	Oral contraceptive pill
OD	Optical density
ORR	Objective response rate
OS	Overall survival
PAR	Poly(ADP-ribose)
PARG	Poly(ADP-ribose) glycohydrolase
PARP	Poly(ADP-ribose) polymerase
PBL	Peripheral blood lymphocytes
PBS	Phosphate buffered saline
PBS-MT	Phosphate buffered saline-milk tween
PCNA	Proliferating cell nuclear antigen
PCR	Polymerase chain reaction
PD	Pharmacodynamic
PF_{50}	Potentiation factor at 50%
PFI	Platinum-free interval
PFS	Progression-free survival
PID	PARP inhibitory dose
PIR	PARP inhibitor resistant
PK	Pharmacokinetic
PPC	Primary peritoneal carcinoma
PR	Progesterone receptor
PTEN	Phosphatase and tensin homolog
QC	Quality control
RCF	Relative centrifugal force
RECIST	Response Evaluation Criteria in Solid Tumours
RPA	Replication protein A
RPMI	Roswell Park Memorial Institute
RTV	Relative tumour volume
SD	Standard deviation
SDS	Sodium dodecyl sulphate
SEM	Standard error of the mean
SNP	Single nucleotide polymorphism
SRB	Sulforhodamine B
ss	Single strand
SSA	Single strand annealing
SSB	Single strand break
SSBR	Single strand break repair
TGD	Tumour growth delay
TMZ	Temozolomide
TNBC	Triple negative breast cancer
TOP1	Topoisomerase 1
TSP	Total soluble protein
TTP	Time to Progression

TVS	Trans-vaginal ultrasound
UHP	Ultra-high purity
UKFOCSS	UK Familial Ovarian Cancer Screening Study
UV	Ultra-violet
V	Voltage
v	Variant-type
V(D)J	Variable, diversity and joining
VEGF	Vascular endothelial growth factor
WHO	World Health Organisation
wt	Wild-type
XRCC	X-ray repair cross-complementing
ZnF	Zinc fingers

List of Figures

List of Tables

Chapter One

1. Introduction

1.1 Introducing the cancer, PARP and *BRCA* story

More than one in three of us will develop cancer at some point in our lives and despite advances in treatment over the last twenty years, cancer remains the most common single cause of mortality in the UK (www.cancerresearch.org/cancerstats). The major shortcomings of existing anti-cancer agents are that their efficacy is limited by toxicity, specificity and the development of drug resistance. The search for new targeted, less toxic treatments and methods to improve the specificity and effect of existing therapies is a major focus of cancer research.

Many current chemotherapy agents work by damaging a cell's ability to repair or replicate its DNA. These include: alkylators, topoisomerase I and II inhibitors and DNA cross-linking agents (DeVita *et al*., 2008). Cancer cells, by definition, are characterised by genomic instability, recently described as an 'enabling characteristic' in the 'Hallmarks of Cancer' update (Hanahan and Weinberg, 2011). That is to say they have developed ways to adapt pre-existing DNA damage signalling and repair pathways to enable them to survive DNA damage and evade cell death. One novel approach then, in the treatment of cancer, is to potentiate the DNA damaging effect of chemotherapy agents by *also* targeting the mechanisms by which this DNA damage is repaired. To put it simply: to combine a DNA damaging agent with a DNA repair inhibitor.

One such novel target is the nuclear enzyme Poly(ADP-ribose)polymerase-1(PARP-1). PARP-1 is essential to the repair of single strand DNA breaks (SSBs) via the base excision repair/single strand break repair (BER/SSBR) pathway (Schreiber *et al*., 2006). Inhibiting PARP-1 has been shown to potentiate the cytotoxic effects of ionising radiation and DNA damaging chemotherapy agents such as the alkylators and topoisomerase inhibitors (Calabrese *et al*., 2004; Delaney *et al*., 2000). The first PARP inhibitor to enter anti-cancer clinical trials was AG014699 (Pfizer, Global Research Development).

At this time there was no data to support single agent use; and so AG014699 was combined in a phase I study with the oral monofunctional alkylating agent temozolomide (Plummer *et al*., 2008).

In 2005, two Nature papers reported that cells deficient in the Breast Cancer Susceptibility (*BRCA*) genes *1* and 2 were exquisitely sensitive to single agent PARP inhibition; being 100-1000 -fold more sensitive than *BRCA* heterozygote or wild type cell lines (Bryant *et al*., 2005; Farmer *et al*., 2005). This observation, made independently by two laboratories using different *BRCA1/2* deficient models and different chemical classes of PARP inhibitors suggested that the sensitivity of these cells was due to PARP inhibition. Mutations in either *BRCA1* or *2* result in defective DNA double strand break (DSB) repair by Homologous Recombination (HR) and are associated with a high lifetime risk of breast and ovarian cancer (Gudmundsdottir *et al*., 2006). It is hypothesized that PARP inhibitors can induce 'synthetic lethality' in cells with *BRCA1/2* mutations, which are defective in HR DNA repair by inactivating the BER/SSBR pathway. 'Synthetic Lethality' is the process by which cancer cells are selectively targeted by the inactivation of two genes or pathways when inactivation of either gene or pathway alone is non-lethal (Kaelin, 2005). The term was first used in the 1940s by geneticists but the suggestion that 'synthetic lethality' could be a useful strategy in anti-cancer treatment did not arise until the late 1990s (Friend and Oliff, 1998).

Clinical trials of single agent PARP inhibitors in *BRCA* mutation carriers with advanced ovarian or breast cancer began in 2005, with results of the olaparib phase I and II studies now reported (Fong *et al*., 2009; Audeh *et al*., 2010; Tutt *et al*., 2010). These 'proof of principle' early phase studies demonstrated that the PARP inhibitor, olaparib, is active and well tolerated in selected *BRCA* mutation carrier populations. Results of other classes of single agent PARP inhibitor studies are awaited.

There is now evidence that cells lacking other components of the HR repair pathway or where the *BRCA* genes have been silenced by epigenetic changes are sensitive to PARP inhibitors (Ashworth, 2008). Given that a substantial proportion of sporadic cancers may harbor such defects, a phenotype known as '*BRCA*ness' or HR deficiency (HRD), a wider therapeutic use for PARP inhibitors is emerging. Clinical trials in selected populations are already underway (www.clinicaltrials.gov).

Chapter one of this thesis sets out to provide the background information and scientific rationale for this body of work investigating the role of the potent, selective PARP-1 inhibitor, AG014699, in the treatment of cancers defective in HR DNA repair.

1.2 DNA damage and repair mechanisms

The accurate and efficient repair of DNA damage is essential for normal cellular function and the maintenance of genomic stability (Hoeijmakers, 2001). In humans acquired or inherited defects in DNA repair can result in an increased lifetime risk of cancer (Hoeijmakers, 2009). The integrity of DNA faces continual threat from a variety of agents. These can be classified into two groups. Firstly, endogenous sources which occur as the by-products of normal cellular metabolism. For example, reactive oxygen and nitrogen species, oestrogen and cholesterol metabolites and reactive carbonyl species are all generated by normal cellular activity and can damage DNA (De Bont *et al*., 2004). Spontaneous reactions within the DNA micro-environment such as hydrolysis can also result in damage to bases such as deaminations (Lindahl *et al*., 1993). Secondly, DNA can be damaged by exogenous physical and chemical stressors such as ultra-violet (UV) light, cigarette smoke and chemotherapy agents.

In humans over 130 genes have been identified that are associated with DNA repair and these genes can be sub-grouped, by function, into five distinct DNA repair pathways (Christmann *et al*., 2003). They are the excision repair mechanisms: Base excision repair (BER), Nucleotide excision repair (NER) which consists of two branches: global genome and transcription coupled NER; Mismatch repair (MMR) and finally the double strand DNA break repair mechanisms: Non-homologous end joining (NHEJ) and Homologous recombination (HR). Each pathway, shown in figure 1.1, has evolved to deal with a specific type of DNA damage, although there is some overlap in their functions (Hoeijmakers, 2001).

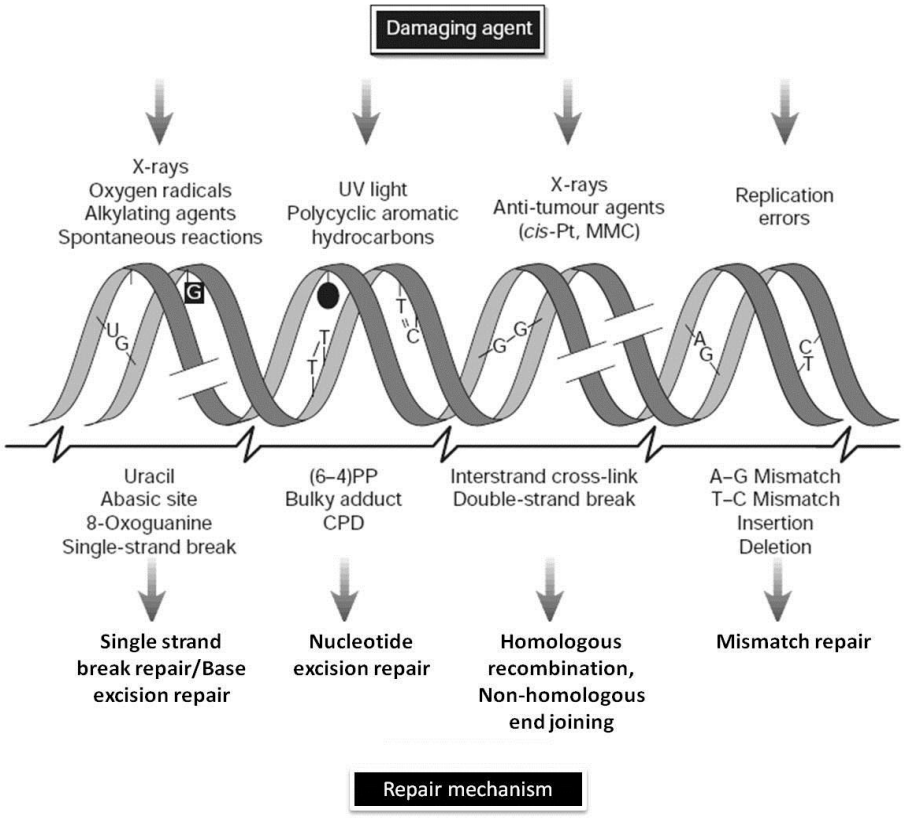

Figure 1.1: DNA damage and repair mechanisms in man (adapted from JHJ Hoeijmakers, 2001). MMC = mitomycin C, Cis-Pt = cisplatin, UV = ultra-violet light.

1.2.1 Base excision repair/ Single strand break repair

Base excision repair or single strand break repair, as it is otherwise known, is the main mechanism by which damaged bases and SSBs are repaired (Bernstein *et al*., 2002). The main function of the BER/SSBR pathway is to protect cells from endogenous DNA damage caused by hydrolysis, reactive oxygen species and other by-products of normal cellular metabolism that modify base structure. Such internal DNA damage occurs at high frequency with > 10^4 depurinations per cell per day (Lindahl *et al*., 1999). BER/SSBR also repairs damage induced by external agents such as cigarette smoke, alkylating chemotherapy agents and ionising radiation. It consists of two sub-pathways; short patch repair which replaces single nucleotides and long patch repair which replaces 2-15 nucleotides. The key steps are summarised in the following section and illustrated in figure 1.2

1.2.1.1 Recognition, base removal and incision (steps I-II)

BER/SSBR can be initiated by the recognition of the damaged base by one of at least 11 known DNA glycosylases. The glycosylases are divided into type I and II, distinguished by function. Glycosylase I enzymes remove modified bases out of the helix creating an apurinic/apyrimidinic (AP) site. This occurs by the action of the Apel AP endonuclease - Ref -1 which makes a 5' nick in the DNA backbone leaving a 5'deoxyribose-5-phosphate (5'dRP) and 3'OH. The type II glycosylases also remove bases but in addition cleave the AP site via endogenous 3' endonuclease activity resulting in a SSB.

1.2.1.2 The role of PARP in BER (step III onwards)

The nuclear enzyme PARP-1 detects DNA strand breaks via its two zinc fingers. PARP-1 binds with high affinity to and is in turn activated by the DNA SSB. Once PARP-1 is activated it catalyses the successive transfer of ADP-ribose units from the substrate nicotinamide adenine dinucleotide (NAD^+) to a variety of acceptor nuclear proteins including itself as shown in figure 1.3 . This produces linear and/or branched polymers of poly ADP-ribose (PAR). The reaction requires the catalysis of the glycosylic bond between the C-1' atom of ribose and the nicotinamide of the NAD^+ and the formation of a new glycosylic bond with the nucleophilic acceptor. Residues of glutamic acid, aspartic acid and lysine act as receptors for poly(ADP-ribosyl)ation on the target proteins (Schreiber *et al*., 2006). This 'poly(ADP-ribosyl)ation' creates a negatively charged target at the SSB which attracts the other DNA damage repair enzymes to the site forming the BER multi-protein complex. This complex is made up of PARP-1, the scaffold protein XRCC1 (x-ray repair cross-complementing 1), DNA ligase III and the DNA polymerase pol β. Following ADP-ribosylation PARP-1 has reduced affinity for DNA and is released, opening up the chromatin and allowing access to the damaged site to the other repair complex proteins. This process involving PARP-1 is required for both short and long patch repair. The PAR polymers are subsequently degraded by the poly(ADP-ribose)glycohydrolase (PARG). The structure of PARP-1 and its other DNA repair functions are discussed later in this chapter in section 1.4.

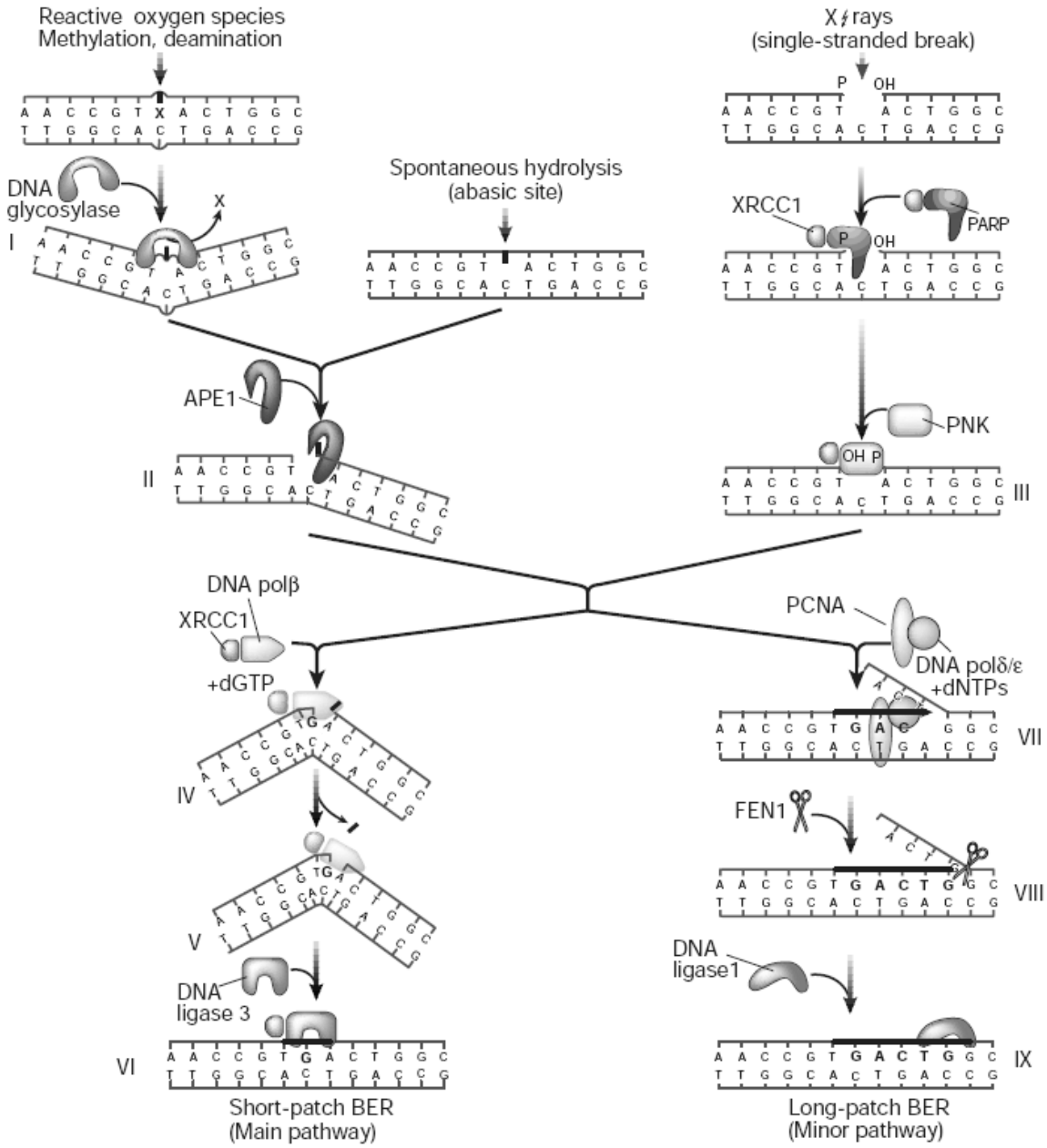

Figure 1.2: The BER/SSBR pathway (adapted from JHJ Hoeijmakers, 2001) showing the role of PARP-1 in both short and long patch repair. XRCC1 (X-ray repair cross-complementing 1), PARP (poly(ADP-ribose) polymerase), APE-1 (Apel endonuclease- Ref -1), PCNA (Proliferating cell nuclear antigen), FEN1 (Flap endonuclease 1). Further figure explanations are provided in the main text under the corresponding Roman numerals.

1.2.1.3 Short patch repair (steps IV-VI)

In mammals short patch BER/SSBR is the dominant pathway. As shown in figure 1.2, the DNA pol β replaces the missing nucleotide using the complimentary strand as a template and removes the 5'-terminal baseless sugar residue via its lyase activity. The XRCC1-DNA ligase 3 complex then seals the nick with XRCC1 acting as a scaffold protein.

1.2.1.4 Long patch repair (steps VII-IX)

In long patch repair the process is more complex with the synthesis of more than one nucleotide required for repair. This synthesis is achieved by DNA pol β, pol δ/ε and the proliferating cell nuclear antigen (PCNA). Flap endonuclease 1 (FEN1) acts to remove the DNA flap and DNA ligase 1 is responsible for sealing.

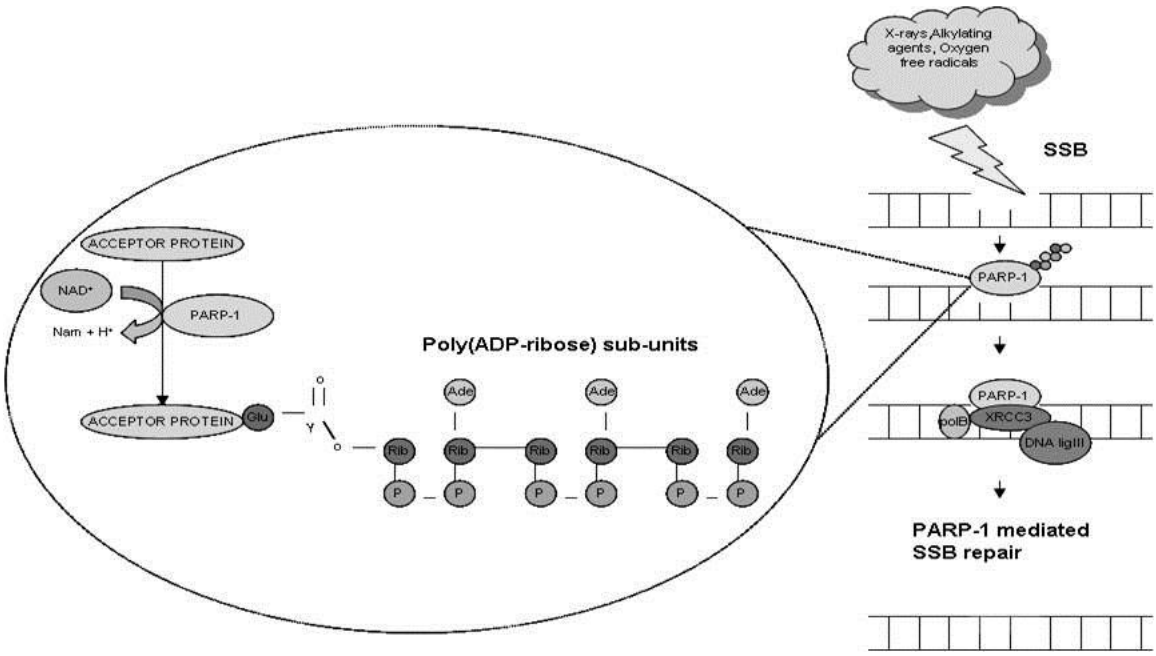

Figure 1.3: The role of PARP-1 in SSB repair pathway (Drew and Calvert, 2007). Following DNA damage PARP-1 is activated and binds to the exposed single strand break (SSB). Once bound it catalyses the successive transfer of ADP-ribose units from the substrate nicotinamide adenine dinucleotide (NAD^+) to a variety of acceptor nuclear proteins. This creates multiple linear or branched polymers of poly(ADP-ribose). This 'poly(ADP-ribosyl)ation' creates a negative charge at the SSB which recruits the other enzymes required for successful long or short patch SSB repair: XRCC1 (X-ray repair cross-complementing 1), DNA ligase III and the DNA polymerase pol B (shown).

1.2.1.5 Human disorders of BER/SSBR

There are no known human disorders associated with inherited BER/SSBR deficiencies. In fact, inactivation of BER/SSBR core proteins in mouse models results in embryonic lethality (Schreiber *et al*., 2002) emphasising the importance of this pathway in genomic maintenance and cell survival.

However, polymorphisms in the BER/SSBR genes do exist and are linked with increased cancer risk and response to chemotherapy. For example, polymorphisms in the *PARP-1* encoding gene - *ADPRT* (adenosine diphosphate ribosyl transferase) and the *XRCC1* gene are linked with an increased risk of lung adenocarcinoma in smokers (Zhang *et al.,* 2005). In addition; *XRCC1* polymorphisms have been shown to predict the response to oxaliplatin- based chemotherapy in patients with advanced colon cancer (Stoehlmacher *et al.,* 2001).

1.2.2 Double strand DNA break (DSB) response

DSBs are regarded as the most lethal of the DNA lesions and if left un-repaired can result in genomic instability, carcinogenesis and ultimately cell death (Hoeijmakers *et al.,* 2001). They occur as a result of direct damage to both strands of DNA from exogenous agents like ionising radiation or chemotherapy (e.g. the topoisomerase inhibitors) (Helleday *et al*., 2008) or as part of normal physiology e.g. to permit genetic recombination during meiosis (Neale *et al*., 2006) and the rearrangements needed for the development of immunoglobulin genes during V(D)J (variable, diversity and joining) recombination (Leavy., 2010). It is now known that a significant number of DSBs arise during DNA replication when a replication fork encounters an un-repaired SSB; and that the HR pathway and PARP-1 have a vital role in repairing such collapsed replication forks (Bryant *et al*., 2009; Helleday *et al*., 2007).

The two major proteins involved in DSB detection are the ataxia-telangiectasia mutated (ATM) and ATM Rad53 related (ATR) proteins, both members of the phosphadtidylinositol 3-kinase-like family (Bakkenist *et al.,* 2004). ATM and ATR sense the DSB and trigger the activation of multiple genes involved in either HR or NHEJ repair, cell cycle arrest, and in some circumstances apoptosis. Substrates for ATM phosphorylation include: BRCA1, p53, the check-point kinases CHK1 and CHK2, Fancona anaemia protein FANCD2, the histone H2AX and the Mre-11-Rad50-NBS1 (Nijmegen breakage syndrome) (MRN) complex. ATR is known to phosphorylate CHK1,

BRCA1 and the DNA helicase BLM1 (Lord *et al*., 2006). It was originally thought that ATM and ATR acted independently in their response to DNA damage. With ATM activated in response to DSB arising from ionising radiation (IR), and ATR phosphorylating its substrates following DNA damage induced by stalled replication forks or insults such as UV light and DNA damaging chemotherapy agents. However, recent evidence suggests that ATM and ATR work together; with reports of both ATM and ATR required for ionising radiation-induced CHK1 phosphorylation and ATM regulating the activity of ATR in response to DSBs (Jazayeri *et al*., 2006).

The role of both ATM and ATR in halting cell cycle progression prior to DSB repair is essential to avoid the passage of deleterious genetic mutations through to daughter cells at mitosis. This cell cycle arrest is facilitated by the activation of CHK1 and CHK2, which results in cell cycle arrest at the G_2/M and S phase check-points. If the DNA damage is considered too severe for effective repair then apoptotic cell death can ensue. This apoptosis is triggered by CHK2 via the phosphorylation of E2F1, PML and p53 (Zhou *et al*., 2004).

The two primary DSB repair mechanisms in humans are NHEJ and HR. These two pathways operate independently but do share some common proteins. Which pathway is used to repair the DNA damage depends principally on the origin of the DSB and the stage in the cell cycle in which the DSB occurs (Takata *et al*., 1998). HR is an error-free pathway which is dependent on the proximity of the sister chromatid and so only takes place in late S and the G_2 phases of the cell cycle (O'Driscoll *et al*., 2006). NHEJ, as the name suggests, simply joins together two ends of broken DNA and therefore does not require the synthesis of a complementary template and so can occur at *any* stage in the cell cycle. However, its main action occurs prior to replication in G_0 and G_1 (Chu *et al*., 1997).

1.2.3 DNA DSB repair: Non-homologous end joining

Non-homologous end joining is the main mechanism in mammalian cells by which DSBs are repaired (Chu *et* al., 1997). It is an error-prone pathway and may result in the deletion or insertion of base pairs. The core protein components of NHEJ (shown in figure 1.4) are DNA-PK (DNA - protein kinase), DNA ligase IV, X-ray cross complementation group 4 (XRCC4) and the nuclease Artemis (Collis *et al*., 2005). DNA-PK, the main NHEJ player, is a nuclear serine/threonine protein kinase that consists of a catalytic subunit (cs) (DNA-PKcs) and a DNA binding/regulatory subunit (Ku). Following a DSB, NHEJ is thought to be initiated by the heterodimer of Ku (Ku70 + Ku80) which binds to both DNA ends (Bernstein *et al*., 2002). The Ku heterodimer then recruits DNA-PKcs, which is in turn activated. The complex of Ku + DNA-PKcs now becomes the active protein kinase – DNA-PK. This brings together the ends of the DSB for processing prior to re-ligation. This processing is thought to be carried out by a number of proteins. For example, the MRN complex has exo/endonuclease and helicase activity to remove the excess DNA at the 3' flaps. Whilst FEN1 is recruited to remove the 5' overhangs, the protein Artemis is recruited and, acting in a complex with DNA-PK, primes the site of damage via its endo/exonuclease activity, resecting DNA at both the 3' and 5' flaps. New DNA ends are synthesised by a DNA polymerase thought to be pol μ and finally, ligation is achieved by the actions of XRCC4 and DNA ligase 4 (Christmann *et al*., 2003)

DNA-PK has been a target for anti-cancer drug developers for some years. NU7441, a 2-N morholino-8-dibenzothiophenyl-chromen 4, is a potent and selective DNA-PK inhibitor developed at Newcastle University in collaboration with KuDOS pharmaceuticals (now owned by Astrazeneca) (Zhao *et al*., 2006). Inhibition of DNA-PK by NU7441 has been shown to enhance the cytotoxicity of ionising radiation and doxorubicin in DNA-PK proficient but not deficient hamster and human cancer cell lines (Tavecchio *et al*., 2011). Interestingly, Tavecchio *et al* demonstrated that inhibiting DNA-PK with NU7441 resulted in reduced HR activity, as represented by reduced Rad51 foci formation, suggestive of DNA-PK activity within the HR repair process. NU7441 is still in pre-clinical drug development but it is envisaged that DNA-PK inhibitors will enter early phase clinical trials in the next few years.

1.2.4 DNA DSB repair: Homologous recombination

Homologous recombination plays a major role in repairing DSBs that arise as a result of replication fork stalling following un-repaired SSBs (Helleday *et al.,* 2007). HR can be subdivided into two pathways; Gene Conversion (GC), illustrated in figure 1.4, and Single Strand Annealing (SSA). GC is the predominant pathway but they share common beginnings. It was always proposed that HR is initiated by the MRN complex (Falck *et al.,* 2005) which recruits ATM to the site of DNA damage but the precise mechanism behind this was unknown. However, it was recently discovered that the MRN complex, in processing the DSB end, creates multiple short single strand (ss) DNA oligonucleotides which in turn stimulate ATM (Jazayeri *et al*., 2008). Once activated, ATM phosphorylates a number of proteins including: BRCA1, the histone H2AX, CHK1 and 2 and the MRN complex itself. Following this phosphorylation, the MRN complex resects, via its exo/endonuclease activity, the sequence of DNA damage exposing single strand overhangs of DNA at the 3' ends on either side of the DSB. This process is thought to also involve BRCA1 (Zhong *et al.,* 1999). Next, Rad51, one of the major players in HR, facilitates the assembly of a helical nucleoprotein filament known as the pre-synaptic filament (shown in figure 1.4 II). This is thought to also involve the Rad51 related proteins (XRCC2, XRCC3, Rad51B, C and D). Paradoxically, this process is made more difficult by another component of HR, the replication protein A (RPA). RPA, an abundant ssDNA-binding protein, competes to bind to the sites of exposed ssDNA (Sung *et al.,* 2006). Biochemical and chromatin immunoprecipitation experiments have shown that the Rad52 protein and the heterodimeric Rad55-Rad57 complex help to overcome the inhibitory effects of RPA on the filament formation (Sung *et al*., 1997). In addition recent data has shown that BRCA2 facilitates Rad51 in displacing RPA from the exposed ssDNA (Jensen *et al.,* 2010). Rad51 localises to the site of DSB with the help of BRCA2 which binds directly to Rad51 via its eight conserved BRC repeat zones transporting it into the nucleus. It is proposed that this BRCA2-Rad51 complex binds to the exposed single stranded DNA and this binding then enables the loading of Rad51 onto the break and the formation of the pre-synaptic filament (Yang *et al.,* 2002).

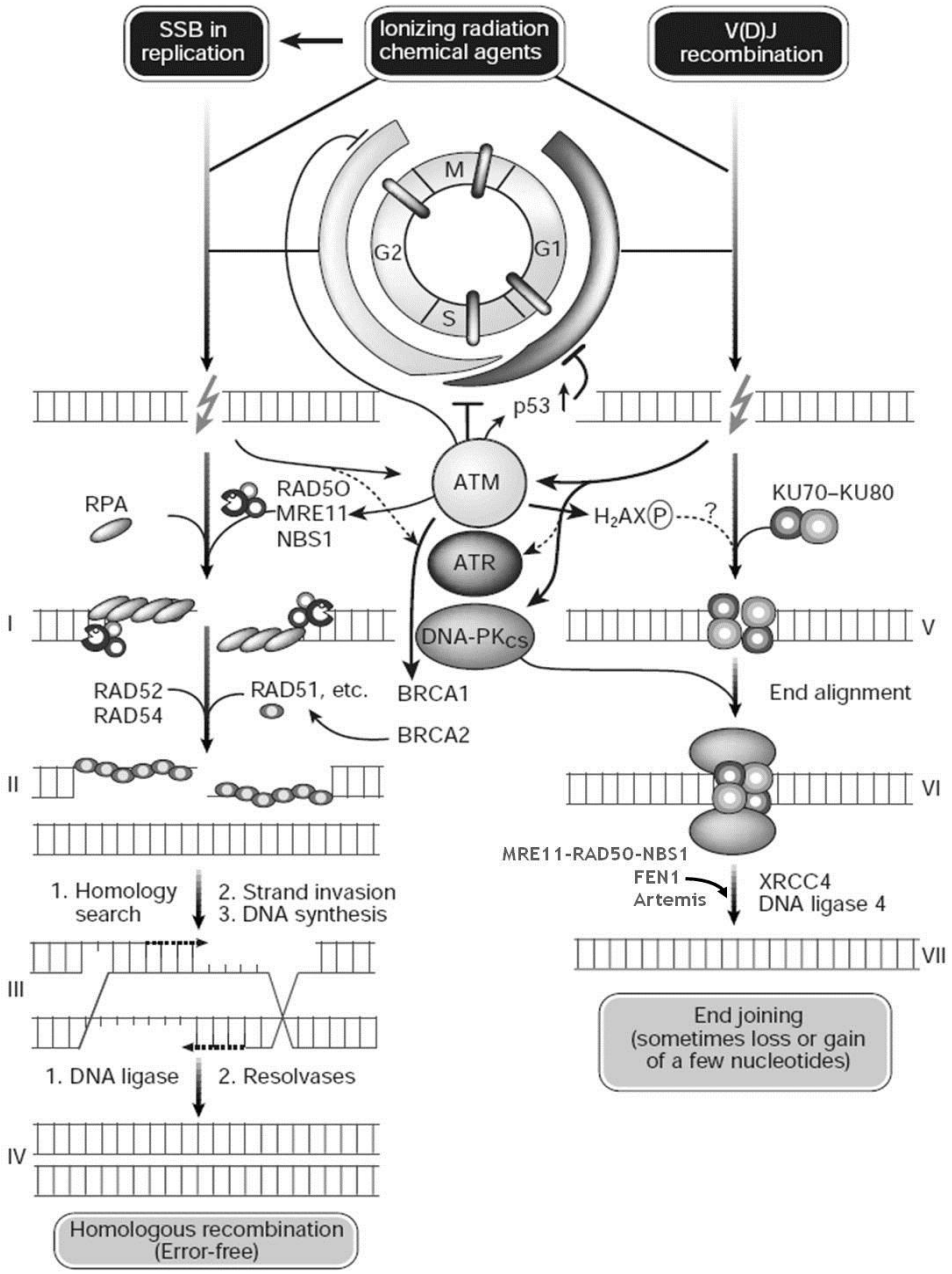

Figure 1.4: DNA DSB repair pathways (adapted from JHJ Hoeijmakers, 2001). Homologous recombination (Gene Conversion): (I) Following DSB DNA excised by the MRN complex and Rad51 localises to DSB via BRCA2. (II) Rad51 and related proteins assemble the pre-synaptic filament. (III) Rad51 and Rad54 identify homologous sequence of DNA and facilitate invasion into break site and new sequence of DNA is synthesised. (IV) Exchanged ends, (Holliday junctions), are rejoined by resolvases. Non-Homologous end joining (NHEJ): (V) Heterodimer of Ku (Ku70 + Ku80) binds to exposed DNA initiating NHEJ. (VI) The active protein kinase – DNA-PK (Ku + DNA-PKcs) brings the ends of DSB for processing prior to re-ligation. (VII) MRN complex, FEN1 and Artemis remove excess DNA ends. New DNA synthesised by a DNA polymerase and ligation occurs via XRCC4 and DNA ligase 4. DSB = double strand break, MRN = Mre-11-Rad50-NBS, XRCC2/3/4 = X-ray cross complementation group 2/3/4, V(D)J = Variable, diversity and joining, BRCA1/2 = breast cancer susceptibility 1/2.

Rad51 with the help of Rad54 identifies a homologous sequence of intact DNA and facilitates its invasion into the site of break. This then acts as a template for a new identical sequence of DNA to be synthesised. Finally the exchanged ends, known as Holliday junctions, are rejoined by resolvases (Constantinou *et al.,* 2001). Recent work has also suggested that BRCA2 also has a role in regulating the DNA-binding activity of Rad51 holding it in an inactive state when it is not needed (Davies *et al.,* 2001; Esashi *et al*., 2007).

If the DSB occurs within matching sequences of DNA it can be repaired by the process of SSA. A much less complex pathway; it involves the matching of homologous sequences on either side of the DSB followed by the deletion of the intermediate non-complementary sequence. The process is facilitated by RPA and Rad52 and is dependent on functioning BRCA1. However, it does not require the full repertoire of HR genes in particular it is Rad51- independent. SSA is likely to generate errors and considered only an alternative pathway in the absence of functioning Rad51 mediated HR (Helleday *et al*., 2007).

It is clear that the BRCA1 and BRCA2 proteins play major roles in the HR repair process. Therefore it would be logical to hypothesise that deficiencies within either *BRCA*1 or 2 genes could result in defective HR. There are a number of human syndromes associated with mutations within genes involved in the HR process. These are shown in table 1.1. The most common and best described is the Hereditary Breast Ovarian Cancer syndrome (HBOCS). This occurs mainly as a result of inheriting a mutation within either the *BRCA*1 or 2 genes and is associated with a high risk of developing breast and ovarian cancer.

Mutations within other genes have been identified which are associated with an increased lifetime risk of breast and/or ovarian cancer. These include *CHEK2* (CHEK2 Breast Cancer Case –Control Consortium., 2004)*, PTEN* (Lynch *et al*., 1997) and most recently *Rad51D* (Loveday *et al*., 2011).

Human syndrome	**Gene**		**Chromosome**	**Cancer risk**	**Reference**
HBOC	*BRCA*1 *BRCA*2/*FANCD*1		17q21 13q12	Breast Ovary Prostate Fallopian Tube Primary peritoneal Pancreas	King *et al.,* 2003
Fanconi anaemia	Other *FANC* genes (A,C,D2,E,F,G,)		16q24.3 9q22.3 3p25.3 6p21-22 9p13	Acute myeloid leukaemia Head and neck cancers Squamous cell carcinoma	Kennedy *et al.,* 2006
Nijmegen breakage syndrome	*NBS1*		8q21	Lymphomas	Demuth *et al.,* 2007
Bloom syndrome	*BLM*		15q26	Leukaemia's NHL Breast	Hickson, 2003
Rothmund-Thomson syndrome	*RECQL4*		8q24.3	Osteosarcoma	Hickson, 2003

Table 1.1: Human syndromes with mutations within genes associated with Homologous recombination and increased risk of cancer. BRCA = bre ast cancer susceptibility, HBOC = hereditary breast and ovarian cancer syndrome, FANC = Fanconi, NBS1 = Nijmegen breakage syndrome, BLM = Bloom, NHL= non-hodgkins lymphoma.

1.3 The *BRCA1* and 2 tumour suppressor genes

The *BRCA*1 gene was first identified in 1990 by Mary King's group working at Berkeley, California, USA. The name BRCA was originally chosen to stand for **B**e**r**keley **Ca**lifornia but was later changed to represent **Br**east **ca**ncer susceptibility (Hall *et al*., 1990). The gene was subsequently cloned in 1994 by Myriad Genetics (Miki *et al*., 1994). Around the same time in 1994, the *BRCA*2 gene was discovered by Stratton and Wooster working at the Institute of Cancer Research, London, UK (Wooster *et al*., 1994). The identification of these genes was a significant breakthrough in the management of breast and ovarian cancer families. It enabled the introduction of risk assessment, genetic counselling and *BRCA* mutational analysis.

The *BRCA1* gene, located on chromosome 17q21, encodes a large, predominantly nuclear protein (1863 amino-acid) with an estimated molecular weight of 220kDa (Venkitaraman *et al.,* 2002). It consists of multiple functional domains including an N-terminal RING, 2 nuclear localisation signals (NLSs) and 2 C-terminal BRCA1 carboxyl terminal (BRCT) domains of ~ 110 residues. The *BRCA2* gene, located on chromosome 13q12.3, and later identified to also be the Fanconi Anaemia gene *FANCD1*, encodes a larger 3418 amino acid protein with an estimated molecular weight of 384kDa (Venkitaraman, 2002). An important feature of the BRCA2 protein is the eight copies of the 30-80 amino acid repeats – BRC, known to be the main binding sites for Rad51 (Bertwistle *et al*., 1998).

The structures of both proteins are shown in figure 1.5. Although the BRCA1 and BRCA2 proteins have different functions involving multiple cellular pathways, both share important regulatory roles in co-ordinating the response and repair of DNA damage. Consequently loss of these functions can result in genomic instability and increased risk of carcinogenesis, as observed in carriers of germline *BRCA* mutations carriers (Venkitaraman, 2009). To understand why inheriting defective *BRCA*1 and 2 genes can confer such a devastating risk of cancer on an individual it is important to review in detail the roles of these proteins play in normal cellular life in particular in DNA repair.

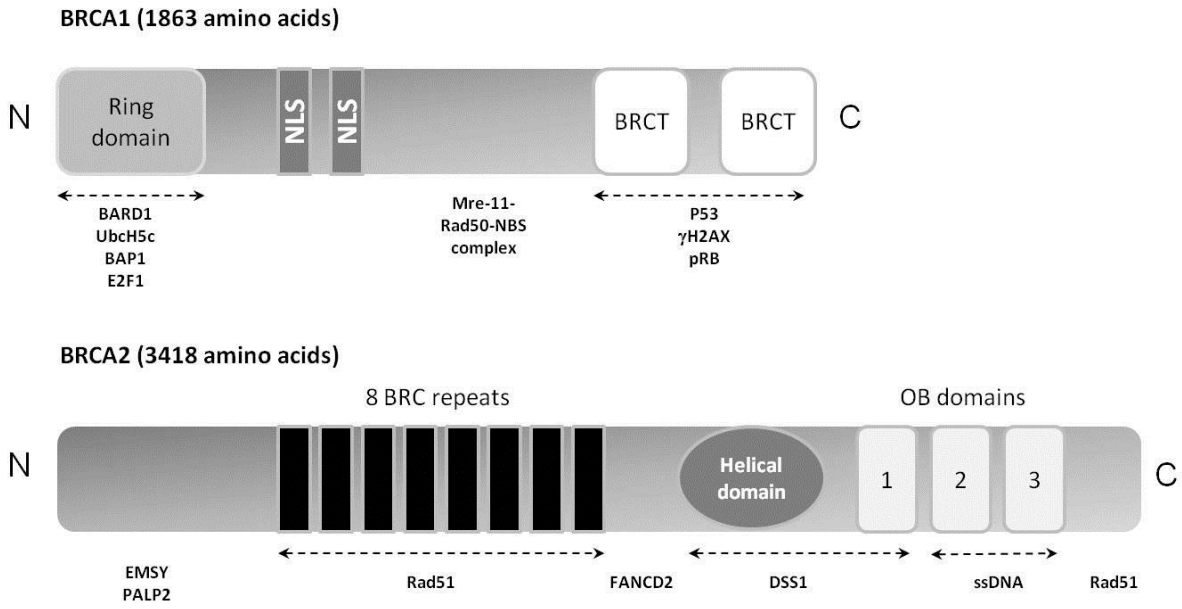

Figure 1.5: Schematic representation of the BRCA1 and BRCA2 proteins. NLS = nuclear localisation signal, BRCT = BRCA1 carboxyl terminal.

1.3.1 Functions of BRCA1

BRCA1 is predominantly a nuclear protein but it is able to shuttle freely between the cytoplasm and nucleus in order to carry out its variety of cellular functions which include: DNA damage signalling response and repair, transcriptional regulation and cell cycle check-point control.

1.3.1.1 BRCA1 and DNA damage response and repair

One of the earliest observations to suggest a role in DNA repair for BRCA1 was its co-localisation with Rad51 in the nuclear foci of mitotic and meiotic cells (Scully *et al.,* 1997). Since then studies have shown that not only does BRCA1 play a vital role in the repair of DNA DSBs but also in the initial detection of the DNA damage. The BRCA1 protein acts as part of a large complex known as the BRCA1- associated genome surveillance complex (BASC). BASC is thought to act as a sensor for DNA damage and includes: the MRN complex, mismatch repair proteins (MSH2, MSH6 and MLH1), BLM syndrome helicase and ATM (Gudmundsdottir *et al.,* 2006). Once DNA DSB damage has been sensed the BRCA1 protein plays a vital role in its repair via HR, as discussed in section 1.2.4. However, there is evidence that BRCA1 plays a role in the other mechanisms of DNA repair in particular NER and NHEJ. BRCA1 has been shown to

regulate the global genomic repair (GCR) sub-pathway of NER. The proposed mechanism is via direct transcriptional control of the NER genes: XPC, DDB2 and GADD45 (Hartman *et al., 2*002). There is also a growing body of evidence suggesting that BRCA1 may regulate a component of NHEJ. NHEJ is an error-prone pathway but more recently the existence of an additional potentially more mutagenic sub-pathway has been proposed (Durant *et al*., 2005). This sub-pathway is thought to operate independently of DNA-PK and is strongly dependent on Mre11 and Rad50. It rejoins chromosomal DNA ends with imperfect micro-homology creating non-random deletions of up to 300 base pairs. This process, which could be highly mutagenic, has been named micro-homology-mediated end joining (MMEJ). Studies have shown that BRCA1 can suppress MMEJ by inhibiting Mre11 activity (Zhuang *et al*., 2006). This proposal is supported by the observation that BRCA1 deficient cells demonstrate an increased tendency to generate large deletions during NHEJ repair.

1.3.1.2 BRCA1 and cell cycle control

The ability to control the timing and sequence of cell cycle events following DNA damage is essential for maintaining genomic stability. This function is governed by a family of cyclin-dependent kinases and their endogenous inhibitors acting at cell cycle check-points. BRCA1 is rapidly phosphorylated after DNA damage and plays a key role in this cell cycle regulation. Firstly, BRCA1 has been shown, via a number of p53 dependent and independent pathways, to stimulate the transcription of the $p21^{WAF1/CIP1}$ promoter of the p21 gene leading to G_1/S cycle arrest (Chai *et al*., 1999). This activation of $p21^{WAF1/CIP1}$ transcription is dependent on the phosphorylation status of BRCA1. Secondly, BRCA1 is thought to be involved in intra-S phase checkpoint activation. Following damage by IR, activation of the intra-S phase checkpoint requires the phosphorylation of BRCA1 by ATR (Tibbetts *et al*., 2000). BRCA1 has also been shown to up-regulate the expression of the cyclin-dependent kinase inhibitor $p27^{KIP1}$, which results in intra-S phase arrest (Williamson *et al*., 2002).

The CHK1 and CHK2 kinases acting downstream of ATM and ATR are responsible for maintaining the G_2-M check-point. In response to IR BRCA1 is phosphorylated by CHK2 and subsequently BRCA1 deficient cell lines have been reported to be unable to activate G_2/M arrest in response to IR (Aprelikova *et al*., 2001). Finally, BRCA1 is known to be a transcriptional regulator of several genes involved in the regulation of

the G_2/M check-point. The strongest evidence for this comes from its regulation of GADD45, which activates the checkpoint by inhibiting the activity of cyclin B-cdc2 complex (Mullan *et al*., 2001).

1.3.1.3 BRCA1 and transcriptional regulation

BRCA1 can regulate transcription by its direct interaction with the core component of transcription; RNA polymerase II and its co-activation or co-repression of a number of known transcription factors (Irminger-Finger *et al*., 1999). Two such transcription factors are the oestrogen receptor-alpha (ERα) and the tumour suppressor protein *p*53.

Given the fact that carriers of *BRCA*1 mutations have a high lifetime risk of developing breast and ovarian cancer, both oestrogen responsive tissues, the relationship of *BRCA*1 to ERα is the focus of much research (Gorski *et al*., 2009). Studies have shown that BRCA1 is able to induce ERα mRNA expression and negatively regulate ERα signalling pathways (Fan *et al*., 1999). BRCA1 has also been reported to inhibit the induction of over 90% of the known oestrogen-inducible genes (Xu *et al*., 2005). One such gene is vascular endothelial growth factor (VEGF), which is important for the angiogenesis required to sustain cancer cells. Confirming this is the observation that VEGF is severely impaired in the presence of exogenous, wild type *BRCA*1 and not mutated *BRCA*1 (Kawai *et al*., 2002).

In response to cellular stress *p*53, known as the 'guardian of the genome', is activated to induce target genes involved in DNA repair, cell-cycle arrest and apoptosis. BRCA1 has been shown to interact with the C-terminus of p53. This interaction results in a re-direction from the activation of pro-apoptotic target genes to those involved in cell-cycle arrest and DNA repair (Chai *et al*., 1999). Interestingly, mutations in *p*53 are common in *BRCA*-mutated cancers and that this loss of p53 function may be important to mediate tumourigenesis (Parant *et al*., 2003).

1.3.2 Functions of BRCA2

The main function of BRCA2 is its role in HR mediated DNA DSB repair through its direct interaction with Rad51 (discussed earlier in this chapter in section 1.2.4). Loss of BRCA2 can result in the repair of DSBs via error-prone pathways and subsequent genomic instability (Tutt *et al.,* 2001). Furthermore, cells deficient in BRCA2 have

impaired formation of Rad51 foci following exposure to DNA damage (Yuan *et al*., 1999; Drew *et al*., 2011b).

In addition to its role in DNA DSB repair, BRCA2 may have a role as a regulator of cell cycle progression at the mitotic check-point. BRCA2 associates with the DNA binding protein BRAF35 and both proteins co-localise on mitotic chromosomes. Injections of antibodies which block either BRCA2 or BRAF35 into cells were shown to block progression through mitosis (Marmorstein *et al*., 2001).

In summary the BRCA1 and 2 proteins are essential to the mechanism of HR DSB repair and major players in the maintenance of genomic stability. It is therefore not surprising that carriers of mutations within the *BRCA* genes have a high lifetime risk of developing cancer.

1.3.3 BRCA1/2 mutations and the risk of cancer

Inheriting a mutation in either of the *BRCA*1 or 2 genes confers a high lifetime risk of developing breast and/or ovarian cancer. The lifetime risk of breast cancer in female *BRCA*1 mutation carriers has been reported to be as high as 84% and between 60-80% in *BRCA*2 mutation carriers (King *et al.,* 2003). In men, breast cancer is rare, accounting for < 1% of all cases, but in *BRCA* mutation carriers the lifetime risk is estimated to be between 58 and 100 times that of the general male population (Brose *et al.,* 2002; Liede *et al*., 2004). The life-time risk of developing ovarian cancer is lower and estimated at 40-50% and 10-20% for *BRCA*1 and *BRCA*2 mutation carriers respectively (Ford *et al*., 1994).

The frequency of carrying a germline *BRCA*1 or 2 mutation in the general population is thought to be between 0.1 – 0.8% (Risch *et al*., 2006). However in patients with breast and/or ovarian cancer it is estimated that between 10-15% will be associated with carrying a *BRCA*1 or 2 germ-line mutation (Stratton *et al*., 1997; Venkitaraman *et al*., 2002).

Carriers of the mutations are not limited to a particular population but specific groups with high prevalence have been identified, such as women of Ashkenazi Jewish descent (Stuewing *et al*., 1997). The autosomal dominant mode of genetic transmission means that *both* the male and female children of a carrier have a 50%

chance of inheriting the mutation in their germline. One defective allele is sufficient to predispose to cancer, but the somatic loss of function of the second allele is required in cancer cells confirming the classic Knudson two hit hypothesis for tumour suppressor genes (Knudson, 1971).

Breast and ovarian cancer are the most commonly observed but an increased risk of other cancers including: prostate, pancreatic, fallopian tube and primary peritoneal carcinoma has been documented (Brose *et al.,* 2002, The Breast Cancer Linkage Consortium (BCLC)., 1999). Primary peritoneal carcinoma (PPC) can arise from an occult ovarian cancer focus or *de novo* in the peritoneal mesothelium. In one study follow-up of women who had undergone prophylactic bilateral oophrectomies reported a frequency of PPC of 2-4%; occurring more often in *BRCA*1 than *BRCA*2 carriers (Casey *et al*., 2005). Primary fallopian tube carcinoma is unusual in the general population but life-time risk in *BRCA*1/2 carriers is reported to be more common at 3% (Brose *et al.,* 2002). In male *BRCA* 1 mutation carriers, the prostate is the commonest cancer site. In a study by the BCLC an elevated risk of prostate cancer was observed in carriers < 65 years old but not in those > 65yrs (Thompson *et al.,* 2002). This is probable explained by the fact that prostate cancer risk increases with age in all men. Pancreatic cancer is more common in *BRCA*2 carriers. They have a younger than average age of disease onset and the estimated lifetime risk is thought to be as high as 5% (BCLC, 1999). Pancreatic cancer risk in *BRCA*1 carriers is less well established.

The risk of childhood cancer is not increased in *BRCA* mutation carriers except in the uncommon situation where an individual inherits mutated *BRCA*2 genes from both parents resulting in Fanconi anaemia (Kennedy *et al*., 2006).

1.3.4 Tissue specificity of BRCA-related cancers

Why *BRCA*1/2 gene mutation carriers are so highly predisposed to cancers of the breast and ovary is not fully understood. However several theories exist attempting to part-explain this phenomenon. Firstly, these cancers arise in oestrogen-dependent epithelial tissues. *BRCA*1 is known to regulate transcription (see section 1.3.3) and inhibit oestrogen receptor signalling; loss of this function could result in un-controlled cell proliferation in these tissues and ultimately cancer (Fan *et al*., 1999). Another proposal is that BRCA function somehow protects cells from the local effects of

mutagenic oestrogen metabolites thus preventing genomic instability. For example, *in vivo* studies in *Brca*1 and *Brca*2 heterozygous mice report alterations in the mammary gland and ovarian tissue architecture following exposure to the highly oestrogenic compound diethylstilbestrol (Bennett *et al*., 2000).

It is often hypothesised that breast and ovarian tissues are highly proliferative and that it is this cell-turnover that increases the chances of mutation and subsequent tumourigenesis. This theory however is questionable as cancers of the highly proliferative gastrointestinal tract and lymphoid tissue are not commonly seen in *BRCA* mutation carriers.

Elledge and Amon propose an alternative reason for this tissue specificity which they coined the 'suppressor hypothesis'. This suppressor hypothesis suggests that *BRCA*-mutated cancers do not arise in other tissues because they cannot tolerate the loss of *BRCA* heterozygosity required for cancer development and that breast and ovarian tissues can. They suggest a variety of reasons for this including a protective anti-apoptotic effect of oestrogen (Elledge and Amon, 2002).

Another proposal is that there must be something specific about breast and ovarian tissues that makes them more dependent on the function of BRCA1 and 2 than other tissues or that loss of another essential gene product co-exists within these tissues resulting in the high risk of cancer. One such gene is the tumour suppressor gene *p*53. Studies have shown that the additional loss of p53 in mice already deficient in Brca1 accelerates the formation of tumours (Xu *et al*., 1999). *p*53 is mutated in almost 100% of all high grade serous ovarian cancers (Ahmed *et al*., 2010) and it may be that in the presence of a germ-line *BRCA* mutation this may be enough to promote cancer.

In summary it is likely that the tissue specificity of *BRCA* mutated cancers is due to multiple genetic and environmental factors.

1.3.5 Management options for BRCA1/2 mutation carriers

Over the past ten years the main focus for those identified as *BRCA* mutation carriers has been cancer prevention through prophylactic surgery and early cancer detection through screening.

1.3.5.1 Prophylactic surgery

Prophylactic bilateral salpingo-oophorectomy (BSO) reduces the risk of ovarian cancer by up to 95% and in pre-menopausal women the risk of breast cancer by around 50%. Prophylactic bilateral mastectomy (BM) reduces the risk of breast cancer by 90% (Domchek *et al*., 2006b). National guidelines in the UK recommend that women undergo prophylactic BSO by age 40-45 and support various strategies for reducing breast cancer risk including BM (National Comprehensive Cancer Network, www.nccn.org). *BRCA* mutation carriers face difficult decisions in terms of whether and when to opt for prophylactic surgery and the support of a multi-disciplinary team including clinical psychologists should be offered to all patients. As surgery does not totally eliminate cancer risk these patients also require long-term follow-up including the management of BSO- induced premature menopause.

1.3.5.2 Screening

The purpose of any cancer screening programme is to detect cancer early enough to enable interventions that will have an impact on patients survival. Any such programme also has to be acceptable in terms of financial and patient costs. The National Breast Screening Programme (NBSP) invites women in the UK to attend for a mammogram every three years between the ages of 47 and 73 (www.cancerscreening.nhs.uk). The NBSP is considered to be worthwhile with a recent report that between 5.7 and 8.8 breast cancer deaths are prevented for every 1000 women screened and between 2 and 2.5 lives saved per every over-diagnosed patient, that is someone treated for a cancer that might never have revealed itself in their life-time (Duffy *et al*., 2010). However, the questions for *BRCA* mutation carriers are; how early to start screening and with what modality? Women with *BRCA* mutations develop cancer at an earlier age than the national screening programme would pick up and at a time when X-ray mammography is less sensitive due to denser breast tissue. Following the results of a large multi-centre cohort study (the MARIBS trial) which demonstrated the superiority of it magnetic resonance imaging (MRI) over mammography in detecting breast cancer in 649 women aged between 35 and 49; it is now recommended that screening should start at age 30 and consist of a combination of annual MRI and mammogram (Leach *et al*., 2005).

There is no evidence that screening for ovarian cancer using trans-vaginal ultrasound (TVU) scanning and blood monitoring of the tumour marker CA125 (cancer antigen 125) saves lives and as a result there is no UK national screening programme for ovarian cancer. However, within the UK, women are currently being offered screening as part of a national trial known as the UK Familial Ovarian Cancer Screening Study (UKFOCSS). UKFOCSS offers women annual TVS and four monthly CA125 measurements. The study is now closed to recruitment and results are expected in 2013. If this shows a benefit then surveillance may be offered on a national level. But until then the main option to prevent ovarian and fallopian tube cancer for *BRCA* mutation carriers remains surgery.

1.3.5.3 Chemoprevention

The use of the oral contraceptive pill (OCP) as chemoprevention, to reduce the risk of ovarian cancer and delay the need for BSO in younger women wishing to have families has been explored in this population. In 1998 one study involving 207 *BRCA*1/2 mutation carriers with ovarian cancer and 161 of their sisters, acting as case-controls, reported a 60% reduction in the risk of ovarian cancer with the use of the OCP for at least six years (Narod *et al*., 1998). One major concern with this preventative strategy is the associated increased risk of breast cancer with the prolonged use (> 4 years) of the OCP (Brohet *et al*., 2007). In addition, chemoprevention has not been shown to be as effective as BSO in preventing ovarian cancer and therefore the use of OCP outside of a clinical trial is not recommended in the UK. The potential use of PARP inhibitors as chemoprevention will be discussed later in this chapter.

1.3.6 Medical treatments of BRCA mutated cancers

Surveillance and surgery will not prevent all *BRCA*1/2 carriers developing cancer and many will already have cancer at the time their mutation status is diagnosed. The current management of *BRCA* mutation associated cancer is identical to the treatment of the non-hereditary forms of the same staged-matched cancer. However, data are emerging to suggest that they should be treated as a distinct disease entity. For example, it is clear that *BRCA* mutated cancers show increased sensitivity to some chemotherapy regimens. Several *in vitro* studies have demonstrated that *BRCA*1 and 2 deficient cells are more sensitive than their wild type controls to the platinum analogue cisplatin and less sensitive to anti-microtubule agents such as the taxanes

(Bhattacharyya *et al*., 2000; Tan *et al*., 2008; Tassone *et al*., 2003). Preliminary patient data are now emerging to support this theory. A retrospective study of 102 *BRCA*1 mutation carriers receiving neoadjuvant chemotherapy for breast cancer showed an increased complete pathological response rate to cisplatin compared to the more standard regimens of CMF (cyclophosphamide, methotrexate and 5-fluorouracil) and AT (doxorubicin and docetaxel) (Byrski *et al*., 2009). A small study by Tan *et al*. also demonstrated higher complete response rates (81.8% *vs*. 43.2%; $P = 0.004$) and improved overall survival to first line platinum based chemotherapy in 22 ovarian cancer patients with germline *BRCA*1/2 mutations over a matched non-hereditary control group. Improved responses were also seen in the *BRCA* mutation carriers who received second and third line chemotherapies (Tan *et al*., 2008). Interestingly, an improved response to platinum has also been reported in ovarian cancers with reduced *BRCA*1 mRNA expression (Quinn *et al*., 2007). This retrospective study analysed *BRCA1* mRNA levels in 70 sporadic ovarian cancers. The results showed that women with low to intermediate levels had a significantly increased median survival following treatment with platinum based chemotherapy than those with high *BRCA*1 mRNA expression (57.2 *vs*. 18.2 months; $P = 0.0017$). Of note, the *BRCA*1 mutation status of patients in this study was unknown; thus the reduced levels of *BRCA*1 expression observed could be attributed to *BRCA*1 germline mutations but additionally somatic mutations or gene promoter methylations.

These data suggest that *BRCA* mutation carriers have a better outcome following treatment for cancer and that it is associated with an increased response to the platinum chemotherapy agents. This question of increased platinum sensitivity in *BRCA*-related breast cancer will hopefully be answered by a current randomised clinical trial. This randomised phase II trial, conducted by the Breakthrough Breast Cancer Research Centre in conjunction with Cancer Research UK (CRUK) (www.brcatrial.org) is randomising patients with a known *BRCA*1/2 mutation at first presentation of metastatic/advanced disease to six cycles of the platinum- carboplatin or standard treatment with the anti-microtubule agent-docetaxel.

Recently a novel strategy for treating these germline *BRCA* mutated cancers has emerged; to use small molecule inhibitors that target the nuclear enzyme Poly(ADP-ribose polymerase-1 (PARP-1). This is discussed in detail in section 1.5.3.

1.4 PARP-1 and the PARP family

The discovery of the first poly(ADP-ribose) polymerase (PARP) began over forty years ago when in 1963 researchers in Paul Mandel's laboratory observed the synthesis of a new polyadenylic acid after adding nicotinamide mononucleotide to rat liver extracts (Chambon *et al*., 1963). Shortly after this discovery independent research groups demonstrated that this new polymer, named poly(ADP-ribose), was made up of two ribose moieties and two phosphate units (Chambon *et al*., 1966; Nishizuka *et al*., 1967; Sugimura *et al*., 1967). The enzyme that could generate large amounts of this poly(ADP-ribose) was later purified and designated the name ADP-ribosyl transferase (ADPRT) (Okayama *et al*., 1977). By 1980 it was discovered that ADPRT was activated by single and double strand DNA breaks (Benjamin and Gill., 1980) and seminal work by Sydney Shall's group demonstrated that it was not only involved in DNA repair but inhibiting it with 3-aminobenzamide (3-AB) enhanced the cytotoxic effects of methylating agents in leukaemic mice cells (Durkacz *et al*., 1980). Durkacz *et al.* were the first to suggest that inhibitors of ADPRT could act as chemosensitizers. ADPRT was later renamed PARP (De Murcia and Menissier de Murcia., 1994) and there are now 17 members of the PARP super-family (Rouleau *et al*., 2010). A true PARP is defined as an enzyme that is able to transfer ADP-ribose units from NAD^+ (nicotinamide adenine dinucleotide) to acceptor proteins, including itself, resulting in the formation of multiple branched and linear poly(ADP-ribose) (PAR) chains. A process known as 'poly(ADP-ribosyl)ation' and shown in figure 1.3 (Schreiber *et al*., 2006). Using this definition only PARP-1, 2, 3, 4, 5 and 5a would be true PARPs. PARP-1, 2 and 3 are the only members known to be activated by DNA damage with PARP-1 playing the dominant role in DNA repair (Ame *et al*., 1999; Ame *et al*., 2004) and the main focus of this thesis.

1.4.1 Structure of PARP-1

The *PARP-1* gene is located on chromosome 1, position q41-42, and encodes the 1014 amino acid, 113KDa, PARP-1 protein (Auer *et al*., 1989). PARP-1 is an abundant nuclear enzyme that is expressed in all nucleated human cells except neutrophils (Oei *et al*., 1994). It is reported to be over-expressed in some cancers (Alderson, 1990). PARP-1, as shown in figure 1.6, consists of three principle domains.

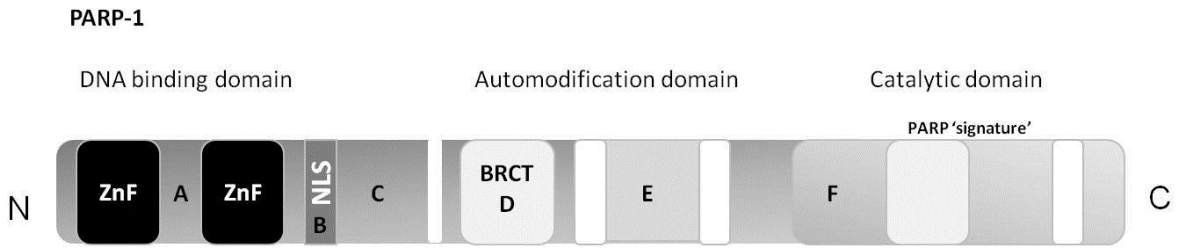

Figure 1.6: Schematic representation of the PARP-1 protein showing the three domains. ZnF = zinc fingers, NLS = nuclear localisation zone, BRCT = BRCA1 carboxyl terminal

Firstly, at the amino-terminal region, is the DNA binding domain, which consists of two zinc fingers and a nuclear localisation signal (NLS). These zinc fingers are essential to the sensing and binding of PARP-1 to DNA single and double strand breaks (De Murcia and Menissier de Murcia., 1994). A third PARP-1 zinc finger (not shown) has recently been identified using spectroscopic and crystallographic analysis; its role is not proposed in DNA binding but in the coupling of the activities of the DNA binding and the catalytic domains (Langelier *et al*., 2008). The second domain of PARP-1 is the auto-modification zone which is located centrally within the enzyme (Tao *et al*., 2009). It contains 15 glutamate residues which enable the enzyme to poly(ADP-ribosyl)ate itself. Interestingly, this domain also contains a BRCT motif which is a protein-protein interaction zone that is found in other DNA repair pathways. The third and final domain is the catalytic domain which is located at the C-terminus. It is the most conserved region between species and is aptly referred to as the PARP 'signature' (De Murcia and Menissier de Murcia, 1994). This region acts to bind the substrates of PARP-1 (Kurosaki *et al*., 1987). ADP-ribose tranferase activity is limited to a 40 KDa region at the far C terminus of the enzyme and loss of this 45-amino acid section results in total absence of enzyme activity (Simonin *et al*., 1990).

1.4.2 Functions of PARP-1

One of the main roles of PARP-1 is in the repair of DNA SSBs via the BER/SSBR pathway, as discussed in section 1.2.1. Its other functions are discussed here in particular its role in DNA DSB repair

1.4.2.1 PARP-1 and DSB repair

It has been known for many years that PARP-1 is activated by DSBs (Benjamin and Gill, 1980) but its exact role in their repair is only just emerging. The observations that PARP-1 activity is required to rapidly recruit Mre-11, NBS1 and ATM to sites of DSBs suggest a role for PARP-1 in mediating the HR repair pathway (Haince *et al*., 2007; Haince *et al*., 2008). Furthermore Bryant *et al*. recently published *in vitro* data showing that PARP-1 binds to and is activated by stalled replication forks arising from un-repaired SSBs; PARP-1 acts together with Mre-11 to re-start the collapsed replication fork and enable HR repair of the damaged DNA (Bryant *et al*., 2009).

PARP-1 may also have a function within the NHEJ pathway. For example, work by Ruscetti and colleagues demonstrated that PARP-1 can modify the protein-kinase activity of, the crucial NHEJ protein, DNA-PK (Ruscetti *et al*., 1998). In particular that, in the presence of NAD^+, PARP-1 can ADP-'ribosylate' and stimulate DNA-PK, which can in-turn phosphorylate PARP-1. Consistent with this observation are reports, based on studies using PARP and DNA-PK inhibitors in cells lacking either PARP-1 or DNA-PKcs that PARP-1 co-operates with DNA-PK to repair ionising radiation-induced DSBs (Mitchell *et al*., 2009). Results of other studies have proposed that PARP-1 participates in an alternative 'DNA-PK/Ku independent' NHEJ pathway which may operate as a back-up to the classical pathway. For example, Wang *et al* have shown that PARP-1 directly competes with Ku to bind to DNA DSBs and with the aid of XRCC1 and DNA ligase III is able to repair the damage. This mechanism is however prone to error and the generation of genomic instability (Wang *et al*., 2006).

Further supporting the role of PARP-1 in NHEJ DSB repair is the evidence that the combined use of a PARP-1 and a DNA-PK inhibitor is synergistic in terms of radiosensitization and the fact that inactive PARP-1 inhibits DNA-PK activity and vice versa (Veuger *et al*., 2003; Veuger *et al*., 2004).

1.4.2.2 PARP-1 and gene transcription

Gene expression profiling of *PARP-1* $^{-/-}$ mice cells (Simbulan-Rosenthal *et al*., 1997) and MCF7 human breast cancer cells treated with PARP-1 short hairpin RNAs (Frizzell *et al*., 2009) shows PARP-1 to be implicated in the transcription of many genes. These studies reveal that loss of PARP-1 results in the down-regulation of the expression of multiple

genes which can be divided by their function into four main groups: cell cycle control, DNA damage response, chromosomal processing and assembly and finally, those involved in the response to inflammation and oxidative stress.

1.4.2.3 PARP-1 response to inflammation and capase-independent cell death

Results from several studies have shown that PARP-1 is involved in the inflammatory response to acute conditions such as cerebral ischaemia, septic shock, and myocardial infarction; and in chronic inflammatory diseases such as diabetes mellitus (Oliver *et al*., 1999; Schreiber *et al*., 2006). Over ten years ago, Burkart and colleagues observed that *PARP-1* $^{-/-}$ mice and mice treated with PARP-1 inhibitors were resistant to developing type one diabetes mellitus following exposure to the pancreatic β islet cell toxin Streptozocin. They concluded that NAD^+ depletion caused by the massive over-activation of PARP-1 was the main mechanism behind the islet cell destruction and that this process was blocked in the mice with non-functional PARP-1 (Burkart *et al*., 1999). Studies investigating the response to acute cerebral ischaemia reported that following inflammatory stress or reperfusion large numbers of DNA SSBs were generated by the synthesis of nitric oxide (NO) from endothelial cells and macrophages. These DNA SSBs resulted in over-activation of PARP-1, depletion of NAD^+, generation of free radicals by mitochondria and ultimately necrotic cell death (Szabo and Dawson, 1998). It is now known that in response to inflammation PARP-1 activates the nuclear factor-κB (NF-κB) and the AP-1 transcription factors (Hassa *et al*., 2003). This results in the release of pro-inflammatory mediators including inducible nitric oxide synthase (iNOS) generates NO and reactive oxygen species that cause DNA SSBs. It is proposed that free PAR formed from the over-activated PARP-1 and PARP-2 is somehow transmitted to the mitochondria resulting in a reduction of the mitochondrial membrane potential and the release of apoptosis inducing factor (AIF) and endonuclease G (EndoG) into the nucleus. This, in combination with overwhelming NAD^+ and adenosine tri-phosphate (ATP) depletion, leads to cell death. This process of PARP-1-mediated, capase-independent cell death could be exploited for therapeutic benefit. If PARP-1 could be inactivated either pharmacologically or genetically in acute conditions such as myocardial infarction and acute brain injury or in chronic diseases such as diabetes mellitus in theory it should be possible to reduce the inflammatory response and improve patient outcome.

1.4.3 PARP-1 activity

PARP-1 enzyme activity is reported to be higher in cancer tissue than normal tissue. For example, increased PAR formation compared to levels in adjacent non-cancerous, normal tissue has been documented in colon carcinoma (Hirai *et al*., 1983), hepatocellular carcinoma (Nomura *et al*., 2000), melanoma, basal skin carcinoma (Ikai *et al*., 1980) and in cervical cancer (Fukushima *et al*., 1981). In addition, it has recently been proposed that PARP-1 activity is hyper-activated in *BRCA* deficient cancers (Gottipati et al., 2010) and that this may in part explain the mechanism behind their sensitivity to PARP inhibitors suggesting an over-reliance on the BER/SSBR. Endogenous PARP activity levels have been shown to vary between cancer patients (Zaremba *et al*., 2011) and it has recently been suggested that PARP activity levels may prove a useful biomarker to determine which patients will be sensitive to PARP inhibitor therapy (Redon *et al*., 2010).

1.4.4 PARP-1 expression

The PARP-1 protein is constitutively expressed in all nucleated human cells except neutrophils (Schreiber *et al*., 2002) and higher levels have been reported in cancer tissue compared with non-malignant tissues. For example, significantly higher levels of PARP-1 protein in hepatocellular carcinoma compared to normal liver (Shimizu *et al*., 2004) and increased mRNA PARP-1 levels in early stage colorectal adenocarcinomas *vs*. adenomas (Nosho *et al*., 2006) have been observed.

1.4.5 Genetic factors influencing PARP-1 activity and expression

Changes within the PARP-1 gene are thought to play a role in determining PARP-1 activity, expression and the risk of cancer in humans (Zaremba *et al*., 2009). To date, 66 *PARP-1* single nucleotide polymorphisms (SNPs) have been reported in man (http://snp500cancer.nci.nih.gov). The T2444C SNP results in a valine to alanine (V762A) change in codon 762 of exon 17 (Cottet *et al*., 2000). This amino acid exchange is located within the catalytic domain of the PARP-1 enzyme and is reported to result in a 30-40% reduction in PARP-1 catalytic activity (Lockett *et al*., 2004; Wang *et al*., 2007). The variant form has also been associated with increased risk of prostate cancer (Locket *et al*., 2004), squamous oesophageal carcinoma, lung cancer in Chinese smokers (Hao *et al*., 2004; Zhang *et al*., 2005) and thyroid cancer (Chiang *et al*., 2008). Polymorphisms within the promoter region of the gene may influence PARP-1

expression. For example, a microsatellite polymorphic DNA fragment consisting of a variable number of CA repeats [$(CA)_{11} – (CA)_{20}$] has been identified which may contribute to the regulation of PARP-1 expression (Fougerousse *et al*., 1992; Oei and Shi, 2001).

1.5 The development of PARP inhibitors

It has long been recognised that inhibiting PARP-1 in patients could have great therapeutic potential in the treatment of many diseases such as ischaemic events (cerebrovascular and myocardial infarction), diabetes and cancer. This has been the focus worldwide of over 20 medicinal chemistry programmes with a peak in development between the years 2001 and 2005 (Ferraris, 2010), see figure 1.7.

The first PARP inhibitor, 3-aminobenzamide (3-AB), was identified over thirty years ago following the observation that nicotinamide and 5-methylnicotinamide competed with NAD^+ as a PARP substrate (Purnell and Whish, 1980). 3-AB causes 96% PARP inhibition but requires millimolar intracellular concentrations to achieve this. Furthermore it lacks specificity as it is also inhibits de novo purine synthesis (Milam and Cleaver, 1984).

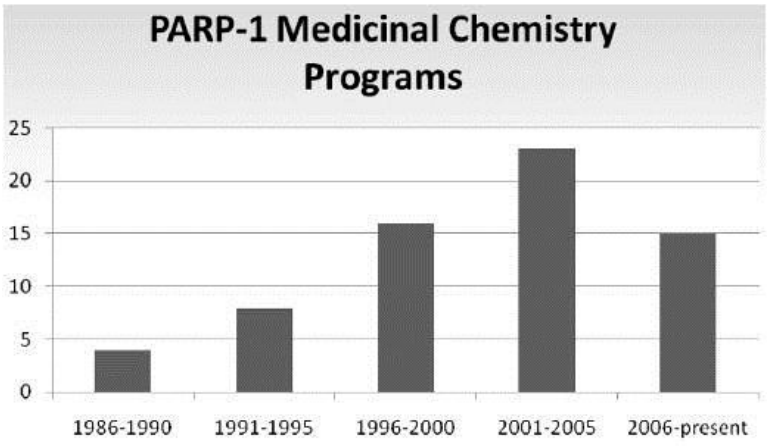

Figure 1.7: Worldwide PARP-1 medicinal chemistry programmes (Ferraris, 2010). Information acquired from the current patent and publication data.

These short-comings in 3-AB led to the development of more potent, more specific inhibitors, which inhibit PARP-1 by the same mechanism: competitive inhibition of NAD^+. In 2003, the first PARP-1 inhibitor entered anti-cancer clinical trials. It was the

potent tricyclic indole PARP-1 inhibitor, AG014699 (Pfizer) (Plummer *et al*., 2008). There are now at least nine PARP-1 inhibitors in anti-cancer clinical trial development, shown in table 1.2. The PARP inhibitory potency of these compounds is indicated by IC_{50} and K_i values. IC_{50} is the concentration required to inhibit PARP activity by 50%; K_i is the dissociation constant of the enzyme. As shown in table 1.2, some of these inhibitors are reported to inhibit PARP-1 *and* PARP-2

1.5.1 AG014699

The studies undertaken for submission of this thesis investigate the role of the PARP inhibitor AG014699. As previously stated, AG014699 was the first PARP inhibitor to enter anti-cancer clinical trials. It was developed by the laboratories of Roger Griffin and Bernard Golding at Newcastle University in collaboration with Cancer Research UK and Agouron Pharmaceuticals (now owned by Pfizer). The structures of the lead compounds discussed below are shown in figure 1.8. In the early 1990s, the initial interest of the Newcastle group was in two core series; the quinazolinones and the benzamidazole carboxamides (from which the clinical candidate was later generated) (Ferraris, 2010). By the late 1990s, it was clear that the benzamidazole carboxamides were the more potent core structures (K_i = 95 nM). The substitution of aryl groups at the para position of this core structure resulted in better interactions with the Tyr889 and Tyr 907 within the nicotinamide binding site of the PARP-1 protein. This led to improved potency of the compound and the generation of the first lead compound – NU1085 (K_i = 6 nM). NU1085 was confirmed to be more potent than previous compounds in its ability to enhance the cytoxicity of temozolomide and topotecan in a panel of human cancer cell lines (Delaney *et al*., 2000). Despite its early promise, NU1085 was found to be poorly water soluble and so the search for a clinical candidate continued. In order to address the issue of aqueous solubility, the groups at Agouron and Newcastle identified a series of [5, 6, 7]tricyclicimidazole lactams. Optimisation of these imidazole lactams led to the discovery of the lead PARP-1 inhibitor - AG014361 (Shalitzky *et al*., 2003). AG014361 shared a feature common to other PARP inhibitors in development at the time, a secondary or tertiary amine, as shown by the light grey circle in figure 1.8 on the compound. It was this amine that was responsible for the improved potency (Ki = 5.8 nM) and water solubility of AG014361. AG014361, at concentrations as low as 0.4 μM, was later shown to potentiate the anti-tumour

effects of temozolomide causing complete tumour regressions in SW620 colorectal cancer cell line xenografts (Calabrese *et al*., 2004). Agouron's final lead candidate, AG014699, emerged from a series of [5, 6, 7]tricyclic indole lactams. AG014699 was selected to be the clinical candidate after it was shown to be the most potent PARP-1 inhibitor in terms of anti-tumour activity in combination with temozolomide in xenograft models, reported to be at least ten times more potent than AG014361 (Thomas *et al*., 2007). AG014699 is the phosphate salt of the tricyclic indole AG014447, with the structure 8-fluoro-2-(4-methylaminomethyl-phenyl)-1,3,4,5-tetrahydro-azepino[5,4,3-cd]indol-6-one illustrated in figure 1.8. AG014699 is a water soluble yellow solid with a molecular weight of 421.36. Crystallographic analysis demonstrates AG014699 binds within the NAD^+ binding domain of PARP via 3 hydrogen bonds. The K_i determined using ^{32}P-NAD^+ incorporation into polymer by purified full-length human PARP, is 1.4 nM.

Metabolism of AG014699 is thought to be predominantly via cytochrome (CY) P2D6, CYP1A2 and CYP3A4 (unpublished data by Pfizer Inc). Pharmacokinetic studies performed as part of the phase I study of AG014699 in cancer patients with advanced solid malignancies have shown the drug to have linear pharmacokinetics with C_{max} at the end of the infusion and a mean terminal half-life of 9.5 hours (Plummer *et al*., 2008). The mean volume of distribution was 212 L indicating extensive tissue distribution with only 11% mean recovery of dose in the urine 24 hours post-dose suggesting that the major route of drug elimination is not renal.

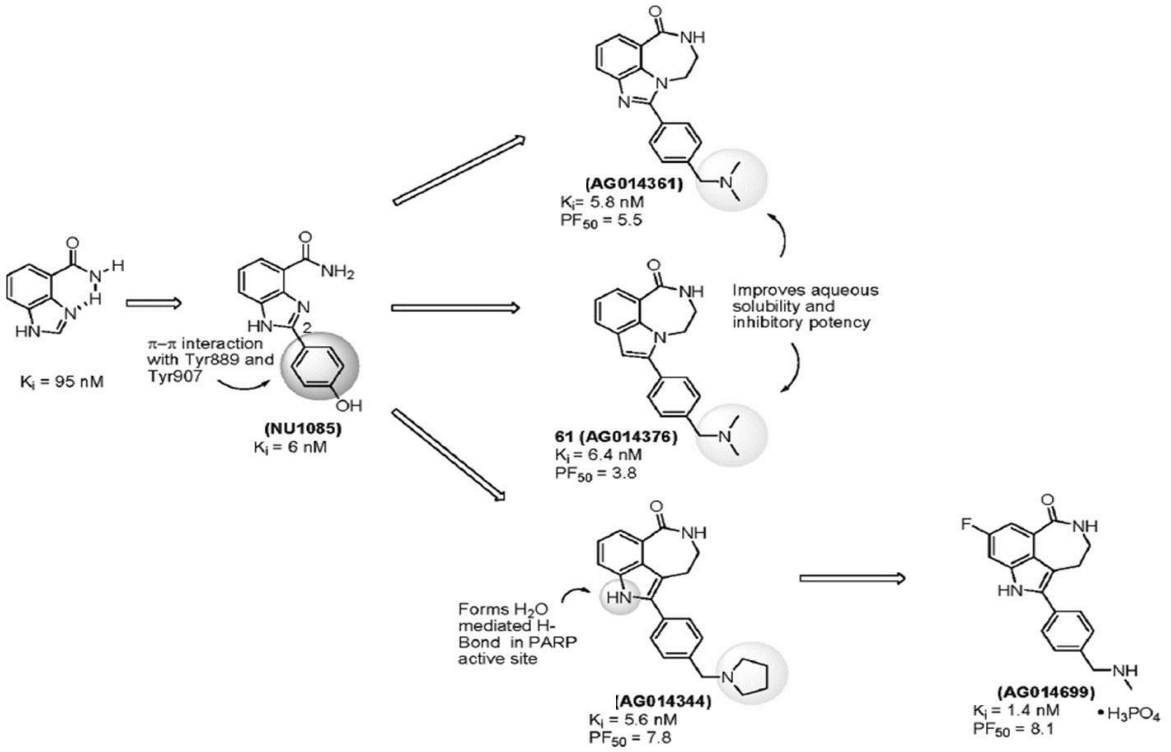

Figure 1.8: The structures of the lead PARP inhibitors developed by Newcastle University and Agouron (adapted from Ferraris, 2010). K_i = dissociation constant of the inhibitor, PF_{50} = potentiation factor at 50% survival.

Agent	Company	Potency	Phase	Therapeutic intention	References
Olaparib (AZD2281)	AstraZeneca	IC_{50} = 5 nM (PARP-1) IC_{50} = 1 nM (PARP-2)	II	*BRCA* mutated breast + ovarian cancer, TNBC, HGSOC, combination with chemotherapy in solid tumours	Fong *et al*., 2009; Tutt *et al*., 2010; Audeh *et al*., 2010; Giaccone *et al*., 2010; Lederman *et al*., 2011
Iniparib (BSI-201)	BiPar	ND	III	Triple negative breast cancer in combination with chemotherapy	O'Shaughnessey *et al*., 2009; O'Shaughnessey *et al*., 2011
Veliparib (ABT-888)	Abbott	K_i = 5.2 nM (PARP-1) K_i = 2.9 nM (PARP-2)	II	Solid tumours, *BRCA* mutated breast and ovarian cancers, MM, brain tumours	Giaccone *et al*., 2010; Ji *et al*., 2010; Kummar *et al*., 2010; Isakoff *et al*., 2010; LoRusso *et al*.,2011
AG014699	Pfizer	K_i = 1.4 nM (PARP-1)	II	MM in combination with TMZ, *BRCA* mutated advanced breast + ovarian cancer	Plummer *et al*., 2006; Plummer *et al*., 2008; Drew *et al*., 2011a
MK-4827	Merck	IC_{50} = 3.2 nM (PARP-1) IC_{50} = 4 nM (PARP-2)	I	Solid tumours, *BRCA* mutated breast + ovarian cancer, TNBC	Schelman *et al*., 2011
INO-1001	Inotek	ND	II	MM in combination with TMZ	Bedikian *et al*., 2009
CEP-9722	Cephalon	IC_{50} = 20 nM (PARP-1) IC_{50} = 6 nM (PARP-2)	I	Advanced solid tumours in combination chemotherapy	
BMN673	Biomarin	ND	I	Advanced solid tumours	
E7016	Eisai	ND	I	Advanced solid tumours in combination chemotherapy	

Table 1.2: PARP inhibitors in anti-cancer clinical trial development, 2011. ND = not determined

1.6 The role of PARP inhibitors in the treatment of cancer

PARP inhibitor development pipelines are pursuing two therapeutic applications: (1) PARP inhibitors as potentiators of chemotherapy and radiotherapy; and (2) PARP inhibitors as single agents, selectively killing cells with defects in DNA repair pathways such as those with *BRCA*1/2 mutations. The pre-clinical evidence to support these two strategies will now be reviewed.

1.6.1 PARP inhibitors as chemopotentiators

1.6.1.1 The monofunctional alkylating agents

The first suggestion that PARP inhibitors could be used in the treatment of cancer as chemosensitisers came from seminal work by Durkacz and colleagues demonstrating that the weak PARP inhibitor 3-AB enhanced the cytotoxicity of DNA methylating agents in mouse leukaemia cells (Durkacz *et al*., 1980). Monofunctional DNA methlyating agents are the most potent activators of PARP-1 (and -2) and they include dacarbazine and temozolomide (TMZ). Both these chemotherapies undergo metabolism within the plasma to the active metabolite 5-(3-methyltriazeno)-imidazole-4-carboxamide (MTIC). MTIC is able to methylate DNA at the O^6- and N^{7-} position of guanine and the N^3 position of adenine (Denny *et al*., 1994), with the most lethal lesion being the O^6-methyl guanine. PARP-1 (and PARP-2) through BER/SSBR are required to repair this damage rapidly. It would therefore seem logical to assume that inhibiting these enzymes results in the increase in the cytotoxicity of MTIC. Evidence to support this are the observations that *PARP-1* knockout mice and cells derived from them are hypersensitive to DNA methylating agents (Menissier de Murcia *et al*., 1997; Masutani *et al*., 2000) and knockdown of PARP-1 in melanomas increases their sensitivity to TMZ, which can further be increased by co-treatment with a PARP inhibitor (Tentori *et al*., 2008; Tentori *et al*., 2010). To date several classes of PARP inhibitors in combination with TMZ have demonstrated potent anti-cancer activity not only in brain tumours and melanomas but a variety of different models. For example, Calabrese and colleagues showed that AG14361, (K_i < 5.8 nM; a fore-runner to the clinical candidate AG014699) enhanced the cytotoxicity of TMZ in the human colon cancer, mismatch repair (MMR)-defective LoVo xenografts by 3-fold and caused

complete regressions in mice bearing human colon cancer MMR-proficient SW620 xenografts (Calabrese *et al*., 2004). Veliparib (ABT-888), a PARP inhibitor currently in clinical evaluation, has been shown to enhance the anti-tumour activity of TMZ in a variety of tumour models including human breast and prostate xenografts; models of metastasis to lung, brain and bone and sub-cutaneous xenografts of ovarian, pancreatic and non small cell lung cancers (Donawho *et al*., 2007, Palma JP *et al*., 2009).

1.6.1.2 The topoisomerase I inhibitors

The topoisomerase 1 inhibitors irinotecan and topotecan (both semisynthetic derivatives of camptothecin) play a major role in the treatment of many cancers including colo-rectal, ovarian and small cell lung cancer. Topoisomerase 1 (TOP1) is an important cellular enzyme which is able to form transient complexes with DNA catalysing the cleavage, unwinding and religation of DNA to reduce the torsional strain caused by transcription and replication. TOP1 cleaves and religates single strands of DNA. The TOP1 inhibitors bind to and stabilise these TOP1 – DNA complexes (cleavable complexes) in their broken state. The collision of a cleavable complex and the advancing replication fork results in the formation of a double strand break and possible cell death. The anti-tumour activity of these inhibitors requires cells to be replicating and TOP1 to be active. In fact, response to the topoisomerase I inhibitors is directly proportional to amount of topoisomerase activity within cells (Pommier, 2006).

As early as 1987 it was shown, in the murine lymphocytic leukaemic cell line L1210, that inhibiting PARP with 3-AB could potentiate the effects of camptothecin (Mattern *et al*., 1987). Following this, Bowman *et al* reported that PARP activity was stimulated by camptothecin in L1210 cells and inhibition of PARP with NU1025 increased both camptothecin-induced DNA breaks and cytotoxicity to a similar extent, suggesting the two events were related (Bowman *et al*., 2001).

In addition the PARP inhibitors NU1025 and NU1085 were shown to increase the cytotoxicity of topotecan up to 5-fold in a panel of human breast, colon, lung and ovarian cancer cell lines (Delaney *et al*., 2000). *In vivo* studies have now confirmed the findings of these *in vitro* studies; the PARP inhibitor AG14361 increased irinotecan-induced tumour growth delay by 2 to 3-fold in human colon cancer xenografts

(Calabrese *et al*., 2004) and the PARP inhibitor GPI 15427 enhanced irinotecan anti-tumour activity in colon cancer models (Tentori *et al*., 2006).

Several mechanisms have been proposed to explain the potentiation of TOP1 poisons by PARP inhibitors. One hypothesis is that PARP is involved in the repair of TOP1 associated DNA damage. AG14361 has been shown to delay the repair of camptothecin-induced DNA breaks and this could not be explained by differences in levels of TOP1 activity as no difference was detected in the nuclear extracts from AG14361-treated compared to control cells (Smith *et al*., 2005). In addition, the Chinese hamster ovary EM9 cell line, which lacks the BER scaffold protein XRCC1, has been shown to be hypersensitive to camptothecin (Caldecott and Jeggo 1991). This suggests that XRCC1 plays a role in the repair of TOP1 inhibitor-induced DNA damage and perhaps PARP-1 participates in this process by recruiting XRCC1 to the site of the TOP1-DNA -associated break.

Another explanation for the potentiation of TOP1 poisons by PARP inhibitors is that PARP inhibitors can in some way modulate the activity of TOP1. PARP-1 is known to poly(ADP-riboslate) TOP1 and down-regulate its activity (Krupitaza *et al*., 1989). Therefore, inhibiting PARP-1 will result in an up-regulation of TOPI, increased DNA breakage and ultimately an increase in sensitivity to topoisomerase I poisons. Supporting this hypothesis is the observation that following DNA damage, poly(ADP-ribosylation) of TOP1 inhibited its activity, or its association with automodified PARP-1, inhibited TOP1 activity. TOP1 was re-activated by 1 mM benzamide (Bauer *et al*., 2001; Yung *et al*., 2004).

1.6.1.3 The platinums

The platinum analogues cisplatin and carboplatin act by covalently binding to DNA to form intra-strand and inter-strand DNA cross-links. These DNA adducts then inhibit DNA synthesis, function and ultimately its transcription. Carboplatin and cisplatin form the backbone of treatment for many cancers including ovarian cancer, small and non-small cell lung cancers, germ cell tumours and head and neck cancers (Chu E and DeVita V., 2010). PARP-1 has recently been identified as a platinum-DNA damage response protein (Zhu *et al*., 2010). However, reports as to whether PARP inhibitors can actually enhance the cytotoxic effects of the platinums are conflicting (Bernges and Zeller, 1996; Nguewa et al., 2006). What is clear from the literature is that any *in*

vitro chemopotentiation seen is cell line dependent. For example, cells lacking homologous recombination function are hypersensitive to cisplatin and PARP inhibition. Synergistic cytotoxicity of the PARP inhibitor AZD2281 (now olaparib) in combination with cisplatin was observed in *BRCA*2-deficient cells, but not with *BRCA*2-proficient cells (Evers *et al*., 2008). In a recent study, triple negative breast cancer cells (TNBC) were hypersensitised to cisplatin and gemcitabine following siRNA knockdown of PARP-1 and this chemopotentiation was not seen in non-TNBC cells (Hastak *et al*., 2010). Results from experiments undertaken for this thesis (presented in chapter four) show that the PARP inhibitor AG014699 enhances the cytotoxicity of carboplatin by 461% in *BRCA*2 defective CAPAN-1 xenografts (Drew *et al*., 2011). The interaction between PARP inhibitors and platinums is still not fully understood but these studies suggest it may be connected to an underlying defect in HR.

1.6.2 PARP inhibitors as radio-potentiators

About a third of all cancer patients will require radiotherapy as part of their treatment (cancerresearchuk.org/cancerstats). Radiotherapy induces DNA damage by multiple mechanisms including base damage and single and double-strand DNA breaks, damage that is dependent on PARP activity for its repair. The idea that PARP inhibitors could be used to improve the efficacy of radiotherapy is over 25 years old. It was in the mid-1980s that one of the first studies was published demonstrating that the 3-AB could enhance the effects of ionising radiation in Chinese hamster cell lines (Ben-Hur *et al*., 1985). Since then, numerous *in vitro* and *in vivo* studies (reviewed in Powell *et al*., 2010) using different classes of PARP inhibitors have shown that PARP inhibitors enhance the cytotoxicity of radiation in a number of tumour types including colorectal cancers (Calabrese *et al.,* 2004) and gliomas (Dungey *et al*., 2009; Russo *et al*., 2009). More recently work by Anthony Chalmers's group has shown that this radio-potentiation is enhanced in rapidly proliferating cells and cells defective in DNA DSB repair compared to normal tissue (Laiser *et al*., 2010). These data support a role for combining radiotherapy and PARP inhibitors in patients with cancer and clinical trials are finally underway (www.clinicaltrials.gov) with results eagerly awaited.

1.6.3 PARP inhibitors as single agents in BRCA-mutated cancers…concept of synthetic lethality

In 2005, two Nature papers reported that cells deficient in *BRCA1* and *2* were 100-1000 -fold more sensitive to PARP inhibitors than *BRCA*1/2 heterozygote or wild type cell lines (Bryant *et al*., 2005; Farmer *et al*., 2005). Bryant *et al.* used the PARP inhibitors NU1025 and AG14361, both forerunners to AG014699. They demonstrated reduced survival of V-C8 (*BRCA*2 deficient Chinese hamster) cell lines after continuous exposure to the NU1025 or 24 hours exposure to AG14361. In mice xenografts, 3 out of 5 V-C8 tumours responded to a 5 day dosing of AG14361 with one mouse showing complete remission and no sign of tumour at autopsy. In addition, they reported an induction in γH2AX foci formation (representing DNA DSBs) and Rad51 foci formation (indicating functional HR repair) in the *XRCC*1 deficient EM9 (Chinese hamster ovary) cell lines. In the V-C8 cells, an increase in γH2AX foci formation but not Rad51 was observed following exposure to NU1025.

In the sister Nature paper, Farmer *et al*. demonstrated the sensitivity of *both BRCA*1 and *BRCA*2 deficient cell lines to the specific inhibition of PARP-1 by two small molecule inhibitors KU0058684 and KU0058948 (Farmer *et al*., 2005). They demonstrated that 24 hours exposure to the PARP inhibitor resulted in permanent G_2/M cell cycle arrest or apoptosis. They also reported a three-fold increase in sensitivity over the DNA damaging agent cisplatin for *BRCA*1/2 deficient cells.

Both groups independently concluded that *BRCA* deficient cells were sensitive to PARP inhibition and that *monotherapy* with a PARP inhibitor could *selectively* kill *BRCA* deficient cancer cells by a mechanism of 'synthetic lethality'.

Synthetic lethality describes the relationship between two genes when loss of either gene i.e. *BRCA or PARP* is viable but loss of both genes i.e. *PARP and BRCA* is lethal (Kaelin, 2005). The proposed mechanism for the synthetic lethality of PARP inhibitors in *BRCA* deficient cells is as follows: PARP inhibition leads to the accumulation of DNA single-strand breaks that result in un-repaired stalled replication forks and ultimately double-strand breaks. These DNA DSBs are normally repaired by the HR pathway (JHJ Hoeijmakers, 2001). In HR-defective cells, i.e. those with *BRCA*1/2 mutations, these DSBs are left un-repaired or are repaired in an error-prone way by alternative NHEJ

DNA repair; both outcomes can result in genomic instability and ultimately cell death. Whereas in cells with functional HR, i.e. those with heterozygous mutations or wild type *BRCA,* DSBs will be accurately and efficiently repaired and inhibiting PARP will not result in cell death. This process is illustrated in figure 1. 9.

The safety of inhibiting PARP in *BRCA* mutant carriers was previously investigated in a study by Drew and colleagues using *BRCA*2 heterozygous (129/C57BL6/DBA) mice (Drew *et al*., 2011b). *BRCA*2 heterozygote mice and wild type controls were treated with either AG014699 (25 mg/kg) i.p. once daily on days 1-5 of a 21 day cycle for six cycles or control saline (10ml/kg) i.p. once daily on days 1-5 of a 21 day cycle for six cycles. Results show, with a follow-up of 365 days, no difference in mean body weight or survival between the four groups suggesting that inhibiting PARP in patients may be safe.

The use of PARP inhibitors to exploit this 'synthetic lethality' in patients with *BRCA*1/2 -mutated cancer is a novel and exciting strategy. It may result in anti-tumour activity without normal tissue toxicity – the ultimate aim of any anti-cancer treatment.

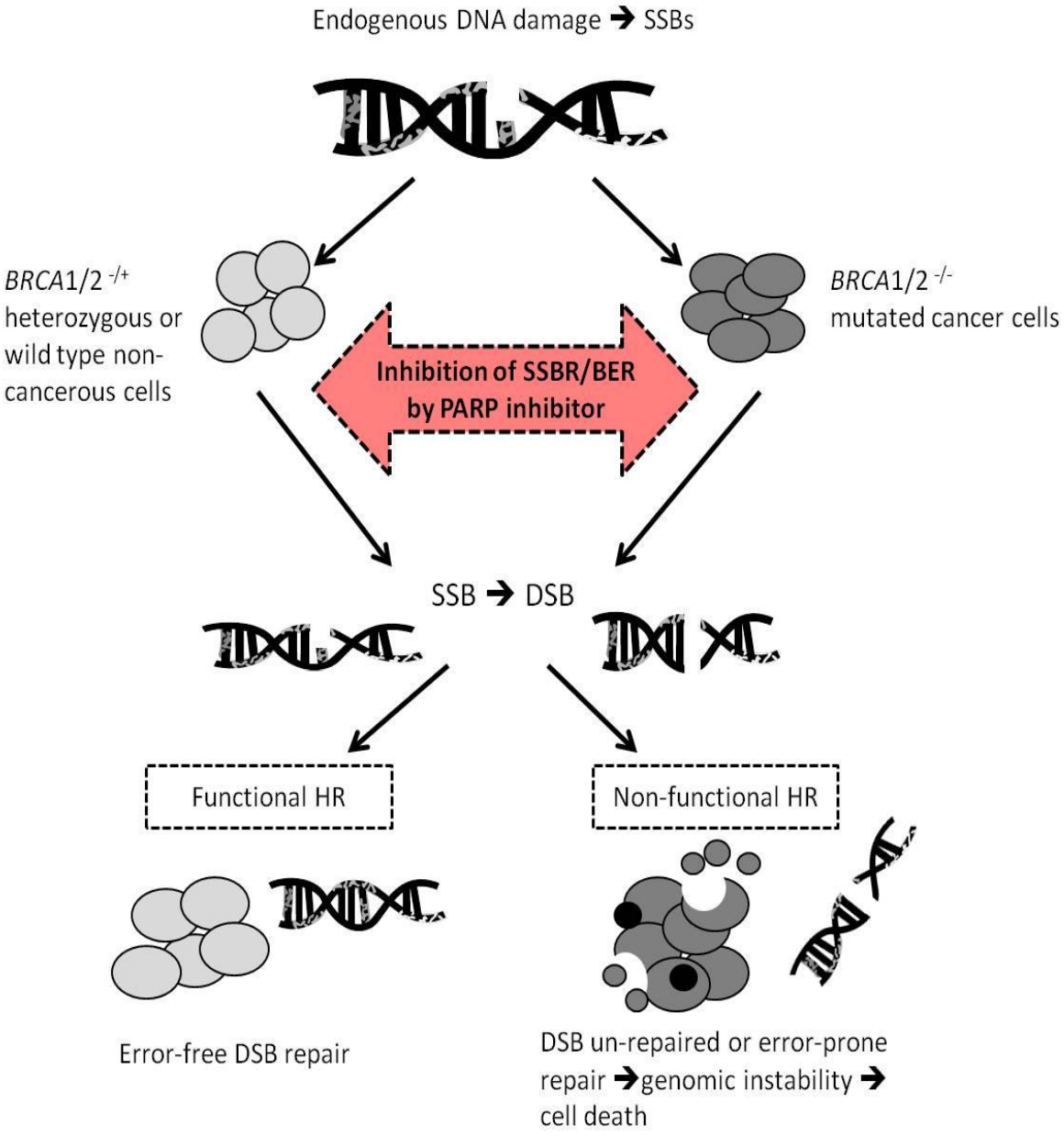

Figure 1.9: Synthetic lethality of PARP inhibitors in *BRCA* deficient cancer cells. SSB = single strand break, SSBR/BER = single strand break repair/base excision repair, DSB = double strand break, HR = homologous recombination

1.6.4 PARP inhibitors as single agents in sporadic HR defective cancers

The majority of cancers are not attributed to hereditary germline mutations in the *BRCA*1 and 2 genes (Venkitaraman, 2002), and so a key question is whether single agent PARP inhibitors can be used to treat patients within the larger cancer population? There is increasing evidence that HR deficiency (HRD) can occur in sporadic cancers resulting in sensitivity to PARP inhibition. For example, it is now known that high grade serous ovarian carcinomas (HGSOC), in addition to mutated *p53* (Bell *et al*., 2005; Ahmed *et al*., 2010), frequently harbour *BRCA*1/2 dysfunction (Hennessy *et al*., 2010; Press *et al*., 2008). Press *et al* reported that germline or somatic *BRCA1 or 2* mutations or epigenetic loss of *BRCA1* (through promoter CpG island methylation) occurred in 60% of high grade serous ovarian cancer cases. Dysfunction of *BRCA1* is also reported in basal-like breast cancers (BLBC) and triple negative breast cancers (TNBC) which are phenotypically similar to *BRCA1* breast cancers with oestrogen receptor negativity and high nuclear grade (Cleator *et al*., 2007; Turner *et al*., 2007; Lee *et al*., 2011). Turner *et al* reported that BLBC have reduced mRNA BRCA1 expression and increased expression of ID4, a negative regulator of BRCA1.

BRCA2 gene methylation is rarely reported but over-expression of the BRCA2 interacting protein EMSY can result in repression of BRCA2 function which may, although this remains uncertain, include its role in HR DNA repair. EMSY over-expression has been observed in up to 13% of breast cancers and 17% of high-grade ovarian cancers (Hughes-Davies *et al*., 2003) suggesting another group which may benefit from PARP inhibition.

Pre-clinical studies have shown that cells lacking other components of the HR pathway such as Rad51, ATR, and CHK2 are sensitive to PARP inhibitiors (McCabe *et al*., 2006). Furthermore mutations within the *ATR* and *CHK2* genes have been reported in some cancers (Swift *et al*., 1991; Miller *et al*., 2002). Cells deficient in the phosphatase and tensin homolog (PTEN) have recently been shown to be sensitive to PARP inhibitors (Mendes-Pereira *et al*., 2009) and *PTEN* is commonly deleted in sporadic cancers with the highest frequencies reported in endometrial cancer (Salmena *et al*., 2008).

Hypoxia within cancer cells drives genomic instability and metastasis and can result in resistance to conventional therapies. It has been reported that hypoxic

microenvironments within cancer cells can lead to reduced expression of essential HR proteins (Bindra et al., 2005; Chan et al., 2008). A recent study by Chan and colleagues demonstrated that this hypoxia-induced HR dysfunction can be exploited by the use of PARP inhibitors (Chan *et al*., 2010). They observed increased cytotoxicity and accumulation of γH2AX and 53BP1 foci in hypoxic cells with the addition of PARP inhibitor; an effect partially reversed by Rad51 over-expression. In addition, hypoxic gassing resulted in growth inhibition of PARP $^{-/-}$ murine embryonic fibroblasts (MEF) but not in PARP $^{+/+}$ MEF cells. *In vivo* studies confirmed this *in vitro* work; tumours from mice treated with PARP inhibitors displayed increased γH2AX and cleaved caspase-3 expression in Rad51-deficient, hypoxic sub-regions; indicating increased DNA damage and apoptosis in a HR-defective environment. This concept that under hypoxic conditions PARP inhibitors can be lethal has been termed 'contextual synthetic lethality'. Given that all cancers are likely to have hypoxic regions this suggests that PARP inhibitors may have an even broader role in the treatment of cancer.

Another mechanism by which cancers could become sensitive to PARP inhibitors is to disrupt their HR repair machinery artificially by the addition of another targeted DNA response/repair agent. The discovery that CDK1-mediated phosphorylation of BRCA1 is required in order for BRCA1 to form repair foci led to the investigation of the effects of combining of CDK1 inhibitors and PARP inhibitors. In a recent study Johnson and colleagues tested the combination of the PARP inhibitor AG014699 and a CDK1 inhibitor (Johnson *et al*., 2011). Following treatment with the PARP-CDK1 inhibitor combination, they observed reduced colony formation and reduced Rad51 formation in *BRCA*- wild type cells and tumour regressions in *BRCA*-wild type xenografts. No increase in toxicity was seen in the mice. Previous studies have shown that PARP inhibitors alone are non-toxic to *BRCA* wild type models (Bryant *et al*., 2005; Farmer *et al*., 2005; Drew *et al*., 2011). However these recent findings suggest that combining PARP inhibitors with CDK1 inhibitors could extend the therapeutic scope into non-*BRCA* mutated cancer populations.

1.7 Results of PARP inhibitor anti-cancer clinical trials

At the time this PhD was instigated there were only two PARP inhibitors in the clinical trial stage of development (AG014699 and olaparib) and no clinical trial results fully published. However, the last 5 years have seen a major leap forward in the development of these novel agents with at least nine inhibitors in various stages of clinical trial development, see table 1.2. The results of any published trials will be reviewed here.

1.7.1 PARP inhibitors in combination with chemotherapy

The pre-clinical data (discussed in section 1.6.1) demonstrating the potent anti-cancer activity in a variety of cancer models of combining PARP inhibitors with the monofunctional, alkylating agent TMZ provided the rationale for the first in-human PARP inhibitor study. The phase I trial of AG014699 in combination with TMZ in patients with advanced solid tumours began at the Northern Centre for Cancer Treatment, Newcastle, UK in 2003 (Plummer *et al*., 2008). In the trial a test dose of single agent AG014699 was given on cycle one D -7 to allow safety, pharmacokinetic (PK) and pharmacodynamic (PD) evaluation of the investigational agent before it was combined with TMZ. The study was driven by a PD end-point which was to establish a PARP inhibitory dose (PID) of AG014699, before attempting to evaluate the maximum tolerated dose (MTD) of the combination. PID was defined as 'the dose of AG014699 at which PARP activity in peripheral blood lymphocytes (PBLs) was reduced to less than 50% of the baseline activity value at 24 hours after the first dose' (Plummer *et al*., 2008). The PID was established at 12 mg/m^2. No dose-limiting toxicities (DLTs) of single agent AG014699 were reported and the DLT of the combination was myelosuppression (a recognised normal tissue DLT of TMZ). Sustained PARP inhibition was demonstrated in PBLs and tumour biopsies; this combination was taken forward into a phase II study in metastatic melanoma. This phase II trial reported enhanced TMZ-induced myelosuppression when combined with PARP inhibitory doses of AG014699 (Plummer *et al*., 2006). A 25% dose reduction in the TMZ to 150 mg/m^2 was therefore required for the regimen to be tolerated. Importantly, the study reported an increase in the response rate and median time to progression compared to historical reports of TMZ alone. These data have yet to be confirmed in a large phase III trial.

Since these first in-human studies, multiple phase I/II trials using different PARP inhibitors with different chemotherapy combinations have recruited patients and some results have been reported in abstract data and are discussed here.

The Phase Ib combination study of the intravenous PARP inhibitor INO-101 (Inotech/Genetech) and TMZ in patients with malignant melanoma reported in 2009 (Bedikian *et al*., 2009). DLTs were myelosuppression and elevated transaminases with the MTD established in combination with full dose TMZ. No PD data were reported so it is not clear what degree of PARP inhibition was achieved and as only 12 patients with metastatic melanoma were treated across the dose ranges it is not possible to comment of any improved efficacy. Interestingly, since these results were published Genentech has suspended further recruitment to this trial and returned the rights for INO-101 to Inotech, who are currently pursuing a role for their PARP inhibitors in retinal diseases (Ferraris, 2010).

The chemo-sensitising potential of the AstraZeneca (AZ) PARP inhibitor, olaparib, is being investigated in a number of on-going combination phase I trials including with: carboplatin, topotecan, dacarbazine, doxorubicin, gemcitabine and irinotecan (www.clinicaltrials.gov). The National Cancer Institute (NCI) sponsored combination study of olaparib with cisplatin and gemcitabine reported DLT of myelosuppression at the first dose level explored. Investigators were subsequently forced to de-escalate to establish tolerable PARP inhibitory doses of olaparib with gemcitabine at 400 mg/m^2 and cisplatin at 40 mg/m^2. The study was undertaken in *non*-heavily pre-treated patients (Giaccone *et al*., 2010). Similarly the phase I combination study of topotecan and olaparib reported DLTs of neutropenia and thrombocytopenia at doses of topotecan 1 mg/m^2/daily for 3 days and olaparib 100 mg twice daily. Further dose levels were not explored due to the myelosuppression (Samol *et al*., 2011). The phase I study of olaparib with dacarbazine also observed neutropenia and thrombocytopenia as DLTs establishing a recommended phase II dose of olaparib 100 mg twice daily with dacarbazine 600 mg/m^2 (Khan et al., 2011).

Preliminary results from four combination studies of the Abbott PARP inhibitor, veliparib (ABT-888), with topotecan, metronomic cyclophosphamide, TMZ or irinotecan have been reported (Ji *et al*., 2010; Kummar *et al*., 2010; Isakoff *et al*., 2010;

LoRusso *et al*., 2011). In the topotecan study, a DLT of myelosuppression was observed at the first dose level and the MTD established with the PARP inhibitory dose was topotecan 0.6 mg/m^2 days 1-5 (Ji *et al*., 2010). The cyclophosphamide – veliparib combination study did not reach MTD and activity was reported in only a small number of *BRCA* mutated ovarian and triple negative breast cancers (Kummar *et al*., 2010). The TMZ – veliparib study investigated efficacy of the combination in metastatic breast cancer and again myelosuppression was seen resulting in a dose reduction of the PARP inhibitor Isakoff *et al*, 2010). In the irinotecan combination study, DLTs were diarrhoea and neutropenia, and a MTD of irinotecan 100 mg/m^2 (LoRusso *et al*., 2011).

A major theme is emerging from these PARP inhibitor-combination studies; enhanced normal tissue toxicity, in particular myelosuppression, is a predictable and common problem. This increased toxicity may limit the dose and choice of chemotherapy used and thus the clinical application of these PARP inhibitor combinations.

1.7.2 PARP inhibitors as single agents in BRCA mutated cancers

The first clinical trials investigating PARP inhibitors as single agents in *BRCA* mutated cancers commenced in 2005. The first to report was the pivotal phase I study of the oral PARP inhibitor, olaparib (Fong *et al*., 2009). The study was conducted in patients with advanced solid tumours (n=60) and enriched for *BRCA1* or *BRCA2* mutation carriers (n=23). Olaparib was well tolerated in all patients, including those with germline *BRCA* mutations. DLTs were myelosuppression and central nervous system side effects with the MTD of 400 mg olaparib twice daily. PARP inhibition was confirmed in surrogate and tumour tissue, and responses were seen in a number of patients with *BRCA* mutations. Anti-tumour activity was reported in both *BRCA1* and *2* mutation carriers which included patients with breast, ovarian or prostate cancer.

Of the 19 evaluable *BRCA* mutation carriers, 12 (63%) had a clinical benefit to treatment (defined as radiologic or tumour marker response or disease stabilisation ≥ four months). Responses were seen in the 100 mg, 200 mg and 400 mg dosing cohorts. No responses were observed in non-*BRCA* mutation carriers. The study incorporated an expansion phase which focused specifically on patients with *BRCA1/2* mutations, and efficacy in a total of 50 patients with ovarian cancer was recently reported, with a clinical benefit rate of 46% (Fong *et al*., 2010). Olaparib was subsequently taken

forward in separate phase II *BRCA*-mutated breast and ovarian cancer studies. Both trials investigated response and toxicity in sequential cohorts of patients, who had progressed following at least one chemotherapy regimen, treated with olaparib 400 mg or 100 mg twice daily (the lowest PARP inhibitory dose with clinical activity from the phase I) on a 28 day cycle. The breast cancer study recruited 54 *BRCA1* or *2* mutation carriers (Tutt *et al*., 2010). In the 400 mg dose group (n=27) an objective response rate (ORR) of 41% (11/27) was seen with a progression free survival (PFS) of 5.7 months. Response rate was lower (22%) in the 100 mg group (n=27). The ovarian cancer study enrolled 57 *BRCA1* or *2* mutation carriers with recurrent epithelial ovarian cancer, primary peritoneal or fallopian tube carcinoma (Audeh *et al*., 2010). In the 400 mg dose group (n=33) ORR was 33% (11/33) and again ORR was lower (13%) in the 100 mg group (n=24) suggesting that the degree of PARP enzyme inhibition may be important. The toxicity profile in both studies was acceptable with the most common toxicities being grade 1 or 2: nausea, vomiting, fatigue and anaemia (ovarian study only). The breast cancer study involved patients who had been heavily pre-treated with chemotherapy and the overall response rate compares well with that seen with standard chemotherapy regimens in the advanced setting (20-30%). The ovarian study included both platinum sensitive and resistant patients and response to olaparib was seen across both groups. It is however important to note that not all patients responded to olaparib and that these are small studies with no randomised control arms and where the two dosing cohorts were not designed to be statistically compared. Furthermore, with any early phase II results, confirmation of these results is needed in larger phase III trials.

These are however proof of concept studies, the first to report single agent activity of a PARP inhibitor in breast and ovarian cancer with defective homologous recombination DNA repair through *BRCA* mutation, which is an exciting breakthrough in the treatment of cancer.

In addition to olaparib there are a number of PARP inhibitors in development for this indication (see table 1.2). Preliminary results of some of these studies have been presented this year at the 2011 American Society of Clinical Oncology (ASCO) annual meeting. A phase I study of the oral Merck PARP inhibitor, MK-4827, in patients with advanced solid tumours enriched for *BRCA* mutated cancers reported a partial

response rate of 20% (12/60) (Schelman *et al*., 2011). The study established a MTD of 300 mg daily continuous dosing. Interim results of the Phase II trial investigating the single agent activity of the PARP inhibitor, AG014699, (Pfizer) in patients with *BRCA*-mutated breast and/or ovarian cancer were also presented at ASCO 2011 (Drew *et al*., 2011a) and are presented in chapter five of this thesis.

1.7.3 PARP inhibitors as single agents in the wider cancer population

The data discussed in section 1.6.5 suggests that there is a wider role for PARP inhibitors in the treatment of cancer. Clinical studies are now underway investigating the efficacy of PARP inhibitors in non-germline *BRCA*-mutated cancers, in particular triple negative breast cancer and high grade serous ovarian cancer.

1.7.3.1 PARP inhibitors and high grade serous ovarian cancers

In order to investigate the role of the oral PARP inhibitor olaparib in non-germline *BRCA* mutant cancers Gelmon *et al* embarked on a four-arm phase II correlative study recruiting (1) HGSOC patients with *BRCA* mutations and (2) HGSOC patients with unknown *BRCA* status (3) *BRCA*- mutated breast cancer and (4) triple negative breast cancer patients with unknown *BRCA* status (Gelmon *et al*., 2011). All patients received continuous olaparib dosing at 400 mg twice daily. All patients underwent *BRCA* mutation testing as part of the study. Results recently reported demonstrated a response rate, as assessed by the Response Evaluation Criteria in Solid Tumours (RECIST), of 24% in the patients with non germline *BRCA* mutated HGSOC. Responses in the confirmed *BRCA* mutation ovarian cancer patients was 41%, similar to that reported in the seminal phase II olaparib study (Audeh *et al*., 2010). Responses were seen in both the platinum sensitive and resistant patients. Interestingly, no responses were observed in the two breast cancer arms of the study which conflicts the data from Tutt *et al* showing that *BRCA* mutated breast cancer is sensitive to olaparib (Tutt *et al*., 2010). The Gelmon study required biopsy samples to be taken before and after olaparib treatment in order to assess *BRCA* mutation status and epigenetic changes to *BRCA1* and these results are eagerly awaited. It should be noted however that this is the *first* study to show single agent PARP inhibitor activity in non-germline *BRCA* mutated cancers, indicating that sporadic high grade serous ovarian cancers could be targeted with PARP inhibitors due to an underlying *BRCA* defect and that accurate sub-classification of these cancers is essential to guide treatment.

The role of PARP inhibitors as maintenance therapy in HGSOC is currently being investigated with interim results of a phase II study recently announced (Ledermann *et al*., 2011). The study randomised patients with platinum sensitive, (defined by the protocol), high grade serous ovarian cancer on a 1:1 basis to olaparib 400 mg twice daily or placebo until disease progression. Preliminary results showed a significant benefit in progression-free survival (8.4 vs. 4.8 months; $P < 0.00001$) favouring the maintenance olaparib. Overall survival data are not yet mature and are awaited.

1.7.3.2 PARP inhibitors and basal-like, triple negative breast cancers

Gene expression profiling has clustered breast cancer into five distinct molecular subgroups, one of which is the basal-like breast carcinoma (BLBC) (Perou *et al*., 2000). The majority lack expression of the oestrogen receptor (ER), progesterone receptor (PR) and HER2/neu receptor. Triple negative breast cancers, by definition, lack ER, PR and HER2/neu expression and make up around 15% of all breast cancers. Although the terms BLBC and TNBC are often used interchangeably, it is important to note that the overlap is not complete. As there is no universal agreement on distinguishing triple negative BLBC from TNBC, clinical trials recruiting patients are likely to be heterogeneous for both groups.

In the phase II study previously discussed Gelmon *et al* reported no single agent activity with the PARP inhibitor olaparib in 15 patients with triple negative breast cancer (Gelmon *et al*., 2011) and at present there is no evidence of *single* agent activity in TNBC using this approach. However, remarkable data were presented at ASCO 2009 of a chemotherapy-PARP inhibitor combination trial, using the PARP inhibitor BSI-201 (now known as Iniparib) in patients with TNBC (O'Shaughnessey *et al*., 2009). This randomised phase II study, recently reported, investigated iniparib in combination with carboplatin and gemcitabine in metastatic TNBC (O'Shaughnessey *et al*., 2011a). The study randomised 120 patients to receive gemcitabine (1000 mg/m^2) plus carboplatin (AUC2) days 1 and 8 +/- iniparib given days 1, 4, 8, 11 of a 21 day cycle. Results showed an increased ORR (52 *vs.* 32%, *p=0.02*), median PFS (5.9 *vs*. 3.6 months, *p<0.01*) and OS (12.3 *vs.* 7.7 months, *p=0.01*) with the addition of the PARP inhibitor. These data represented a significant result in a breast cancer sub-group with limited targeted treatment options. However, what was not clear from the study was the underlying mechanism for potentiation of the chemotherapy response. The original hypothesis

was that iniparib, as a PARP inhibitor, was potentiating the chemotherapy by inhibiting repair of the chemotherapy-induced DNA damage. However, in contrast to other combination studies (discussed in section 1.5.1), no increased toxicity was seen in the iniparib plus chemotherapy arm. At the time this trial was reported it raised many questions about the lack of toxicity. Was the lack of toxicity due to the intermittent dosing of the inhibitor or the lower than standard dose of carboplatin used (AUC2) or that the PARP inhibitor was not enhancing the chemotherapy but acting via independent mechanisms? It may even be possible that the intermittent chemotherapy, by providing exogenous DNA damage is potentiating the PARP inhibitory properties of iniparib. Some of the questions surrounding iniparib were answered earlier this year at ASCO 2011 with the reporting of the phase III study of this combination. In the phase III trial 519 patients were randomised 1:1 to receive gemcitabine (1000 mg/m^2) plus carboplatin (AUC2) days 1 and 8 with or without the PARP inhibitor given days 1, 4, 8, 11 of a 21 day cycle (O'Shaughnessey *et al*., 2011b). Before the results were presented the study team announced that they had new data to confirm that Iniparib was 'not acting as a PARP inhibitor' at the concentrations achieved in the study population and that iniparib acts by arresting cell cycle at the G_2/M checkpoint. The trial also failed to meet its primary endpoint and did not show a significant benefit in terms of improved OS in patients receiving iniparib plus the chemotherapy. Data presented by independent researchers at the same meeting proposed that iniparib has numerous off-PARP targets including inhibition of the enzyme caspase-3 (Maegley *et al*., 2011). What is certain is that the mechanism of action of iniparib is still unclear and requires further investigation and that this study does not add to the case for the use of PARP inhibitors in TNBC.

1.8 Predictive biomarkers for defective HR

It is clear that many cancers harbour defects in the HR DNA repair pathway and that many cancer patients outside of the *BRCA* mutation carrier population could benefit from PARP inhibitor therapy. The problem is how to identify them given the heterogeneous mechanisms by which sporadic cancers can develop defective homologous recombination. The development of assays to determine homologous recombination deficiency (HRD) is the next big challenge for researchers.

Sequencing all cancers for mutations within the individual genes known to be involved in HR is one method. However, this is likely to be costly and time-consuming. It also limits the search to genes already known to be involved in HR and it will not detect HRD secondary to epigenetic silencing. One alternative method is to use gene expression arrays to determine a *BRCA*-like profile in tumours. Konstantinopoulos *et al* identified a 60 gene signature of *BRCA*ness using a publicly available micro-array dataset that included 61 patients with epithelial ovarian cancers including those with germline *BRCA* mutations. In a further 70 patient population enriched for sporadic cancers this *BRCA*ness profile was shown to correlate with response to PARP inhibitors, response to platinums and the ability to form Rad51 foci (Konstantinopoulos *et al*., 2010). More recently, Mulligan *et al* used DNA-microarray technology to profile a cohort of breast cancers enriched for BRCA mutants and thus DNA damage response and HR deficient (Mulligan *et al*., 2011). They were able to identify a 44 gene signature of the DNA damage response deficient molecular subtype. This signature was then validated retrospectively using independent breast cancer data sets and shown to be able to predict response to DNA damaging anthracycline chemotherapy. This method could be useful to predict response to PARP inhibitors.

Another approach is to measure Rad51 foci by immunofluoresence. Based on *in vitro* data presented in chapter three of this thesis, Mukhopadhyay *et al* investigated Rad51 focus formation as a marker of HRD in primary ovarian cancer cell cultures (Mukhopadhyay *et al*., 2010). The inability to form foci following AG014699 was observed in 16 out of 24 cultures and this correlated with *ex vivo* sensitivity to AG014699 with a negative predictive value of 100% and positive predictive value of 93%. These primary cultures were not developed from known *BRCA*1/2 mutation carriers, highlighting again the extent of HRD in the sporadic cancer population.

Another option to measure Rad51 foci is in tumour biopsies after *ex vivo* damage. For example, in a small study Willers and colleagues measured Rad51 foci following *ex vivo* irradiation in core breast cancer biopsies (Willers *et al.,* 2009). No increase in Rad51 foci was seen in four out of the seven cancers suggesting an underlying HRD. Interestingly, three of these tumours were triple negative breast cancers, a phenotype that associated with *BRCA*1 deficiency (Turner et al., 2007). There are problems with these approaches: in the study by Mukhopadhyay *et al* it is the need to obtain viable,

replicating cells; in Willer's study there are technical difficulties in inducing DNA damage *ex vivo*. These assays may not be practical in the normal clinical practice out with a translational study.

In the UK most patients with a confirmed diagnosis of cancer will have had the diagnosis made by immunohistochemistry (IHC) analysis of formalin fixed paraffin embedded (FFPE) tumour blocks. IHC of FFPE tissue is another option to help identify HR defects. This approach is practical in terms of the availability of tumours but maybe very time consuming in terms of the number of proteins that would potentially need to be measured. Nevertheless, expression of BRCA1 by IHC has been shown to correlate with mRNA BRCA1 expression in such FFPE samples and may prove a simple and useful indicator of HR function (unpublished data Dr Judith Carser, Queens University, Belfast). In a recent study by Gottipati and colleagues investigating HR competence in BRCA2 deficient CAPAN-1 cells and PARPi- resistant revertant clones, hyperactivated PARP was observed in the cells with HRD; IHC could be a useful way to detect this (Gottipati *et al*., 2010).

Finally, the use of circulating tumour cells (CTCs) may eventually prove a useful tool in the selection of patients with HRD for PARP inhibitor therapy. For example, induction of γH2AX after treatment with DNA damaging agents has been demonstrated in CTCs and studies evaluating Rad51 foci formation are ongoing (Wang *et al.,* 2010). The advantage of CTCs is that the actual tumour can be assessed rather than surrogate tissues with only minimal invasion such a venepuncture. Such methods are likely to be more acceptable to patients and enable serial measurements of biomarkers before and after treatments.

To summarise many of these assays are still in the early stages of development and some may prove too expensive or too impractical to use. In addition, these assays will require further evaluation and validation within prospective clinical trials before they can be adopted as predictive tools directing treatment decisions in patients.

1.9 Resistance to PARP inhibitors

The results from the reported clinical trials of PARP inhibitors in selected cancer patient populations are encouraging but it is important to note that not all patients respond and most responders eventually develop resistance (Fong *et al*., 2009; Fong *et al*., 2010). While it may seem premature to determine resistance mechanisms early in the development of these novel agents, mechanism-based resistance has frequently been found to occur with targeted therapy as it has with chemotherapy. Understanding why this happens is important if the clinical outcomes of these novel agents are to be improved. Recent studies in cancer cell lines have demonstrated that second mutations in the *BRCA1 or BRCA2* genes can lead to resistance to PARP inhibitors (Edwards *et al*., 2008; Sakai *et al*., 2008; Sakai *et al*., 2009). Secondary mutations may restore *BRCA* function and HR DNA repair in the face of PARP inhibition in order to maintain genomic integrity. Edwards and colleagues developed a model for drug resistance by producing cells from the *BRCA2*-deficient cell line CAPAN-1 that were insensitive to PARP inhibitors (Edwards *et al*., 2008). CAPAN-1 cells are derived from a pancreatic epithelial tumour arising in a carrier of a c.6174delT *BRCA2* frameshift mutation (Goggins *et al*., 1996). They lack a wild-type *BRCA2* and the c.6174delT allele encodes a truncated protein of 2,002 amino acids (approximately 224 kDa), compared with the wild-type 3,418–amino acid protein (approximately 390 kDa). The mutant protein lacks two whole BRC repeats, the DNA binding/DSS1 interaction domain (DBD) and the C-terminus, which contains the TR2 RAD51 binding domain and nuclear localization sequences (Esashi *et al*., 2007). CAPAN-1 cells are thus unable to form damage-induced Rad51 foci and are extremely sensitive to treatment with potent PARP inhibitors (Drew *et al*., 2011; MacCabe *et al*., 2006).

The PARP inhibitor–resistant (PIR) clones developed following exposure to the potent PARP inhibitor KU0058948 by Edwards *et al* were shown to be are highly resistant (>1,000-fold) (Edwards *et al*., 2008). PIR clones are also cross-resistant to the DNA cross-linking agent cisplatin, but *not* to the microtubule stabilizing drug docetaxel.

Platinum chemotherapy is a well-established strategy in the treatment of ovarian cancer, including patients with *BRCA*1 or *BRCA*2 mutations. Clinical observations suggest that *BRCA*1/2 mutation ovarian cancer patients respond better to platinum therapy, in contrast to patients with no family history of the disease, although

resistance does eventually occur (Tan *et al*., 2008). In addition, systemic chemotherapy with the platinums may exert their *BRCA*1/2-selective effects through similar mechanisms to PARP inhibitors. In view of these findings, the *BRCA*2 gene was sequenced in tumours from patients bearing the *BRCA*2 c.6174delT mutation whose ovarian carcinomas were resistant to carboplatin chemotherapy (Sakai *et al*., 2009). These studies revealed deletions in the *BRCA*2 gene, which restored the open reading frame. This suggests that a specific mutation (c.6174delT) in *BRCA2* and sensitivity to therapeutics in cell lines and patients can be reversed by intragenic deletion. Similar results have been reported for *BRCA*1 mutated tumours in patients treated with platinum based chemotherapy (Swisher *et al*., 2008). Although resistance to both platinums and PARP inhibitors can be mediated by secondary mutations, restoring BRCA function, it is likely that the mechanism of resistance is more complex. It is important to note that the clinical data have shown that PARP inhibitor resistance does not equate to platinum resistance. For example, not all platinum-sensitive ovarian cancer patients were sensitive to PARP inhibition and anti-tumour activity was seen in platinum-resistant patients in the first single agent trial of olaparib in *BRCA*1/2 mutation carriers (Fong et al., 2009). However, post-hoc analysis of the data from all 50 ovarian cancer patients treated in this study (including the expansion phase) showed a significantly higher clinical benefit rate (69.2%) in patients who were platinum-sensitive compared to those who were resistant (45.8%) or refractory (23.1%), (Fong *et al*., 2010). It is not clear how much of an issue this will be in clinical practice and we await the results of the on-going studies and the mature data from those already concluded.

2.0 Project aims

This aims of this research project were to investigate through *in vitro*, *in vivo* and clinical studies the effects of the PARP-1 inhibitor AG014699 in human cancers defective in homologous recombination DNA DSB repair. The project focuses particularly on cancers defective in the tumour suppressor genes *BRCA*1 and *BRCA*2. Detailed objectives for each study are found at the beginning of the three results chapters.

Chapter Two

2. Materials and Methods

2.1 General laboratory chemicals and materials

All chemicals were obtained from Sigma (Poole, Dorset, UK) unless otherwise stated. Sterile plasticware for use in tissue culture experiments was supplied by Fisher Scientific (Manchester, UK). The PARP inhibitor AG014699 was supplied by Pfizer GRD (La Jolla, California, USA). AG014699 was dissolved in dimethyl sulfoxide (DMSO) to give a stock solution of 10 mM and stored at -20^0C for *in vitro* studies. For use within *in vivo* experiments it was dissolved in sterile water to give a 1 mg/ml (2.4 mM) solution. The sources of other reagents and materials are described, as appropriate, in the text.

2.2 Good Clinical Laboratory Practice

Laboratory work, undertaken for the phase II PARP-BRCA PH2/052 clinical trial, presented in chapter five, was performed in keeping with the principles of the International Conference on Harmonisation- Good Clinical Practice (ICH-GCP) (www.ich.org). To ensure that these standards were achieved the project work and the laboratory systems were assessed regularly by in-house audits and a two-day study audit by CRUK.

2.3 Culture of cell lines

Cell lines were maintained in exponential growth in tissue culture grade flasks, petri dishes and 6 well plates at 37°C in a humidified incubator atmosphere of 5% CO_2 and 95% air (SANYO; Illinois, USA). All cells were handled separately with their own unique reagents, under sterile conditions, in class II tissue culture cabinets. Cells were cultured in Roswell Park Memorial Institute (RPMI) 1640 media supplemented with 10% foetal bovine serum, penicillin (100 U/ml), and streptomycin (1.0 mg/ml) unless otherwise stated. Adherent cells were brought into suspension for sub-culture by aspirating off the medium, washing twice with phosphate buffered saline (PBS), followed by five

minute incubation with 0.25% trypsin solution in PBS. Cell cultures were confirmed mycoplasma negative by regular testing using the MycoAlert mycoplasma detection kit (Lonza; Rockland, Maine, USA).

2.3.1 Cell lines

A panel of 11 cell lines, including nine human cancer cell lines, with differing HR repair status were selected for use within the *in vitro* experiments presented in chapter three. These cell lines have been subsequently authenticated by an in-house NICR programme. Details for each cell line are provided below and a summary is provided in table 3.1 of chapter three to aid interpretation of results. In addition to these cell lines two cell lines were cultured for use within PD assays. The mouse lymphocytic leukaemic cell line, L1210, was used as quality control (QC) samples for the PARP activity assay described in section 2.9. The human lymphoblast cell line, K562, was used for QC samples for the PARP-1 expression assay described in section 2.10. Both L1210 and K562 are grown in suspension in RPMI 1640 media supplemented with 10% foetal bovine serum, penicillin (100 U/ml), and streptomycin (1.0 mg/ml) and originally supplied by the American Type Culture Collection (ATCC).

2.3.1.1 MCF7

Breast adenocarcinoma cells derived from the pleural fluid of a 69 year old Caucasian female. *BRCA* 1 hemizygous/*BRCA*2 wild type, *p*53 wild type and oestrogen receptor positive adherent cells with a doubling time of approximately 28 hours. Original supplier: ATCC (Manassas, Virginia, USA).

2.3.1.2 MDA-MB-231

Breast adenocarcinoma adherent cell line derived from the pleural fluid of a 51 year old Caucasian female. It is hemizygous for *BRCA*1 and the remaining non-mutated allele contains two non-pathogenic single-nucleotide polymorphisms. Original supplier: ATCC.

2.3.1.3 MDA-MB-436

Breast adenocarcinoma adherent cell line derived from the pleural fluid of a 43 year old Caucasian female. *BRCA*1 mutated (5396 +IG>A), *BRCA*2 wt type (Elstrodt *et al*., 2006). An adherent cell line grown in RPMI 1640 –Leibovitz medium (50:50 vol/vol)

supplemented with 4 mM L-glutamine, 10% fetal bovine serum, penicillin (100 U/ml) and streptomycin (1.0 mg/ml). Original supplier: ATCC.

2.3.1.4 HCC1937

Primary breast carcinoma adherent cell line derived from 23 year old Caucasian female. Mutated *BRCA*1 (5283insC), wild type for *BRCA*2 (Tomlinson *et al*., 1998), oestrogen and progesterone receptor negative. Original supplier: ATCC.

2.3.1.5 HCC1937 – BRCA1

Primary breast carcinoma adherent cell line derived from 23 year old Caucasian female (HCC1937) with transfected wild type *BRCA*1 (Tassone *et al*., 2003). Original supplier: ATCC.

2.3.1.6 UACC3199

Primary breast carcinoma, adherent cell line with ≥ 60% *BRCA*1 promoter methylation, which has been shown to result in reduced *BRCA*1 gene copy number and chromosome 17 aneusomy as observed in *BRCA*1 mutated breast cancer cells (Wei *et al*., 2005). Cell line obtained from the University of Arizona Cancer Research Centre, Tucson, USA. The methylation status of *BRCA*1 in these cells was confirmed by Valerie Deregowski (University of Leuven, Belgium) by methylation-specific polymerase chain reaction.

2.3.1.7 CAPAN-1

Pancreatic adenocarcinoma cells derived from liver metastasis of a 40 year old Caucasian male. *BRCA*2 mutated (6174 delT allele encoding truncated BRCA2 protein; other BRCA2 allele is lost), *BRCA1* wt type (Goggins *et al*., 1996). Adherent cell line grown in RPMI 1640 media supplemented with 15% foetal bovine serum, penicillin (100 U/ml), and streptomycin (1.0 mg/ml). Original supplier: ATCC.

2.3.1.8 OSEC1

Immortalized human ovarian surface epithelial, adherent cell line; heterozygous for the *BRCA*2 mutation 4630insA and wild type for *BRCA*1. Both OSEC cell lines were provided by Richard Edmondson and immortalised with the catalytic subunit of

telomerase (hTERT) and a temperature-sensitive form of SV40 large T antigen (unpublished data Richard Edmondson, Newcastle University, UK).

2.3.1.9 OSEC2

Immortalized human ovarian surface epithelial, adherent cell line; wild type for both *BRCA*1 and 2 (Davies *et al*., 2003).

2.3.1.10 AA8

Chinese hamster ovary cell line wild type for *XRCC*3 (Pierce *et al*., 1999); provided by Prof Penny Jeggo at the University of Brighton, UK.

2.3.1.11 IRS-1SF

Chinese hamster ovary cell line deficient in the HR gene *XRCC*3 (Pierce *et al*., 1999); provided by Prof Penny Jeggo at the University of Brighton, UK.

2.4 Preparation of clinical samples from the phase II BRCA-PARP trial

2.4.1 Preparation of peripheral blood lymphocytes from whole blood for pharmacodynamics assays

Peripheral blood lymphocytes (PBL) were extracted from whole blood for analysis of PARP-1 activity and expression. For PARP-1 activity blood samples (10 ml x 4 or x 8 for stage one patients) were collected on day (D)1 prior to treatment, at the end of infusion, 4 hours post and 24 hours post AG014699 (which is the D2 pre-dose sample). For assessment of PARP-1 expression a single 10 ml whole blood sample was taken within two weeks prior to starting AG014699. Blood was collected into potassium ethylenediaminetetraacetic acid (EDTA) vacutainer tubes (BD, Oxford, UK), stored immediately on ice and PBL isolated by lymphopreparation using pre-prepared Lymphoprep™ tubes (Axis-shield; Cambridgeshire, UK) within one hour of sampling. Each Lymphoprep™ tube contains 10 ml of Lymphoprep™ solution contained below a porous membrane disc. 10 ml of chilled PBS was freely added to the Lymphoprep™ tube followed by 10 ml of whole blood. The tube is then centrifuged for 10 minutes (min) at 1100 relative centrifugal force (RCF) in a horizontal rotor (swing-out head) centrifuge at 4°C. After centrifugation, the PBL cells form a distinct band at the sample/medium interface. This band of PBL was then collected from the interface

using a Pasteur pipette (Axis-shield; Cambridgeshire, UK) and transferred to a 50 ml Cellstar tube (Greiner Bio-one; Gloucestershire, UK) and placed on ice. The PBL were then diluted by the addition of 20 ml of ice cold PBS and centrifuged for 10 min at 500 RCF in a horizontal rotor (swing-out head) centrifuge at 4°C. The supernatant was then discarded and the cell pellet re-suspended in 2 ml of pre-chilled freezing medium consisting of RPMI1640 medium supplemented with 10% foetal calf serum, 10% DMSO and x1 strength Halt protease inhibitor cocktail (Pierce; Illinois, USA). Finally, the PBL are then placed in 2 separate 1.8 ml cyrotubes (Nunc, supplied by Fisher Scientific; Loughborough, UK) and stored at –70^{o}C prior to use.

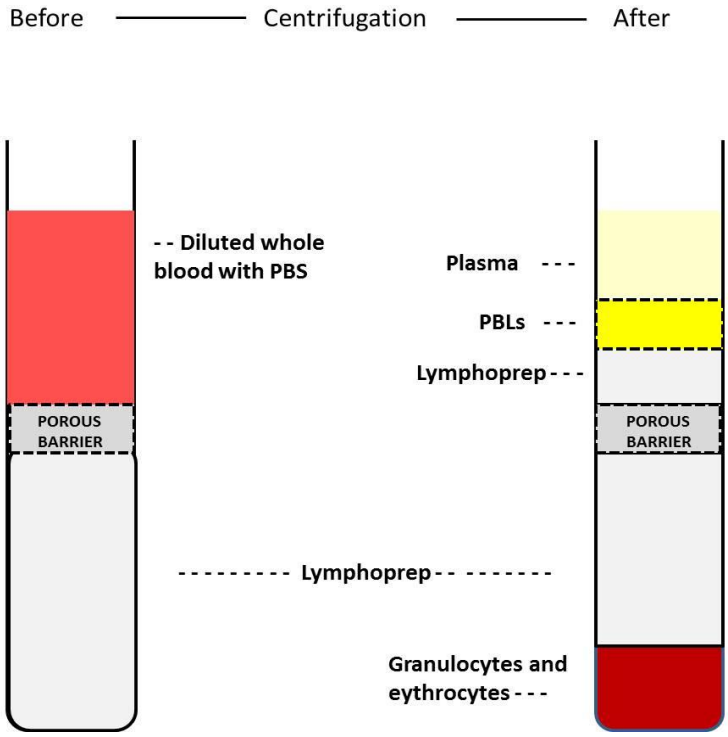

Figure 2.1: Extraction of peripheral blood lymphocytes (PBL) from whole blood using Lymphoprep™ tubes.

2.4.2 Preparation of plasma from whole blood for pharmacokinetic assay

Blood samples (5 ml x 9 or x 18 for stage one patients) were collected at the following time-points: D1 pre-AG014699, end of infusion, 1-3 hours post AG014699; D2 pre-AG014699; D4 pre-AG014699, end of infusion, 1-3 hours post AG014699 and D5 pre-AG014699 and D5 end of infusion. Blood was collected into heparinised vacutainer tubes (BD, Oxford, UK) and plasma separated within 30 min of sampling by

centrifugation at 1000 RCF at room at 4°C. The plasma supernatant was removed and separated into 2 x 1 ml samples and stored in 1.8 ml cyrotubes (Nunc, supplied by Fisher Scientific; Loughborough, UK) at - 20^{o}C prior to use.

2.4.3 DNA purification from whole blood for genotyping assays

For each patient a single sample of whole blood (5 ml) was collected into potassium ETDA vacutainer tubes (BD, Oxford, UK) and stored at – 20^{0}C prior to use. Samples were then thawed at room temperature and DNA extracted using the QIAamp DNA Blood Maxi (50) kit, (Qiagen; West Sussex, UK). The concentration (ng/µl) of the eluted DNA was determined using the Nanodrop N-D 1000 spectrophotometer system (Nanodrop Technologies; Delaware, USA) operating on Nanodrop 3.0.1 software. DNA aliquots were then stored as working and stock solutions at 4^{0}C and – 20^{0}C respectively. Working stock solutions were diluted using ultra-high purity (UHP) sterile water to give a concentration = 10 ng/µl.

2.5 Clonogenic cell survival assay

2.5.1 Background principles

The clonogenic cell survival assay allows a measurement of cell survival after exposure to pharmacological agents. The assay measures viable cells that have undergone at least 5-6 rounds of replication to produce a colony and have therefore survived the drug exposure. All cell lines listed in section 2.3.1 (with the exception of the HCC1937 and HCC1937-BRCA1) were used in this assay.

2.5.2 Assay

Exponentially proliferating cells were plated into six-well plates and incubated for 48 hours to allow cells to reach their optimum proliferation rate. AG014699 at 0, 0.1, 1.0, 10.0, 30.0, 50.0, or 100 µM in 1% DMSO was added to the wells and incubated for 24 hours. Control cells received no AG014699 but were treated with medium containing 1% DMSO for 24 hours. Cells were harvested and cultured in drug-free medium in 90-mm Petri dishes for up to 21 days, depending on the proliferation rate of the individual cell line. Colonies were fixed in methanol and acetic acid (3:1 vol/vol), stained with methyl violet 10B, and counted with an automated colony counter (Oxford Optronix; Oxford, UK).

2.5.3 Analysis of results

Data are expressed as the percentage of colonies in AG014699-treated cultures compared with that in control cultures. The concentration that results in death of 50% of cell population (LC_{50}) was calculated for each cell line in each independent experiment. Each assay contained triplicate samples for each concentration. Results represent data from at least three independent experiments. Graphs were produced and statistical analysis performed using the GraphPad prism software version 4.0 (GraphPad Software Inc; La Jolla, California, USA)

2.6 Sulforhodamine B Assay for Cell Growth Inhibition

2.6.1 Background principles

The HCC1937 and HCC1937-BRCA1 cell lines have poor cloning efficiency and were not appropriate for the clonogenic cell survival assay. As an alternative, cell growth inhibition was measured using the sulforhodamine B (SRB) protein dye assay (Vichai and Kirtikara, 2006). This assay determines cell density by measuring cellular protein content. Adherent cells are incubated in 96-well plates for a given period of time in media containing a range of concentrations of the drug under investigation. Cell monolayers are then fixed in trichloroacetic acid and stained for 30 minutes in SRB protein dye. After removal of excess dye the protein-bound dye is dissolved in a Tris-base solution ready for optical density determination (at 520 nm) using a microplate spectrophotometer system. This method enables large numbers of samples to be investigated in a short period of time. In addition to the HCC1937 and HCC1937-BRCA1 cell lines, the MDA-MB-231 cells were also evaluated with this assay so that a direct comparison could be made between results from the clonogenic survival assay and the SRB assay.

2.6.2 Assay

Cells were seeded into 96-well plates at 2000 cells per well and allowed to attach overnight. AG014699 at 0.0, 1.0, 10.0, 30.0, 50.0, or 100 µM in 1% DMSO was added, and cells were incubated for 120 hours at 37°C, fixed in 50% (wt/vol) trichloroacetic acid, and stained with 0.4% SRB solution (diluted in 1% acetic acid) for 30 minutes. Absorbance of sulforhodamine B was measured at 520 nm with a SpectroMax 250

microplate spectrophotometer system (MDS Analytical Technologies; Toronto, ON, Canada) to determine cell density.

2.6.3 Analysis of results

The concentration required to produce 50% inhibition of cell growth (GI_{50}) based on absorbance measurement was calculated for each cell line in each independent experiment. Each assay contained triplicate samples for each concentration. Results represent data from at least three independent experiments. Graphs were produced and statistical analysis performed using the GraphPad prism software version 4.0 (GraphPad Software Inc, La Jolla, California, USA)

2.7 DNA Double strand break determination by γH2AX immunofluorescence assay

2.7.1 Background Principles

H2AX is one of three types of histone H2A molecules found in eukaryotic cells. Phosphorylation by ATM or DNA-PK of H2AX is an early step in the cellular response to DNA DSBs. Within 1-3 minutes of a DSB the unique carboxy-terminal tail of H2AX serine 139 is phosphorylated forming γH2AX foci (Rogakou *et al.,* 1998). The γH2AX foci localise to sites of DSBs and one γH2AX focus is thought to correspond to one DSB within the cell nucleus (Rogakou *et al.,* 1999, Paull *et al.,* 2000). This assay uses immunocytochemistry to detect the γH2AX foci. A primary antibody specific to γH2AX is used, this is then combined with a secondary fluorescent antibody and a DNA counter-stain to allow the nucleus of each cell to be visualised by microscopy.

2.7.2 Cell preparation and assay

Cells were grown to 50-70% confluence to the day of experiment on sterile circular glass cover-slips (22 mm diameter, 1 mm thickness) in 60 mm petri dishes. For cells exposed to AG014699; the medium was aspirated and replaced with medium containing, at final concentration, 1 or 10 µM AG014699 at time zero on the day of experiment. Cells were then incubated for 24 hours at 37^0C. Cells treated with X-ray irradiation were irradiated with 2 Gy (2.5 Gy/min at 310 kV, 10 mA) using the Gulmay Medical RS320 Irradiation system (Gulmay Medical Limited; Surrey, UK). Ionising

radiation was used as a positive control in all experiments. Cells were returned to the incubator for the described length of time before fixation. The cover-slips containing cells were then washed twice in 2 ml cold PBS in 6 well plates and subsequently fixed in chilled 100% methanol at -20^0C for 10 min. The cells were then re-hydrated by washing in PBS for two 10 minute washes. Fixed control, AG014699-treated, or irradiated cells then were blocked for 1 hour at room temperature in KCM buffer (120 mM KCl, 20 mM NaCl, 10 mM Tris–HCl at pH 8.0, 1 mM EDTA, 0.1% Triton X-100, 2% bovine serum albumin, and 10% milk powder). The cells were then incubated overnight at 4^0C in Upstate primary mouse monoclonal IgG_1 anti-phospho-histone H2A.X Ser 139, clone JBW301 antibody (Millipore; Billerica, Massachusetts, USA) diluted 1:400 in the KCM blocking buffer described above. Following incubation with the primary antibody the cover-slips were transferred to 6 well plates and washed in KCM with 0.1% (v/v) Triton X-100 for three 10 minute washes on a platform shaker. Next the cover-slips were incubated in the dark for 1 hour at room temperature in secondary fluorescent antibody Alexa Fluor 546 goat anti-mouse IgG (Invitrogen; Paisley, UK) diluted 1:200 in blocking buffer. Cells were then washed as described above in KCM with 0.1% (v/v) Triton X-100 but shielded from light and with the addition of one extra 5 min wash. Following this cover-slips were mounted onto slides using Vectorshield hard set mounting medium with DAPI (Vector Laboratories; Peterborough, UK), which counter-stains the DNA.

2.7.3 Analysis

Images were obtained using Leica DMR microscope and RT SE6 Slider camera Advanced Spot software version 3.408 (Diagnostic Instruments Inc; Sterling Heights, Michigan, USA). γH2AX foci were manually quantified in 30 nuclei from three different areas of each treatment slide. This method of quantification has been shown to be reliable and reproducible (Mukhopadhyay *et al*., 2010). Graphs were produced and statistical analysis performed using the GraphPad prism software version 4.0 (GraphPad Software Inc, La Jolla, California, USA)

2.8 Rad51 focus formation immunofluoresence assay

2.8.1 Background Principles

As already discussed in chapter one section 1.2.4 the Rad51 recombinase protein, structurally related to the E. coli RecA protein, is a pivotal player in the HR DSB repair pathway. In response to DNA damage Rad51 forms nuclear complexes that can be detected using microscopy as individual foci. These foci are seen at high levels in cells with intact HR pathways following damage with ionizing radiation (IR) and co-localise over time with sites of H2AX phosphorylation at the sites of DNA damage (Paull *et al*., 2000). Thus the formation of Rad51 foci following DNA damage could serve as a biomarker of HR function and to be able to quantify them could enable HR proficient and deficient cells to be identified.

2.8.2 Cell preparation and assay

The method used was similar to the γH2AX immunofluoresence assay with the following changes: Primary antibody used was anti-Rad51 rabbit polyclonal antibody (Calbiochem; Merck Serono Ltd, Middlesex, UK) diluted 1:400 with blocking buffer and incubated overnight at 4^0C. Secondary antibody used was Alexa Fluor 488 goat anti-rabbit IgG (Invitrogen; Paisley, UK) diluted 1:100 in blocking buffer and incubated in the dark for two hours at room temperature. For all assays the concentration of AG014699 was 10 µM and dose of IR treatments was 2 Gy.

2.8.3 Analysis

Images were obtained using Leica DMR microscope and RT SE6 Slider camera with Advanced Spot software version 3.408 (Diagnostic Instruments Inc; Sterling Heights, Michigan, USA). Rad51 foci were manually counted in 30 nuclei from three different areas as described above. Graphs were produced and statistical analysis performed using the GraphPad prism software version 4.0 (GraphPad Software Inc, La Jolla, California, USA).

2.9 PARP activity assay

2.9.1 Background principles

PARP activity after treatment with AG014699 is measured using the GCP validated immunoblot PARP assay used in the Phase I and II clinical trials of AG014699 in combination with TMZ (Plummer *et al.,* 2006, Plummer *et al*., 2008). The assay measures PARP activity by quantifying the amount of PAR synthesized during a maximum PARP enzyme stimulation step in which cells are exposed to blunt-ended oligonucleotide in the presence of excess NAD^+ for a six minute period. The oligonucleotide simulates DNA strand breaks. The reaction is then stopped by the addition of an ice-cold concentrated AG014699 'stop solution'. Samples are subsequently placed on ice. A known number of cells (between 2000 and 10,000) are then blotted onto a membrane which is then exposed to a primary anti-PAR antibody. Bound primary antibody is subsequently exposed to secondary antibody conjugated to horse-radish peroxidise. On exposure to chemiluminesence detection reagent, light is emitted from areas of the blot containing the primary-secondary antibody complexes in proportion to the amount of PAR present. This chemiluminescence is detected and expressed as 'luminescent arbitrary units' (LAU). It is important to note that this LAU value reflects the PAR produced during the reaction step *plus* the PAR already present in the cell prior to the assay. Therefore for each sample a control sample of un-reacted cells is also loaded onto the immunoblot. The LAU value for these control samples is then subtracted from the former result to give the maximum-stimulated PARP activity for the cells. During the validation of this assay a large inter-assay variability was observed (unpublished data Dr Chris Jones, Newcastle University, UK), making it questionable to compare PARP activity directly between blots using the LAU values. To combat this and standardise results between assays the following serially diluted standards of PAR: 25, 5, 1, 0.2, 0.04 and 0 pmol ADP-ribose monomer are loaded onto the immunoblot at the same time as the cell samples. In addition, for the clinical trial, each individual patient's samples were run on the same blot in order to assess changes in PARP activity accurately over time following AG014699.

2.9.2 Buffers and solutions

The isotonic buffer comprised of 36 mM Hepes, 130 mM potassium chloride, 0.57 mM dextran, 2.0 mM ethylglyceroltetraacetic acid (EGTA), 2.31 mM magnesium chloride and 223 mM sucrose all dissolved in distilled water and pH adjusted to 7.8. The solution was then stored at 4^0C and given an expiry date of three months. The reaction buffer consisted of 100 mM Tris.HCl and 120 mM magnesium chloride dissolved in distilled water and pH adjusted to 7.8. The solution was stored at 4^0C and given an expiry date of three months. Tris/ Ethylenediaminetetraacetic acid (EDTA) solution comprised of 10 mM Tris and 1 mM EDTA dissolved in distilled water; stored at room temperature for a maximum of three months. The stop solution was prepared fresh on the day of each experiment by diluting 25 µl of 10 mM AG014699 into 20 ml of PBS to give a 12.5 µM AG014699 solution. This was then stored on ice until required in the assay. Blocking buffer again made fresh on the day of the assay consisted of PBS with 5% Marvel milk powder (Premier Foods; St Albans, Hertfordshire, UK) and 0.05% Tween-20.

2.9.3 Preparation of 7 mM NAD^+

2.5 mg of solid NAD^+ (stored at -20^0C) was weighed on the day of experiment and dissolved in 500 µl of distilled water. A 10 µl aliquot of this solution was diluted further 1:100 with distilled water, transferred into a silica cuvette and the optical density read at 260 nm against a control of distilled water using the Lambda 2 Spectrometer (Perkin Elmer; Fremont, USA). The molarity of the stock solution was calculated using the equation: 1 mM = 18 OD (optical density). The stock solution was subsequently diluted in distilled water to give a 7 mM solution.

2.9.4 Preparation of oligonucleotide

A pellet of synthesised oligonucleotide with the sequence CGGAATTCCG (Invitrogen; Paisley, UK) was dissolved in 10 mM Tris/EDTA and heated to 60^0C in a water bath. Re-annealing of the DNA was achieved by cooling the solution to 24^0C by 1^0C per minute by the addition of ice to the water bath. The solution was then diluted 1:50 with Tris/EDTA and the optical density read at 260 nm against a blank cuvette containing Tris/EDTA. 1 optical density is equal to 50 µg/ml double stranded oligonucleotide. Using this calculation the original oligonucleotide solution was diluted with 10 mM

Tris/EDTA to give a 200 µg/ml solution. The solution was then transferred to microtubes in 250 µl aliquots and stored at -20^{0}C. On the day of experiment one aliquot was thawed at room temperature and then stored on ice until required.

2.9.5 Preparation of PAR standards

Purified PAR, branched and linear polymers of an average 25 (3-300) monomers, (Biomol; Plymouth Meeting, Pennsylvania, USA) was supplied as a 10 µg/ml solution where 1 µg is equivalent to 1850 pmol of ADP-ribose monomer and stored at -80^{0}C. On the day of the experiment one aliquot of PAR was thawed at room temperature and 292 µl of distilled water added resulting in a 25 pmol ADP-ribose monomer/100 µl solution. This was then serially diluted in 200 µl distilled water to give the following standards: 25, 5, 1, 0.2, 0.04 and 0.00 pmol. 100 µl of each standard was then mixed with 300 µL PBS. For the zero PAR standard 100 µl of distilled water was mixed with PBS. These standards were stored on ice until needed.

2.9.6 Preparation of cell line samples

Cells were grown to 50-75% confluence on the day of experiment in 35 mm x 10 mm Petri dishes containing 10 ml of media. For each cell line the following treatments were compared: no treatment (DMSO control) and 10 µM AG014699. On the day of experiment medium was aspirated and replaced by medium containing 10 µM AG014699 or DMSO for the no treatment control samples. Cells were then incubated in this medium for 30 minutes. Following this, cells were washed in PBS x 2, trypsinised, re-suspended in 10 ml of medium in universal containers and centrifuged at 500 g for 5 min at 4^{0}C. The media was then aspirated and the cell pellet placed immediately on ice. The cell pellet was then re-suspended in 20 ml ice-cold PBS and centrifuged at 500 g for 5 min at 4^{0}C twice. The supernatant was discarded and the cell pellet re-suspended in 50 µl of ice-cold 0.15 mg/ml digitonin for 5 minutes to permeabilise the cells. 450 µL of ice-cold isotonic buffer was then added to the permeabilised cells. Permeabilised cells were then counted using an improved Neubauer haemocytometer (Weber Scientific, Teddington, UK) after diluting 6 µl of cell suspension 1:1 with trypan blue. The cell suspensions were then diluted using isotonic buffer to give a final concentration of between 2000-10,000 cells per 60 µl and placed back on ice.

2.9.7 Preparation of clinical trial samples

Extraction of peripheral blood lymphocytes (PBL) from whole blood for use within this assay is described in section 2.4.1. On the day of the experiment the relevant patients' PBL were removed from -80^{0}C storage and thawed at room temperature. The sample was then transferred into a clean eppendorf and centrifuged at 500 g for 5 minutes at 4^{o}C. The supernatant was removed and discarded and the cell pellet re-suspended in 1 ml of ice-cold PBS. After vortexing the sample was then centrifuged again at 500 g for 5 minutes at 4^{o}C. The supernatant was discarded and the cell pellet re-suspended in 1 ml of ice-cold PBS and washed and centrifuged again as above. Following the second wash the supernatant was discarded and the cell pellet re-suspended in 50 µl of ice-cold 0.15 mg/ml digitonin for 5 minutes to permeabilise the cells. The next steps were identical to that described above for the cell line preparation, resulting in a cell suspension of PBL of between 2000-10,000 cells per 60 µl. This was then placed back on ice and used within one hour of preparation.

2.9.8 Quality control samples

As described in section 2.3.1 L1210 cells were used as QC samples in all assays. L1210 were cultured and stored as necessary in 1 ml aliquots of media (with 10% DMSO) containing 1 x 10^6 cells at -80^{0}C. Each time a new batch of L1210 cells was used they were tested against the previous batch to ensure that there was no significant inter-batch difference in the amount of PAR the cells contained. For each assay one aliquot of L1210 cells was used and prepared as described in section 2.9.7.

2.9.9 PARP reaction

For each sample triplicate reaction tubes were prepared containing 30 µl of Reaction Buffer, 5 µl 7 mM NAD^+ and 5 µl of oligonucleotide. The reaction tubes and eppendorf tubes containing the cell suspensions were warmed to 26^{0}C in a shaking water bath. After 7 min the cell suspensions were vortexed and 60 µl of each pipetted into the reaction tubes. After exactly 6 min for each tube the reaction was stopped by the addition of 400 µl of ice-cold 12.5 µM AG014699 and the reaction tubes placed on ice.

2.9.10 Immunoblot technique

Two layers of filter paper followed by a membrane of Hybond N (Amersham Biosciences, UK), all pre-soaked in PBS, were placed onto the base plate of 48-well purpose built manifold. The top plate of the manifold was screwed down tightly to align the wells over the membrane. Following completion of the PARP reaction, 400 µl of each reaction tube cell suspension was gently blotted on to each well using a p1000 Gilson pipette. For each reacted cell suspension sample, an equivalent number of un-reacted cells from the original cell suspension were loaded onto the membrane, in order to give the baseline PAR levels in the cells prior to the reaction. The PAR standards and quality control reacted L1210 cells were also loaded. The blotting pattern for each assay was recorded in the relevant laboratory books. Suction was then applied to the manifold using a Vacusafe aspirator (Integra Biosciences, Switzerland) until all the contents of each well had been absorbed onto the membrane. 400 µl of 10% trichloroacetic acid / 2% sodium pyrophosphate was then pipetted into each well and drawn through the membrane using suction. This step was repeated using 800 µl 70% ethanol as a fixative. The membrane was then removed from the manifold and following 3 x 5 min PBS washes placed in a blocking solution of 5% Marvel milk powder (Premier Foods; St Albans, Hertfordshire, UK) and 0.05% Tween-20 in PBS known as PBS-MT for one hour at room temperature.

2.9.11 Primary and secondary antibody incubations

The membrane was then incubated overnight at 4^0C in mouse monoclonal anti- PAR antibody 1.5 mg/ml, donated by Professor Alex Bürkle (University of Konstanz, Germany from an established hybridoma clone supplied by Dr Takashi Sugimura, National Cancer Centre Research Institute, Tokyo, Japan) diluted 1:1000 in PBS-MT. Following this the membrane was then washed in PBS-T to remove any unbound primary antibody and incubated in the secondary antibody polyclonal goat anti-mouse HRP-conjugated (DAKO; Ely, Cambridgeshire, UK) diluted 1:1000 in PBS-MT for 1 hour at room temperature. Following secondary antibody incubation the membrane was washed for 1 hour in PBS-T with 5 min changes of the wash.

2.9.12 Detection and analysis of chemiluminescence:

Following the final PBS-T wash, ECL western blotting detection fluid (GE Healthcare; Buckinghamshire, UK), (2.5 ml of reagent A + 2.5 ml of reagent B), was pipetted onto the membrane ensuring all blotted areas were covered. After one minute the membrane was transferred to a dark box and an image of the membrane was acquired using a Fuji LAS 3000 camera and imaging software system (Raytest, Sheffield, UK). The membrane was placed on the tray in position four; the camera was set to 'pro' mode to detect chemiluminescence with the iris set to 0.85. A flat frame was applied and exposure set to five minutes. The image was then analysed using Aida Image Analyser software version 3.28.001 (Raytest; Sheffield, UK). Circular regions were marked out over the image corresponding to each blotted well and the luminescence quantified to give a result of LAU/mm^2 per well. An example of this is shown in figure 3.5 of chapter three. The LAU/mm^2 values for the un-reacted cells were then subtracted from the equivalent reaction cell values giving a result of the PAR produced during the reaction step. A standard curve, using non-linear regression, was created using the LAU/mm^2 for the PAR standards using GraphPad prism software version 4.0 (GraphPad Software Inc, La Jolla, California, USA). The resulting equation was then used to calculate the amount of PAR in each cell sample. PARP activity was then calculated as a % of the untreated control samples for each concentration of AG014699 or in the case of the clinical samples for each time-point following the AG014699 dosing.

2.10 PARP-1 expression assay

2.10.1 Background principles

Western blotting is a technique developed more than thirty years ago for the detection of specific proteins or amino acid sequences (epitopes) in a given cell or tissue extract (Burnette, 1981). The process involves the transfer of electrophorectically separated proteins from a sodium dodecyl sulphate (SDS)-polyacrylamide gel to a solid nitrocellulose membrane. This membrane is then probed with specific monoclonal or polyclonal primary antibodies which detect specific epitopes. These bound primary antibodies are then detected by secondary antibodies or other immunological agents whose interaction can be detected by chemiluminescence or autoradiography.

2.10.2 Buffers and solutions

Laemelli Buffer minus mercaptoethanol and bromophenol blue (LB-ME-BB) consisted of 250 nM Tris-HCl (pH = 6.8), 5% SDS and 40% Glycerol. The solution was deemed stable for six months. Running buffer (x 1 strength) was prepared on the day of the experiment by diluting 100 ml of commercially available Tris/Glycine/SDS running buffer (x 10 strength) (BioRad; Hertfordshire, UK) with 900 ml deionised water. Transfer buffer (x 2 strength) was prepared on the day of the assay by diluting 160 ml of commercially available Novex-Tris Glycine transfer buffer (x 25 strength) (Invitrogen; Paisley, UK) with 1840 ml deionised water. Loading dye comprised 52.5 mM dithiothreitol and 1% bromophenol blue dissolved in water (pH = 6.8). Blocking buffer consisted of PBS with 0.05% Tween-20 and 5% milk powder (Premier Foods; St Albans, Hertfordshire, UK).

2.10.3 Preparation of the PBL lysates

On the day of the assay the relevant patients' PBL samples (previously stored in freezing medium) were removed from – 80^{0}C thawed at room temperature, transferred to 1.5 ml eppendorfs and centrifuged at 4^{0}C, 500 G for five minutes. The supernatant was then removed and discarded. Next 100 μl of LB-ME-BB was added to the cell pellet together with Pierce protease inhibitor cocktail (x 1 strength), (Pierce; Illinois, USA).

The cell pellet was then resuspended by vortexing and pipetting and placed on ice for 30 minutes. During this 30 minute period each eppendorf was vortexed every five minutes. The lysate was then sonicated (20 microns amplitude) on ice for three times five second periods using a Vibra-Cell sonicator (Vibracell; Connecticut, USA). The sonicated lysate was then centrifuged at 14000 g for seven minutes at room temperature. The supernatant was then transferred to a clean 1.5 ml eppendorf and placed on ice.

2.10.4 Preparation of QC lysates

For each experiment two aliquots of the K562 cells (cultured as described in section 2.3.1) were removed from – 80^{0}C storage thawed at room temperature and lysates

prepared as described in section 2.10.3. The only difference to this was that only 50 µl not 100 µl of LB-ME-BB was added to the cell pellet after the initial centrifugation step.

2.10.5 BCA protein assay

In order to determine the amount of protein loaded onto the gel for each sample a bioinchoninic acid (BCA) protein assay using the Pierce BCA assay (Pierce; Illinois, USA) was performed with each Western Blot. The assay is based on the reduction of Cu^{2+} to Cu^{+} by peptide bonds in an alkaline medium. BCA chelates with Cu^{+} in a ratio of 2:1 forming a purple coloured reaction product. Absorbance of this product can then be measured on a MRXTC II Plate Reader (Dynex Technology INC; Virginia, USA) at 570 nm. A stock solution of 2 mg/ml bovine serum albumin (BSA) was prepared by diluting 0.04g BSA in 20 ml LB-ME-BB. This stock was then diluted, as described in table 2.1, to produce the following BSA standard concentrations: 2.00, 1.50, 1.00, 0.50, 0.25, 0.125, 0.0625 and 0.00 mg/ml. These standards were then loaded in quadruplicate onto a 96-well plate as shown in table 2.2. 5 µl of each patient and 5 µl of each QC sample were then transferred to clean labelled eppendorfs containing 45 µl of LB-ME-BB to give a 1:10 dilution.

10 µl of each sample was then loaded in quadruplicate onto the 96-well plate. Next 190 µl of the BCA reagent, mixed as per the manufacturer's instructions, was added to each well. The plate was then incubated at 37^{0}C for 30 minutes. The absorbance was then measured on the MRXTC II Plate Reader (Dynex Technology INC; Virginia, USA. The known concentration of each BSA standard was then plotted against the corresponding mean absorbance result at 570 nm. Linear regression analysis was then used to calculate the unknown protein concentrations from each patient and QC sample. This result was then multiplied by ten to account for the original dilution of the sample in LB-ME-BB. For each BCA assay to be valid the R^2 must be > 0.9.

BSA standard (mg/ml)	Volume (µL) of 2 mg/ml stock	Volume (µL) LB-ME-BB	Total Volume (µL)
2.00	500.00	0.00	500.00
1.50	375.00	125.00	500.00
1.00	250.00	250.00	500.00
0.50	125.00	375.00	500.00
0.25	62.50	437.50	500.00
0.125	31.25	468.75	500.00
0.0625	15.63	484.37	500.00
0.00	0.00	500.00	500.00

Table 2.1: Dilution of 2 mg/ml BSA stock to create the eight BSA standards

BSA Standards (mg/ml)				Patient and QC samples							
2.00	2.00	2.00	2.00	Sample 1	Sample 1	Sample 1	Sample 1	Sample 2	Sample 2	Sample 2	Samples 2
1.50	1.50	1.50	1.50	Sample 3	Sample 3	Sample 3	Sample 3	Sample 4	Sample 4	Sample 4	Sample 4
1.00	1.00	1.00	1.00	Sample 5	Sample 5	Sample 5	Sample 5	Sample 6	Sample 6	Sample 6	Sample 6
0.50	0.50	0.50	0.50	Sample 7	Sample 7	Sample 7	Sample 7	Sample 8	Sample 8	Sample 8	Sample 8
0.25	0.25	0.25	0.25	Sample 9	Sample 9	Sample 9	Sample 9	Sample 10	Sample 10	Sample 10	Sample 10
0.125	0.125	0.125	0.125	Sample 10	Sample 10	Sample 10	Sample 10	Sample 11	Sample 11	Sample 11	Sample 11
0.0625	0.0625	0.0625	0.0625	Sample 12	Sample 12	Sample 12	Sample 12	Sample 13	Sample 13	Sample 13	Sample 13
0.00	0.00	0.00	0.00	Sample 14	Sample 14	Sample 14	Sample 14	Sample 15	Sample 15	Sample 15	Sample 15

Table 2.2: Loading pattern of standards and samples for BCA assay on the 96-well plate

2.10.6 Preparation of PARP-1 standards for electrophoresis

10 µg/ml PARP-1 standards (Biomol; Exeter, UK) were stored in 15 µl aliquots at – 80^0C. On the day of experiment one vial was removed from storage and placed on ice to thaw. To prepare the lower concentrations of the standard curve 2 µl of this PARP-1 aliquot was removed and mixed by pipetting with 18 µl of LB-ME-BB in a clean eppendorf to give a 1:10 dilution. The PARP-1 standards were then made up as shown in table 2.3 and placed on ice until needed.

Volume (µL) of 10 µg/ml PARP-1 stock	Volume (µL) of 1:10 µg/ml PARP-1 stock	Volume (µL) of LB-ME-BB	Final PARP-1 standard (ng) in 15 µL volume
6.00	0.00	9.00	40.00
3.80	0.00	11.20	25.00
1.50	0.00	13.50	10.00
0.00	7.50	7.50	5.00
0.00	3.70	11.30	2.50
0.00	0.00	15.00	0.00

Table 2.3 Preparation of PARP-1 standards for electrophoresis

2.10.7 Preparation of cell lysates for electrophoresis

Cell lysates were diluted in LB-ME-BB with calculations adjusted for the addition of 4 x load dye (2.10.2) to each sample. One volume of load dye (x 4) was added to three volumes of each sample such that the load dye became x 1 strength for use on the gel. When possible both the QC, K562, samples and the patient PBL lysates were loaded at 30 µg total soluble protein (TSP) protein in a maximum volume of 15 µl per well. In the previous validation of this assay it was noted that this level of protein should not be exceeded or the signal could become saturated. Once diluted to the required concentration the samples were placed into a boiling water bath, for five minutes to enable protein denaturation and exposure of the epitope. Samples were then immediately loaded into appropriate wells of the gels as described in section 2.10.8.

2.10.8 Gel electrophoresis

One Criterion™ pre-cast (4-20% Tris-HCL) gel (BioRad; Hertfordshire, UK) was removed from its case, the white cover slip from the bottom of the gel removed and the gel washed briefly in distilled water. The gel was then placed in a BioRad Criterion™ gel rig (BioRad; Hertfordshire, UK) and the gel comb removed. The inner well reservoir was then immediately filled with the Tris/Glycine/SDS running buffer (x 1), described in section 2.10.2, followed by the outer reservoir which was filled to the marked fill line. If two gels were run simultaneously the second gel was prepared as above. The gel was then loaded from left to right as follows: the first lane was loaded with 4 µl of the protein molecular weight marker –MagicMark (Invitrogen; Paisley, UK). MagicMark was stored at -20^{o}C and only required defrosting prior to use. 10 µL of each PARP-1 standard was then loaded in duplicate, followed by duplicate patient samples and finally duplicate QC samples. Once loading was completed the top was placed on the tank and the BioRad Power Pac 300 (BioRad; Hertfordshire, UK) was set to run for two hours at a constant voltage (V) of 100 V.

2.10.9 Western Blotting technique

Prior to blotting, two Criterion™ material pads (BioRad; Hertfordshire, UK), two filter paper sheets (Whatman; Kent, UK) and one Hybond-C nitrocellulose membrane (Amersham Biosciences; Buckinghamshire, UK) all cut to 14 cm x 9 cm, were pre-soaked in (x 2) Novex transfer buffer. After the gel had run for two hours at 100 V, the power was switched off and the gel casing removed. The lower protruding lip of the gel was discarded and the pre-cast gel case opened using a flat bladed knife. The top 10 mm comb section of the gel was then also removed using the blade. The gel was then ready for transfer onto the nitrocellulose membrane in the BioRad Criterion™ Blotter (BioRad; Hertfordshire, UK). One material pad was placed on the inner side of the black section of the transfer case, followed by one filter paper and then the gel. The nitrocellulose membrane was then placed on top of the gel (with the upper right corner cut), followed by the second piece of filter paper and the second material pad. Any air bubbles between the material pads, gel and filter papers were removed by the use of a mini-roller. The cassette was then closed and placed into the transfer tank, ensuring that the black side of the cassette was closest to the black side of the transfer rig. If a second gel was run in section 2.10.8 the procedure was repeated. Finally the transfer rig was filled with x 2 transfer buffer and allowed to run for two hours at 100 V.

To prevent over-heating during the transfer an ice pack was placed into the rig and the rig itself was placed into a container of ice.

2.10.10 Primary and secondary antibody incubations

Following transfer the membrane was removed from the cassette and briefly blotted dry on tissue paper. It was then transferred to a clean tray, ensuring that the cut right hand corner was in place, and blocked for one hour at room temperature under gentle agitation with 25 ml of PBS-MT blocking buffer. Next the primary antibody Anti PARP-1 C2-10 (Trevigen; Maryland, USA) was applied to the membrane diluted 1:2000 in 20 ml PBS-MT overnight at 4^0C using a rotation shaker. The next day the membrane was rinsed in three five minute washes of PBS-T (25 ml per wash), before transfer to a clean blocking tray and the application of the secondary antibody. The secondary antibody - polyclonal goat anti-mouse IgG HRP secondary antibody (Dako; Cambridgeshire, UK) was diluted 1:1000 in 20 ml PBS-MT and mixed for one hour with gentle agitation on a rotation shaker at room temperature. Following this the membrane was finally washed at for one hour at room temperature in PBS-T with frequent changes of wash (approximately every five minutes).

2.10.11 Detection and analysis of chemiluminescence

Next the membrane was thoroughly drained by holding the edge against absorbent paper to remove excess moisture and placed on a sheet of cling film protein transfer side up. Then 5.85 ml of solution A was combined with 150 µl of solution B from the ECL PlusWestern Blot Detection Kit (GE Healthcare; Buckinghamshire, UK) and mixed using vortexing. The entire surface of the membrane was then covered with ECL Plus detection fluid and exposed for five minutes. Any excess fluid was drained onto absorbent paper and the membrane wrapped in clean cling film, removing any air bubble by the use of a roller. The membrane was then transferred to the Fuji LAS 3000 camera and imaging software system (Raytest, Sheffield, UK).). The membrane was placed on the tray in position two; the camera was set to 'pro' mode to detect chemiluminescence with the iris set to 0.85. A flat frame was applied and exposure set to ten minutes. The image was then analysed using Aida Image Analyser software version 3.28.001 (Raytest; Sheffield, UK). Rectangular regions were marked out over the image corresponding to each of the PARP-1 standards, QCs and visible patient samples as shown in figure 3.7 of chapter three and the luminescence quantified to

give a result of LAU per each area (mm^2). A standard curve, using non-linear regression, was created using the LAU/mm^2 for the PARP-1 standards using GraphPad prism software version 4.0 (GraphPad Software Inc, La Jolla, California, USA). The resulting equation was then used to calculate the amount of PARP-1 (ng) in each cell sample. Using the results of the BCA protein assay, this value could then be expressed as a value of ng PARP-1 detected per µg of TSP. Patient samples were run in duplicate wells on two separate assays and their mean value (ng per µg TSP) calculated as above.

It was proposed that on completion of the Western blotting assay for all patients within the trial, the expression values would be compiled and patients PARP-1 activity stratified into five groups based on the scoring system described in table 2.4. The rationale behind this was that a semi quantitative scale would limit data errors from both intra and inter assay variability, whilst still providing absolute numerical values on an individual patient's expression level.

0	No signal visible after exposure of the membrane or variability of the generated replicates resulting in a CV > 50.
1	Patients mean expression value falls into the lowest quartile of values
2	Patients mean expression value falls into the second quartile of expression values
3	Patients mean expression value falls into the third quartile of expression values
4	Patients mean expression value falls into the highest quartile of expression values

Table 2.4: Semi-quantitative system for scoring PARP-1 expression levels in patients. CV = coefficient of variation.

2.11 Development and validation of an analytical method for the determination of AG014447 in human plasma.

2.11.1 Background Principles

AG014447 is the parent drug of AG014699 and it is AG014447 that is detected in human plasma following administration of AG014699. The AG014699 pharmacokinetic (PK) studies for the phase I and II combination TMZ studies were performed by Quintiles Preclinical Services, Edinburgh, UK on behalf of Pfizer. However, for this

BRCA-PARP phase II study, PK analysis was to be performed in-house. One of the objectives of this research fellowship and thesis was to develop and validate an analytical method to determine the concentration of the analyte AG014447 in human plasma using protein precipitation extraction followed by high performance liquid chromatography (LC) with tandem Mass Spectrometry (MS). Validation of this assay to GCLP standards was performed by testing an assessment of linearity, range, accuracy and recovery, intra and inter-assay precision, lower limit of detection, specificity and freeze/thaw stability of AG014447. The assay method is described below. The validation report is not included as part of this thesis.

2.11.2 Analytical system

The analytical system used was the API4000 LC/MS/MS from Applied Biosystems (California, USA) with a series 200 Micro pump, autosampler and Peltier column oven, all from Perkin Elmer (Beaconsfield, UK). The column used was the Gemini 3u C18 110A, 20 x 4 mm supplied by Phenomenex (Macclesfield, UK). A Phenomenex guard column (C18 (ODS Octadecyl), 4mm L x 2.0mm) was also used for every run and changed after every fifty patient samples. Analysis was performed using Analyst software version 1.5 (Applied Biosystems; California, USA)

2.11.3 Preparation of mobile phases

Prior to use the deionised water and the acetonitrile (Fisher Scientific; Loughborough, UK) used to make the mobile phases were filtered through 0.45 µm phenex filter membranes using the Phenomenex filtration apparatus (Macclesfield, UK). Mobile phase A (10:90 acetonitrile: water + 0.1% formic acid) was prepared by adding 50 ml of acetonitrile to 450 ml of deionised water in a 1000 ml measuring cylinder plus 0.5 ml formic acid (Fisher Scientific; Loughborough, UK). The solution was then mixed, transferred to a 500 ml Duran bottle (Duran group; Wertheim, Germany) and given an expiry date of seven days. Mobile phase B (65:35 acetonitrile:water + 0.1% formic acid) was prepared by adding 325 ml of acetonitrile to 175 ml deionised water in a 1000 ml measuring cylinder followed by 0.5 ml formic acid. The solution was mixed, transferred to a 500 ml Duran bottle with an expiry date of seven days. The needle-wash (solution C) was prepared by adding 250 ml acetonitrile to 250 ml deionised water in a 1000 ml measuring cylinder to give a 50: 50 mix. The solution was then mixed, stored in a 500 ml Duran bottle and stable for one month.

2.11.4 Preparation of AG014447 and deuterated d7-AG014447 stock solutions

AG014447 and its corresponding internal standard (IS) deuterated d7-AG014447 were supplied by Pfizer. Compounds were all weighed out using a Mettler 5 place balance (Mettler-Toledo; Leicester, UK). AG014447 1mg/ml stock solution was made by weighing out 2 mg AG014447 and dissolving in 2 ml of 100% methanol and stored, protected from light, at -20^{0}C. Internal standard d-7 AG014447 200 µg/ml stock solution was prepared by weighing out 2 mg and dissolving in 10 ml of 100% methanol. This was then separated into 1 ml aliquots and stored, protected from light, at -20^{0}C.

2.11.5 Preparation of AG014447 standard curve

For each analytical run a new standard curve was prepared on the day of experiment. The following eight concentrations of AG014447 were prepared in duplicate: 2, 4, 10, 20, 50, 100, 250 and 500 ng/ml by diluting the 1 mg/ml stock solution in blank plasma (supplied by the Blood Bank Service, Newcastle-upon-Tyne, UK) shown in table 2.5. The standard curve was determined from the plasma standards by linear regression with a $1/x^2$ weighting of the analyte to IS area ratios using the Analyst programme version 1.5.

1000ng/ml 447 (ml)	100ng/ml 447 (ml)	10ng/ml 447 (ml)	Volume plasma (ml)	Final concentration AG014447 (ng/ml)
0.50			0.50	500.00
0.25			0.75	250.00
0.10			0.90	100.00
	0.50		0.50	50.00
	0.20		0.80	20.00
	0.10		0.90	10.00
		0.40	0.60	4.00
		0.20	0.80	2.00

Table 2.5: Preparation of AG014447 standard curve

2.11.6 Preparation of QC samples

For use within each analytical run QC samples for the three concentrations: lowest QC (LQC) 2 ng/ml, medium QC (MQC) 50 ng/ml and the highest QC (HQC) 500 ng/ml were prepared. These were made up in advance of use and stored at – 20^{0}C (stable for five months). New batches were tested to ensure consistency with the preceding batch prior to use within patient sample analysis. On the day of a run triplicate QCs for each

concentration were removed from - 20^{0}C and thawed at room temperature. In addition to the nine QCs a single blank plasma sample, containing only the IS and a double blank sample of plasma only were also prepared.

2.11.7 Preparation of samples

On the day of the run 200 µl of each sample (blank plasma, standards, QCs, patient samples) were pipetted into 1.5 ml labelled microtubes. To each sample 10 µl of the IS at concentration 100 ng/ml was added except to the double blank plasma.
Some patient samples required dilution 1:10 with blank plasma prior to extraction process depending on the dose of AG014699 administered and the sampling time-point to ensure that the results lay within the standard curve (2 ng/ml to 500 ng/ml). Protein precipitation was achieved by the addition of 0.4 ml acetonitrile to each sample whilst vortexing. The samples were then centrifuged at 12,000 RCF for 5 min in a Heraeus biofuge15 centrifuge (Heraeus Sepatech GmbH; Osterode, Germany). The supernatant was then transferred to a labelled 12 x 75 mm borosilicate tube (Fisher Scientific; Loughborough, UK) and evaporated to dryness in nitrogen at 40^{o}C using a Zymark evaporator (Caliper Life Sciences; Cheshire, UK). The residue was then reconstituted in 180 µl of mobile phase A (described above), vortexed and placed in autosampler limited volume inserts ready to be run on the LC/MS/MS.

2.11.8 Order of sample injections

For each analytical run the samples were tested in the sequence shown in figure 2.2. An un-extracted AG014447 sample was always tested before any clinical samples were removed from -20^{0}C to ensure that the LC/MS/MS system was operational that the analyte could be detected to a similar sensitivity to previous runs.

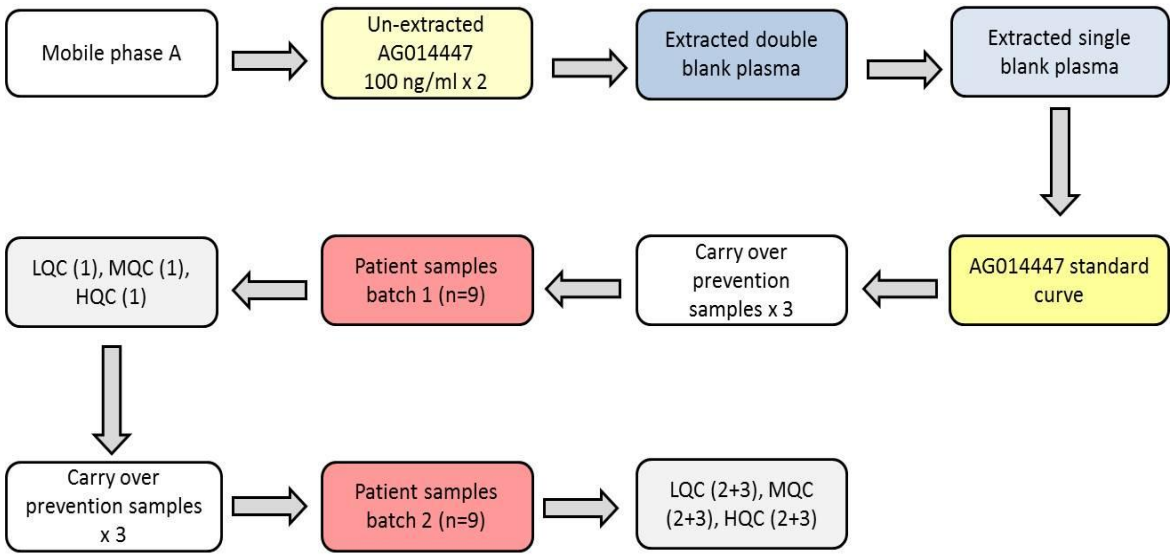

Figure 2.2: Flow diagram showing the sequence in which samples were run on the LC/MS/MS for each analytical run

2.11.9 Preparation of carry over prevention samples

To eliminate carry-over of the analyte between high and low concentrations, three samples of mobile phase A were run after the highest standard (500 ng/ml), the highest QC samples and any anticipated high patient samples, for example the end of infusion time-points.

2.11.10 LC/MS/MS conditions

Mobile phase: pump A - 10:90 acetonitrile: water + 0.1% formic acid, pump B - 65:35 acetonitrile: water + 0.1% formic acid. Needle wash – 50:50 acetonitrile: water. Retention time of the analyte was 2.33 minutes. The time-table used for the gradient elution is shown in table 2.6. The settings for the mass spectrometer for analyte detection and the parameters for the mass spectrometer environment are shown in table 2.7

Step	Time (min)	Flow rate (ml/min)	Gradient	% Mobile phase A	% Mobile phase B
1	0.00	0.50	1	100.00	0.00
2	1.00	0.50	1	100.00	0.00
3	1.50	0.50	1	0.00	100.00
4	2.00	0.50	1	0.00	100.00
5	2.50	0.50	1	100.00	0.00
6	6.00	0.50	1	100.00	0.00

Table 2.6: Chromatography gradient of mobile phases across the column

Compound	Q1 mass	Q3 mass	Dwell (msec)	DP (volts)	CXP
AG014447	324.00	293.20	150.00	41.00	14.00
IS	331.30	297.10	150.00	51.00	10.00
Parameter					
Collison gas (CAD)	5.00				
Curtain gas (CUR)	50.00				
Ion source gas 1	65.00				
Ion source gas 2	50.00				
Ion spray voltage (IS)	5500.00				
Temperature	500.00				

Table 2.7: Mass spectrometer parameters

2.12 Taqman® Real-Time PCR genotyping

2.12.1 Background Principles

To determine the single nucleotide polymorphisms (SNPs) within the *CYP2D6* gene (*2 and *4) associated with the metabolism of AG014699 (Plummer *et al*., 2008) and the *PARP-1* gene (T2444C) associated with reduced enzyme activity (Lockett *et al*., 2004; Wang *et al*., 2007), genotyping was performed using Taqman® Real-time Polymerase chain reaction (PCR). All reagents and equipment described in this section were purchased from Applied Biosystems (Warrington, UK), unless otherwise stated. The Real-time and 'allelic discrimination' runs were performed on the ABI 7500 Fast System operating 7500 Fast system software (Applied Biosystems; Warrington, UK). Taqman® Real-time PCR for each SNP under investigation was performed by incubating the DNA template with Taqman® genotyping master mix and the specific SNP genotyping assay mix which contained two fluorescent probes: VIC and FAM. During the extension cycle of PCR these reporter probes are cleaved off specific target sequences and fluoresce. This fluorescence is subsequently detected using the 'allelic discrimination' software

on ABI 7500 Fast system. The programme is set for the VIC probe to denote the presence of the wild-type (wt) allele and the FAM probe to denote variant (v) alleles. Therefore for any given SNP, wild-type homozygotes (wt/wt) fluoresce only VIC, variant homozygotes (v/v) fluoresce only FAM and any heterozygotes (wt/v) will contain equal amounts of both VIC and FAM fluoresence. An example of this 'allelic discrimination' process is shown in figure 2.3. Specific primers for the SNPs under investigation were obtained ready for use from Applied Biosystems. The details of these 'off the shelf' genotyping assays are found in table 2. 8.

Gene	SNP	Taqman® Genotyping assay
PARP-1	T2444C rs 113640	X 40 assay C_1515368_1
CYP2D6	C245R (*2) rs 16947	X 20 assay C_27102425_10
	G1846A (*4) rs 3892097	X 20 assay C_27102431_10

Table 2.8: Details of the Taqman® Genotyping assays used for the specific SNPs.

2.12.2 Preparation of the DNA template

DNA was purified from patients' whole blood (method described in section 2.4.3) and stored at 4^0C as 10 ng/µl working solutions. For each genotyping assay 1 µl of each patient's working solution was added to the reaction mixture. Sample testing was not duplicated unless the primary results were inconclusive.

2.12.3 Preparation of the PCR plate

All reactions were run on 96-well MicroAmp Fast Optical 0.1 ml PCR plates. The plates were loaded with one DNA sample per patient; in addition, three no DNA template controls (NTC) and any available known genotype controls for validation were also run. Each well of the plate was loaded to contain 1 µl of sample DNA, x1 Taqman® Genotyping PCR Master Mix and x1 Genotyping Assay mix (as per table 2.9) made up to a total volume of 25 µl with sterile UHP water. The NTC were made as above but without the sample DNA. The plate was then sealed with MicroAmp Optical adhesive film (to avoid evaporation of reagents during PCR) and centrifuged at 1500g for one minute at 4^0C. 4.2.7. The plate was then immediately loaded into the ABI 7500 Fast machine. If there was any delay in loading the plate was stored at 4^0C whilst waiting for machine.

2.12.4 PCR

For all real-time assays the default conditions on the 'Absolute Quantitation' plate documents were selected. The conditions were: initial hold at 95^0C for 10 minutes followed by a total of 40 cycles at 95^0C for 15 seconds then 60^0C for one minute.

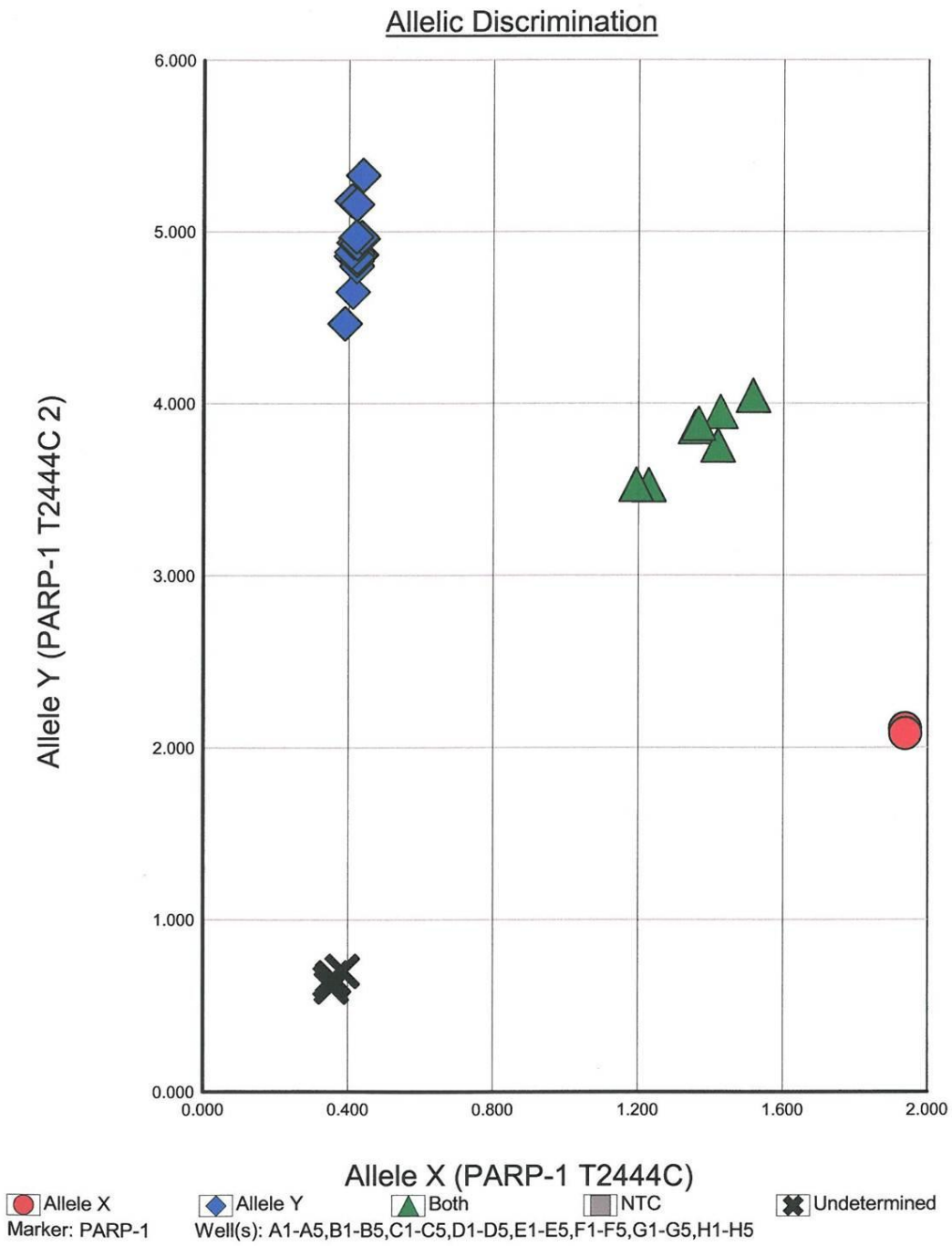

Figure 2.3: Taqman® Real-time PCR allelic discrimination results chart of analysis of the PARP-1 SNP T2444C (rs 113640, C-1515368) for the BRCA-PARP clinical trial patients.

2.12.5 Data analysis

Following PCR amplification an end-plate read was performed using the Applied Biosystems Sequence Detection System. The Sequence Detection System software uses the fluorescence measurements made during the plate read to plot fluorescence values based on the signals within each well. These plotted fluorescence signals indicate which alleles are present in each well and thus the genotype for each patient sample can be determined.

The frequencies of the genotypes were tested in accordance with the principles of Hardy-Weinberg. The validity of each assay was confirmed by cross-checking the results of known genotype controls.

Chapter Three

3. *In vitro* studies of the effect of AG014699 in a panel of human cell lines with differing *BRCA* status

3.1 Introduction

Assumptions regarding the selective cytotoxicity of single agent PARP inhibitors to Homologous Recombination deficient models have been based on studies in non-cancerous, genetically naïve, *BRCA1/2*-negative embryonic stem cells; *BRCA2*-deficient Chinese hamster lung fibroblasts and genetically modified human cell lines using the potent PARP inhibitors AG14361, KU0058684 and KU0058948 (Bryant *et al*., 2005; Farmer *et al*., 2005). In contrast, results of experiments examining the sensitivity of *human cancer* cell lines to single agent PARP inhibitors have been conflicting. For example, Gallmeier *et al* reported that the *BRCA2*-defective human pancreatic cancer CAPAN-1 cells were not sensitive to PARP inhibition (Gallmeier *et al*., 2005) whereas McCabe *et al* did demonstrate sensitivity of CAPAN-1 cells to the PARP inhibitors KU0058684 and KU0058948 (McCabe *et al*., 2005). In addition, De Soto *et al* observed, in a panel of human breast cancer cell lines, that the *BRCA*1 negative cell lines: HCC1937 and SUM1315MO2, were *not* significantly more sensitive to the PARP inhibitors 3-Aminobenzamide, NU1025 and AG14361 compared to non *BRCA* mutated controls (MCF7 and MDA-MB-231) (De Soto *et al*., 2006).

A possible explanation for the conflicting data is that some of these studies were conducted using less potent PARP inhibitors than the current clinical candidates. Another theory is that these experiments were conducted with human cancer cells originating from naturally occurring *BRCA*1/2 mutations and that the lack of sensitivity may reflect the ability of cancer cells to adapt to mutation defects to promote survival; a recently recognised enabling characteristic of cancer cells (Hanahan and Weinberg, 2011).

Therefore tumours from patients with *BRCA*1/2 mutations may not be as exquisitely sensitive to PARP inhibitors as reported by the pivotal 2005 Nature publications

(Bryant *et al*., 2005; Farmer *et al*., 2005). In view of the conflicting pre-clinical data, a comprehensive study of the therapeutic potential of the PARP inhibitor AG014699 in human cancer cell lines with differing *BRCA/* HR status and an investigation into the mechanism behind any observed selective sensitivity was undertaken.

3.2 Objectives

The aims of this study were as follows:

- To investigate the effect of AG014699 on cell viability and growth using clonogenic cell survival assays and sulforhodamine B assays.
- To determine baseline levels of PARP-1 activity in cell lines and investigate the effect of AG014699 on PARP-1 activity.
- To test the hypothesis that DNA double strand breaks accumulate in cells after exposure to AG014699 and that Homologous Recombination functions only in the *BRCA*1/2 proficient cell lines.

3.3 Materials and Methods

Materials and methods for the assays listed are described in full in chapter two. Deviations from these methods and their reasoning's are detailed in the individual assay results sections.

A panel of 11 mammalian cell lines were used in this study, characteristics of which are detailed in chapter two, Materials and Methods. A summary is provided here in table 3.1 as an aide-memoire. The panel included two paired HR proficient and deficient cell line models; the human *BRCA*1 mutant breast cancer HCC1937 cell line and the *BRCA*1 corrected counterpart HCC1937-BRCA1; and the Chinese hamster ovary (CHO) cell line AA8 and its XRCC3-deficient derivative IRS-1SF. The panel also included the immortalised human ovarian surface epithelial (OSE) *BRCA2* heterozygote cell line, OSEC1, and the immortalised human OSE *BRCA* wt type OSEC2 cell line.

Cell line	**HR/BRCA status**	**Origin**
MCF7	*BRCA 2* wt type, *BRCA1* hemizygous	Breast carcinoma cells derived from pleural fluid
MDA -MB -231	*BRCA2* wt type, *BRCA1* hemizygous	Primary breast carcinoma cells
OSEC-2	*BRCA1/2* wt type	Ovarian surface epithelial cells
OSEC-1	*BRCA2* heterozygote (4630insA ,exon 11), *BRCA1* wt type	Ovarian surface epithelial cells
UACC3199	Epigenetically silenced *BRCA1* by promoter methylation	Primary breast carcinoma cells
MDA -MB -436	*BRCA1* mutated (5396 +IG>A), *BRCA2* wt type	Breast carcinoma cells derived from pleural fluid
HCC1937	*BRCA1* mutated (5283insC), *BRCA2* wt type	Ductal breast carcinoma
HCC1937 – BRCA1	Transfected wild type *BRCA1* , *BRCA2* wt type	Ductal breast carcinoma
CAPAN -1	BRCA2 mutated (6174delT), *BRCA1* wt type	Pancreatic adenocarcinoma cells derived from a liver metastasis
IRS-1SF	XRCC3 deficient	Chinese Hamster Ovarian surface epithelial cells
AA8	XRCC3 wt type	Chinese Hamster Ovarian surface epithelial cells

Table 3.1: Cell line characteristics

3.4 Results

To make for easier discussion of the results, cells with *BRCA*1/2 or *XRCC3* mutations are grouped by the term 'HR deficient' (HR-) and cells with wt type *BRCA*1/2, *XRCC3* or heterozygous for *BRCA*1/2 are grouped 'HR proficient' (HR+). As the level of BRCA1 function in the UACC3199 (*BRCA*1 methylated) cell line is not known, results for this cell line were analysed separately.

3.4.1 Clonogenic cell survival and Growth inhibition in response to AG014699

For these studies cells were exposed to increasing concentrations of AG014699 ranging from 0.00 to 100.00 μM. Methods for which are described fully in chapter two, Materials and Methods. Results are illustrated in figure 3.1 and LC_{50} values summarized in table 3.2. These clonogenic cell survival assays were undertaken jointly by Yvette Drew and Suzanne Kyle.

Clonogenic cell survival assays demonstrated that *BRCA* mutated human cancer cell lines are significantly more sensitive to AG014699 than human cell lines with wild type or heterozygote BRCA (mean LC_{50} = 4.0 ± 2.9 *vs*. mean LC_{50} = 25.1 ± 9.2; $P < 0.0001$). Reviewing the data for all nine cell lines tested, the known HR- cells (CAPAN-1, IRS-1SF and MDA-MB-436) were 9-fold more sensitive to AG014699 than the HR+ cell lines (AA8, MCF7, MDA-MB-231, and OSEC2) (*P=0.0001*, unpaired t-test).

Of note, the UACC3199 cell line, with epigenetically silenced *BRCA*1*,* had 3-fold greater sensitivity than the HR proficient cells (*P=0.002*, unpaired t-test) and a mean LC_{50} within the range of the HR deficient cells (0.9 – 8.3 μM). Using the mean LC_{50} concentrations of each cell line there was a significant difference between all 3 groups - the HR deficient cells, the *BRCA1* methylated UACC3199 cells and the HR proficient cells (LC_{50} = 3.3 μM *vs*. LC_{50} = 7.6 μM *vs*. LC_{50} = 29.7, P *<0.0001,* 1 way ANOVA), see figure 3.2.

The most sensitive human cancer cell line to AG014699 was the *BRCA*1 mutated MDA-MB-436 cell line (LC_{50} = 1.3 μM).

Encouragingly, the sensitivity of the *BRCA*2 heterozygote, OSEC1 cells (mean LC_{50} = 44.8 µM) was within the range observed in the HR proficient cells (16.2 – 58.6 µM) and interestingly, less sensitive than the *BRCA*2 wt type OSEC2 cell line (mean LC_{50} = 31.6 ± 11.1 µM). These results infer that PARP inhibition is non-toxic to heterozygote models and thus may be safe in *BRCA* mutation carrier patients.

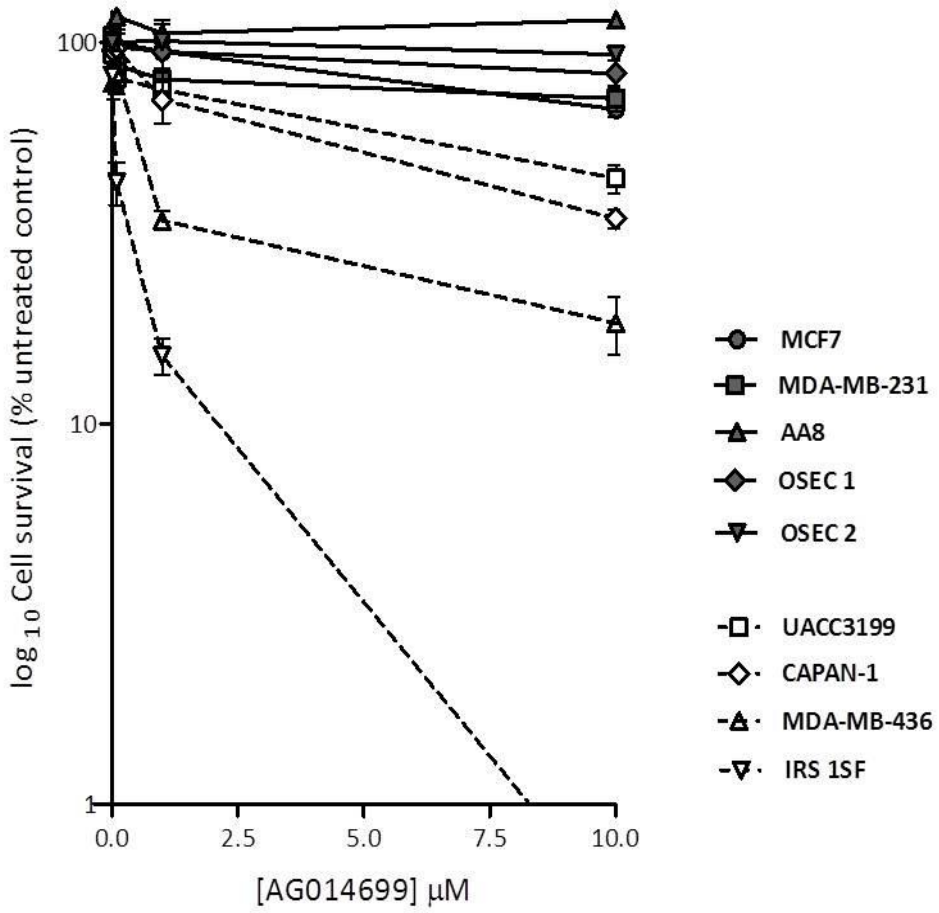

Figure 3.1: Clonogenic survival assays of cells treated with 24 h AG014699 (data presented 0.0-10.0 µM). Solid symbols/lines = HR proficient' cells, open symbols/dashed lines = 'HR deficient' cells. Data are the mean and SEM values for each concentration from ≥ 3 independent experiments.

Cell line	Mean IC_{50} μM ± SD	Mean % survival at 10 μM AG014699
MCF7	20.2 ± 3.5	66.8
MDA-MB-231	21.9 ± 2.6	71.2
OSEC1	44.8 ± 14.3	82.7
OSEC2	31.6 ± 11.1	83.2
AA8	50.7 ± 6.9	114.4
UACC3199	7.6 ± 1.2	43.9
MDA-MB-436	1.3 ± 0.6	18.3
CAPAN-1	5.5 ± 2.5	34.4
IRS-1SF	1.4 ± 0.4	00.5

Table 3.2: Mean IC_{50} and % Survival at 10 μM AG014699 data for cell lines from the clonogenic cell survival assays.

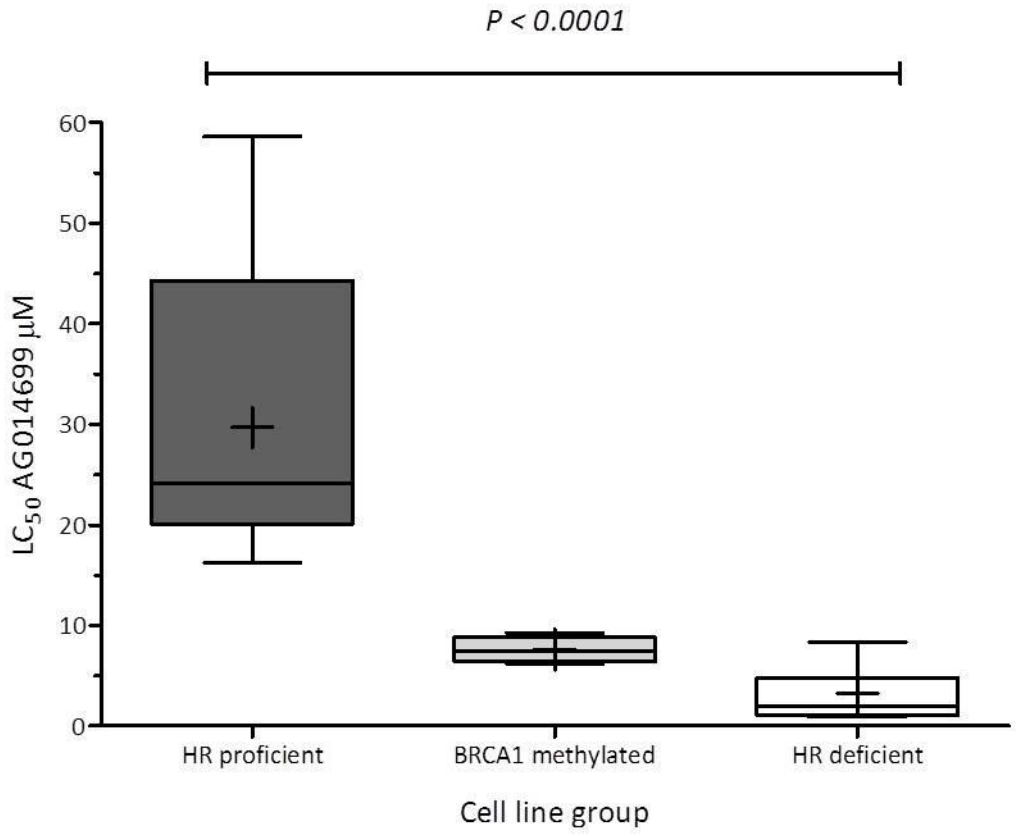

Figure 3.2: Box and whiskers plot (minimum to maximum) with + showing mean LC_{50} data for the HR proficient, HR deficient and the UACC3199 *BRCA1* methylated cell lines. P value calculated using 1 way ANOVA demonstrates a significant difference between the 3 groups (*P=0.0001*).

The HCC1937 and HCC1937-BRCA1 cell lines had poor cloning efficiency and were not appropriate for the clonogenic cell survival assay. As an alternative, the sulforhodamine B (SRB) protein dye assay was used to determine cell growth in response to AG014699. MDA-MB-231 cells were also evaluated in the SRB assay to provide a direct comparison between results from the two cell viability assays. Using the SRB assay, *BRCA*1 deficient HCC1937 cells were significantly more sensitive to AG014699 than the *BRCA*1 complemented HCC1937-BRCA1 cell line (mean GI_{50} = 10.5 µM *vs*. 16.7 µM, *P=0.001*, unpaired t-test) and the sensitivity of the HCC1937-BRCA1 cell line was similar to that of the MDA-MB-231 (mean GI_{50} = 16.5 µM), shown in figure 3.3. Comparing the two assays the results for the MDA-MB-231 cell line were similar with a mean LC_{50} = 21.9 µM and a mean GI_{50} = 16.5 µM.

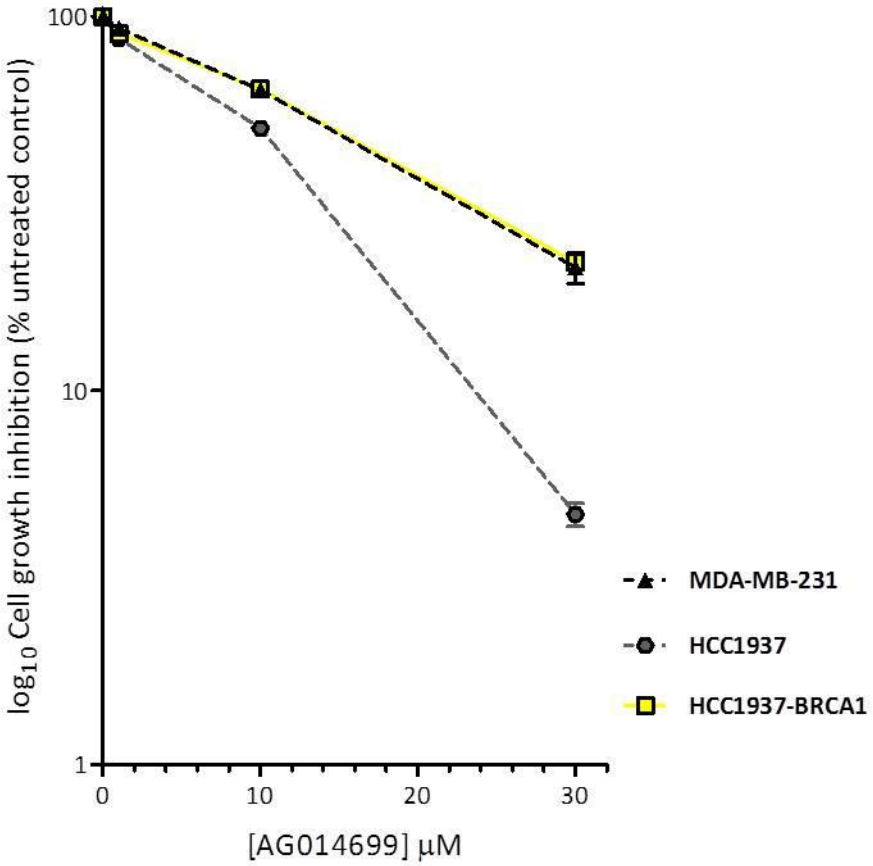

Figure 3.3: SRB cell growth assays of HCC1937, HCC1937-BRCA1 (blue) and MDA MB 231 cells treated with AG014699 (0 - 100µM) for 6 days, data presented for 0.00-30.00 µM. Data are mean and SEM values from 3 independent experiments.

Cell line	Mean GI_{50} µM ± SD	Mean % growth at 10 µM AG014699
MDA-MB-231	16.5 ± 0.7	63.7
HCC1937	10.5 ± 0.7	50.3
HCC1937-BRCA1	16.7 ± 1.1	64.0

Table 3.3: Mean GI_{50} and % Growth at 10 µM AG014699 data for three cell lines from the SRB assays

These experiments demonstrate that HR deficient human and non-human cells of cancerous and non- cancerous origin are much more sensitive to AG014699 induced cytotoxicity than HR proficient cells of similar origin. These data suggest that this increase in AG014699-induced toxicity is secondary to the HR deficiency and the underlying mechanism behind this is investigated in the subsequent experiments.

Reviewing the LC_{50} and GI_{50} data in tables 3.2 and 3.3 respectively, the cut off of 50% survival following the exposure of cells to 10 µM AG014699 discriminated between those cells with functional HR (>50% survival) and cells with dysfunctional HR (< 50% survival) and for this reason a dose of 10 µM AG014699 was chosen for use in subsequent experiments.

3.4.2. Baseline PARP-1 activity and inhibition in response to 10 µM AG014699

To investigate whether differences in cell line sensitivity to AG014699 were secondary to variations in baseline levels of PARP activity or the degree of AG014699-induced PARP inhibition we used the validated PAR formation immunoblot assay (Plummer *et al*., 2008). The assay, described in chapter two, Materials and Methods, detects maximally stimulated PARP activity as pmol PAR. An example of an immunoblot and a typical PAR standard curve are shown in figures 3.4 and 3.5 respectively. PARP activity, based on detected pmol PAR, was calculated from the non-linear regression equation. Inhibition of activity following AG014699 was then expressed as % of the un-treated control value. Un-stimulated PARP activity i.e. endogenous PAR levels for each line was also calculated from cell samples that did not undergo the reaction as described in the chapter two, section 2.9.1.

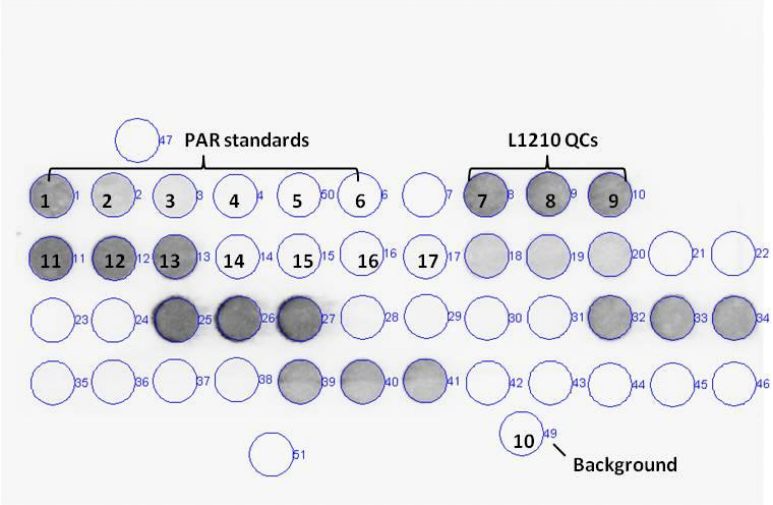

Figure 3.4: PAR formation immunoblot. Wells 1-6 = PAR standards (pmol) 25, 5, 1, 0.2, 0.04, 0.00. Wells 7-9 = QC L1210 samples. Well 10 = background. Wells 11-17 = a single patient time-point with 11-13 being the control reacted samples, 14-16 the reacted cells + AG014699 and well 17 = the un-reacted sample showing the endogenous PAR present.

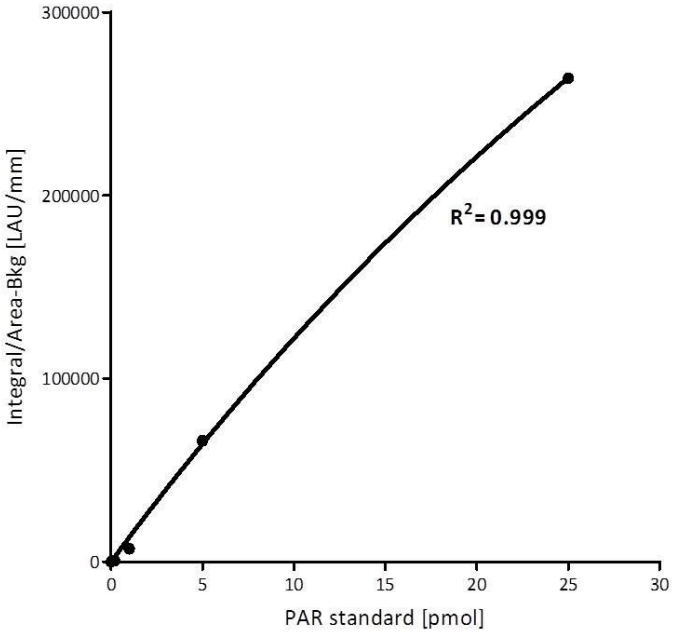

Figure 3.5 A standard curve showing the non-linear relationship between PAR standards and the luminescent arbitrary units (LAU) for a given area detected by the Fuji -LAS imaging system.

For this study, cells in culture were pre-exposed to 10 µM AG014699 or control (DMSO) for 30 minutes and maximum stimulated PARP activity subsequently assessed. PARP activity is expressed as pmol PAR per 10^6 cells. Results for all cell lines are summarised in table 3.4.

There was a large variation in the baseline levels of PARP enzyme activity between the cell lines. For all cell lines mean endogenous baseline PARP activity was 157.40 pmol PAR per 10^6 cells. This ranged from as low as 27.67 up to 594.70 pmol PAR per per 10^6 cells, with a CV of 101%. As expected the baseline (maximum stimulated) PARP activity levels were higher but there was less inter-cell variation with a mean of 4507.00 pmol PAR per per 10^6 cells, range 881.70 to 8760.00 pmol and CV of 42%. There was a trend towards higher baseline endogenous PARP activity in the HR- cell lines compared to the HR+ cell lines but this was not statistically significant (mean = 210.2 *vs.* 112.8 pmol PAR per 10^6 cells, *P = 0.34*, un-paired t-test). In addition higher activity was seen in the HR- cells in a sub-group analysis of the *human cancer* cell lines but no statistical significance (mean = 246.2 *vs.* 146.2 pmol PAR per 10^6 cells, *P = 0.52*), (figure 3.6).

The results for baseline maximum stimulated activity showed a similar trend with higher baseline PAR in the HR- cells (mean = 5046.00 *vs.* 3968.00 pmol PAR per 10^6 cells, *P = 0.15*, un-paired t-test) and the subset analysis of the HR-human cancer cells, but again levels of statistical significance were not met, see figure 3.7.

To determine whether there was any relationship between the baseline PARP activity and sensitivity to AG014699 (represented as LC_{50}), a Pearsons correlation analysis was performed. Results, shown in figure 3.8, demonstrate no significant relationship between the two parameters ($R^2 = 0.05$, $P = 0.32$).

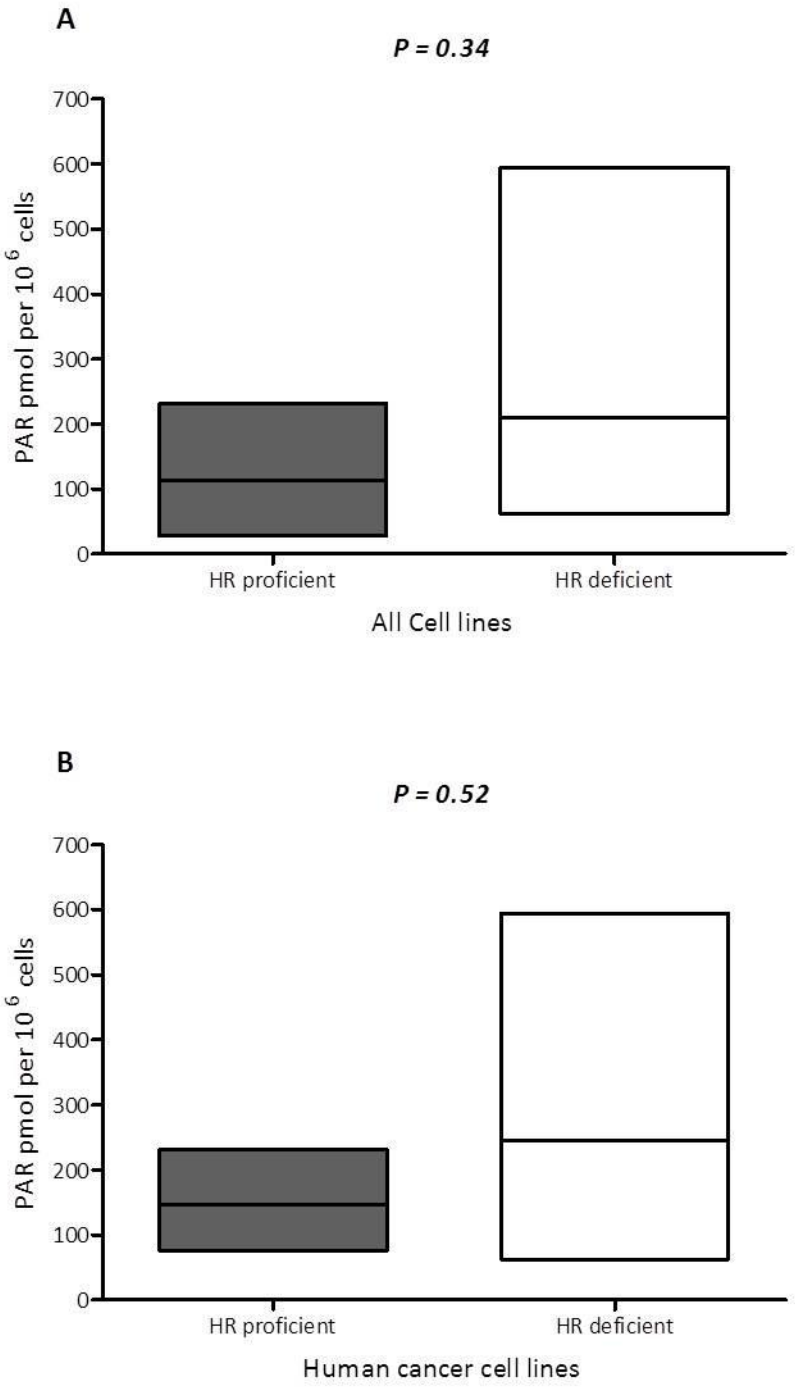

Figure 3.6: Floating bars showing maximum to minimum and mean values (line) of baseline endogenous PARP activity levels by pmol PAR per 10^6 cells in HR proficient and HR deficient cells for **A:** all cell lines and **B:** human cancer cell lines only. Line = mean value and P values calculated using un-paired t-test shows no significant difference between the groups.

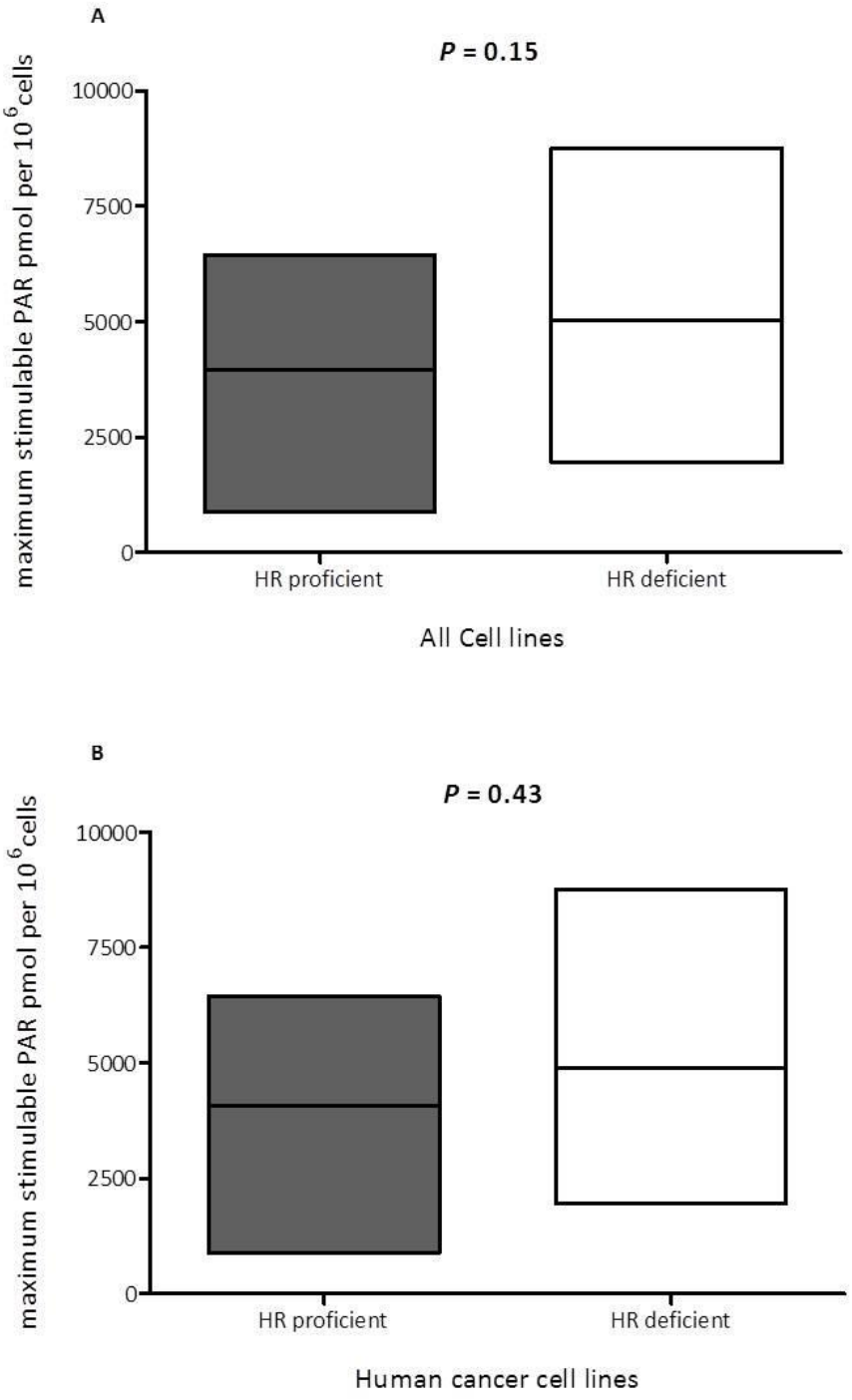

Figure 3.7: Floating bars showing maximum to minimum and mean values (line) of baseline maximum stimulated PARP activity levels by pmol PAR per 10^6 cells in HR proficient and HR deficient cells for **A:** all cell lines and **B:** human cancer cell lines only. Line = mean value and P values calculated using un-paired t-test shows no significant difference between the groups.

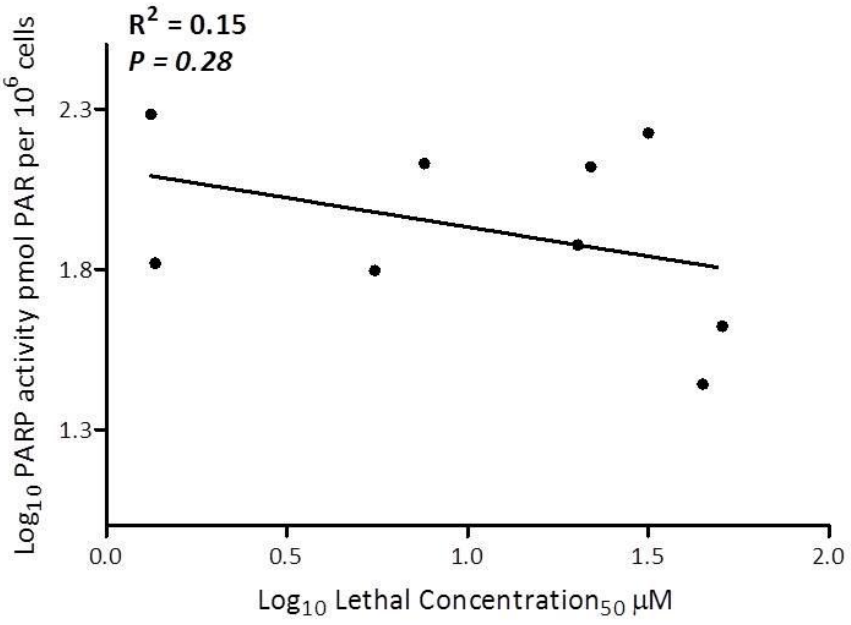

Figure 3.8: Relationship between baseline PARP activity and AG014699 sensitivity (log_{10} LC_{50}).

A dose of 10 µM AG014699 resulted in > 95% inhibition of PARP activity in all cell lines (mean = 96.6%) with no significant difference observed in the degree of inhibition between the HR + and the HR- cell lines. Results for certain cell lines are shown visually with an immunoblot example in figure 3.9 and the absolute % activity for all cell lines is shown graphically in figure 3.10.

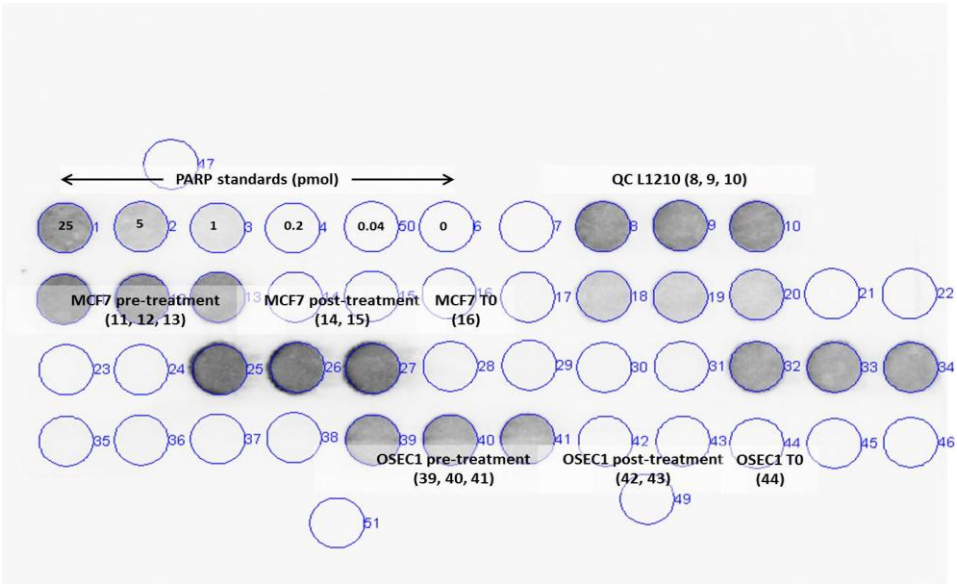

Figure 3.9: PAR formation immunoblot showing the affect on PAR levels by reduced luminescence following AG014699 treatment in MCF7 and OSEC1 cell lines.

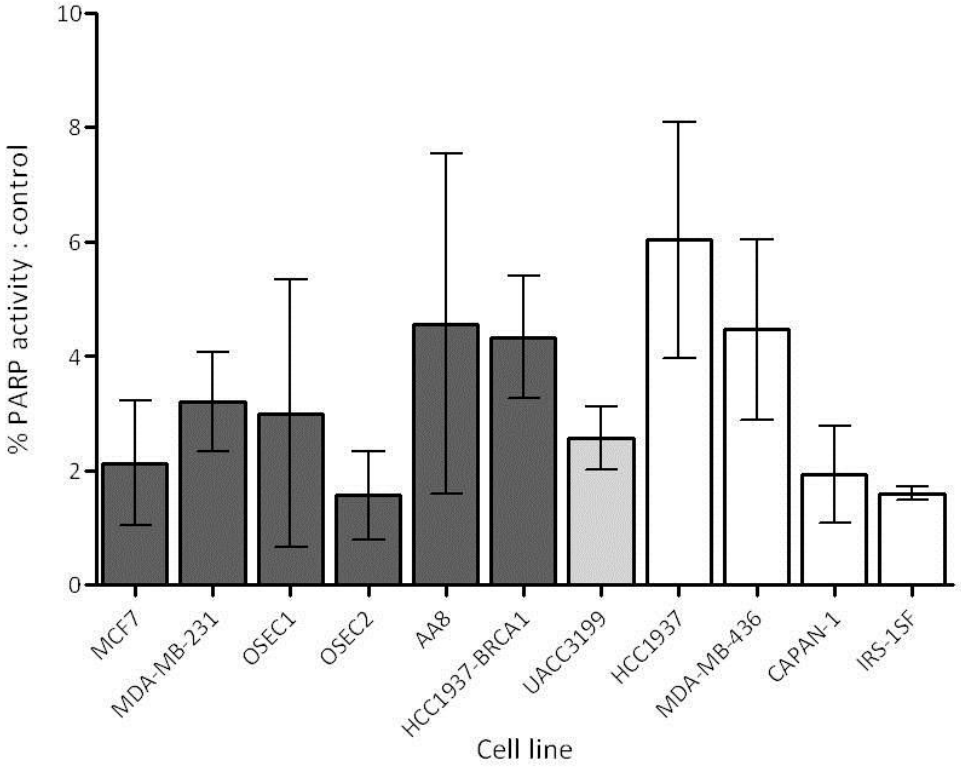

Figure 3.10: PARP activity following a 30 min exposure to 10 µM AG014699. Data expressed as % activity compared to the un-treated control are the mean (+ SEM) of three independent experiments. Note maximum value on y axis is 10%

Cell line	HR status	Mean PARP activity pmol PAR per 10^6 cells ± SD			PARP inhibition (%) over baseline levels (maximum stimulated)
		Endogenous baseline	Maximum stimulated Control	Maximum stimulated + 10 μM AG014699	
MCF7	+	75.30 ± 72.20	3901.00 ± 994.00	76.00 ± 73.60	98.05
MDA-MB-231	+	132.00 ± 31.20	2047.00 ± 1648.00	65.70 ± 21.60	96.79
OSEC1	+	27.70 ± 27.50	3500.00 ± 2357.00	145.30 ± 214.50	95.85
OSEC2	+	168.50 ± 21.90	3884.00 ± 2066.00	77.30 ± 79.20	98.01
AA8	+	42.00 ± 9.20	5633.00 ± 2589.00	72.30 ± 58.60	98.72
HCC1937-BRCA1	+	231.30 ± 75.40	6373.00 ± 94.30	294.00 ± 86.40	95.39
UACC3199	-	135.30 ± 20.40	4688.00 ± 1867.00	136.00 ± 14.00	97.10
HCC1937	-	594.70 ± 157.80	5615.00 ± 2874.00	352.00 ± 230.40	93.73
MDA-MB-436	-	192.30 ± 51.90	2649.00 ± 975.60	131.00 ± 47.50	95.05
CAPAN-1	-	62.70 ± 27.10	5830.00 ± 1395.00	106.70 ± 75.00	98.17
IRS-1SF	-	66.00 ± 56.90	5532.00 ± 2125.00	68.30 ± 43.00	98.77

Table 3.4: Summary data for PARP activity expressed as pmol PAR per 10^6 cells for all 11 cell lines. SD = standard deviation. Homologous Recombination (HR) status + denotes cells with proficient HR and – denotes deficient HR.

3.4.3 DNA double strand break formation in response to AG014699

To determine whether DNA double strand breaks (DSBs) accumulate after exposure to AG014699, DSBs were measured using the γH2AX focus Immunofluoresence assay, described in chapter two, section 2.7. Time-course experiments were undertaken to measure γH2AX foci after cell lines were treated with 10 μM AG014699 in 1% DMSO *or* vehicle control (1% DMSO) for up to 24 hours in culture medium at 37^{o}C. In addition, as a positive control for DNA damage, cells were exposed to 2 Gy (2.5 Gy/minute at 310 kV and 10 mA) of x-ray irradiation followed by incubation for 30 minutes in culture medium at 37^{o}C.

Results show a very rapid accumulation of DNA DSBs in all cell lines within the first hour following exposure to AG014699. Examples of the full time-course for the MCF7, UACC3199, MDA-MB-436 and CAPAN-1 cell lines are shown in figure 3.11.

In contrast, exposure to 2 Gy ionising radiation (IR) resulted in a peak of γH2AX foci at 30 minutes and disappearance of all foci by 8 hours indicating that DSB repair had occurred. The majority of the repair occurred during the first two hours. An example of these time-courses for the MCF7 human breast cancer cell line is included in figure 3.11.

Results for all 11 cell lines comparing the fold-change in γH2AX after 24 hours of AG014699 over the un-treated controls are shown in figure 3.13. 24-hours of 10 μM AG014699 resulted in a mean increase of 6-fold (range 1.9-10.2) in γH2AX foci compared with untreated control cells. Fold change was calculated by dividing the mean number foci per 30 nuclei in treated cells by the mean number of foci per 30 nuclei in control cells. There was no difference between the fold-change between the HR+ and the HR– cells when comparing the paired cell lines.

Of note, the number of γH2AX foci after 10 μM AG014699 counted were similar to that measured in the cells exposed to 2 Gy IR, see figure 3.14, highlighting the fact that AG014699 causes significant DNA damage. This point is also made visually by the fluorescent microscopy images of γH2AX foci in MCF7 cells following DNA damage from IR and AG014699 in figure 3.12.

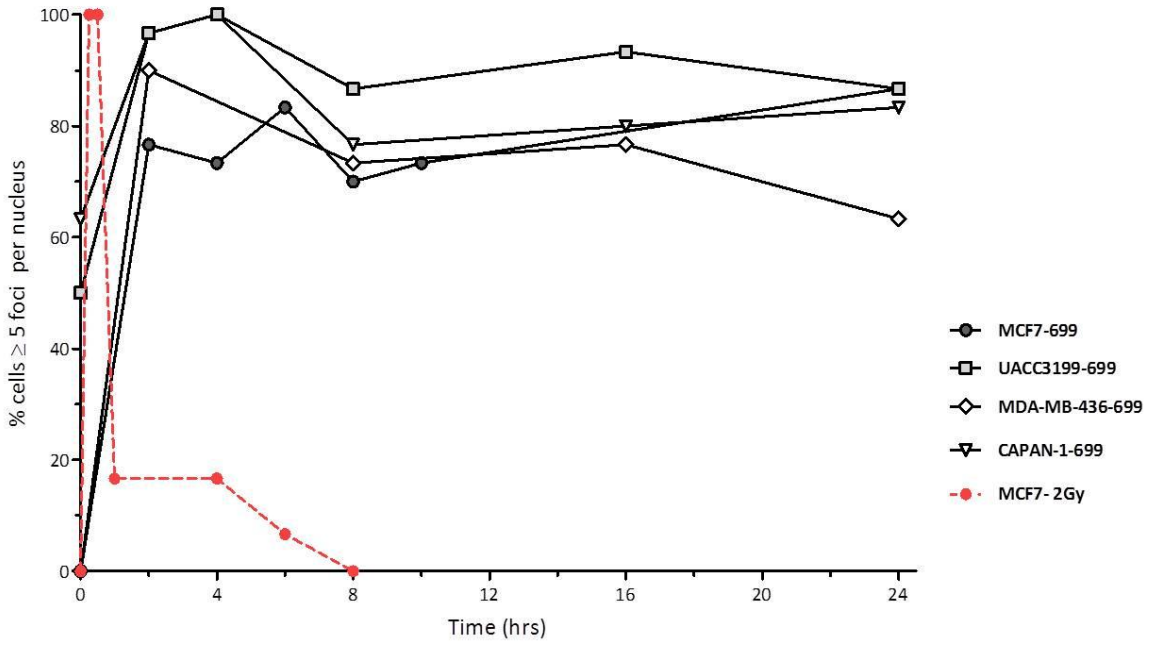

Figure 3.11: γH2AX foci time-course experiments in MCF7, UACC3199, MDA-MB-436 and CAPAN-1 cells following continuous exposure to 10 μM AG014699. For comparison, a time-course experiment following 2 Gy in MCF7 cells is shown. Results are the mean no. of cells with ≥ 5 foci per nucleus from three independent assays.

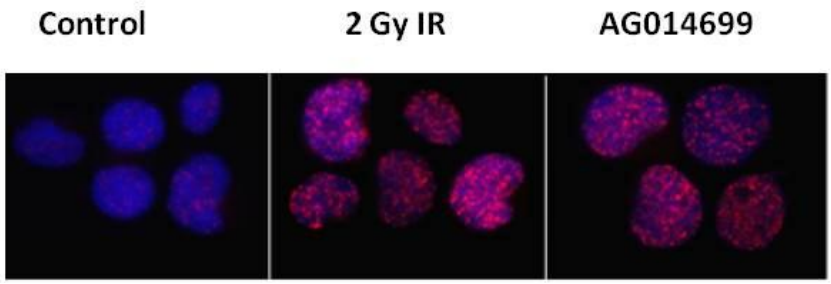

3.12: Immunofluoresence images for control, 2 Gy IR plus 30 minutes incubation and 24 hours of 10 μM AG014699 treated MCF7 cells. Nuclei are stained blue with DAPI and γH2AX foci detected fluoresce in red.

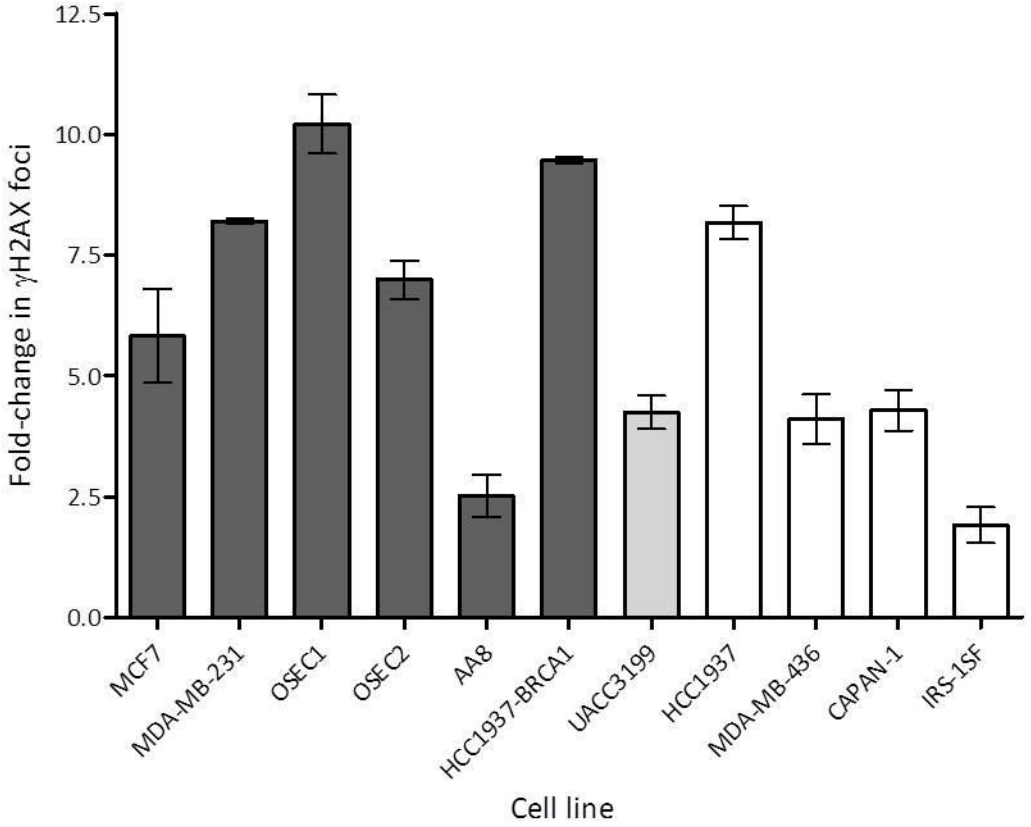

Figure 3.13: γH2AX foci following continuous exposure to 24h 10 µM AG014699. Data are fold change in foci + SEM for each cell line in 3 independent assays.

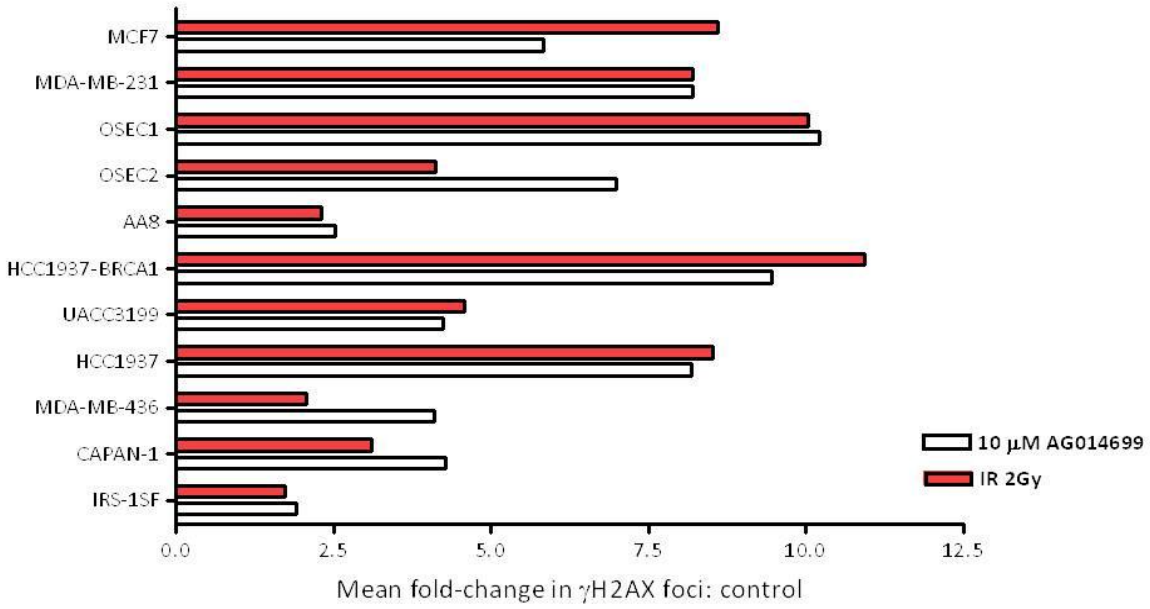

Figure 3.14: γH2AX foci following continuous exposure to 24h 10 µM AG014699 and following 2 Gy + 30 minutes. Data are mean fold change in foci in 3 independent assays.

3.4.4 Rad51 foci formation assay as a marker of Homologous recombination following AG014699

Localisation of Rad51 foci at DNA double strand breaks is an essential step in the HR repair pathway (Shinohara *et al*., 1992). The presence of nuclear Rad51 foci is considered a marker of functional homologous recombination in cells. To determine whether cells were able to repair AG014699-induced DNA DSB by HR, Rad51 foci were detected using the immunofluoresence assay described in chapter two, section 2.8. Cells were treated with 10 μM AG014699 in 1% DMSO *or* no drug (vehicle control; i.e. 1% DMSO) for 24 hours in culture medium at 37^{o} C *or* 2 Gy IR plus 2 hours incubation at 37^{o} C. An incubation of 2 hours following 2 Gy IR was chosen for these experiments as previous time-course experiments had demonstrated peak of Rad51 foci two hours following DNA damage with IR (unpublished data Yvette Drew, Newcastle University, UK).

Results show the number of Rad51 foci significantly increased in response to AG014699-induced DNA damage in cells with no known defect in HR but not in HR deficient cells. Examples of fluorescent microscopy images for control, 2 Gy IR plus two hours incubation and 24 hours 10 μM AG014699 treated MCF7 cells are shown in figure 3.15 below. Fold changes in the numbers of nuclear Rad51 foci in the human cancer cell lines in response to the three treatments are illustrated in figure 3.16

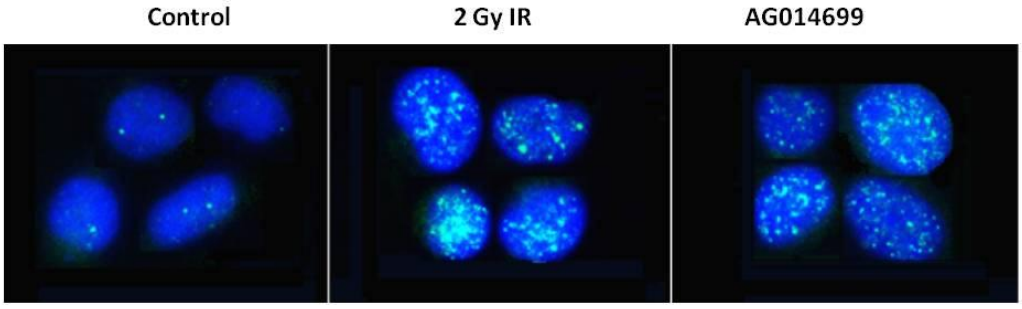

Figure 3.15: Immunofluoresence images for control, 2 Gy IR and AG014699 treated MCF7 cells. Nuclei stained blue with DAPI and Rad51 foci fluoresce in green.

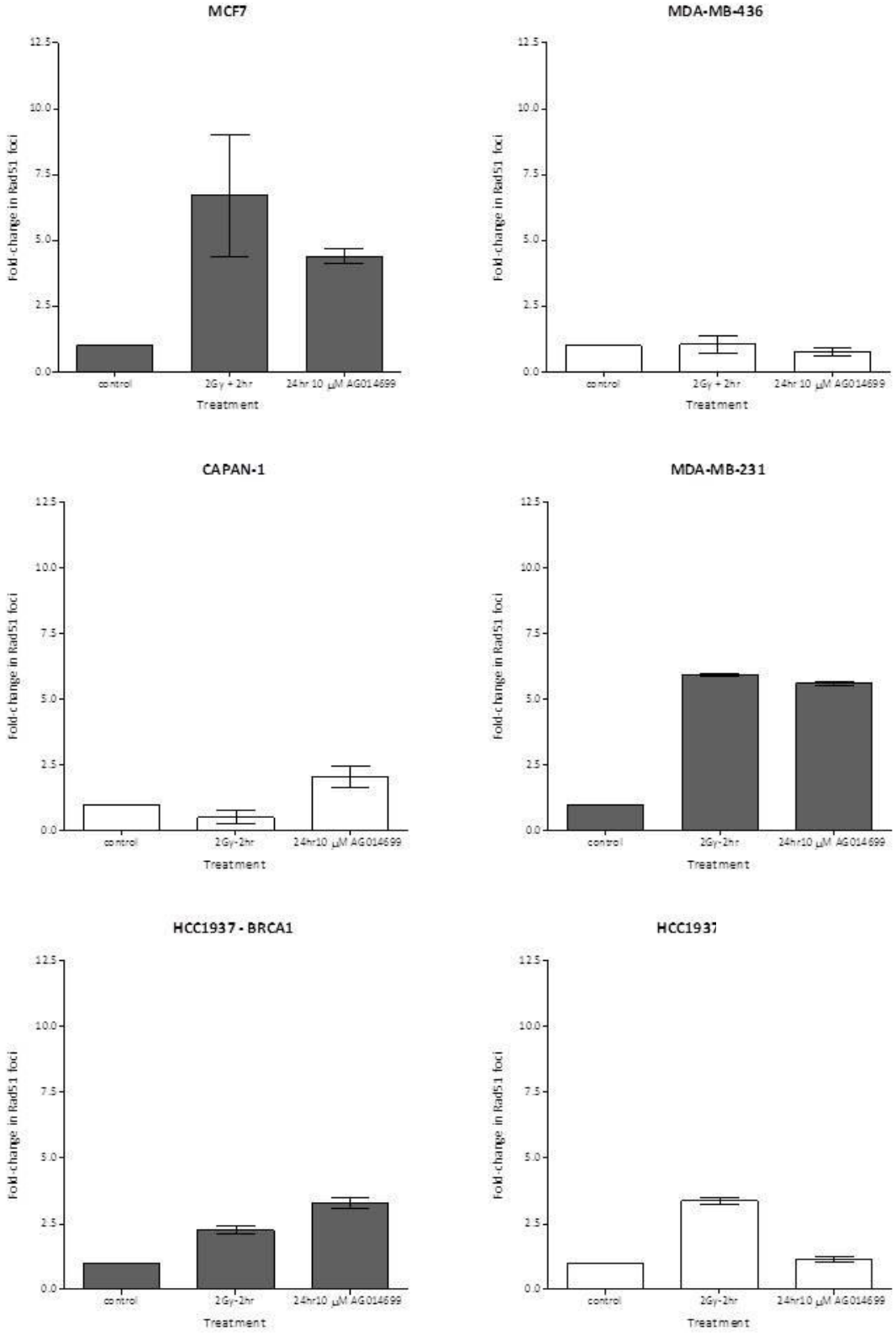

Figure 3.16: Fold-change in Rad51 foci in selected cell lines following; 24h 10 μM AG014699, 2Gy IR + 2 h incubation over un-treated controls. Data for each cell line (as labelled) is mean fold-change + SEM from 3 independent assays.

Results for all cell lines following treatment with AG014699 are seen in figure 3.17. The data demonstrate a statistically significant increase (mean increase = 3.8-fold, *P<0.001)* in the number of Rad51 foci compared with corresponding untreated control cells in the cell lines with functional HR (MCF7, MDA-MB-231, OSEC-2, AA8 and HCC1937-BRCA1) and in cells heterozygous for *BRCA2* (OSEC1). However, AG014699 exposure did *not* cause a significant increase in Rad51 foci in the *BRCA1/2* mutated MBA-MB-436, CAPAN-1 and HCC1937 cells, the *BRCA1* epigenetically silenced UACC3199 cells, or the *XRCC3*-mutated IRS-1SF cells (mean change = 1.0-fold).

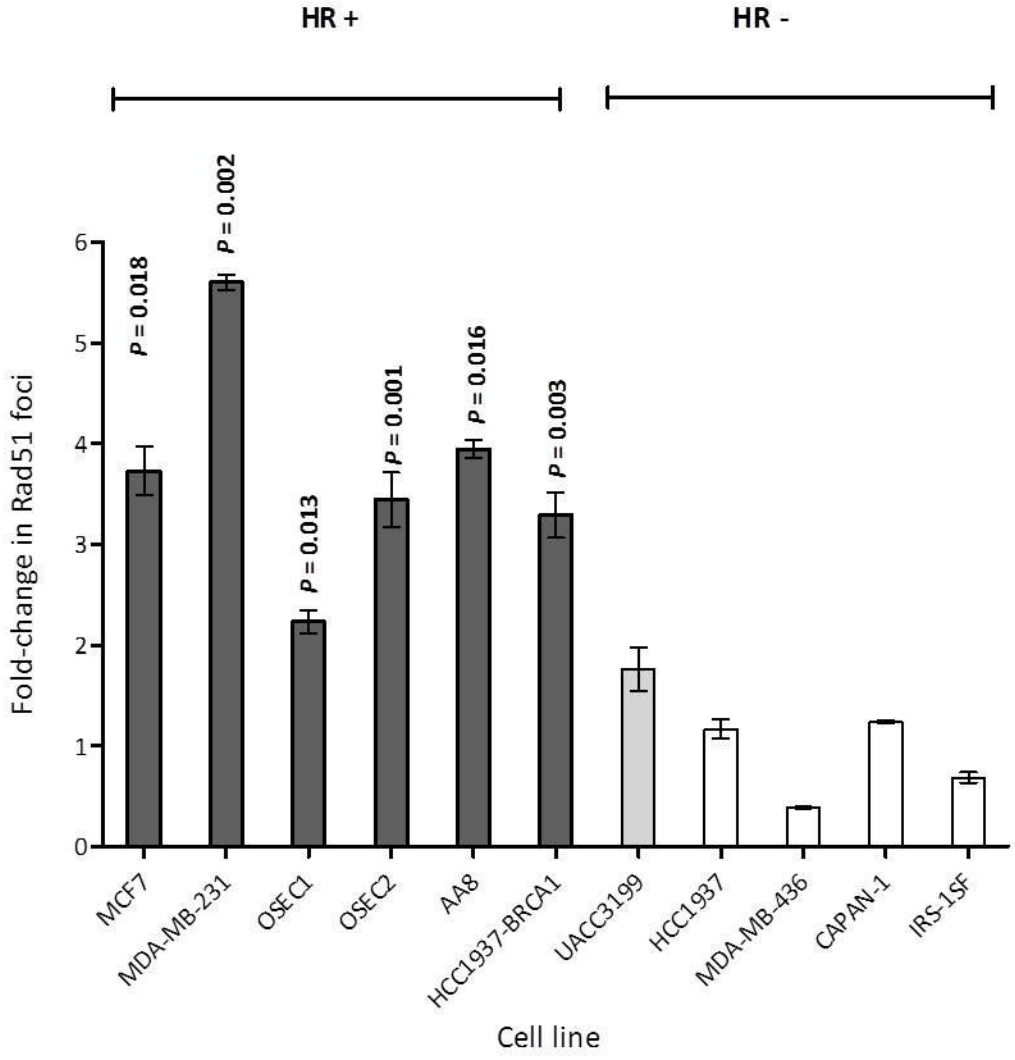

Figure 3.17: Rad51 foci Immunofluoresence following continuous exposure to 24h 10 µM AG014699. Data are fold change in foci + SEM for each cell line in 3 independent assays.

The cell lines were subsequently separated into two groups based on their ability (yes or no) to increase nuclear Rad51 levels by ≥ 2-fold over baseline levels following AG014699 corresponded exactly to the original HR – and HR+ groupings; with the UACC3199 cell line falling into the 'No' group. There was, as expected, a difference in the sensitivities to AG014699 between the two groups with mean LC_{50} = 4.6 μM in the No group significantly lower than the mean LC_{50} = 29.7 μM in the yes group.

These data suggest that changes in nuclear Rad51 foci in response to AG014699 could be used a biomarker of functional HR and should be further investigated.

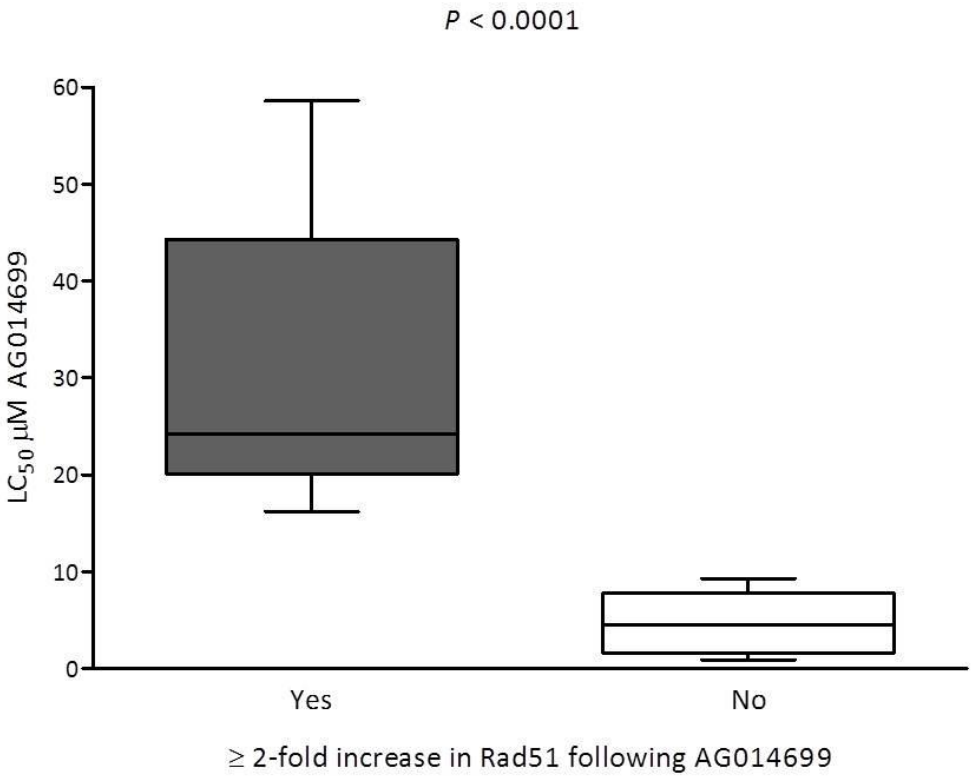

Figure 3.18: Box and whiskers plot of LC_{50} of AG014699 by cell lines ability to increase Rad51 foci by ≥ 2-fold in response to 10 μM AG014699. The line represents the median values.

3.5 Discussion

Several important observations have emerged from these studies. Firstly, the results of cytotoxicity assays demonstrate that PARP inhibition is selectively toxic to human cancer cell lines with mutated *BRCA*1/2 confirming the concept of synthetic lethality. In addition, these data demonstrate that inhibiting PARP-1 is synthetically lethal to non-germline *BRCA* mutated cells i.e. those with epigentically silenced *BRCA*1 or cells deficient in *XRCC3,* suggesting a wider therapeutic role for these novel agents. The immunofluorescence studies have shown that DNA damage accumulates with on-going AG014699 exposure highlighting the mechanism of action of PARP inhibitor-induced cytotoxicity. Results of PARP activity assays confirm that this selective toxicity is not due to differences in degree of PARP enzyme inhibition. Finally, Rad51 immunofluorescence assays have demonstrated that a ≥ 2-fold increase change in Rad51 foci after AG014699 can discriminate between HR proficient and deficient cells suggesting that this may be useful as a biomarker in patients and requires further investigation.

3.5.1 AG014699 is synthetically lethal in BRCA*1/2 mutated and epigenetically silenced* BRCA*1*

Human cancer cell lines with mutated *BRCA1* and *BRCA*2 are sensitive to PARP inhibitor therapy. These results support those previously published showing selective sensitivity to PARP inhibitors in non-cancer, non-human BRCA1/2-deficient models (Bryant *et al*., 2005; Farmer *et al*., 2005) and contrast with previous studies that failed to show such sensitivity in human cancer models (Gallmeier and Kern, 2005; De Soto *et al*., 2006). The *BRCA*1 mutant MDA-MB-436 cells were the most sensitive human cancer cell line to AG014699-induced cytotoxicity. They also formed the lowest number of Rad51 foci in response to AG014699, suggesting that these cells had the most profound HR deficiency. The highlight of these cytotoxicity experiments is the discovery that *BRCA*1 methylated UACC3199 breast cancer cells were sensitive to AG014699 with mean LC_{50} significantly lower than the HR proficient cells (7.6 μM *vs*. 29.7; $P = 0.002$).

The methylation status of *BRCA*1 in these cells had been confirmed by Valerie Deregowski (University of Leven, Belgium) by methylation-specific polymerase chain

reaction and a defect in HR is suggested by the observation in these studies that prolonged exposure to AG014699 failed to induce a significant increase in Rad51 foci.

These UACC3199 data are highly relevant as they suggest that PARP inhibitors could have therapeutic potential in sporadic, non-germline *BRCA* mutated tumours with epigenetic changes in the HR genes. *BRCA1* dysfunction by epigenetic gene silencing has been reported in 18% of high grade serous ovarian cancers (HGSOC) (Press *et al*., 2008) and reduced BRCA1 mRNA expression is known to be a common feature of triple negative breast cancers (Turner *et al*., 2007). Clinical trials of PARP inhibitors in these populations are on-going (www.clinicaltrials.gov). A phase II study investigating the single agent role of the PARP inhibitor olaparib recently reported a response rate, as assessed by the RECIST; of 24% in the patients with non-germline *BRCA* mutated HGSOC (Gelmon *et al*., 2011). In addition, PARP inhibitors as maintenance therapy in HGSOC is currently being investigated with the interim results of a phase II study recently announced (Ledermann *et al*., 2011). The study randomised patients with platinum sensitive (defined by the protocol) HGSOC on a 1:1 basis to olaparib 400 mg twice daily or placebo until disease progression. Preliminary results showed a significant benefit in progression-free survival (8.4 vs. 4.8 months; $P < 0.00001$) favouring the maintenance olaparib.

To date no single agent activity has been seen in patients with triple negative breast cancer and this may mean that the degree of *BRCA*1 dysfunction is not enough to induce HRD. However the results of further studies are awaited.

The results of *in vivo* studies investigating the anti-tumour effect of AG014699 on *BRCA* deficient animal models, including UACC3199 xenografts, are presented and discussed in chapter four.

3.5.2 PARP activity and response to AG014699

In order to further investigate the underlying mechanisms behind the selective sensitivity of HR defective cells to AG014699, levels of baseline PARP activity and PARP enzyme inhibition following AG014699 were determined. Results for all 11 cell lines showed an increase in the mean baseline PARP activity of the HR deficient *vs*. the HR proficient cell lines but this did not reach statistical significance ($P = 0.34$). Data for the human cancer cell lines showed a higher mean activity in the HR deficient cells *vs.*

proficient cells but again this was non-significant ($P = 0.52$). Data for the paired human breast cancer HCC1937 and HCC1937-BRCA1 cell lines however did show a significant difference in endogenous PAR levels with higher levels seen in the HR deficient HCC1937 line (mean = 594.7 *vs*. 231.3 pmol PAR per 10^6 cells, $P = 0.02$, un-paired t-test). These data suggest that PARP activity might be higher in HR deficient cells and is supported by the recent report by Gottipati *et al* that PARP-1 is hyperactivated (measured by baseline PAR levels) in *BRCA2* deficient replicating cells. The authors proposed that HR defective cells may have an over-reliance on PARP-1 and that this may, in part, explain their increased sensitivity to PARP inhibitors (Gottipati *et al*., 2010).

PARP activity levels have been measured in patient samples in a number of PARP inhibitor clinical trials to determine the efficiency of PARP inhibitors. A recent review of these studies proposed that baseline PARP activity levels may be able to determine which patients are sensitive to these agents and prove a useful biomarker of HR function (Redon *et al*., 2010). Results of baseline PARP activity and patient response to AG014699 from the phase II BRCA-PARP study are presented and discussed in chapter five of this thesis.

Following a dose of 10 μM AG014699 profound inhibition of PARP-1 (>95%) was achieved in all cell lines; demonstrating that the PARP inhibitor freely permeated cells, binds to and inactivates PARP-1, and that the PARP inhibition persists during cell permeabilization and subsequent PARP enzyme stimulation. There was no statistically significant difference in the degree of PARP inhibition across the cell lines. This suggests that the difference in sensitivity seen in the cytotoxicity assays is unlikely to be due to differences in drug delivery or binding and more likely due to differences in pathways downstream of PARP enzyme inhibition.

3.5.3 The mechanism of AG014699 selective cytotoxicity

The proposed mechanism of selective AG014699 toxicity in HR defective cells is that PARP-1 inhibition leads to accumulation of DNA single-strand breaks which during replication are converted to DNA double-strand breaks, represented by γH2AX foci. In HR competent, BRCA1/2-proficient cells, these double-strand breaks will eventually be repaired by the error-free HR repair pathway, accompanied by Rad51 foci formation. However, in HR-deficient cells, repair does not occur resulting in the accumulation of

double-strand breaks and cell death. To investigate this, γH2AX and Rad51 foci immunofluoresence experiments were undertaken. Results of γH2AX immunofluoresence assays demonstrate an increase in γH2AX foci in all 11 cell lines treated with 24 hours 10 μM AG014699 compared with the untreated control cells. Results of time-course experiments seen in figure 3.10 confirm that DNA DSBs do accumulate with continuous AG014699 exposure with little resolution despite functional HR.

The variation in the absolute numbers of γH2AX foci seen between cell lines could be secondary to differences in DNA content, S-phase cell fraction, and cell-number doubling times between individual cell lines. It is less likely as a result of differences in HR status because no difference was found in control cells for the parental BRCA1-mutated HCC1937 and the BRCA1-corrected HCC1937–BRCA1 cell lines (mean no. foci per nucleus = 11.5 ± 3.4 *vs*. 6.5 ± 0.7, *P = 0.12*, un-paired t-test).

The data presented in figure 3.13 shows that a 24-hour exposure to 10 μM AG014669 induces a level of DNA DSBs similar to that caused by 2 Gy IR. This raises the question could continuous PARP inhibition in *BRCA* mutation carrier patients be dangerous resulting in an accumulation of DNA damage and subsequent genomic instability?

Encouragingly, the cytotoxicity data from these studies have not shown the *BRCA*1/2 heterozygous cell lines to be sensitive to short-term AG014699 exposure. In addition, early clinical trials using the continuous dosing schedule of the PARP inhibitor, olaparib, have reported the drug to be well tolerated; although long-term safety data from these studies is not yet available (Fong *et al*., 2009; Tutt *et al*., 2010; Audeh *et al*., 2010; Gelmon *et al*., 2011).

3.5.4 Rad51 as a biomarker of HR

Rad51 foci formation was assessed in all 11 cell lines following a 24 hour exposure to AG014699 or 2 Gy IR plus 2 hour incubation. Results following AG014699, presented in figure 3.13, show that all cell lines have some level of baseline nuclear Rad51 foci but a significant increase is only seen in the HR proficient cells, confirming the proposed mechanism of PARP inhibitor-induced synthetic lethality.

The UACC3199, *BRCA1* methylated, cells also failed to increase Rad51 foci significantly in response to AG014699 suggesting that the sensitivity to AG014699 observed in clonogenic assays is most likely secondary to defective HR.

A ≥ 2-fold increase in Rad51 foci after AG014699 appears to discriminate between the HR proficient and deficient cells. This observation was further tested in a clinical study of 25 primary cell cultures derived from ascites from ovarian cancer patients with unknown HR status. The study demonstrated that a 2-fold or greater increase in Rad51 foci following *ex vivo* treatment with AG014699 could predict subsequent sensitivity to the PARP inhibitor AG014699 in cytotoxicity assays with 100% positive predictive value. The authors concluded that Rad51 should be further investigated as biomarker for HR (Mukhopadhyay *et al*., 2010).

However, the use of Rad51 as a biomarker to predict for HR function is problematic. For example, these studies have shown the presence of Rad51 foci in the control, un-treated cells of the known HR – cell lines. This confirms published work by Tarsounas *et al* demonstrating that Rad51 foci form in un-irradiated CAPAN-1 cells. Using laser-scanning cytometry to determine cell cycle stage, they unequivocally showed the Rad51 foci to be S-phase replication associated (Tarsounas *et al*., 2003). In addition, Henry-Mowatt *et al* demonstrated that Rad51 localises to chromatin and plays a role in the progression of stalled replication forks when they encounter DNA lesions during S phase (Henry-Mowatt et al., 2003). These studies show that Rad51 foci form not *only* as part of the HR response to DNA damage but also in a *BRCA*2-independent manner as part of the normal cell cycle. Interestingly, data for the HR-, *BRCA1* mutant HCC1937 cell lines shows a significant increase in Rad51 foci following IR over un-treated controls (mean = 40.33 *vs.* 12 foci per nucleus, $P < 0.0001$, un-paired t-test) and no significant increase in Rad51 foci following exposure to 10 μM AG014699. One possible explanation for this is that these foci were all S-phase related and not part of the DNA damage HR repair process. Another is that radiation-induced DNA damage is heterogeneous and can result in base modifications, inter-strand crosslinks, single strand and double strand breaks and recent work by Petermann *et al* demonstrates that IR -induced DNA damage can contribute to the formation of replication-induced DSB which can be detected as Rad51 foci (Petermann *et al*., 2010).

These studies all suggest that two distinct Rad51 mediated pathways exist; one involved in HR the other localising to the exposed single strand DNA ends during replication and that the presence of nuclear Rad51 foci *per se* cannot be used to reflect functional HR. What is needed are functional assays that can assess changes in Rad51 foci in real time following DNA damage. But there are problems with these approaches, the most obvious is the need to obtain viable, replicating cells; another is the technical difficulties in inducing DNA damage *ex vivo*. In the end such assays may not be practical in the normal clinical practice out with a translational study.

3.6 Conclusions

To conclude, these *in vitro* studies demonstrate that the PARP inhibitor AG014699 is selectively toxic to cancers defective in HR DNA repair. They have shown that DNA DSBs accumulate following treatment with AG014699 and that a subsequent failure to activate HR repair underlies this selective toxicity. No significant differences were seen in the degree of PARP inhibition or baseline PARP activity levels between the cell lines to account for the selective cytotoxicity. In addition these data have shown the epigenetically silenced *BRCA*1 UACC3199 cell line to be sensitive to PARP inhibition suggesting a wider role for PARP inhibitors in cancers defective in homologous recombination repair in the absence of germline *BRCA* mutations.

Chapter Four

4. *In vivo* studies of the effects of AG014699 in *BRCA* deficient xenografts

4.1 Introduction

Data presented in chapter three of this thesis and recently published (Drew *et al*., 2011b) have shown that AG014699 is selectively toxic to human cancer cell lines with mutations within the *BRCA*1 and 2 genes. This supports the theory of synthetic lethality and adds weight to the original reports demonstrating PARP inhibitor sensitivity in *non*-cancerous and *non*-human cell lines (Bryant *et al*., 2005; Farmer *et al*., 2005). The results of experiments presented in chapter three also highlight that cells with defects in the HR repair pathway, other than by *BRCA* mutation, i.e. by methylation of *BRCA*1 or loss of *XRCC3*, can also be sensitive to PARP inhibition by AG014699.

At the time this work was undertaken published *in vivo* data supporting the theory of the synthetic lethality of PARP inhibitors in *BRCA* defective cancers were limited. In 2005 Bryant *et al* had reported that treatment of tumours derived from *BRCA*2 deficient V-C8 Chinese hamster lung fibroblast cell line with the PARP inhibitor AG14361 [5 days intra-peritoneal (i.p.)] resulted in 3/5 responses including one complete remission. There were no responses in the *BRCA*2 complimented (V-C8+B2) xenografts (Bryant *et al*., 2005), suggesting that anti-tumour activity with AG14361 occurs only in the xenografts with defective DNA repair capacity. In the sister Nature paper Farmer *et al* investigated the role of the PARP inhibitor KU0058684 in preventing the formation of teratocarcinomas in athymic mice after transplantation of *BRCA*2 deficient embryonic stem (ES) cells or *BRCA*2 proficient ES cells. A significant reduction was observed in the number of tumours formed in the *BRCA*2 deficient ES cell lines compared to the proficient ES cells. It should be noted that these studies have limitations; they used only *BRCA*2 deficient models and tested *non*-human and *non*-cancerous cell lines. It may be difficult to reproduce these results in genetically more

complex models such as human cancers. Therefore the question remained unanswered: can PARP inhibitors selectively kill human cancers with *BRCA* mutations?

De Soto and colleagues set out to answer this question by investigating the effects of different PARP inhibitors on both BRCA1 $^{-/-}$ and *BRCA*1 $^{+/+}$ human breast cancer xenografts (De Soto *et al*., 2006). They first compared the *in vitro* sensitivity of a panel of 12 cell lines, including *BRCA1*$^{-/-}$*, BRCA1*$^{+/-}$ *and BRCA1* $^{+/+}$ embryonic stem (ES) cells, three murine mammary tumour cell lines and four human breast cancer cell lines with differing *BRCA*1 status, to the PARP inhibitors AG14361, NU1025 and 3-AB. The human breast cancer cell lines were MCF7 (BRCA1$^{+/+}$), MDA-MB-231 (BRCA1$^{+/-}$), HCC1937 (BRCA1$^{-/-}$) and SUM1315M02 (BRCA1$^{-/-}$). Using clonogenic cell survival and growth inhibition assays they observed that the *BRCA1*$^{-/-}$ mutant ES cells were significantly more sensitive to the PARP-1 inhibitor AG14361 than the wild type or heterozygous *BRCA*1 ES cells. The mouse mammary cell lines displayed a similar result, with the BRCA1$^{-/-}$ mutant cell being the most sensitive to AG14361. However it was not significantly more sensitive than its *BRCA*1 complemented controls and it was much less sensitive to PARP inhibition than the *BRCA*1$^{-/-}$mutant ES cell line. Finally the human breast cancer cell lines failed to show any selective toxicity by *BRCA*1 status to AG14361-induced PARP-1 inhibition. These findings were confirmed in the *in vivo* studies when nude mice with human breast cancer xenografts of differing *BRCA*1 status were exposed to three consecutive days of AG14361 (30 mg/kg) i.p. starting on D2, 9 and 16. The authors concluded that non-cancerous, non-human genetically naïve *BRCA* mutant cells were selectively sensitive to PARP-1 inhibitors but *not BRCA*1 mutated human cancers. They proposed that this was because human cancers have acquired resistance through secondary mutations and suggested that PARP inhibitors as single agents do not have a therapeutic role in the treatment of *BRCA*-mutated cancers.

In view of the limited and conflicting published data, studies were undertaken as part of this thesis to develop xenograft models of the *BRCA*1 mutated human breast cancer cell line MDA-MB-436, the *BRCA*2 mutated human, pancreatic carcinoma cell line CAPAN-1 and the *BRCA*1 methylated breast cancer cell line UACC3199, to investigate both the anti-tumour effects and the toxicity of differing schedules of the potent, specific PARP-1 inhibitor AG014699 in these models. UACC3199 cells were investigated

in order to confirm or refute the *in vitro* data presented earlier that UACC3199 cell lines are also sensitive to PARP inhibition.

Additionally, i*n vitro* studies have shown *BRCA* mutant cells to be hypersensitive to platinum agents (Bhattacharyya *et al*., 2000). Therefore the cisplatin analogue, carboplatin, was also used to act as a positive control and to investigate combined PARP inhibitor anti-tumour activity.

4.2 Objectives

The aims of this study were as follows:

- To establish xenograft models in mice using the following human cancer cell lines mutated *BRCA*1 (MDA-MB-436), mutated *BRCA*2 (CAPAN-1) and epigenetically silenced *BRCA*1 (UACC3199).
- To investigate the anti-tumour activity and toxicity of AG014699 in these xenografts.
- To determine whether different scheduling of AG014699 in the above xenograft models could affect anti-tumour activity.
- To investigate the activity of AG014699 combination with carboplatin

4.3 Materials and Methods

4.3.1 General animal husbandry

CD-1 nude mice (female and aged 10–12 weeks) from Charles River laboratories (Wilmington, MA) were used in all xenograft experiments. These mice were maintained and handled in isolators under specific pathogen-free conditions, with five mice per cage and 20 cages per isolator. All experiments involving mice were reviewed and approved by the relevant institutional animal welfare committee and then performed according to the UK Coordinating Committee on Cancer Research Guidelines for the Welfare of Animals in Experimental Neoplasia and UK law. For these experiments, mice were treated with drug or control vehicle between the hours of 09.00 and 11.00. Treatments were all administered by i.p. injection in the animal's home cage within the animal facility. Mice were killed by cervical dislocation for the

following reasons: tumour size was greater than 10 × 10 mm, weight loss was more than 15% of baseline, or the study ended as defined a priori.

4.3.2 Cell line implantation

MDA-MB-436, CAPAN-1, and UACC3199 xenografts in CD-1 nude mice were used to test the efficacy of AG014699 because these models represent *BRCA1*-mutated, *BRCA2*-mutated, and *BRCA1*-silenced tumours, respectively. Further characteristics of these cell lines and including details of their respective *BRCA* mutation are found in table 3.1 in chapter three.

Exponentially growing MDA-MB-436, CAPAN-1 and UACC3199 cells were re-suspended in phosphate-buffered saline at a concentration of 1×10^7 cells per 50 µl. 50 µl of the cell suspension was then injected subcutaneously into one site on the right flank of each mouse. When sufficient mice (to allow five mice per treatment group) had palpable tumours (i.e. ≥5 x 5 mm), the mice were randomly assigned, to avoid bias, to treatment groups. Investigators were not blinded to the treatment groups.

This work was undertaken by Dr Yvette Drew and Dr Evan Mulligan under the supervision of Mr Huw Thomas. Details of the individual experiments undertaken for each xenograft model are listed below.

4.3.3 UACC3199

Treatment groups for mice bearing UACC3199 xenograft tumours in experiment one were as follows: control normal saline (10 ml/kg) administered once daily for 10 days, AG014699 (25 mg/kg) administered once daily for 10 days or a single dose of carboplatin (75 mg/kg) administered on day 1. Treatment groups in experiment two were as follows: control normal saline (10 ml/kg) administered once daily for 5 days of a 7-day cycle for six cycles, AG014699 (10 mg/kg) administered once daily for 5 days of a 7-day cycle for six cycles or a single dose of carboplatin (75 mg/kg) on day 1.

4.3.4 MDA-MB-436

Treatment groups were as follows: control normal saline (10 ml/kg) administered once daily for 5 days of a 7-day cycle for six cycles, AG014699 (10 mg/kg) administered once daily for 5 days of a 7-day cycle for six cycles or a single dose of carboplatin (75 mg/kg) on day 1.

4.3.5 CAPAN-1

The six treatment groups were as follows: (i) control normal saline (10 ml/kg) daily for 10 days, (ii) AG014699 (10 mg/kg) once a day for 10 days, (iii) AG014699 (10 mg/kg) once daily for 5 days of a 7-day cycle for six cycles (iv) a single dose of carboplatin (75 mg/kg) on day 1, (v) a combination of carboplatin (75 mg/kg) on day 1 and AG014699 (10 mg/kg) once a day for 10 days or (vi) a combination of carboplatin (75 mg/kg) on day 1 with AG014699 (10 mg/kg) once a day for 5 days of a 7-day cycle for six cycles.

4.3.6 Rationale for dose and schedule of AG014699

The initial schedule and dose of AG014699 selected for these *in vivo* experiments was 25 mg/kg i.p. once daily for ten consecutive days. A dose of 25 mg/kg in mice has been shown (unpublished data by Huw Thomas, Newcastle University, UK) to give equivalent plasma drug concentrations to that measured in patients who received a 12 mg/m^2 dose of AG014699 in the phase II combination study (Plummer *et al*., 2006). This dose, when given intermittently i.e. D1-5 of a 21 D cycle for six cycles, has also been shown to be safe and non-toxic in *BRCA*$2^{+/-}$ transgenic mice (Drew *et al*., 2011). At the time these experiments began a more prolonged or even a continuous dosing schedule of AG014699 had not been considered. It was not until preliminary data from these *in vivo* experiments and clinical efficacy data from the PARP-BRCA phase II clinical trial became available that this was proposed. These interim data suggested that longer, more sustained PARP inhibition might be necessary to improve the anti-tumour activity of AG014699 in *BRCA*-defective cancers. Therefore subsequent experiments investigated the prolonged AG014699 regimen of 10 mg/kg once daily for 5 days of a 7 day cycle for six cycles.

4.3.7 Use of carboplatin

The cytotoxic platinum analogue carboplatin was developed in the late 1980s at the Institute for Cancer Research, London, UK (Harrap, 1985). It acts by covalently binding to DNA to form intra-strand and inter-strand DNA cross-links. These DNA adducts then inhibit DNA synthesis, function and ultimately its transcription. Carboplatin forms the backbone of treatment for many cancers including ovarian cancer, small and non-small cell lung cancers, germ cell tumours and head and neck cancers (Chu E and DeVita V., 2010). It is postulated that a patient's *BRCA* status may modulate their subsequent response to the platinum agents. Pre-clinical studies have shown that cancer cell lines

with mutations in either the *BRCA*1 or *BRCA*2 genes are more sensitive to the platinum analogue - cisplatin than their wild type matched controls (Bhattacharyya *et al*., 2000; Tan *et al*., 2008; Tassone *et al*., 2003). Tassone and colleagues demonstrated that the *BRCA*1 mutated human breast cancer cell line HCC1937 was significantly more sensitive to cisplatin than MCF7 (*BRCA*1 wild type) and the MDA-MB-231 (*BRCA*1 heterozygote) cell lines. In addition, the HCC1937 cancer cell line was shown to be less sensitive or even resistant to the anti-microtubule agent paclitaxel (Tassone *et al*., 2003). Small retrospective studies in patients with ovarian cancer (discussed in chapter one, section 1.3.6) also suggest that *BRCA* mutation carriers respond better to carboplatin than non-carriers (Tan *et al*., 2008).

This question of platinum sensitivity and taxane resistance in *BRCA* mutation carriers has not yet been proven in a randomised clinical trial setting. However, a phase II trial is currently ongoing randomising patients with *BRCA*1/2 mutated breast cancer at first presentation of metastatic disease to six cycles of carboplatin or standard treatment with the anti-microtubule agent docetaxel (www.brcatrial.org).

In light of all these data, it was considered important to investigate carboplatin in these experiments. Firstly, to act as a positive control for DNA damage, secondly to enable any observed anti-tumour effects of the PARP inhibitor AG014699 to be directly compared with a cytotoxic to which these xenografts should be sensitive, and finally to investigate anti-tumour effect and toxicity of the combination.

4.3.8 Anti-tumour response assessment

Mice were weighed and tumour volumes determined daily from two-dimensional calliper measurements using the equation:

$a^2 \times b/2$, where a = width and b = length of the tumour.

Tumour data are presented in the results section as the dimension-less parameter, relative tumour volume (RTV). For example, RTV1 is the tumour volume on the first day of treatment (day 0), RTV2 is two times larger than RTV1; RTV3 is three times larger than RTV1 and so on. Tumour growth delay (TGD) was measured in days using the formula:

TGD = Time to specified RTV in treatment group (days) – Time to specified RTV in control group (days)

Any additional effect of combining AG014699 to the cytotoxic carboplatin on tumour growth delay (TGD) was assessed by measuring % Enhancement (E) using the formula:

% E = [(TGD of the combination treatment/TGD of cytotoxic alone) × 100] - 100.

4.3.9 Statistical analysis

Values relating to the comparison of means are generated using un-paired t-tests for comparisons of two means or one way analysis of variance (ANOVA) for comparisons of greater than two means. All statistical tests were considered significant if the *P* value < 0.05. Statistical tests were two-sided.

4.4 Results

All *in vivo* data and statistical analysis are summarised in table 4.1 and results of individual experiments are analysed and discussed in the relevant text. To facilitate interpretation of these results a key is provided in figure 4.1 below. Each symbol and line pair represents a different treatment arm and is used consistently throughout the figures in this chapter. The only exception is in figure 4.8 and 4.9 where the D 1-10 schedule of AG14699 is dosed at 10 mg/kg rather than 25 mg/kg.

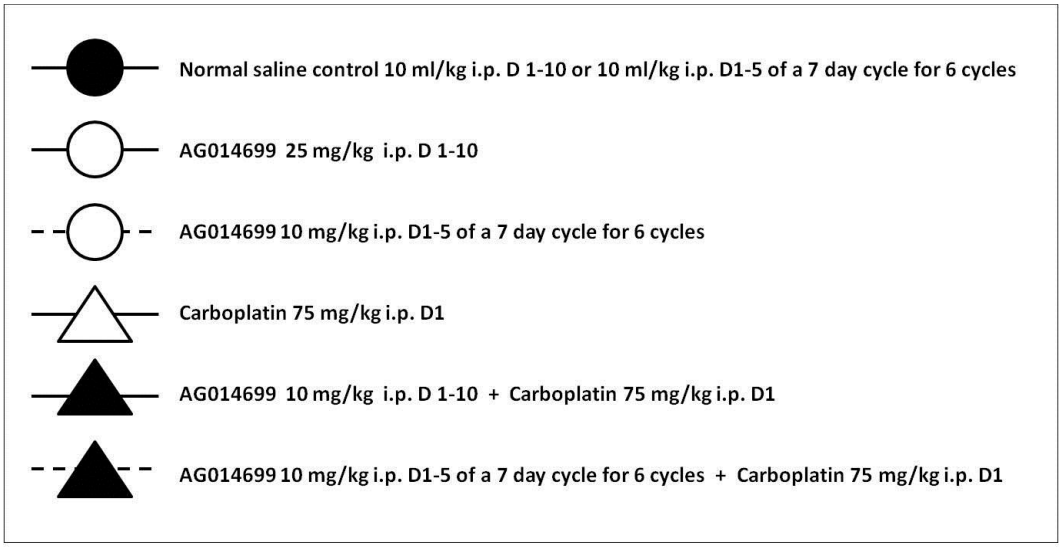

Figure 4.1: Key for *in vivo* experimental treatment arms.

4.4.1 Epigenetically silenced BRCA1 UACC3199 xenografts: experiment one

Of the 30 mice implanted with epigenetically silenced *BRCA1* UACC3199 cells, only 15 developed tumours by day 40. These 15 mice were then randomly assigned to the following treatment groups (five mice per group): normal saline control (10 ml/kg D1-10), AG014699 (25 mg/kg daily for D1-10) or carboplatin (single dose of 75 mg/kg on D1). The fifteen tumours that developed did so at different rates with a lag time from implantation to palpable tumour (≥ 5 mm x 5 mm) ranging from 21 to 32 days. Due to this variable lag time, there was an up to seven-fold variation in the individual tumour volumes (range = 33 mm^3 – 242 mm^3) when the treatments were initiated on day one. However, the mean tumour volumes of the five mice in each treatment group: control (99 mm^3), AG014699 (105 mm^3) and carboplatin (122 mm^3) did not differ significantly (99 *vs*. 105 *vs*. 122 mm^3; $P = 0.87$). Following day one of treatment, the UACC3199 tumours in all three groups grew relatively slowly; the control tumours reached only a mean RTV of 2.63 at day 10. However, because of the large range of tumour volumes at day one, by day 12 at least 2/5 mice in each group had to be killed because their individual tumour burden was greater than the specified 10 × 10 mm. For this reason and to make for more accurate comparisons of the results, only the data collected up to and including day 12 are presented here. Results for the RTV over time of each individual mouse within each treatment group are shown in figure 4.2 with mean data for each treatment arm presented in figure 4.3.

RTV at day 10 in the AG014699-treated group was significantly less than that in the saline-treated control mice (RTV = 1.55 *vs*. 2.63; $P = 0.02$). Reviewing the data shown in figure 4.3 it appears that during the 10-day dosing period of AG014699 tumour growth is retarded or even arrested, with no significant change in mean RTV at D10 from the mean RTV at D2 (RTV D10 = 1.55 *vs.* RTV D2 = 1.27; $P = 0.44$). However, as the graph shows, when AG014699 treatment was stopped tumour growth increased significantly; comparing mean RTV at D12 with D10 (RTV D10 = 1.55 *vs*. RTV D12 = 2.80; $P = 0.02$).

In response to carboplatin (75 mg/kg D1) no difference in tumour growth was observed until D9 when a slowing of tumour growth was detected. Mean RTV on D10 = 1.72, but this was not significantly different from the mean RTV in the control group at the same time-point (RTV D10 = 1.72 *vs.* RTV D10 = 2.63; $P = 0.13$).

This experiment demonstrated that AG014699 suppressed UACC3199 tumour growth only during the dosing period. One possible explanation for this is that PARP enzyme inhibition was not sustained for long enough in this experiment allowing recovery of PARP activity and tumour re-growth. Therefore a more prolonged AG014699 schedule was subsequently evaluated.

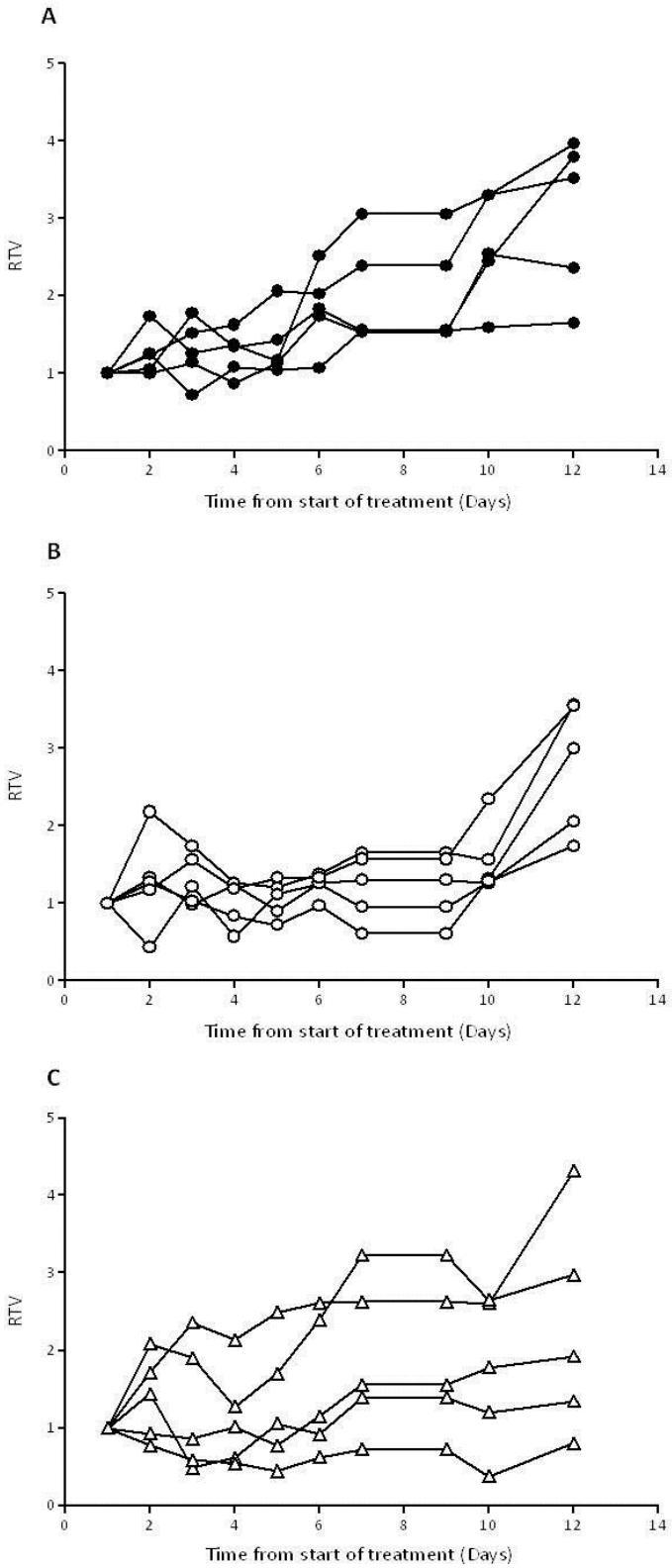

Figure 4.2: Experiment one: UACC3199 xenograft tumour growth in CD-1 nude mice. Growth, calculated as the relative tumour volume (RTV) after each treatment, is shown as a function of time from the start of treatment. **A:** Saline control 10 ml/kg i.p. D 1-10, **B:** AG014699 25 mg/kg i.p. D 1-10 and **C:** Carboplatin 75 mg/kg D1.

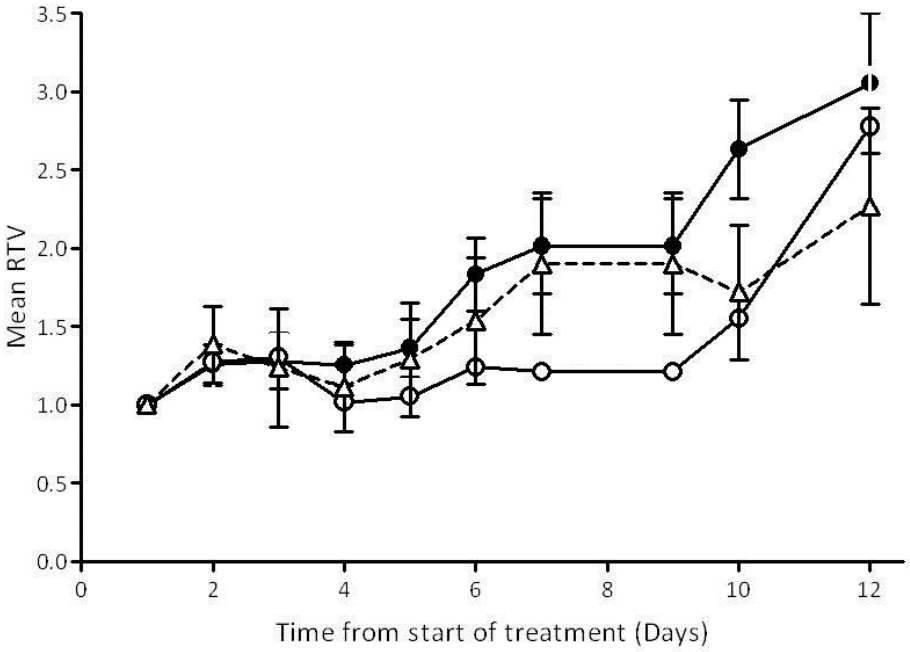

Figure 4.3: Experiment one: UACC3199 xenografts mean tumour growth in CD-1 nude mice. Results are mean RTV + SEM. Solid circles and line = saline vehicle alone; open circles and solid line = AG014699 (25 mg/kg per day for 10 days); open triangles and dashed line = carboplatin (single dose of 75 mg/kg on day 1).

4.4.2 Epigenetically silenced BRCA1 UACC3199 xenografts: experiment two

In this study, 40 mice were implanted with UACC3199 cells. Treatment was commenced 42 days later when nine mice had confirmed tumours (i.e. when there were sufficient mice for at least three per treatment group). Mice were randomised to the following treatment groups: normal saline control (10 ml/kg daily for 5 days of a 7-day cycle for six cycles), AG014699 (10 mg/kg daily for 5 days of a 7-day cycle for six cycles; known as the prolonged schedule), or as in experiment one; carboplatin (75 mg/kg) single dose on D1. Comparing the groups, growth of the xenografts was more consistent than the previous experiment, with up to five-fold variation in the individual tumour volumes (range = 15 mm^3 – 79 mm^3) when treatments were initiated on day one. In addition, there was no significant difference in the mean tumour volumes of each treatment group on day one (control = 38 mm^3 *vs.* AG014699 = 55 mm^3 *vs.* carboplatin = 45 mm^3; $P = 0.31$).

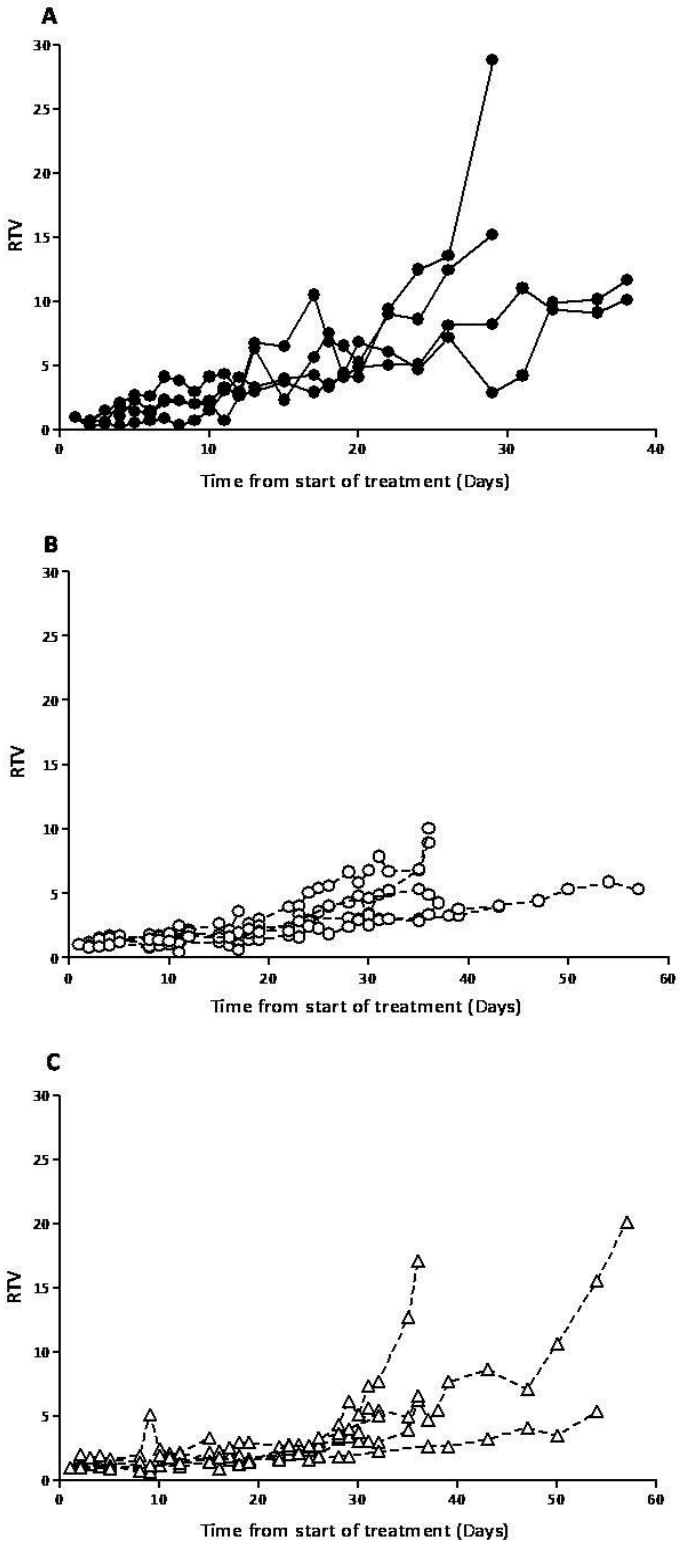

Figure 4.4: Experiment two**:** UACC3199 xenografts tumour growth in CD-1 nude mice. RTV is shown as a function of time from the start of treatment. **A:** Saline control 10 ml/kg i.p. D 1-5 of a 7 day cycle for 6 cycles, **B:** AG014699 10 mg/kg i.p. D 1-5 of a 7 day cycle for 6 cycles and **C:** Carboplatin 75mg/kg D 1.

Results for the RTV over time of each individual mouse within each treatment group are shown in figure 4.4 with mean data for each treatment arm presented in figure 4.5.

The mean time to RTV5 in saline-treated control mice was 25.2 days and this was extended by 37% to 34 days in the AG014699-treated mice, representing a significant tumour growth delay of 9.1 days over untreated controls ($P = 0.05$). For the carboplatin-treated mice, the time to RTV5 increased by 45%, again representing a significant 10.4-day tumour growth delay ($P = 0.02$) (figure 4.5 and table 4.1). Importantly, treatment with AG014699 appeared to be non-toxic to these mice, with the maximum weight loss among treated mice being 6.6% compared to 3% in control mice. Carboplatin caused marginal toxicity, with the maximum weight loss being 9.6%.

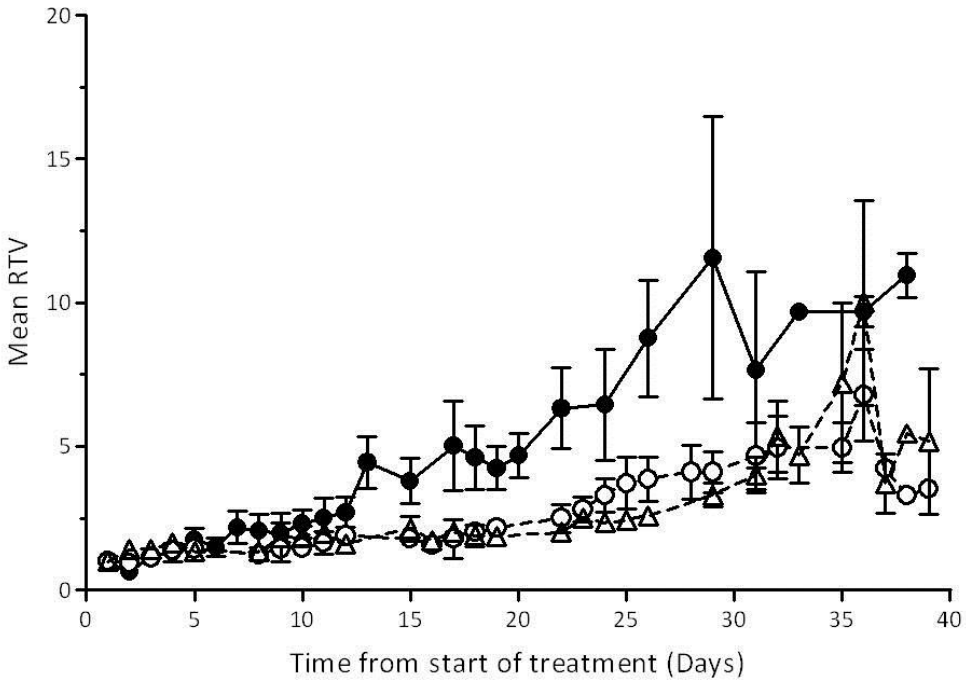

Figure 4.5: Experiment two: UACC3199 xenografts mean tumour growth in CD-1 nude mice. Results are mean RTV +SEM. Solid circles and line = saline vehicle alone; open circles and dashed line = AG014699 (10 mg/kg D1-5 every 7 days for 6 cycles); open triangles and dashed line = carboplatin (single dose of 75 mg/kg on day 1).

4.4.3 BRCA1 mutated MDA-MB-436 xenografts

In light of the data from the UACC3199 xenografts, which suggested that greater anti-tumour activity may be seen following a more sustained PARP inhibition, the prolonged schedule of AG014699 was chosen for the studies with MDA-MB-436 xenografts. Unfortunately, only 15 out of 50 mice that were implanted with MDA-MB-436 cells developed tumours. This poor xenograft take rate (30%) meant that only three treatment arms were possible in this experiment and so the AG014699 schedule was compared to a matched saline control group and a single dose of Carboplatin (75 mg/kg) on D1 group. It had been intended to compare both the schedules of AG014699 tested in the UACC3199 studies. Treatment for all three arms began 44 days after implantation. On day one of treatment there was an up to a nine-fold variation in the volumes of the individual tumours (range 14 mm^3 – 135 mm^3). However there was no significant difference comparing the mean tumour volume of each treatment group (control = 46 mm^3 *vs.* AG014699 = 70 mm^3 *vs.* carboplatin = 44 mm^3; $P = 0.48$).

The results for individual mice within each treatment group are shown in figure 4.6 with mean data presented in figure 4.7 and summary data in table 4.1. These data demonstrate that AG014699 significantly delayed tumour growth with mice reaching RTV4 in 29 days when compared to tumours in untreated control mice, which reached RTV4 after 19 days ($P = 0.03$). Of note, in the AG014699-treated group, one mouse had a transient complete tumour regression (i.e. no detectable tumour) between days 15 and 17. The MDA-MB-436 tumours were extremely sensitive to carboplatin treatment (see figure 4.6 C), with complete tumour regressions observed in three mice; one on days 17–50, the second on days 20–34 and the third mouse experiencing a sustained durable complete tumour regression from day 15 until it was killed at the end of the study. Time to RTV4 in the tumours of the remaining two mice were 57 and 63 days; giving a mean RTV4 of 60 days, significantly higher than that seen in the untreated control group (60 *vs.* 19 days; $P = 0.001$).

AG014699 was again found to be non-toxic in this study, with the maximum weight lost in AG014699-treated mice being 4% and compared to 6.4% in control mice. Carboplatin, however, caused considerable toxicity, with maximum weight loss being 13%.

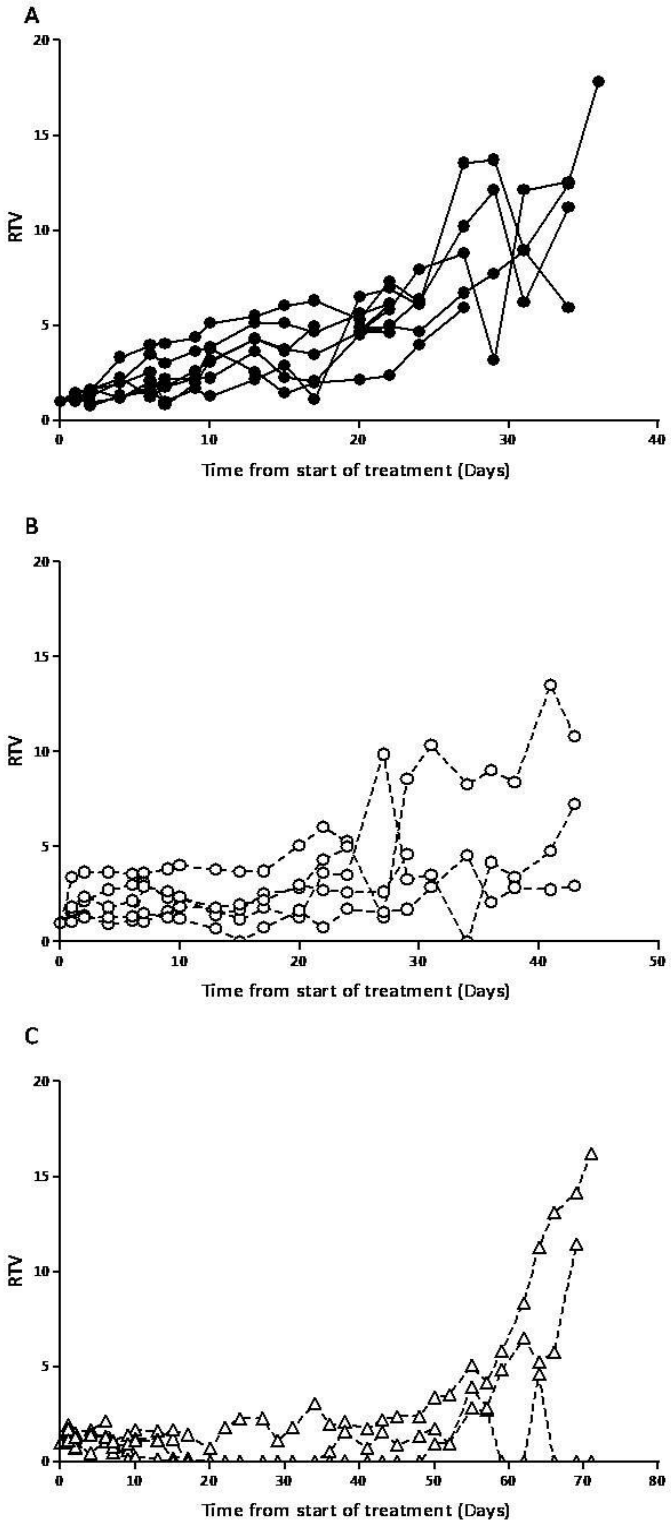

Figure 4.6: MDA-MB-436 xenografts tumour growth in CD-1 nude mice. RTV is shown as a function of time from the start of treatment. **A:** Saline control 10 ml/kg i.p. D 1-5 of a 7 day cycle for 6 cycles, **B:** AG014699 10 mg/kg i.p. D 1-5 of a 7 day cycle for 6 cycles and **C:** Carboplatin 75mg/kg D 1.

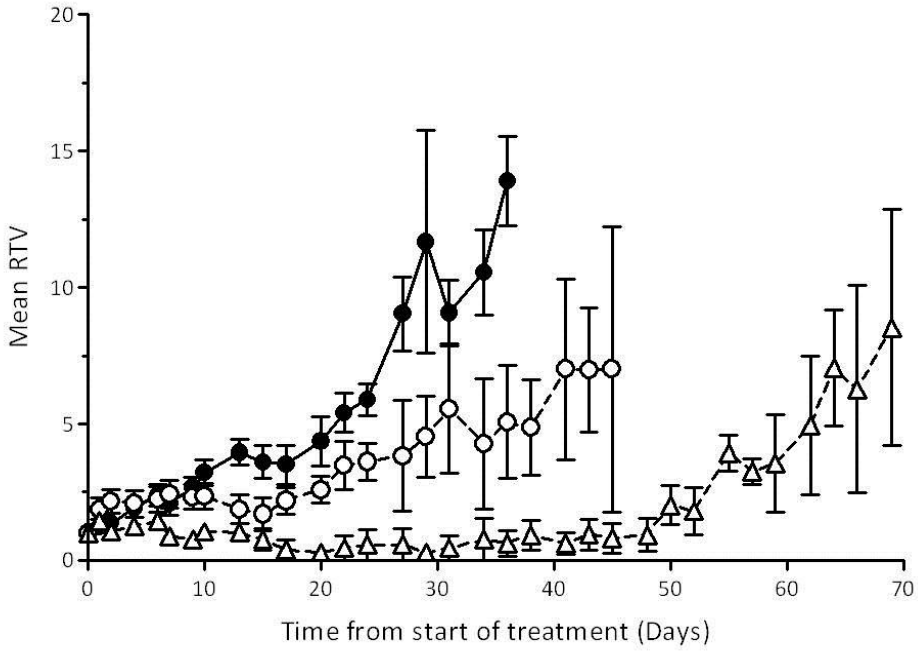

Figure 4.7: MDA-MD-436 xenografts mean tumour growth in CD-1 nude mice. Results are mean RTV +SEM. Solid circles and line = saline vehicle alone; open circles and dashed line = AG014699 (10 mg/kg D1-5 every 7 days for 6 cycles); open triangles and dashed line = carboplatin (single dose of 75 mg/kg on day 1).

4.4.4 BRCA2 mutated CAPAN-1 xenografts

All 40 CD-1 nude mice implanted with CAPAN-1 cells developed tumours. This 100% take rate meant that multiple schedules of AG014699 could be directly compared within the same controlled study. Thus, 15 days after implantation, mice were randomly assigned to one of the following six treatment groups: saline control (10 mL/kg) daily for 10 days, AG014699 (10 mg/kg) once a day for 10 days, AG014699 (10 mg/kg) once daily for 5 days of a 7-day cycle for six cycles, a single dose of carboplatin (75 mg/kg) on day 1, a combination of carboplatin (75 mg/kg) on day 1 with AG014699 (10 mg/kg) once a day for 10 days, or a combination of carboplatin (75 mg/kg) on day 1 with AG014699 (10 mg/kg) once a day for 5 days of a 7-day cycle for six cycles.

On day one of treatment there was an up to a six-fold variation in the size of the individual tumours, with volumes ranging from 10 mm^3 to 61 mm^3. Statistical analysis of the mean tumour volume of each treatment group showed no significant differences between the groups except when comparing the AG014699 prolonged

schedule (45 mm^3) with the combination of carboplatin (75 mg/kg) day 1 and AG014699 (10 mg/kg) once a day for 10 days arm (23 mm^3; $P > 0.05$).

Results for individual mice from each treatment group are shown in figure 4.8 with mean data presented in figure 4.9. The data for mean RTV presented in figure 4.9 is presented as two figures (A and B) to make for easier visual interpretation.

The most toxic regimen in terms of weight loss was Carboplatin in combination with the prolonged AG014699 course which resulted in maximum weight loss of 6.3% compared to < 5% seen in the other groups.

The mean time to RTV4 in the saline-treated control group was 11.5 and this is consistent with previous published reports (Van der Heijden *et al*., 2005).

A single dose of carboplatin (75 mg/kg) on D1) resulted in one complete tumour regression and a statistically significant longer mean time to RTV4 of 18 days ($P = 0.03$) compared with that of the control mice.

Treatment with AG014699 for 10 days resulted in an approximate doubling of the mean time to RTV4 to 24 days equivalent to a 12.5-day growth delay and significantly different from the controls ($P = 0.02$). This TGD was further improved when the longer schedule of AG014699 was applied. The prolonged schedule of AG014699 resulted in a 27.5-day growth delay compared with the control mice (i.e. time to RTV4 of 39 days *vs.* 11.5 days; $P = 0.02$). These results generate the hypothesis that degree of PARP inhibition *and* duration of PARP inhibition are both important for tumour cell kill.

The best anti-tumour responses were seen in the combination of AG014699 and Carboplatin treatment arms. Carboplatin combined with AG014699 (10 mg/kg) once daily for 10 days resulted in two complete tumour regressions (one at day 28 and the other at day 35) and a significant tumour growth delay of 27.5 days over the control group (mean time to RTV4 = 39 days ; $P = 0.04$). The most effective regimen in terms of longer time to RTV4 was the carboplatin with AG014699 given on the prolonged schedule.

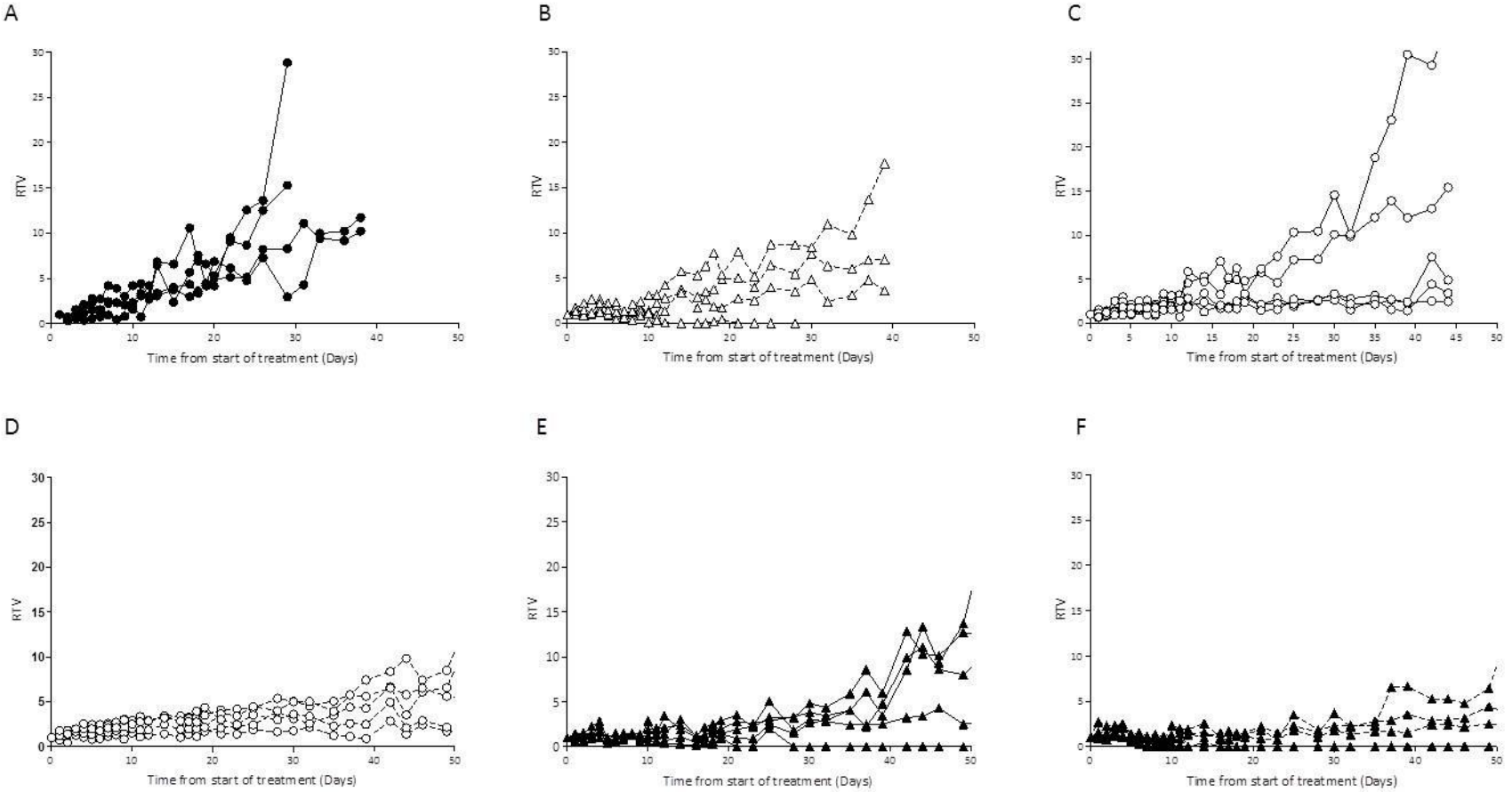

Figure 4.8: CAPAN-1 xenograft tumour growth as RTV in CD-1 nude mice. **A:** Control (saline daily for 10 days). **B:** Carboplatin (75 mg/kg on day 1). **C:** AG014699 (10 mg/kg daily for 10 days). **D:** AG014699 (10 mg/kg daily for days 1-5 of a 7-day cycle for six cycles, prolonged schedule). **E:** Combination therapy with carboplatin (75 mg/kg on day 1) + AG014699 (10 mg/kg daily for 10 days). **F:** Combination therapy with carboplatin (75 mg/kg on day 1) + AG014699 prolonged schedule.

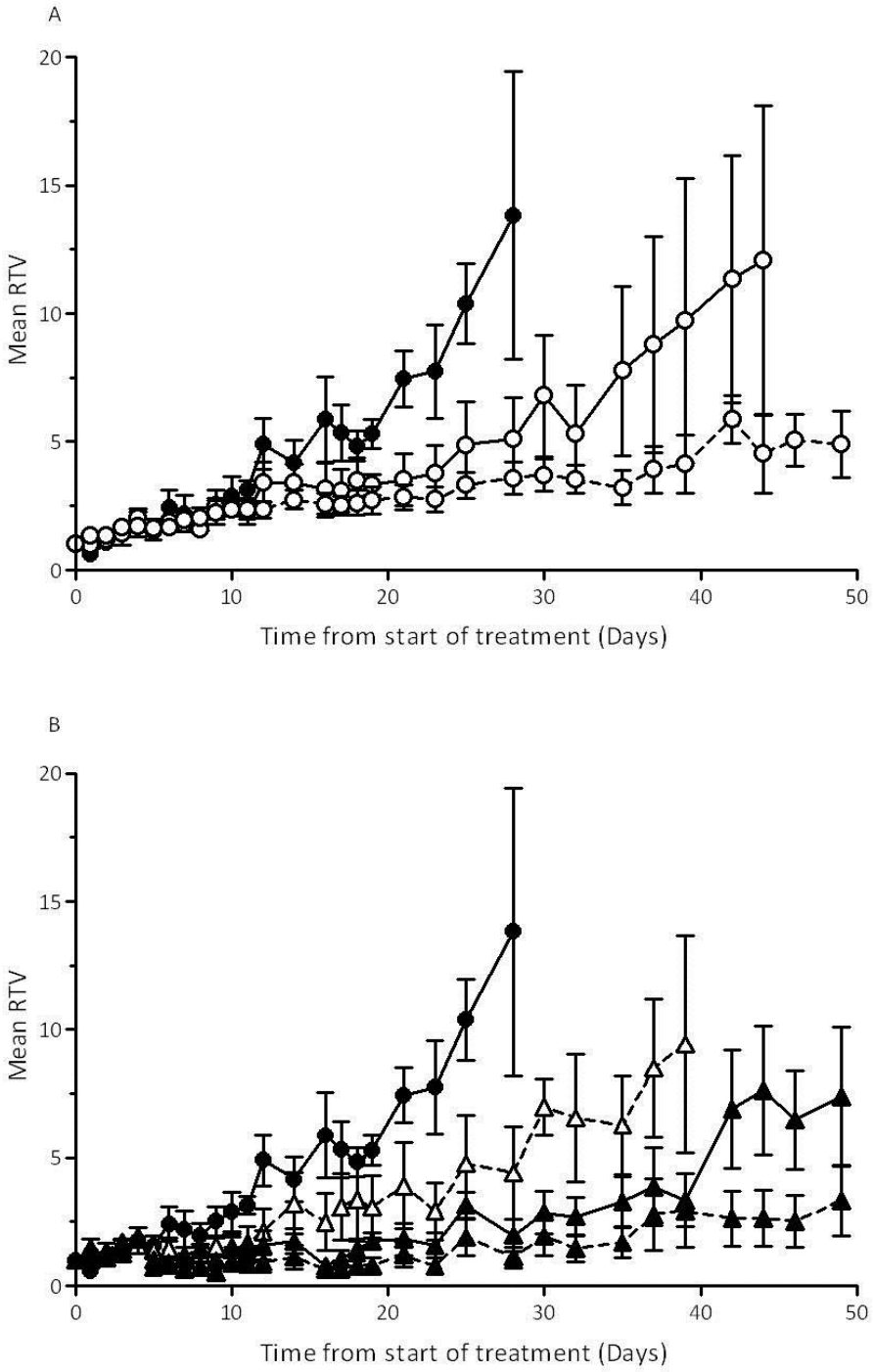

Figure 4.9 CAPAN-1 xenografts mean tumour growth in CD-1 nude mice. Results are mean RTV +SEM. **A:** Solid circles and solid line = saline control; open circles and solid line = AG014699 (10 mg/kg D1-10); open circles and dashed line = AG014699 (10 mg/kg D1-5 every 7 days for 6 cycles) **B:** Solid circles and solid line = saline control; open triangles and dashed line = carboplatin (single dose of 75 mg/kg on day 1); solid triangles and solid line = carboplatin (single dose of 75 mg/kg on day 1) + AG014699 (10 mg/kg D1-10); solid triangles and dashed line = carboplatin (single dose of 75 mg/kg on day 1) +AG014699 (10 mg/kg D1-5 every 7 days for 6 cycles

This regimen resulted in two complete tumour regressions (one at day 7 and the other at day 12) and a mean tumour growth delay of 36.5 days in the remaining tumours. This gave a mean RTV4 = 48 which is significantly higher than the untreated control group (mean time to RTV4 = 48 days *vs.* 11.5 days; $P = 0.01$).

The addition of AG014699 (in both schedules) to carboplatin resulted in greater tumour growth delay than the use of carboplatin alone as measured by % Enhancement (E). With the ten day AG014699 schedule resulting in 323% increase in efficacy and the more prolonged AG014699 schedule of treatment over six weeks a 461% increase, see table 4.1.

Xenograft and treatment	Mean time (D) to RTV4 (95%CI)	Mean time (D) to RTV5 (95%CI)	Mean TGD (D)	Enhancement (%)	No. CRs	*P*
(A) UACC3199						
Control saline (10 ml/kg D1-5 every 7D x6)		25.2 (14-36)	N/A		0/5	
AG014699 (10 mg/kg D1-5 every 7D x 6)		34.25 (25-46)	9.1		0/5	0.05
Carboplatin (75 mg/kg D1)		35.60 (26-44)	10.4		0/5	0.02
(B) MDA-MB-436						
Control saline (10 ml/kg D1-5 every 7D x6)	19 (9.4-25)		N/A		0/5	
AG014699 (10 mg/kg D1-5 every 7D x6)	29 (13-45)		10		1/5	0.03
Carboplatin (75 mg/kg D1)	60 (57, 63)*		41		3/5	
(C) CAPAN-1						
Control saline (10 ml/kg D1-5 every 7D x6)	11.5 (4-20)		N/A		0/5	
AG014699 (10 ml/kg D1-10)	24 (7-44.8)		12.5		0/5	0.02
AG014699 (10 mg/kg D1-5 every 7D x6)	39 (27-50)		27.5		0/5	0.02
Carboplatin (75 mg/kg D1)	18 (1-35)		6.5		1/5	0.03
AG014699 (10 ml/kg D1-10) + Carboplatin (75 mg/kg D1)	39 (22.8-55.4)		27.5	323	2/5	
AG014699 (10 ml/kg D1-5 every 7D x 6) + Carboplatin (75 mg/kg D1)	48 (10.9-86.3)		36.5	461	2/5	0.01†

Table 4.1: Summary of *in vivo* efficacy data, following treatment with: saline control, AG014699 or Carboplatin. Data are mean and 95% CI unless < 3 tumours were available for evaluation* due to tumour regressions. P values are shown comparing treatments to un-treated controls, with the exception of † which compares the combination treatment to carboplatin alone. D = days, CI = confidence interval, CR = Complete remission.

4.5 Discussion

Three important observations have emerged from these studies. Firstly, a prolonged exposure to the PARP inhibitor AG014699 is needed for single agent anti-cancer activity. Secondly, inhibiting PARP-1 is synthetically lethal to epigentically silenced *BRCA*1 xenograft models confirming the *in vitro* data presented in the previous chapter. Thirdly, that the platinum analogue carboplatin has anti-tumour activity in *BRCA1* and 2 defective xenografts as a single agent and in combination with AG014699.

4.5.1 Schedule of AG014699 matters

These xenograft studies have shown that the PARP inhibitor AG014699 has activity against *BRCA* defective cancers and that duration of exposure, in addition to dose, of the PARP inhibitor is important in terms of its single agent anti-tumour effect.

The UACC3199 experiments investigated two schedules of AG014699: (1) 10 mg/kg D1 -10 and (2) 10 mg/kg D1-5 every 7 days for 6 weeks. Reviewing both sets of data, summarised in table 4.1, it appears that the longer and more sustained inhibition of PARP provided by the prolonged schedule two resulted in better anti-tumour effect. This effect was also seen in the CAPAN-1 experiments, which investigated the same two single agent schedules of AG014699. The results, shown in figures 4.8C and 4.8D and table 4.1, are clear; the prolonged regimen of AG014699 resulted in a longer TGD and a significantly longer time to RTV4 than the ten day AG014699 dosing schedule. This is illustrated further in figure 4.10 which shows the data for both schedules head to head together with the exposure to AG014699.

Interestingly, single agent AG014699 (in both schedules) was shown to be at least as equivalent to a single dose of carboplatin in the UACC3199 and CAPAN-1 studies. In addition, the anti-cancer activity of AG014699 came at a lower cost in terms of toxicity than the carboplatin.

These data suggest that PARP inhibitors should be evaluated against carboplatin in randomised clinical trials of selected cancer patients.

Results of the *BRCA*1 mutated MDA-MB-436 *in vivo* experiments, shown in figures 4.6 and 4.7, demonstrate that MDA-MB-436 tumours are sensitive to the anti-cancer

activity of AG014699. Treatment with the prolonged schedule resulted in significant delays in tumour growth; with tumours reaching RTV4 in 29 days compared to 19 days in tumours of untreated control mice. These data support the *in vitro* findings in which the MDA-MB-436 cell lines were the most sensitive to AG014699 in clonogenic cell survival assays (mean IC_{50} = 1.3 μM).

The low implantation rate of the UACC3199 and the MDA-MB-436 cell lines meant that multiple treatment arms in these experiments were not possible and that the two schedules of AG014669 were not investigated within the same controlled experiment. This limits the interpretation of the results; in addition one might question the accuracy of any comparison of the results. However, the studies in the CAPAN-1 xenografts *were* tested within the same controlled experiment and these results demonstrate superiority of the prolonged AG014699 schedule, confirming the hypothesis that prolonged exposure to AG014699 is better.

The scientific explanation for this greater anti-tumour effect is that single agent PARP inhibitor cytotoxicity is dependent on cells replicating. That is, for unrepaired SSBs to become DSBs or lethal stalled replication forks, cells must go through S-phase of the cell cycle. If PARP is inhibited for short periods of time only a fraction of the total cancer cell population will have passed through S-phase and been affected. However, if the time of PARP inhibitor exposure is prolonged, the greater percentage of the cells will have been in S-phase during the PARP enzyme inhibition and the greater the cell kill. Therefore, during schedule two of AG014699 dosing it is proposed that PARP-1 is fully inhibited for five days allowing the accumulation of DNA double strand breaks, stalled replication forks and cell death. The 48 hours without treatment is then not enough time for PARP enzyme activity levels to recover to 100% and the damage to cells continues. PARP activity is furthered inhibited when the treatment cycle re-starts. Whereas in the simple ten day dosing regimen (schedule one) full recovery of PARP enzyme function and loss of the synthetic lethality will eventually occur. This theory may also explain the lack of selective cytotoxicity of AG14361 in *BRCA*1 mutated breast cancer xenografts presented by De Soto and colleagues as intermittent (30 mg/kg i.p. for 3 days on D2, 9 and 16) AG14361 dosing was used (De Soto et al., 2006).

What is not known is how long it takes for PARP enzyme activity to recover following a single dose of AG014699. Pharmacodynamic studies in mice measuring changes to PARP activity levels over time after AG014699 doses are planned and the results will greatly inform future clinical studies.

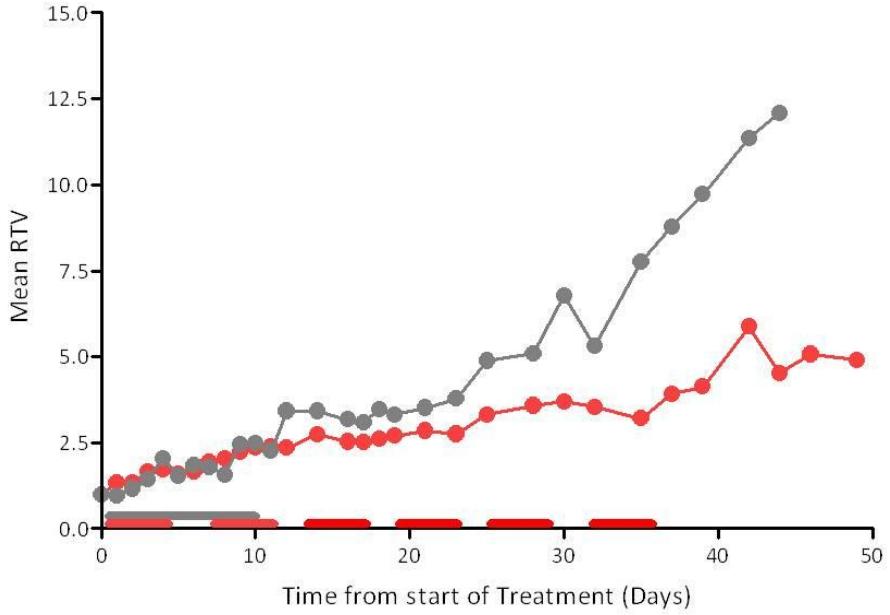

Figure 4.10: 'Schedule matters': CAPAN-1 xenograft mean tumour growth represented by mean RTV following treatment with: AG014699 (10 mg/kg D1-10) = solid grey circles + grey line; AG014699 (10 mg/kg D1-5 every 7 days for 6 cycles) = solid red circles + red line. The treatment periods for the AG014699 arms are represented by the corresponding coloured lines along the x-axis.

This observation that 'schedule matters' as well as dose is also important as it may in-part explain the lack of patient responders to AG014699 in the current phase II PARP-BRCA clinical trial. The intermittent dosing regimen (D 1–5, every 21 days) of AG014699 was selected as it was previously shown to be safe in combination with temozolomide in the phase I trial (Plummer *et al*., 2008). These *in vivo* data strongly suggest that continuous not intermittent dosing may be needed for greater efficacy in *BRCA* mutation carrier population. These results also provide further justification to amend the current clinical trial. This is discussed further in chapter five (section 5.5.6).

4.5.2 AG014699 is synthetically lethal in epigenetically silenced BRCA1

The clinical application of PARP inhibitors as single agents was originally thought to be limited to cancers harbouring germ-line *BRCA* mutations and phase I/II clinical trials have since confirmed the activity of the PARP inhibitor olaparib in this patient population (Fong *et al*., 2009; Audeh *et al*., 2010; Tutt *et al*., 2010). However, it is now proposed that PARP inhibitors may be a therapeutic option in non-*BRCA* mutated cancers which have other defects within the HR repair pathway (discussed in chapter one section 1.6.4).

The breast cancer cell line UACC3199 has epigenetically silenced *BRCA*1 through promoter gene methylation (Wei *et al*., 2005). In chapter three (section 3.4.1) of this thesis, *in vitro* data demonstrate that UACC3199 cells are sensitive to AG014699 and have impaired ability to form Rad51 foci following DNA damage, suggesting that they are HR defective. Results of *in vivo* UACC3199 experiments presented here (see figure 4.5 and table 4.1) demonstrate that AG014699 significantly delays tumour growth compared to untreated controls. Interestingly, this TGD of 11 days was the same as that seen following a single dose of carboplatin (75 mg/kg) on D1. AG014699 was less toxic, in terms of maximum weight loss, than the carboplatin (6.6% *vs.* 9.6%). These findings confirm the *in vitro* data and add further weight to the proposal that PARP inhibitors could have a wider clinical application.

Defective HR DNA repair through epigenetic silencing of *BRCA*1 or other mechanisms is now known to occur commonly in sporadic cancers; in particular high grade serous ovarian carcinomas (HGSOC) (Press *et al*., 2008) and triple negative breast cancers (Turner *et al*., 2007). In a recent study of sporadic epithelial ovarian cancers Mukhopadhyay and colleagues demonstrated a failure to form Rad51 foci (an indicator HR function) following exposure to AG014699 in 67% (16/24) of primary cultures. This failure of Rad51 foci induction correlated with *ex vivo* sensitivity to AG014699 (Mukhopadhyay *et al*., 2010). In another study, Graeser *et al* observed a low Rad51 score in 26% of breast cancer core biopsies taken 24 hours after the first cycle of neo-adjuvant chemotherapy (Graeser *et al*., 2010). These two studies highlight that HR dysfunction is common in non-*BRCA* germline mutated cancers and perhaps more prevalent in ovarian than triple negative breast cancers. Clinical data is now emerging to support this; reports of a phase II study investigating the PARP inhibitor olaparib

showed encouraging activity in non-*BRCA* mutated HGSOC with response rates of 24% (11/46 patients) (Gelmon *et al*., 2011). Disappointingly, no responses have been reported in the 15 patients with non-*BRCA* mutated triple negative breast cancer.

In summary it is clear from these *in vitro* and *in vivo* studies that *BRCA*1 methylated breast cancer cells (UACC3199) are sensitive to the PARP inhibitor AG014699 and future clinical studies of this novel agent should include patients without non-germ-line *BRCA* mutated cancers.

4.5.3 Carboplatin as a single agent and in combination with AG014699

These studies have shown that single agent carboplatin is active in *BRCA* deficient xenografts. The MDA-MB-436 cell line was the most sensitive to AG014699 *in vitro*, had the lowest fold change in Rad51 foci following AG014699 and was the most sensitive to carboplatin in these *in vivo* studies confirming that these cells harbour a severely defective HR phenotype. These experiments also demonstrate that combining AG014699 with carboplatin is better than either treatment alone in *BRCA*2 mutant models. In the CAPAN-1 xenografts the most effective regimen, defined by longer time to RTV4, was the prolonged AG014699 schedule in combination with carboplatin (75 mg/kg) on D1. This resulted in two complete tumour regressions and a mean tumour growth delay of 36.5 days in the remaining tumours.

These results confirm the findings of a number of studies which have investigated the efficacy of the PARP inhibitor-platinum combination; in mice bearing *BRCA1*- and p53-deleted transplanted mouse mammary tumours (Rottenberg *et al*., 2008) and in mice bearing autochthonous *BRCA2*- and p53-deleted mouse mammary tumours using the PARP inhibitor AZD2281 (now known as olaparib) (Hay *et al*., 2009), which demonstrated that the combination of cisplatin and a PARP inhibitor resulted in prolonged recurrence-free and overall survival compared with mice treated with either drug alone. The rationale for combining AG014699 with a platinum analogue is further supported by work by Evers and colleagues who demonstrated selective cytotoxic synergy between cisplatin and the PARP inhibitor AZD2281 (now olaparib) in *BRCA*2-deficient but not proficient mammary mice tumour cell lines (Evers *et al*., 2008).

Reviewing these results and the published literature (chapter one, section 1.6.1) it appears that prolonged, higher doses of PARP inhibitors are required as single agents

to exploit the synthetic lethality concept but that in combination with cytotoxics these doses may be too toxic for patients where only shorter, less potent PARP inhibiton is tolerated. For example, in the case of AG014699, chemopotentiation *in vivo* studies have reported that concentrations as low as 0.1 μM AG014699 are able to cause > 100% enhancement of temozolomide induced tumour growth delay and that the maximum tolerated dose in combination of AG014699 was 1mg/kg (Thomas et al., 2007). However, these studies have shown that higher AG014699 doses (10mg/kg) are needed to produce single agent activity and therapeutic concentrations (around 3.9 μM); such doses were found by Thomas *et al* to be lethal in combination with temozolomide.

Clinical studies are now underway investigating the safety and efficacy of combining PARP inhibitors with chemotherapy including the platinum agents both to act as chemosensitisers and to exploit the HR defective phenotype. One of the problems these trials will face is which dosing schedule of the PARP inhibitor to use in order to get the balance right between efficacy and toxicity.

4.6 Conclusions

To conclude, these studies provide the first evidence that UACC3199 tumour xenografts are sensitive to single agent AG014699, confirming the *in vitro* data presented in chapter three suggesting that PARP inhibitors may be a therapeutic option in non-*BRCA* mutated cancers. Secondly, the data in the CAPAN-1 tumours directly comparing the two schedules of AG014699 shows that TGD is significantly longer with a prolonged continuous dosing schedule of the PARP inhibitor. These results have impacted on the current CRUK PARP-BRCA clinical trial where AG014699 is given only intermittently on D1-5 allowing PARP enzyme recovery during the remainder of the 21 day cycle. These data have provided valuable weight to support the amendment of this multi-centre UK study which is now open to recruitment (October 2011) to investigate an oral continuous AG014699 dosing schedule. Finally, these experiments have shown that carboplatin has anti-tumour activity in *BRCA* defective xenografts and may be a therapeutic option in *BRCA* mutation carrier patients either in combination with a PARP inhibitor or as a single agent and these issues are the subjects of on-going clinical trials.

Chapter Five

5. Pharmacodynamic, Pharmacokinetic, Pharmacogenomic and Clinical outcomes of AG014699 in patients; results of the Phase II PARP-BRCA clinical trial

5.1 Introduction

A better understanding of the molecular biology of cancer is leading to the identification of distinct cancer sub-types, new anti-cancer targets and as a result more individualised patient treatment approaches through the development of targeted agents (Schilsky *et al.,* 2010). An example of this in action can be seen in the development of PARP inhibitors. Since the discovery of the first PARP; PARP-1, over 40 years ago (Chambon *et al*., 1963), the abundant nuclear enzyme has emerged as an important novel target in cancer therapy. The first inhibitor of PARP, 3-AB, was identified in 1980 (Durkacz et al., 1980). Pre-clinical studies using the next generation of more potent more specific inhibitors suggested that the main anti-cancer role of PARP inhibitors would be as chemotherapy and radiotherapy potentiators (Delaney *et al*., 2000; Calabrese *et al*., 2004). Thus the first inhibitor to enter anti-cancer clinical trials was AG014699 (Pfizer GRD) in a phase I combination study with the oral, alkylating agent temozolomide in 2003. At this time this trial was conceived there were no data to support single agent AG014699 activity in the treatment of cancer.

However, whilst this early phase combination AG014699 study was recruiting, two Nature papers reported results from two independent research groups showing that cells deficient in the *BRCA1* and *2* genes were 100-1000 - fold more sensitive than heterozygote or wild type cell lines to PARP inhibitor monotherapy (Bryant *et al*., 2005; Farmer *et al*., 2005). Bryant *et al* demonstrated reduced survival in *BRCA*2 deficient cells to the PARP inhibitors NU1025 and AG14361, both forerunners to AG014699. In the sister paper, Farmer *et al* demonstrated sensitivity of both *BRCA1* and *2* deficient cell lines to two small molecule PARP-1 inhibitors-: KU0058684 and KU0058948, both forerunners to olaparib. Both groups concluded that *BRCA* deficient cells were sensitive to PARP inhibition by the proposed mechanism of 'synthetic lethality'

discussed in chapters one and three. Encouragingly both groups showed that PARP inhibition was non-toxic to models with restored BRCA function. These data suggested that, in patients, PARP inhibitors could selectively kill *BRCA* deficient tumours sparing normal tissue.

Proof of concept clinical trials investigating the efficacy and safety of PARP inhibitors as single agents in *BRCA* mutated cancers commenced shortly after these studies were published in 2005. The first study, a phase I dose escalation study of the oral, potent PARP-1 and 2 inhibitor olaparib (previously known as AZD2281/KU0059436) was actually on-going at the time of the 2005 Nature publications (Fong *et al*., 2009). It was however a standard phase I dose escalation study open to patients with advanced solid malignancies. On reviewing the BRCA-PARP *in vitro* and *in vivo* data (Bryant *et al*., 2005; Farmer *et al*., 2005) the study was promptly amended to enrich for *BRCA1* or *BRCA2* mutation carriers (n=23). Two major findings came out of this study; results discussed in detail in chapter one, section 1.6.3. The first, that olaparib was well tolerated in patients, including those with the germ-line *BRCA* mutations. The second, that olaparib had anti-tumour activity only in the mutation carriers. The study incorporated an expansion phase, which focused specifically on patients with *BRCA1/2* mutations. Efficacy in a cohort of 50 patients all with *BRCA*1/2 mutated ovarian cancer was recently reported a clinical benefit rate of 46% for olaparib (Fong *et al*., 2010).

As a result olaparib was taken forward into two separate phase II studies investigating the response in *BRCA* mutated breast and ovarian cancers respectively. Both these trials have demonstrated that olaparib is active in *BRCA* mutated cancers; confirming the phase I findings (Audeh *et al*., 2010; Tutt *et al*., 2010). The breast cancer study involved patients who had been heavily pre-treated with chemotherapy and the overall response rate compared well with that seen with standard chemotherapy regimens in the advanced setting (20-30%). The ovarian study included both platinum sensitive and resistant patients and response to olaparib was seen across these two groups. The greater response rates in patients receiving the 400 mg twice daily dose in both studies suggested that the degree of PARP inhibition is important.

It is also important to note that not all *BRCA1/2* mutation carriers responded to olaparib and that resistance to PARP inhibition has recently been reported through mechanisms of secondary genetic mutations of *BRCA1* or *BRCA2* restoring their

functions (discussed in chapter one section 1.7, Edwards *et al*., 2008; Sakai *et al*., 2008 and 2009). The DNA repair capacity judged by homologous recombination status was not investigated in these studies and it is not yet clear how often such genetic reversions could occur in patients.

Therefore, as with any early phase trial results; confirmation is required in larger phase III trials and it is prudent to await the results of other on-going trials investigating other classes of PARP inhibitor.

One such study is the phase II Cancer Research UK (CRUK) trial of the activity of the intravenous PARP-1 inhibitor, AG014699, in patients with *BRCA1* or *2* mutated locally advanced/metastatic breast cancer or advanced ovarian cancer (known as the PARP-BRCA PH2/052 trial). At the time of writing, the PARP-BRCA PH2/052 study is ongoing. The protocol has recently been amended to investigate an oral, continuous dosing regimen, the reasons for which will be discussed in later on in this chapter. The pharmacokinetic, pharmacodynamic and pharmacogenomic assays developed and performed on the clinical samples collected within this study fall within the remit of this thesis. Results are presented and discussed in this chapter together with any available clinical outcome data.

5.1.1 The Phase II PARP-BRCA PH2/052 clinical trial

This is a national, multi-centre, phase II study of the PARP-1 inhibitor AG014699 in patients with *BRCA1* or *2* mutated locally advanced/metastatic breast cancer or advanced ovarian cancer. The study is being conducted by CRUK in collaboration with Pfizer GRD and the Northern Institute for Cancer Research, Newcastle upon Tyne. The participating cancer centres are the Beatson West of Scotland Cancer centre, Glasgow, University College London Cancer Trials Centre, The Christie Hospital, Manchester, St James University Hospital, Leeds, The Northern Centre for Cancer Care, Newcastle-upon-Tyne, Plymouth Oncology Centre and Birmingham University Hospital. The study is being conducted under full ethical approval and all laboratory work for the primary and secondary objectives undertaken to Good Clinical Practice (GCP). The study is registered with the European Clinical Trials database (EudraCT no. 2006-002348-27).

5.1.1.1 Trial eligibility criteria

The study is open to patients with confirmed germline *BRCA1* and or *2* mutations and locally advanced/metastatic breast cancer or advanced ovarian cancer. A summary of the main inclusion and exclusion criteria are shown in table 5.1.

5.1.1.2 Trial design and end-points

The trial is an open label, single arm study of AG014699 given over a 30 minute intravenous infusion on day (D) one to five every 21 days for six cycles. The primary end-points of the study are: response rate and toxicity. Response is measured by the Response Evaluation Criteria in Solid Tumours (RECIST) (Eisenhauer *et al*., 2009) and assessed following every two cycles of AG014699. Toxicity is recorded at every patient visit and coded by the Common Terminology Criteria for Adverse Events (CTCAE) version 3.0. Secondary end-points: Time to progression (TTP), Overall survival (OS), PARP-1 activity and AG014447 pharmacokinetics following AG014699. Tertiary end-points include the analysis of PARP-1 expression and the genotyping of single nucleotide polymorphisms (SNPs) within genes involved in the metabolism of AG014699 (*CYP2D6**2, *4) and PARP-1 activity (*PARP-1* T2444C).

At study conception it was not known whether a difference in response to AG014699 would be seen between the patients with *BRCA*1 or 2 mutations and between those with breast or ovarian cancer. Therefore the study was designed to recruit patients into four subgroups of 14 patients each: *BRCA1* ovary, *BRCA1* breast, *BRCA2* ovary and *BRCA2* breast to allow response to be assessed. If one response was seen in the 14 then this was considered to be significant and the null hypothesis of the drug being inactive in this sub-group could be rejected.

At the time of study design, no safety data on the use of PARP inhibitors in this patient population were available. Therefore in order to address concerns about potential toxicity in patients the study was conducted in two stages.

Stage one consisted of two cohorts; cohort one in which three *BRCA*1 and three *BRCA*2 mutation carriers received a daily dose of 4 mg/m^2 for five days for the first cycle. In the previous phase I study a 4 mg/m^2 dose was shown to inhibit PARP-1 but with recovery of enzyme activity within 24 hours (Plummer *et al*., 2008). If no dose limiting toxicity (DLT) was observed these patients received subsequent cycles at a daily dose

of 12 mg/m^2 for five days. In cohort two, three *BRCA*1 and three *BRCA*2 mutation carrier patients received 12 mg/m^2 AG014699 for 5 days for the first cycle and if no DLT was observed patients were dose escalated to receive subsequent cycles at a dose of 18 mg/m^2.

In Stage two of the study patients received 18mg/m^2 for the first cycle and all subsequent cycles unless a dose reduction was required as per the protocol. Patients who were responding to and tolerating AG014699 treatment after six cycles were permitted to continue on study at the discretion of the investigators.

Inclusion criteria:
Proven carriers of a known mutation in *BRCA1* or *BRCA2* Histologically documented locally advanced or metastatic breast cancer or advanced ovarian cancer Patients with ovarian cancer who have ≤ 3 prior chemotherapies and in whom > 2 months have elapsed since their last treatment with a carboplatin- or cisplatin-containing regimen Patients with breast cancer who have had ≤ 3 prior chemotherapy regimens Measurable disease as measured by X-ray, Computerised Tomography (CT), or Magnetic resonance imaging (MRI) scan as defined by the Response Evaluation Criteria in Solid Tumours (RECIST) criteria. Life expectancy ≥ 12 weeks World Health Organisation (WHO) performance status of 0 or 1 Written informed consent and be capable of co-operating with treatment and follow-up ≥ 18 years Haematological and biochemical indices within the ranges shown below: • Haemoglobin ≥9.0 g/dl, Neutrophils ≥1.5 x 10^9/L, Platelets ≥100 x 10^9/L • Serum bilirubin ≤1.5 x upper normal limit • Alanine amino-transferase or aspartate amino-transferase ≤ 2.5 x upper limit of normal, or ≤ 5 if liver metastases present • Glomerular Filtration Rate ≥50 ml/min
Exclusion criteria:
Radiotherapy (except for palliative reasons), endocrine therapy, immunotherapy or chemotherapy during the previous 4 weeks before start of study drug (six weeks for nitrosoureas and Mitomycin-C) Any unresolved toxicities > Grade 1 Common Terminology Criteria for Adverse Events (CTCAE) from previous treatments, except for alopecia. Known brain metastases Pregnant or breast feeding patients. Female patients who have a negative serum or urine pregnancy test before enrolment and agree to use two highly effective forms of contraception 4 weeks before entering the trial, during the trial and for 6 months afterwards are considered eligible. Male patients with partners of child-bearing potential (unless they agree to use one form of highly effective contraception during the trial and for 6 months afterwards). Major thoracic and/or abdominal surgery in the preceding 4 weeks from which the patient has not recovered. At high medical risk because of non-malignant systemic disease including active uncontrolled infection. Current malignancies at other sites, with the exception of adequately treated cone-biopsied *in situ* carcinoma of the cervix uteri and basal or squamous cell carcinoma of the skin and concurrent breast and ovarian carcinoma. Patients with active or unstable cardiac disease or history of myocardial infarction within six months.

Table 5.1: PARP-BRCA PH2/05 trial eligibility criteria

5.1.2 Pharmacodynamic, Pharmacokinetic and Pharmacogenomic end-points

5.1.2.1 PARP-1 activity

In this study PARP-1 enzyme activity levels were measured in patients' peripheral blood lymphocytes (PBL) using the GCLP validated PAR formation immunoblot assay described in chapter two, section 2.9. Baseline pre-AG014699 PARP-1 activity levels were determined to investigate differences in endogenous (un-stimulated) PARP activity or maximum stimulated PARP activity between patients and to investigate if any relationship exists between PARP activity and the clinical response to AG014699, patient's age and PARP-1 protein expression levels. Maximum stimulated PARP-1 activity was also quantified in response to AG014699 to determine the efficiency of on-target effect of the PARP inhibitor and to relate this to the pharmacokinetic evaluation of AG014699.

5.1.2.2 PARP-1 expression

To determine whether inter-patient variation in levels of PARP-1 activity could be attributed to differences in PARP-1 expression and to compare results of this patient population with other published data sets; PARP-1 expression levels were measured from patients' PBL using the validated semi-quantitative Western blotting assay described in chapter two, Materials and Methods, section 2.10.

5.1.2.3 PARP-1 T2444C single nucleotide polymorphism genotyping

For this study, the T2444C SNP was determined from DNA extracted from whole blood using the PARP-1 TaqMan Real-time PCR genotyping assay kit (c1515368-1, rs number 113640; Applied Biosystems, Warrington, UK) as described in chapter two, Materials and Methods, section 2.12. Results of patient's endogenous baseline PARP-1 activity were then correlated with the T2444C SNP results.

5.1.2.4 Pharmacokinetics of AG014699

The pharmacokinetics of AG014447 (the free base of AG014699) was determined from plasma extracted from patient's whole blood using LC/MS/MS. The method, developed and validated to GCLP for this research study, is described in chapter two, section 2.11. The PK sampling schedule for this study permitted only limited analysis but would allow for relationships between the AG014699 pharmacokinetics and pharmacodynamic and clinical response data to be investigated.

5.1.2.5 CYP2D6 single nucleotide polymorphism genotyping

Cytochrome P450 2D6 (CYP2D6, debrisoquine/asparteine hydroxylase) is a member of the Cytochrome P450 super-family. It is involved in the metabolism of ~ 25% of all commonly prescribed drugs (Sistonen *et al*., 2007) and including AG014699 (Pfizer GRD). CYP2D6 gene is highly polymorphic and over 75 major alleles have been identified to date (www.cypalleles.ki.se). Single nucleotide polymorphisms within *CYP2D6* can result in increased, decreased or abolished gene function. This can result in complete deficiency up to excessive metabolism of a given drug resulting in either excess toxicity or lack of efficacy. For this study, the CYP2D6*2 and *4 were determined from DNA extracted from whole blood using TaqMan Real-time PCR genotyping assay kits (Applied Biosystems, Warrington, UK) listed and described in chapter two, Materials and Methods, section 2.12. Results were then used to investigate any association between toxicity and response to AG014699.

5.2 Objectives

The end-points of the phase II PARP-BRCA PH2/052 trial are detailed above but the objectives for the specific studies carried out for this thesis are as follows:

- **Pharmacodynamic (PD) endpoints:** To investigate the effects of AG014699 on PARP-1 activity and investigate baseline PARP-1 activity and PARP-1 expression levels in patients.
- **Pharmacokinetic (PK) endpoints:** To establish and validate a method to determine the concentration of AG014447, the active drug of the pro-drug AG014699, in human plasma samples.
- **Pharmacogenomic (PG) endpoints:** To determine the SNPs within the genes associated with the metabolism of AG014699 (*CYP2D6*) and PARP-1 activity (*PARP-1*).
- **Clinical endpoints:** To determine the response rate, time to progression, overall survival and toxicity following AG014699 in this patient population

- To investigate any possible relationships between the above parameters

5.3 Materials and Methods

Materials and methods for the listed assays are described in full in chapter two, Materials and Methods. Any deviations from these methods for specific experiments are detailed in the individual results sections below. Preparations of the clinical samples for analysis within the listed assays are also described in chapter two. The schedules of the different clinical samples taken for use within this study are detailed in figure 5.1. All stage one patients, who were dose escalated between, cycle one and two, underwent PK and PD blood sampling on both these cycles whereas stage two patients underwent PD and PK sampling in cycle one only.

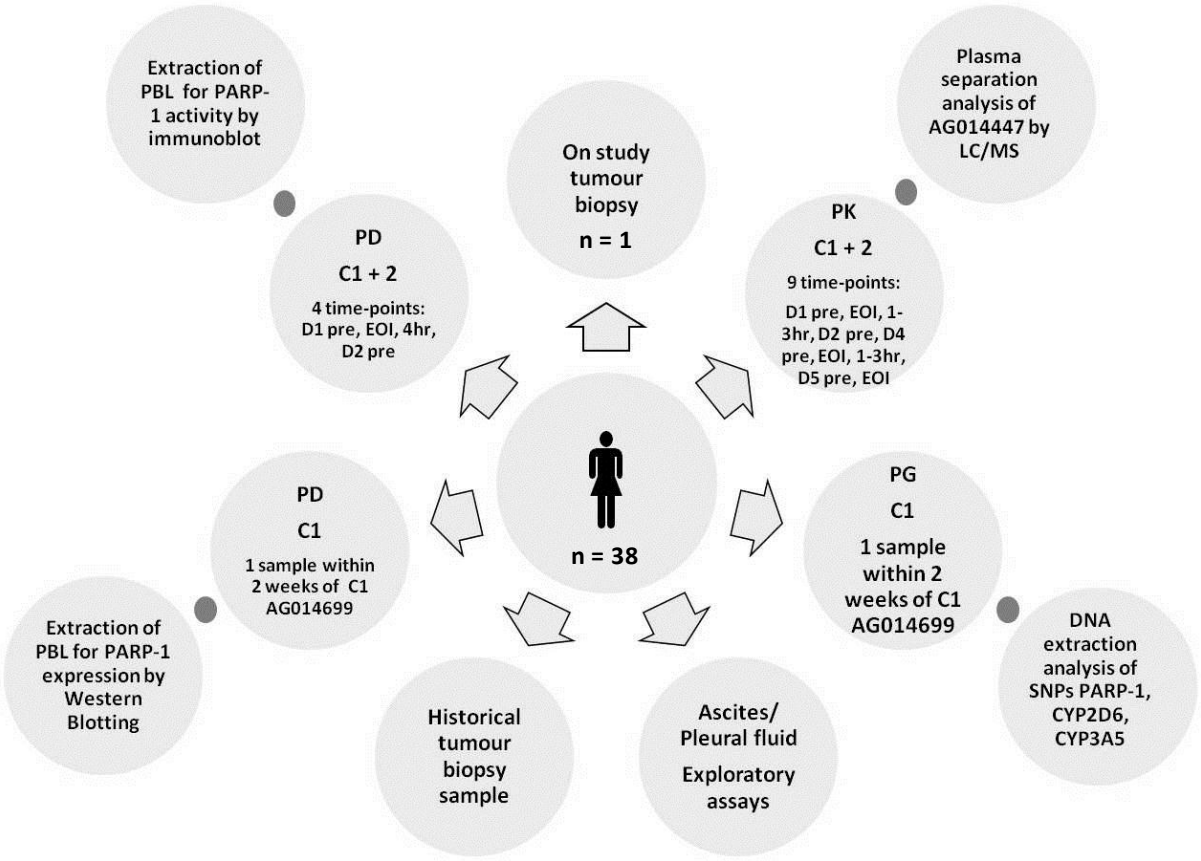

Figure 5.1: Summary of the schedule of clinical samples taken as part of the PARP-BRCA PH2/052 phase II trial. Stage two patients had pharmacokinetic (PK) and pharmacodynamic (PD) sampling in C1 only. Pre = pre-treatment, EOI = end of infusion, PBL = peripheral blood lymphocytes, LC/MS = liquid chromatography mass spectrometry, C = cycle, D = day, SNP = single nucleotide polymorphisms. n=actual number of patients/ biopsies at the time of writing.

5.4 Results

5.4.1 Patient demographics

Between January 2007 and September 2010 38 patients were entered into the study. Baseline characteristics are shown in table 5.2. It was initially envisaged that accrual of the 56 patients would take approximately 24 months, with an average of 2-3 patients recruited per month. However recruitment has been slower than predicted. Possible reasons include the restriction on the prior number of chemotherapies permitted in the breast cancer patients (this has been addressed in a recent protocol amendment) and the restriction of excluding non-UK residents. The low number of *BRCA2* ovarian cancer patients recruited may reflect the lower risk of developing ovarian cancer in *BRCA2* mutation carriers (Ford *et al.,* 2004).

The mean age of the 38 patients is 51.4 years which is lower than the reported average age at diagnosis of breast cancer (61 years) and ovarian cancer (63 years) patients (www.cancerresearch.uk.org/cancerstats). This is not surprising given that one of the hallmarks of *BRCA* mutation carriers is the early age at cancer presentation (King *et al*., 2003).

Patients were all of good performance status and had received a median number of two prior chemotherapies.

For reporting of results patients are identified by their specific study number e.g. 40-001; where the first number represents the treatment centre i.e. 40 is Newcastle and the second number is the patient recruitment number. Two additional patients were recruited to stage one, cohort two; one to replace patient 40-007 who withdrew due to clinical evidence of disease progression during cycle one. The second additional patient arose due to two patients at different treatment centres being given the information about the study at the same time and it was considered unethical to withdraw the offer of treatment.

Patient baseline characteristics n=38	**Patient no. (%)**
Sex – no. (%)	
Female	38 (100)
Male	0 (0)
Age - yr	
Mean	51.4
Range	28 - 72
Tumour type – no. (%)	
Breast	16 (42)
Ovarian	22 (58)
***BRCA* mutation/ Tumour type –no. (%)**	
BRCA1 breast	5 (13)
BRCA2 breast	11 (29)
BRCA1 ovary	16 (42)
BRCA2 ovary	6 (16)
WHO PS – no. (%)	
0	10 (26)
1	28 (74)
Mean no. (range) prior chemotherapies	2 (1 – 4)

Table 5.2 Baseline patient characteristics for the PARP-BRCA PH2/052 phase II trial

5.4.2 Patients baseline PARP-1 characteristics

5.4.2.1 PARP-1 activity in Peripheral Blood Lymphocytes

PBL samples were collected for all 38 patients, but the samples for baseline PARP-1 activity, as described in figure 5.1, were obtained in 35 patients. The main reason for not obtaining a result for a given patient was that either the blood sampling was not possible at a given time-point or blood was taken but insufficient PBL were harvested to enable results to be generated. PARP-1 activity was assessed using the validated immunoblot assay described in chapter two, Materials and Methods and is expressed as pmol of PAR formation per 10^4 PBL. Examples of an immunoblot and PAR standard curve are shown in figures 3.5 and 3.6 respectively in chapter three.

Patients' baseline PARP-1 activity was obtained from the cycle one, D1 PBL sample which was taken immediately prior the first AG014699 dose. This time-point enables

the amount of PARP-1 activity to be assessed in the un-stimulated, un-reacted sample, which represents the endogenous PARP activity and secondly the amount of PARP activity in the sample after maximum stimulation of the enzyme after the addition of oligonucleotide in the assay reaction.

Results for all 35 patients for endogenous un-stimulated PARP activity are shown in figure 5.2. This shows low levels of PARP-1 activity with a mean value = 0.097 pmol PAR per 10^4 PBL (median = 0.05 pmol PAR, range = 0.00-0.75 pmol PAR per 10^4 PBL) and a large variation between patients (coefficient of variation (CV) = 146.5%). Interpreting these data is difficult as the majority of results lie at the lower end of the standard curve and no published data is yet available for comparison of *endogenous* PBL PARP-1 activity measured in similar populations or even in non-*BRCA* mutated cancer populations or healthy volunteers using these methods.

Results for the pre-treatment PARP-1 activity samples after maximum enzyme stimulation for the 35 patients are shown in figure 5.3 and table 5.3. Similar to the endogenous PARP-1 activity data, a large inter-patient variation is seen (range = 0.38 – 40.26 pmol PAR per 10^4 PBL, CV = 144.7%). Mean PARP-1 activity = 6.80 pmol PAR per 10^4 PBL and median = 2.71 pmol PAR per 10^4 PBL. This is almost double the PARP-1 activity levels reported by Zaremba *et al.* (Zaremba *et al*., 2011) of a large cohort of 118 cancer patients with unknown *BRCA* status where a mean baseline PARP-1 activity after maximum enzyme stimulation = 3.60 pmol PAR per 10^4 PBL was seen.

A large variation in PARP-1 activity was also seen in Zaremba's study (CV = 129.9%, range = 0.10 – 26.00 pmol PAR per 10^4 PBL) confirming that PARP-1 activity varies markedly between individuals.

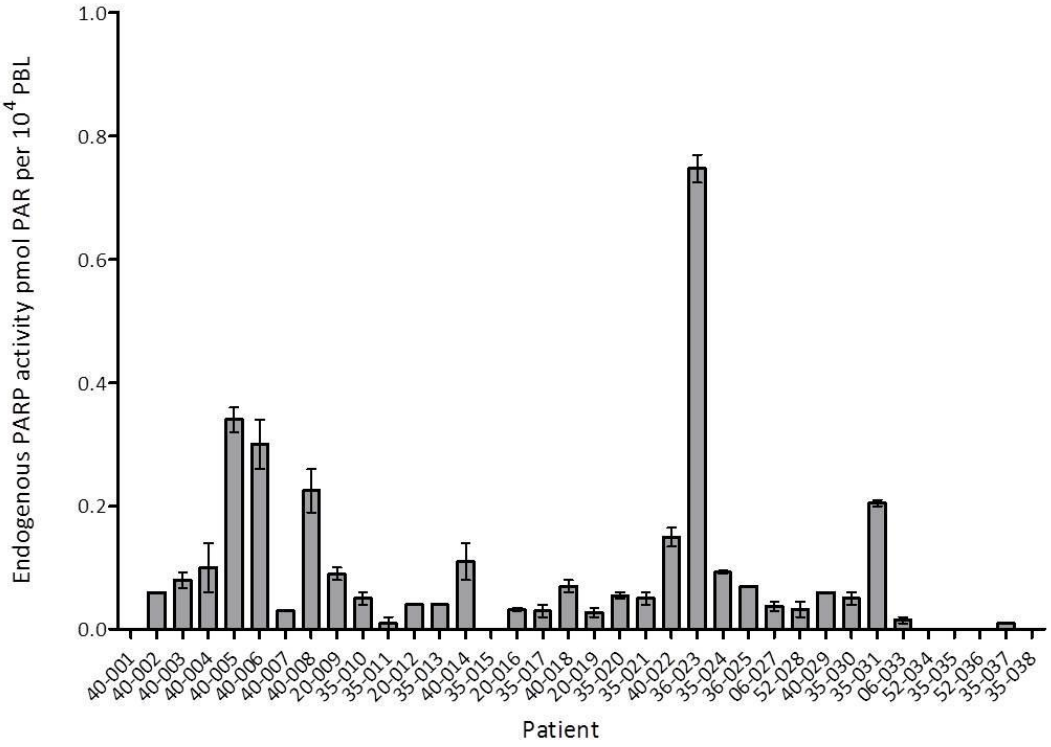

Figure 5.2: Mean endogenous PARP-1 activity in pre-AG014699 treatment PBL samples. Error bars = SEM.

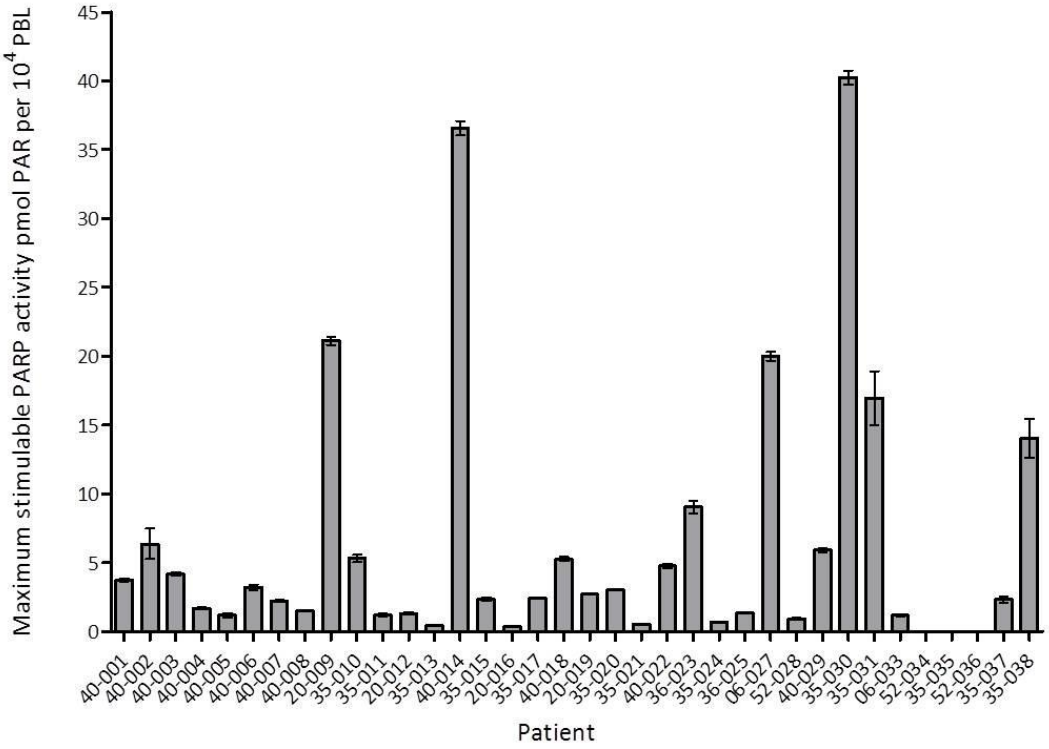

Figure 5.3: Mean maximum stimulated PARP-1 activity in pre-AG014699 treatment PBL samples. Error bars = SEM.

5.4.2.2 PARP-1 protein expression in Peripheral Blood Lymphocytes

PBL samples for PARP-1 protein expression were collected for 30 of the 38 patients. The main reason for not obtaining a result for a given patient was that either the blood sampling was not possible at the specified time-point or blood was taken but insufficient PBL were harvested to enable results to be generated. PARP-1 expression was assessed using the semi-quantitative Western Blotting assay described in chapter two, section 2.10 and is expressed as ng PARP-1 per μg of total protein loaded.

Analysis of PARP-1 expression results, shown in figure 5.4 and table 5.3; demonstrate mean PARP-1 expression of 0.21 ng per μg and a median of 0.16 ng per μg protein loaded. Like PARP-1 activity levels, a large variation is seen between subjects with CV = 92.5% and range of 0.00 to 0.93 ng per μg protein. These results are similar to data reported by Zaremba *et al.* where a mean PARP-1 expression of 0.23 ng per μg protein was seen in a population of 118 cancer patients (Zaremba *et al*., 2011).

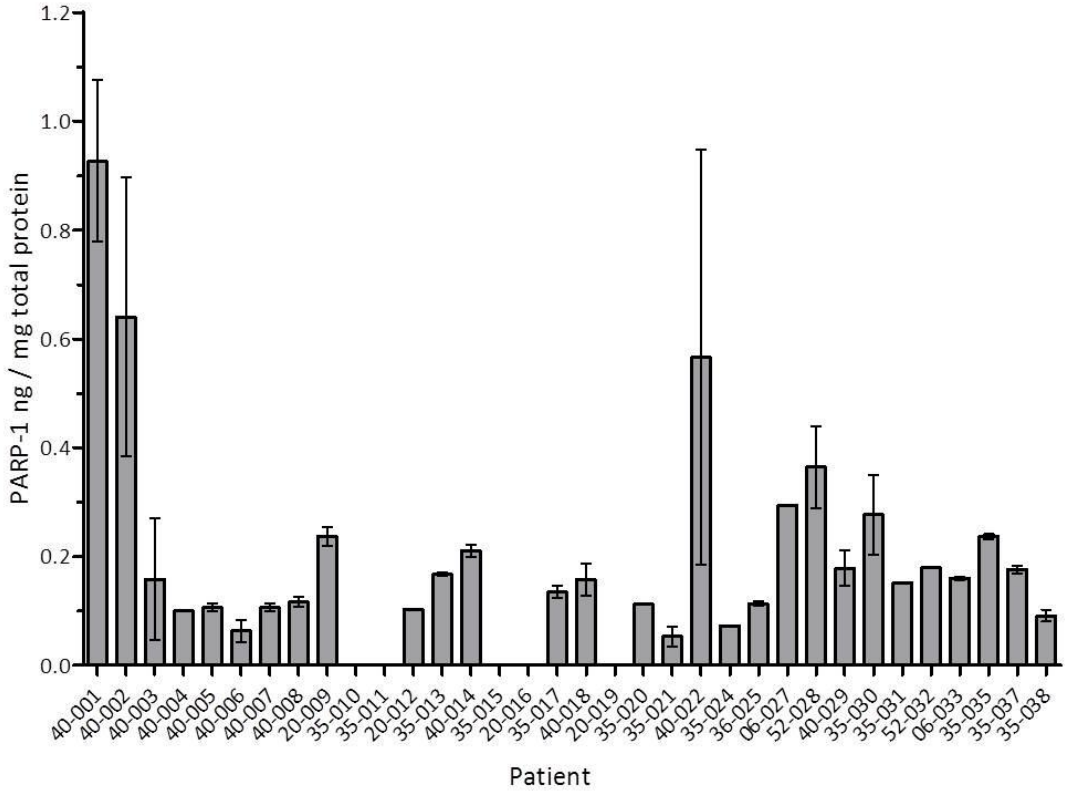

Figure 5.4: Mean baseline PARP-1 protein expression in pre-AG014699 PBL samples. Error bars = SEM.

5.4.2.3 PARP-1 activity vs. PARP-1 expression

To determine whether any relationship exists between PARP-1 protein expression and maximum stimulated PARP-1 enzyme activity; results from both assays were analysed after $\log_{10}$ transformation as both data sets were positively skewed. Results shown in figure 5.5 demonstrate a weak but non-significant correlation with increased protein expression and increased PARP-1 activity ($R^2 = 0.14$, $P = 0.06$, Pearsons correlation coefficient).

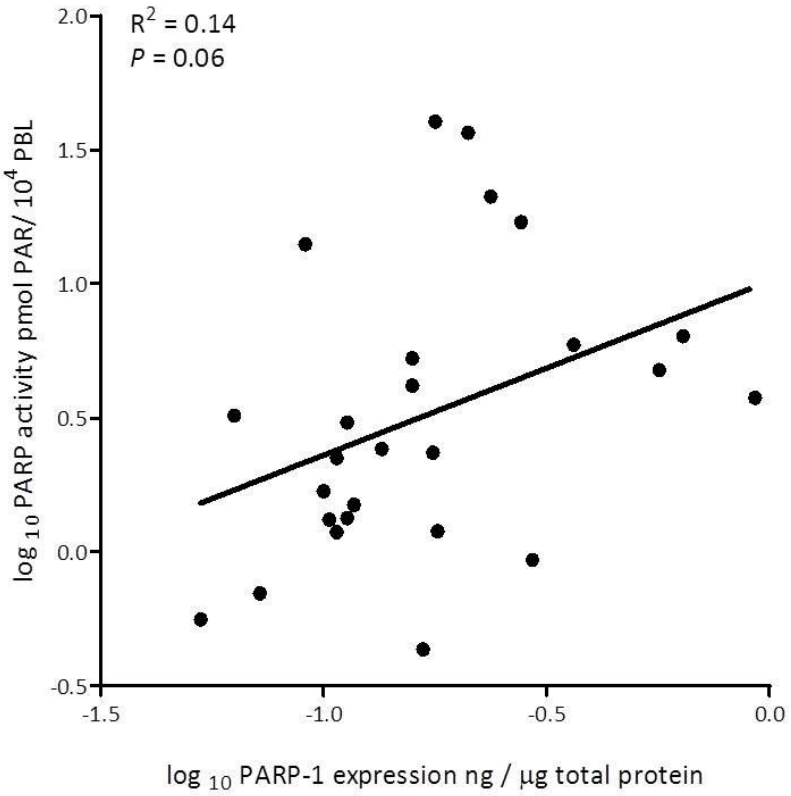

Figure 5.5: Relationship between $\log_{10}$ PARP-1 expression and activity

5.4.2.4 PARP-1 activity and PARP-1 expression vs. age

Studies investigating a link between PARP-1 activity, expression and longevity have been conflicting. Grube and Burkle demonstrated that poly(ADP-ribosylation) capacity decreases with age in both rats and humans. In addition they showed that maximally stimulated PARP activity in PBL of 13 mammalian species directly correlated with species-specific life span with a 5-fold difference between the longest lived (man) and shortest lived (rat) species tested (Grube and Burkle., 1992).

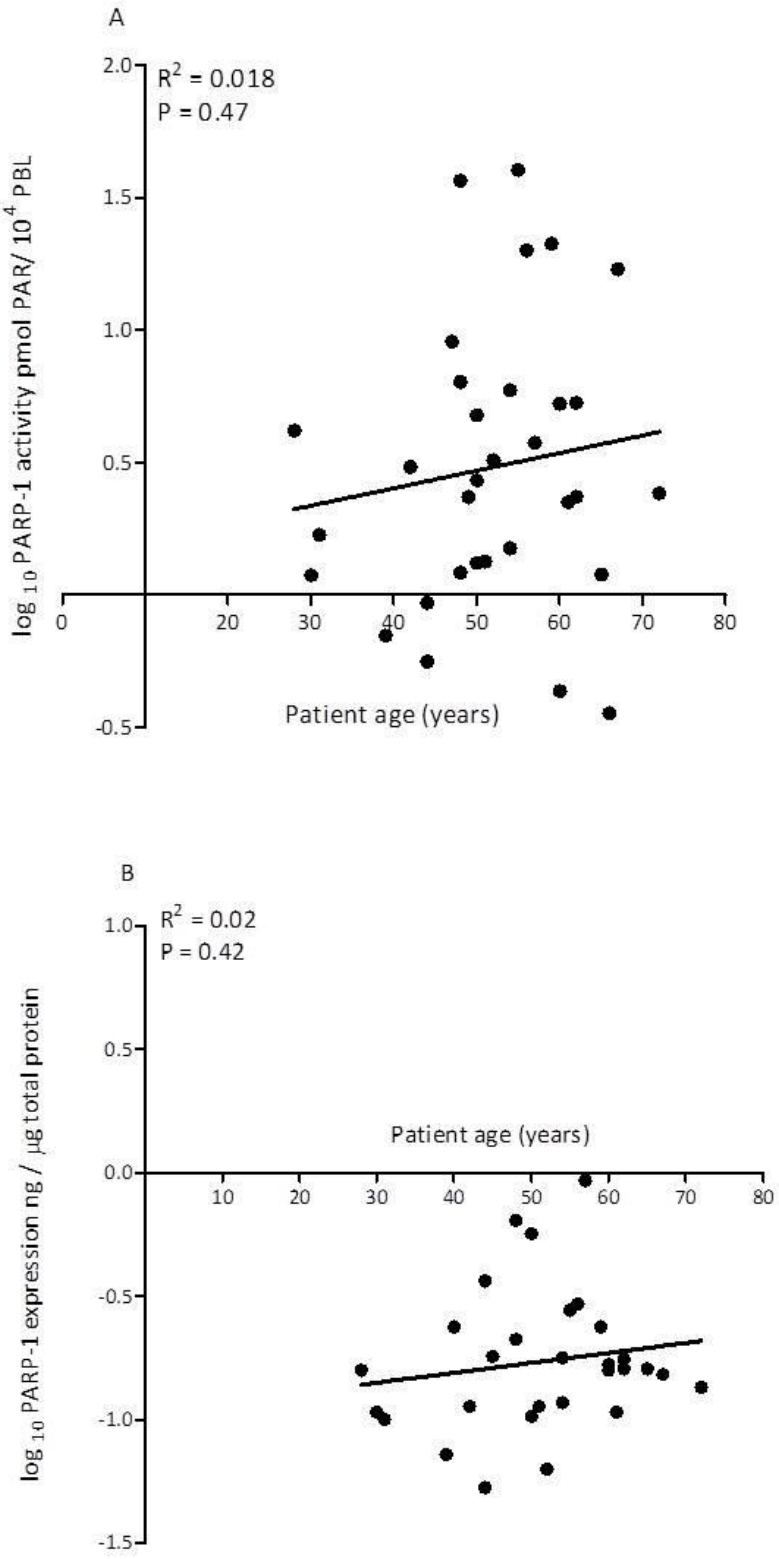

Figure 5.6: Relationship between (A) log $_{10}$ PARP-1 activity (B) log $_{10}$ PARP-1 expression and age

In contrast to this, Muiras *et al* reported significantly higher maximum stimulable PARP activity in a population of 49 French centenarians *vs.* 51 younger controls aged 20-70 years (Muiras *et al.*, 1998).

Analysis of the data from this study using a Pearson correlation coefficient does not show any significant relationship between $\log_{10}$ PARP-1 activity ($R^2 = 0.02$, $P = 0.47$) or $\log_{10}$ PARP-1 expression ($R^2 = 0.02$, $P = 0.42$) and age. See figure 5.6

5.4.2.5 PARP-1 T2444C genotyping

Whole blood samples for analysis of the PARP-1 T2444C SNP were received for 31 out of 38 patients. The main reason for not obtaining a result for a given patient was that the blood sample was not taken due to error at the treatment centre. DNA was extracted from whole blood and analysed using the Taqman kit as described in chapter two, Materials and Methods. Results for all 31 patients are shown in table 5.3 together with the corresponding pre-AG014699 PARP-1 activity levels. The frequencies of the genotypes were as follows: major genotype (T/T) 77.4%, the heterozygote genotype (T/C) 19.4% and the minor variant genotype (C/C) 3.2%. The minor allele frequency of 13% is consistent with the published data reports of between 5-33% and the allele frequency was consistent with Hardy Weinberg Equilibrium ($X^2 = 0.60$, $P = 0.44$). Only one patient (35-013) was found to have the C/C variant genotype and interestingly this patient had the second lowest PARP-1 activity of the group at 0.43 pmol PAR per 10^4 PBL, see figure 5.7. However as this was the only C/C patient it was not possible to do further statistical comparisons of this single result but analysis of PARP-1 activity data by genotype grouping (T/T *vs.* [T/C + C/C]) shows a trend towards lower PARP-1 activity with the variant C allele but this did not reach statistical significance ($P = 0.17$, un-paired t-test).

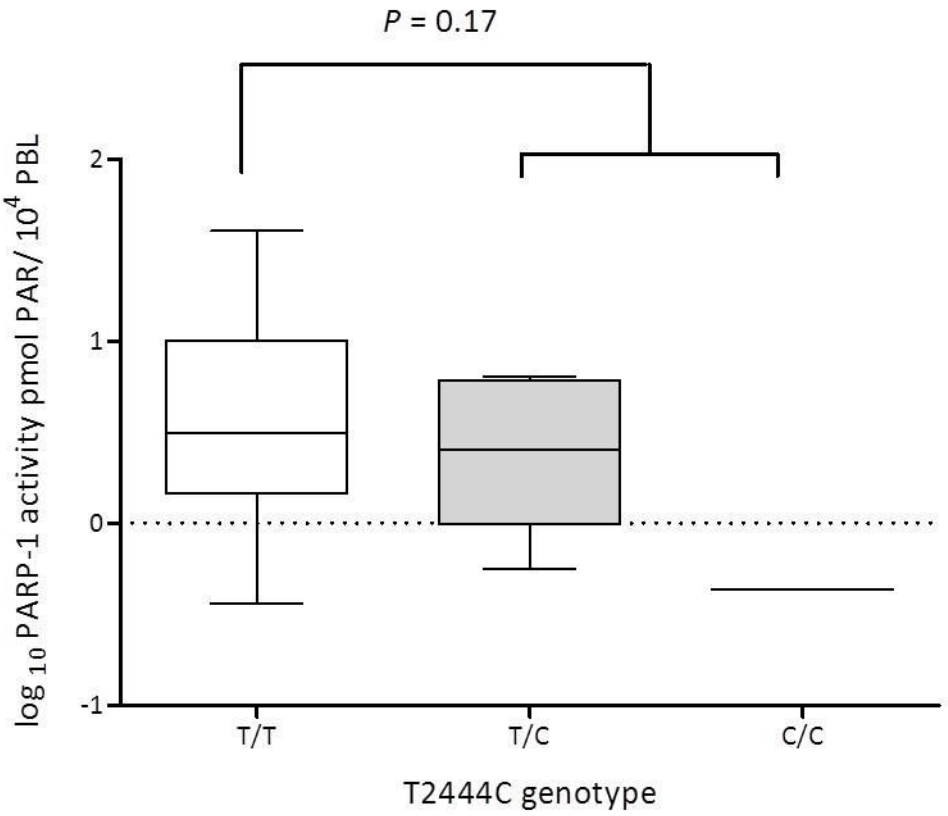

Figure 5.7: PARP-1 activity by *PARP*-1 T2444C genotype

Patient study no.	T2444C SNP	Baseline endogenous PARP-1 activity (mean pmol PAR per 10^4 PBL)	Baseline maximum stimulated PARP-1 activity (mean pmol PAR per 10^4 PBL)	Baseline PARP-1 protein expression (ng/μg protein)
40-001	T/C	0.00	3.75	0.93
40-002	T/C	0.06	6.38	0.64
40-003	T/T	0.08	4.18	0.16
40-004	T/C	0.10	1.69	0.10
40-005	T/C	0.34	1.19	0.11
40-006	T/T	0.30	3.22	0.06
40-007	T/T	0.03	2.24	0.11
40-008	T/T	0.22	1.50	0.12
20-009	T/T	0.09	21.13	0.24
35-010	T/T	0.05	5.32	*
35-011	T/T	0.01	1.21	*
20-012	*	0.04	1.32	*
35-013	C/C	0.04	0.43	0.17
40-014	T/T	0.11	36.56	0.21
35-015	*	0.00	2.34	*
20-016	T/T	0.03	0.36	*
35-017	T/T	0.03	2.42	0.14
40-018	T/T	0.07	5.27	0.16
20-019	T/T	0.03	2.71	0.00
35-020	T/T	0.05	3.04	0.11
35-021	T/C	0.05	0.56	0.05
40-022	T/T	0.15	4.77	0.57
36-023	T/T	0.75	9.05	*
35-024	T/T	0.09	0.70	0.07
36-025	T/T	0.07	1.34	0.11
06-027	*	0.04	20.00	0.29
52-028	T/T	0.03	0.93	0.36
40-029	T/C	0.06	5.93	0.18
35-030	T/T	0.05	40.26	0.28
35-031	T/T	0.20	16.97	0.15
52-032	T/T	*	*	0.18
06-033	*	0.01	1.19	0.16
35-034	*	*	*	*
35-035	T/T	*	*	0.24
52-036	*	*	*	*
35-037	T/T	0.01	2.35	0.18
35-038	T/T	0.00	14.05	0.09

Table 5.3: PARP-1 T2444C SNP genotyping results with patients' C1 baseline endogenous PARP-1 activity, maximally stimulated pre-AG014699 PARP-1 activity levels and pre-AG014699 PARP-1 protein levels.
* indicates result unavailable due to sample not being taken or insufficient sample to do analysis.

5.4.3 PARP-1 activity in PBL in response to AG014699

Blood samples were taken, as described in section 5.3.1, to assess PARP-1 activity levels in PBL pre- and post-AG014699. A complete set of samples (four time-points per cycle) were received for 26 patients but providing the pre-AG014699 sample was taken it was possible to assess the affect of AG014699 on the remaining time-points. This was possible for 33 patients and results, expressed as % PARP-1 activity of the pre-AG014699 baseline sample, for all 33 patients are shown in table 5.4, with summary data provided in table 5.5. The D2 pre-dose blood sample was intended to be taken approximately 24 hours post the D1 dose of AG014699. It is therefore referred to in the text, graphs and tables as D1 24h time-point.

As explained in section 5.1.1, in cohort one of stage one, six patients (3 with *BRCA1* and 3 with *BRCA2* mutations) received the first cycle of AG014699 at a daily dose of 4 mg/m^2. All six patients subsequently received the second cycle at the higher dose of 12 mg/m^2 as no DLT was observed. PARP-1 activity results for this cohort, expressed as a % of the pre-treatment levels, are shown in figure 5.8. A single dose of 4 mg/m^2 AG014699 resulted in profound suppression of PARP-1 activity with mean activity levels at 30 min (end of infusion sample) of 2.2% of baseline. However some recovery was seen at 24h with mean PARP-1 activity up to 31.5% of baseline levels.

Data for the same six patients following a single dose of 12 mg/m^2 AG014699 shows mean PARP activity levels of 1.3% at 30 min and less recovery of activity at 24 h (mean = 3.8%). These are the first examples of intra-patient dose escalation of a PARP-1 inhibitor and show a dose dependent effect of PARP-1 enzyme inhibition at the 24 hour time-point.

In cohort two of stage one a further six patients (3 with *BRCA1* and 3 with *BRCA2* mutations) were treated with AG014699 at a daily dose of 12 mg/m^2 for cycle one and all (except patient 40-007 who withdrew from study due to early disease progression) were dose escalated to 18 mg/m^2 for subsequent cycles as no DLT was observed. As patient 40-007 would not be assessable for response an additional patient was recruited to this cohort. Results for all seven patients are shown in figure 5.9.

Patient study no.	Dose AG014699 (mg/m^2)	Mean PARP-1 activity (± SD) pmol PAR per 10^4 PBL	% PARP-1 activity of D1 pre-dose levels		
		D1 pre-dose	D1 EOI	D1 4 hours	D1 24 hours
40-001	4	3.75 ± 0.20	0.90 ± 0.40	0.33 ± 0.58	95.67 ± 4.19
	12	11.71 ± 0.29	0.23 ± 0.21	3.27 ± 0.55	0.00 ± 0.00
40-002	4	6.38 ± 1.92	0.23 ± 0.21	7.17 ± 0.76	29.03 ± 2.20
	12	1.79 ± 0.14	2.03 ± 0.55	8.20 ± 0.30	10.43 ± 0.98
40-003	4	4.18 ± 0.20	1.17 ± 0.12	6.63 ± 0.75	11.00 ± 1.04
	12	7.70 ± 0.23	1.00 ± 0.20	*	6.17 ± 0.29
40-004	4	1.69 ± 0.13	10.23 ± 1.36	5.23 ± 0.42	38.40 ± 3.50
	12	18.16 ± 0.40	3.17 ± 0.12	5.83 ± 0.42	0.00 ± 0.00
40-005	4	1.19 ± 0.23	0.30 ± 1.23	0.00 ± 0.00	7.91 ± 0.51
	12	0.40 ± 0.01	0.00 ± 0.00	0.00 ± 0.00	0.00 ± 0.00
40-006	4	3.22 ± 0.33	1.13 ± 1.96	29.17 ± 5.31	6.80 ± 0.85
	12	13.01 ± 0.32	*	*	6.17 ± 0.29
40-007†	12	2.24 ± 0.12	1.46 ± 0.14	6.36 ± 1.51	3.22 ± 0.24
40-008	12	1.50 ± 0.05	1.18 ± 2.05	20.61 ± 7.17	147.89 ± 16.85
	18	2.48 ± 0.10	10.97 ± 3.51	17.09 ± 1.95	30.58 ± 2.11
20-009	12	21.13 ± 0.51	12.22 ± 1.20	10.70 ± 0.27	12.97 ± 0.58
	18	21.94 ± 1.01	3.87 ± 0.29	*	7.53 ± 0.38
35-010	12	5.32 ± 0.49	18.97 ± 3.07	26.47 ± 0.49	31.37 ± 3.19
	18	18.28 ± 1.38	18.17 ± 1.57	22.83 ± 0.90	32.13 ± 0.15
35-011	12	1.21 ± 0.17	7.32 ± 1.07	20.72 ± 0.09	44.09 ± 3.50
	18	9.22 ± 1.47	3.77 ± 0.51	6.67 ± 0.42	15.3 ± 0.10
35-017	12	2.42 ± 0.08	0.39 ± 0.21	8.60 ± 0.52	2.74 ± 0.20
	18	6.81 ± 0.14	33.61 ± 0.93	16.24 ± 0.75	13.94 ± 0.22
40-018	12	5.27 ± 0.28	7.09 ± 1.06	2.36 ± 0.12	1.84 ± 0.12
	18	2.92 ± 0.16	2.42 ± 0.06	2.73 ± 0.10	8.43 ± 1.34
20-012	18	1.32 ± 0.12	4.37 ± 0.83	16.83 ± 1.36	4.73 ± 0.51
35-013	18	0.43 ± 0.01	2.03 ± 1.04	0.00 ± 0.00	1.37 ± 1.31
40-014	18	36.56 ± 10.90	11.13 ± 0.75	16.77 ± 1.27	56.13 ± 3.05
35-015	18	2.34 ± 0.18	2.11 ± 0.13	1.23 ± 0.15	6.63 ± 0.06
20-016	18	0.36 ± 0.04	0.22 ± 0.38	11.98 ± 1.32	1.16 ± 1.01
20-019	18	2.71 ± 0.05	0.00 ± 0.00	*	1.90 ± 0.32
35-020	18	3.04 ± 0.05	3.30 ± 0.35	*	14.80 ± 0.89
35-021	18	0.56 ± 0.08	52.59 ± 1.77	42.74 ± 1.60	32.24 ± 3.21
40-022	18	4.77 ± 0.25	11.90 ± 1.17	21.91 ± 3.00	34.63 ± 2.45
36-023	18	9.05 ± 0.78	5.52 ± 0.37	5.02 ± 0.36	*
35-024	18	0.70 ± 0.01	43.23 ± 5.89	42.93 ± 1.55	481.00 ± 83.96◊
36-025	18	1.34 ± 0.03	31.90 ± 3.82	19.87 ± 1.10	39.20 ± 2.51
06-027	18	20.00 ± 0.56	3.09 ± 0.28	4.72 ± 0.12	3.86 ± 0.20
52-028	18	0.93 ± 0.11	17.77 ± 6.19	1.34 ± 1.74	0.00 ± 0.00
40-029	18	5.93 ± 0.27	*	5.16 ± 0.56	3.85 ± 0.37
35-030	18	40.26 ± 0.71	7.17 ± 0.48	21.09 ± 0.54	5.47 ± 0.45
35-031	18	16.97 ± 3.38	49.81 ± 2.58	46.24 ± 10.22	43.69 ± 0.33
06-033	18	1.19 ± 0.11	16.87 ± 1.67	33.09 ± 1.75	26.87 ± 0.42
35-037	18	2.35 ± 0.42	3.46 ± 0.36	1.28 ± 0.27	2.79 ± 0.33
35-038	18	14.05 ± 2.43	9.22 ± 1.05	12.20 ± 2.56	6.33 ± 0.24

Table 5.4: PARP-1 activity in response to AG014699 expressed as % PARP-1 activity of the un-treated control samples. * indicates that result unavailable due to sample not being taken or insufficient sample to do analysis. EOI = end of infusion, SD = standard deviation, CV = coefficient of variation

†Patient withdrew from study after C1 due to disease progression.

◊ Result excluded from further analysis but reported

Dose level	No. Patients	Mean % PARP activity of baseline ± SD (%CV)		
		D1 EOI	D1 4 hours	D1 24 hours
4 mg/m^2	6	2.37 ± 3.89 (167.31)	8.09 ± 10.78 (133.30)	31.47 ± 33.94 (107.84)
12 mg/m^2	13	4.59 ± 5.87 (127.98)	10.28 ± 8.59 (83.53)	20.53 ± 40.51 (197.33)
18 mg/m^2	24	13.94 ± 15.79(113.27)	16.09 ± 14.04 (87.28)	16.40 ± 16.19 (98.71)

Table 5.5: PARP-1 activity in response to AG014699: summary statistics.

As explained, all patients in stage one (with the exception of patient 40-007) underwent PD sampling for PARP-1 activity in cycle one and two of the study. It was therefore possible to investigate whether an individual's baseline PARP-1 activity (D1 pre-dose levels) varied between the first and second cycle of treatment. Figure 5.10 shows the % change in baseline PARP-1 activity levels from the D1 pre-dose sample of cycle one to the D1 pre-dose time-point of cycle two for all 12 patients. In 75% of patients (9/12) there was an increase in the C2 D1 pre-dose PARP-1 activity compared to the C1 levels. The mean fold-change was for all patients a 2.12 increase over baseline. This could be consistent with known intra-subject variability of PARP-1 levels which has been reported as up to 1.9-fold over three blood samples during a period of 72 hours (MD thesis data Chris Jones, Newcastle University, UK, 2006). However it may represent an induction of PARP-1 activity following recovery after inhibition by the AG014699. It would be interesting to investigate whether the same phenomenon occurred with PARP-1 protein expression levels.

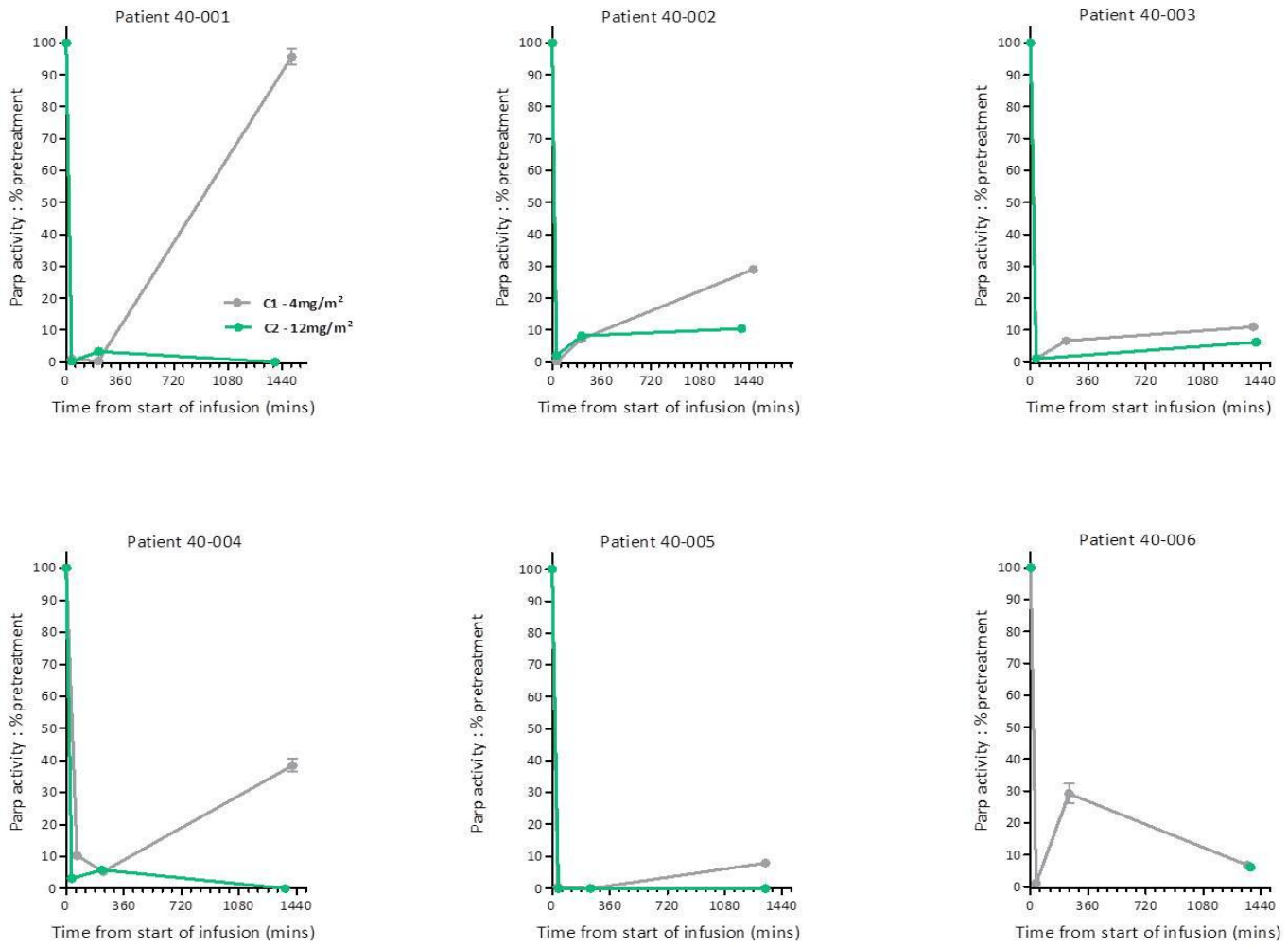

Figure 5.8: PARP-1 activity in response to AG014699 cohort one, stage one patients. Grey lines and symbols represent the 4 mg/m^2 dose and the green symbols and lines are the 12 mg/m^2 dose level.

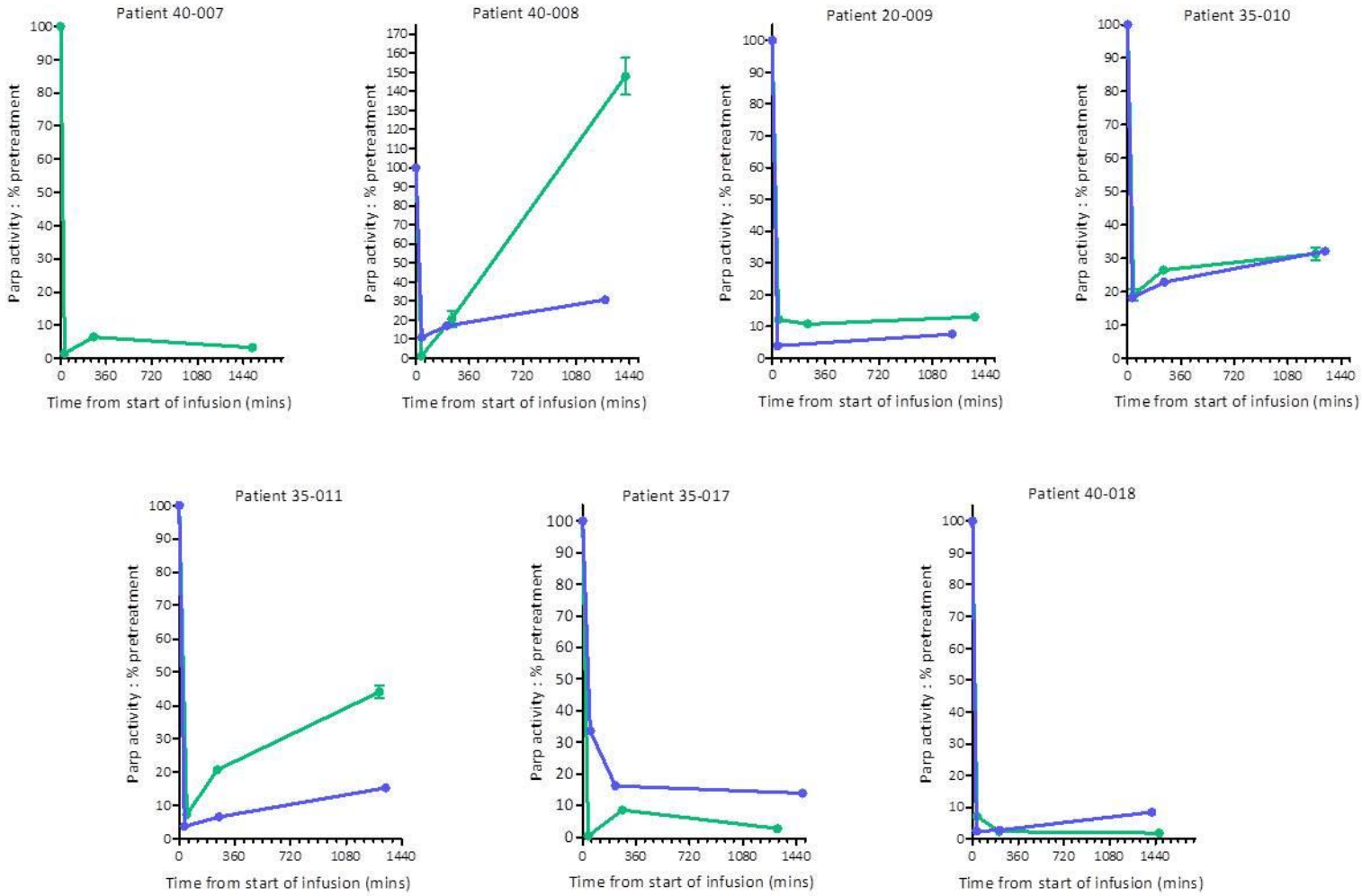

Figure 5.9: PARP-1 activity in response to AG014699 cohort two, stage one patients. Green lines and symbols represent the 12 mg/m^2 dose and the blue symbols and lines the 18 mg/m^2 dose level.

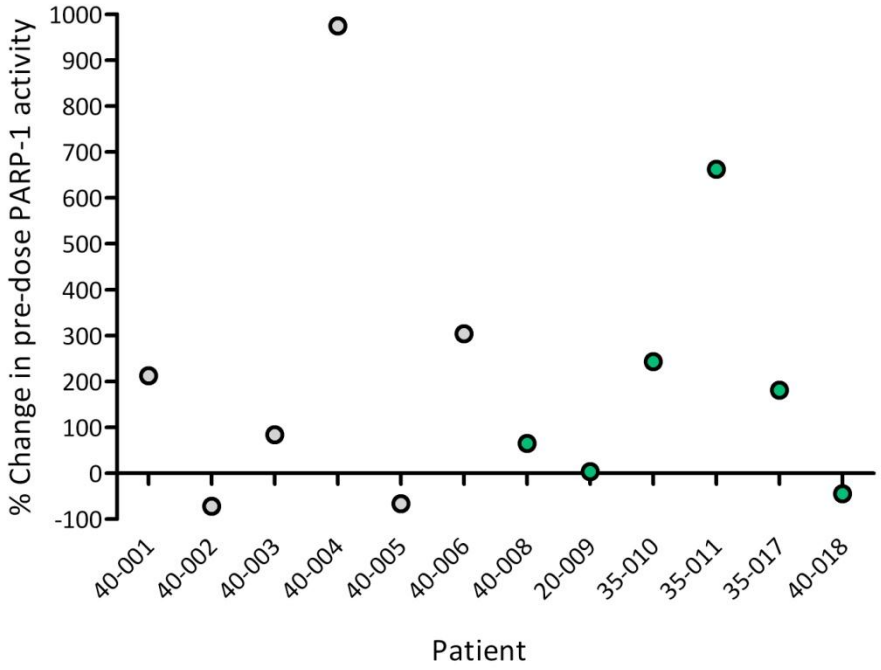

Figure 5.10: Intra-patient % change in PARP-1 activity after dose escalation (from C1 D1 pre-dose to C2 D1 pre-dose levels). Patients who received 4mg/m^2 for C1 are represented by the grey symbols and patients who received 12mg/m^2 in cycle one are shown in green symbols.

Patients in stage two of the study received 18 mg/m^2 daily dosing of AG014699 for all cycles. PARP-1 activity data for these patients, in addition to those in cohort two, stage one, who were also treated at 18 mg/m^2 in C2, are shown in figure 5.11A. Five patients had significantly less inhibition of PARP-1 activity at the EOI time-point than the rest of the group (mean % activity over baseline = 42.22 *vs.* 7.53; $p < 0.001$, un-paired t-test) and their individual results are plotted in figure 5.11B. In all five of these patients PARP-1 activity levels did fall further at the 4 h time-point (mean activity = 33.6 %) but in 3/4 patients (no sample received for patient 35-024) PARP-1 activity levels of > 30% of baseline were seen at the D2 pre-dose time-point.

Overall for stage two patients dosed at 18 mg/m^2, the D2 pre-dose sample shows a mean PARP-1 activity of 16.44% of baseline; demonstrating that AG014699 results in profound PARP-1 inhibition in PBL 24 h after the last dose. However, as figure 5.11A highlights in a number of patients recovery to > 30% of baseline is seen at this time-point. The impact of this in terms of clinical response to AG014699 will be reviewed later. Interestingly no correlation between the degree of AG014699 induced inhibition

of PARP-1 activity and baseline (maximum stimulated) levels of PARP-1 activity was seen in these patients at any of the time-points, see figure 5.12.

A wide inter-patient variation in inhibition of PARP-1 activity by AG014699 was seen at all time-points and dose levels with % CV shown in table 5.4.

For all three dose cohorts the mean PARP activity ~ 24 h (D2 pre-dose sample) after a single dose of 4, 12 and 18 mg/m^2 AG014699 was 31.47%, 20.53% and 16.40% respectively. Figure 5.13A shows a clear dose-response relationship between mean % PARP-1 enzyme inhibition at this time-point and increasing doses of AG014699.

Interestingly this is *not* seen at the earlier time-points with the degree of inhibition at 18 mg/m^2 similar to or less than that at the other dose levels, even when you remove the data points for those patients identified in figure 5.11. This may suggest that higher AG014699 doses result in prolongation of PARP-1 inhibition rather than more profound inhibition.

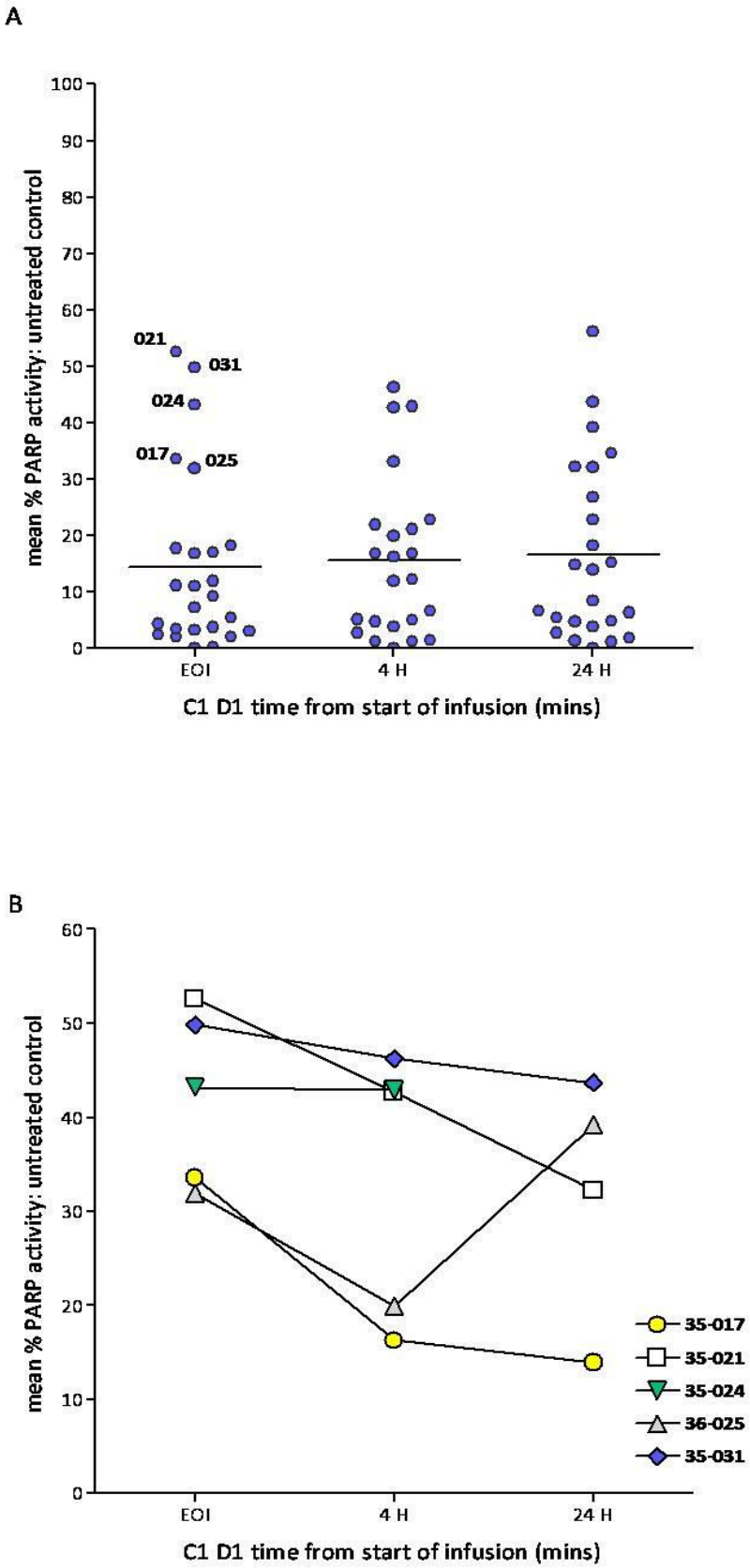

Figure 5.11: PARP-1 activity in response to AG014699 stage two patients **(A)** Scatter-plot showing the effect of 18 mg/m^2 dose of AG014699 on PARP-1 activity in PBL in 24 patients. 5 Patients with the highest EOI activity levels are shown with study number next to the corresponding plots. **(B)** Data for the five patients identified in A

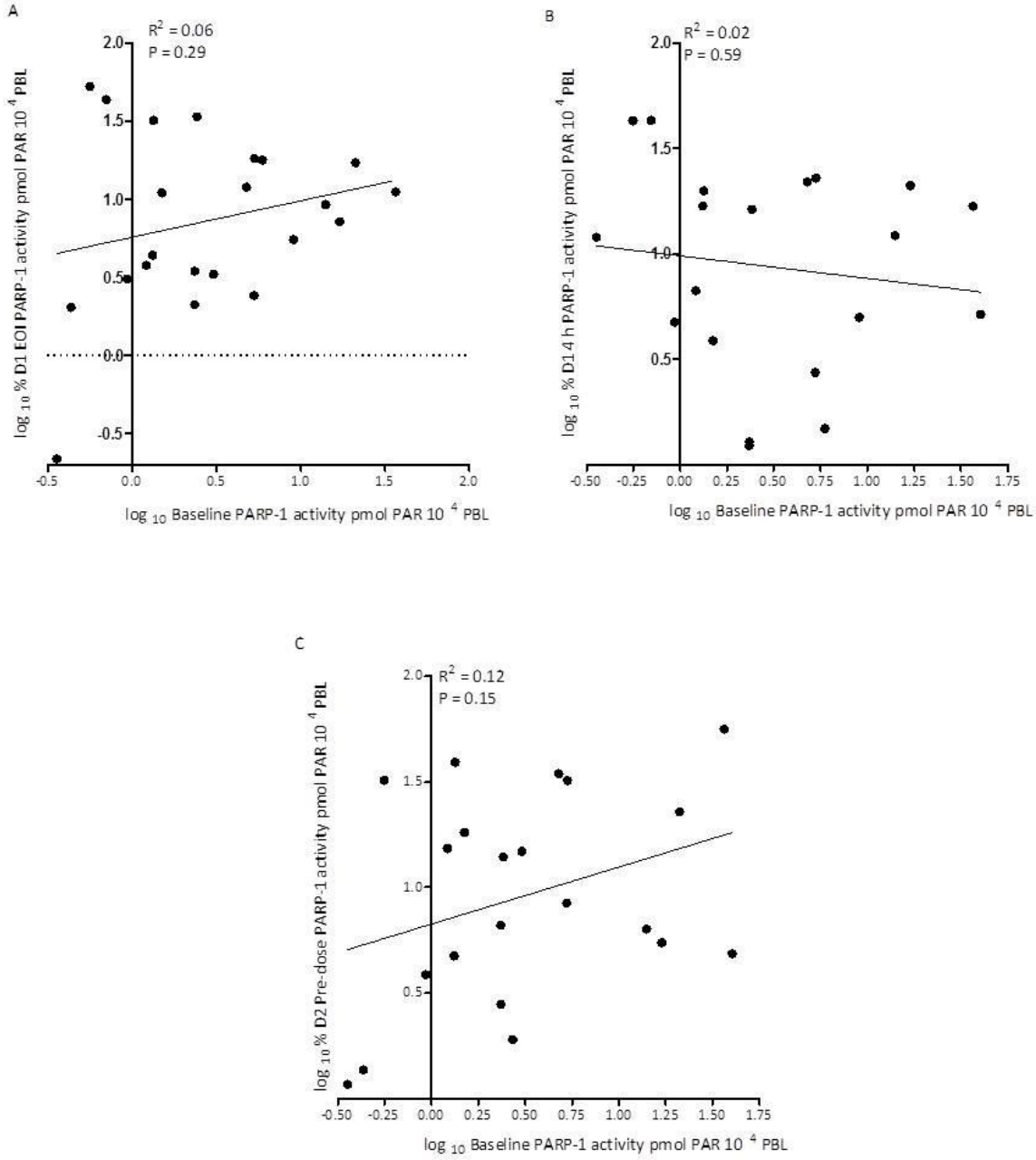

Figure 5.12: Relationship between patients baseline PARP activity and levels after AG014699 exposure. Data shows no relationship between PARP-1 activity levels at the end of infusion **(A)**, 4 h **(B)** and 24 h **(C)** post dose of AG014699 and a patients' baseline pre-treatment PARP-1 activity levels. Correlation calculated using Pearsons coefficient.

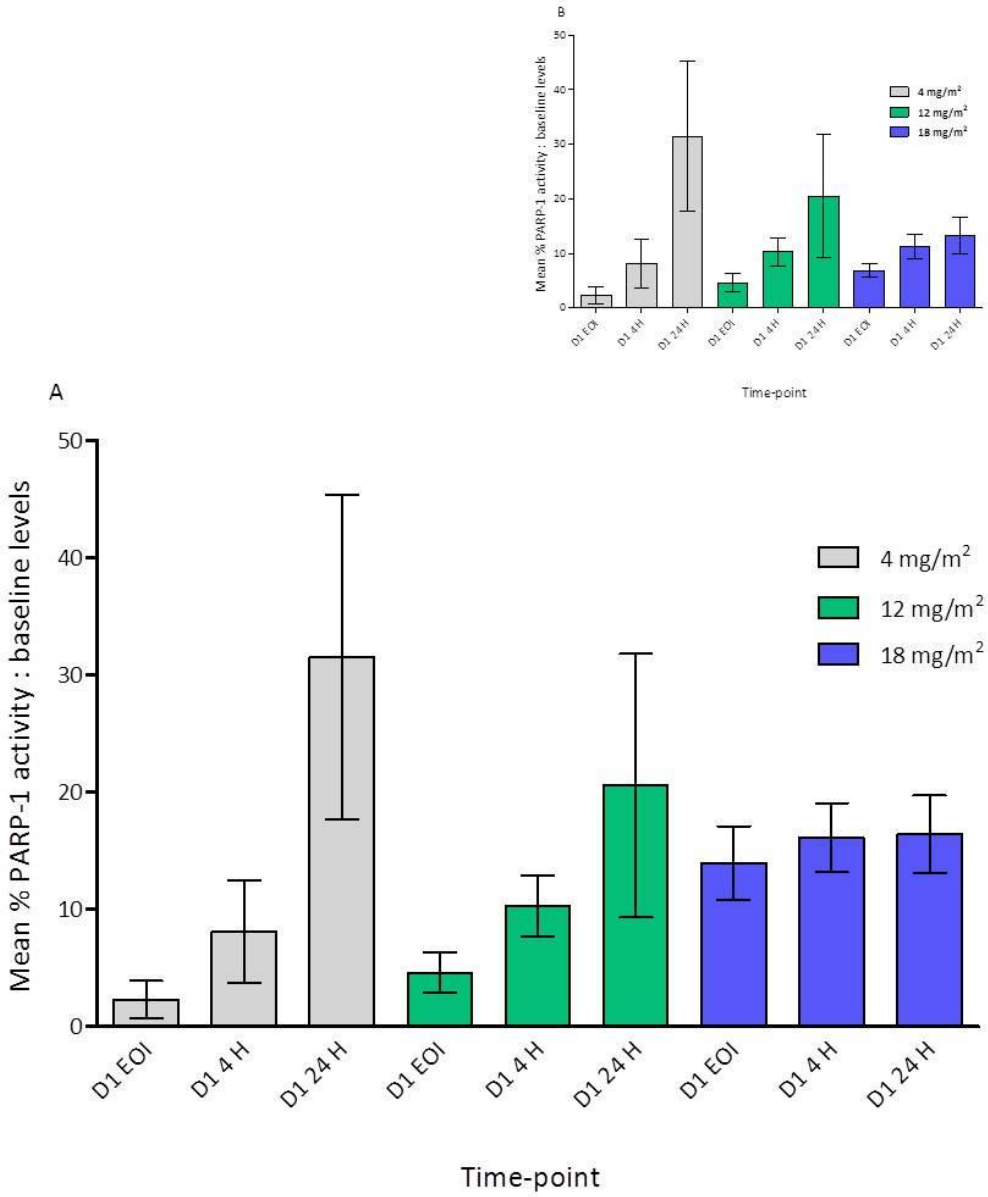

Figure 5.13: (A) Mean % PARP-1 activity for each time-point of each dosing level (represented by the coloured bars). Data show a dose-response at the D2 pre-dose sample with reduction in PARP-1 activity with increasing dose of AG014699. Error bars represent the SEM. **(B)** The same data minus the five patients identified in figure 5.11.

5.4.4 Pharmacokinetics of AG014699

The pharmacokinetics of AG014447 (the free base of AG014699) was determined from plasma extracted from patient's whole blood using LC/MS/MS, as described in chapter two, section 2.11. The blood sampling schedule and preparation of plasma are described in section 5.3.2. A complete set of samples (9 time-points per cycle) was received for 28 patients. However, sufficient samples were received from 35 patients

and are included in this pharmacokinetic study. Results, expressed as concentration of AG014447 in ng/ml, for the individual sampling time-points for all 35 patients are shown in Table 5.6, with summary data presented in Table 5.7.

As described in section 5.4.3 this is the first clinical trial to include intra-patient dose escalation of a PARP-1 inhibitor. Based on data from the previous phase I study of AG014699 in combination with temozolomide (Plummer *et al*., 2008) the maximum or peak concentration of AG014699 after administration (C_{max}) occurred at the end of the 30 minute infusion. Figure 5.14 shows the C_{max} values on D1, 4 and 5 for each dose level and demonstrates a linear pharmacokinetics with increasing AG014699 dose, although there was considerable inter-patient variability.

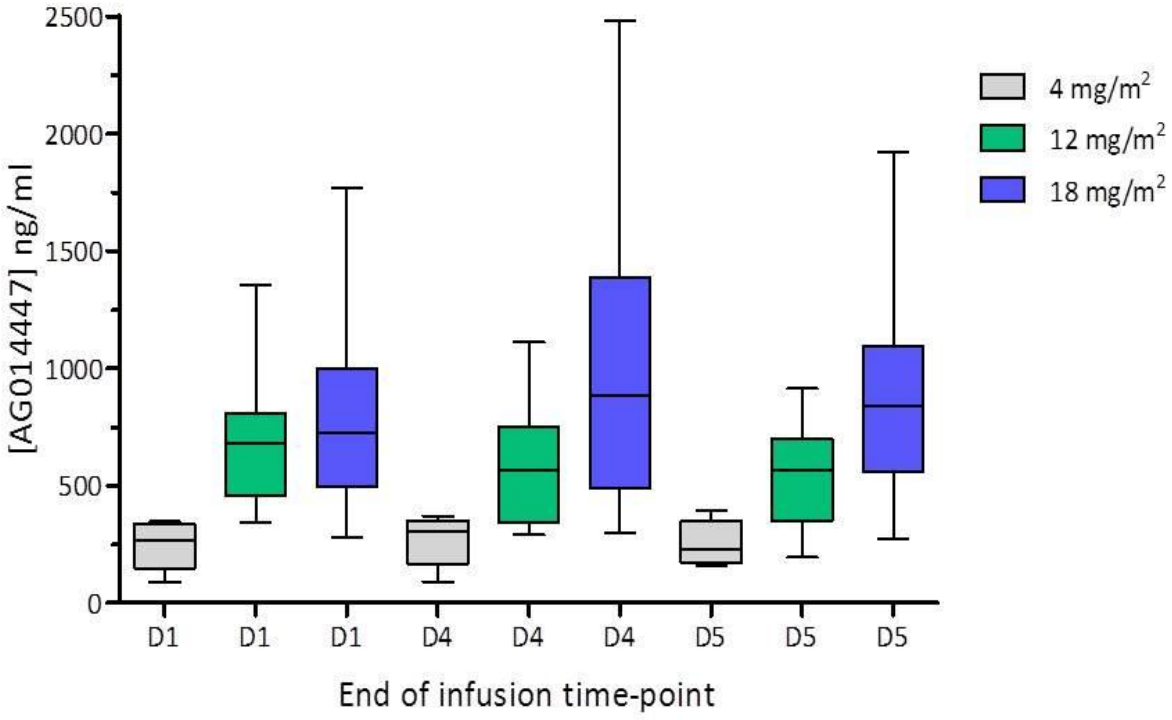

Figure 5.14: Box plot and whiskers plot showing the C_{max} AG014447 (ng/ml) for each time-point in each AG014699 doing cohort. Lines represent median values.

Separate graphs for D1, D4 and D5 C_{max} AG014447 for each of the three dose levels are shown in Figure 5.15.

Linear regression analysis demonstrates a significant relationship ($P < 0.001$) between increasing dose of AG014699 and C_{max} for all three days tested. Mean C_{max} AG014447 on D1 were 246.1 ng/ml, 676.5 ng/ml and 859.7 ng/ml for the 4 mg/m^2, 12 mg/m^2 and 18 mg/m^2 dose levels respectively.

This is comparable with the published phase I study data set with mean C_{max} values on D1 of 134 ng/ml, 551 ng/ml and 837 ng/ml for the 4 mg/m^2, 12 mg/m^2 and 18 mg/m^2 cohorts respectively (Plummer *et al*., 2008). For the 18 mg/m^2 dosing cohort C_{max} was highest on D4 but this was not significantly different to the C_{max} values for D1 and 5 ($P = 0.22$, one way analysis of variance).

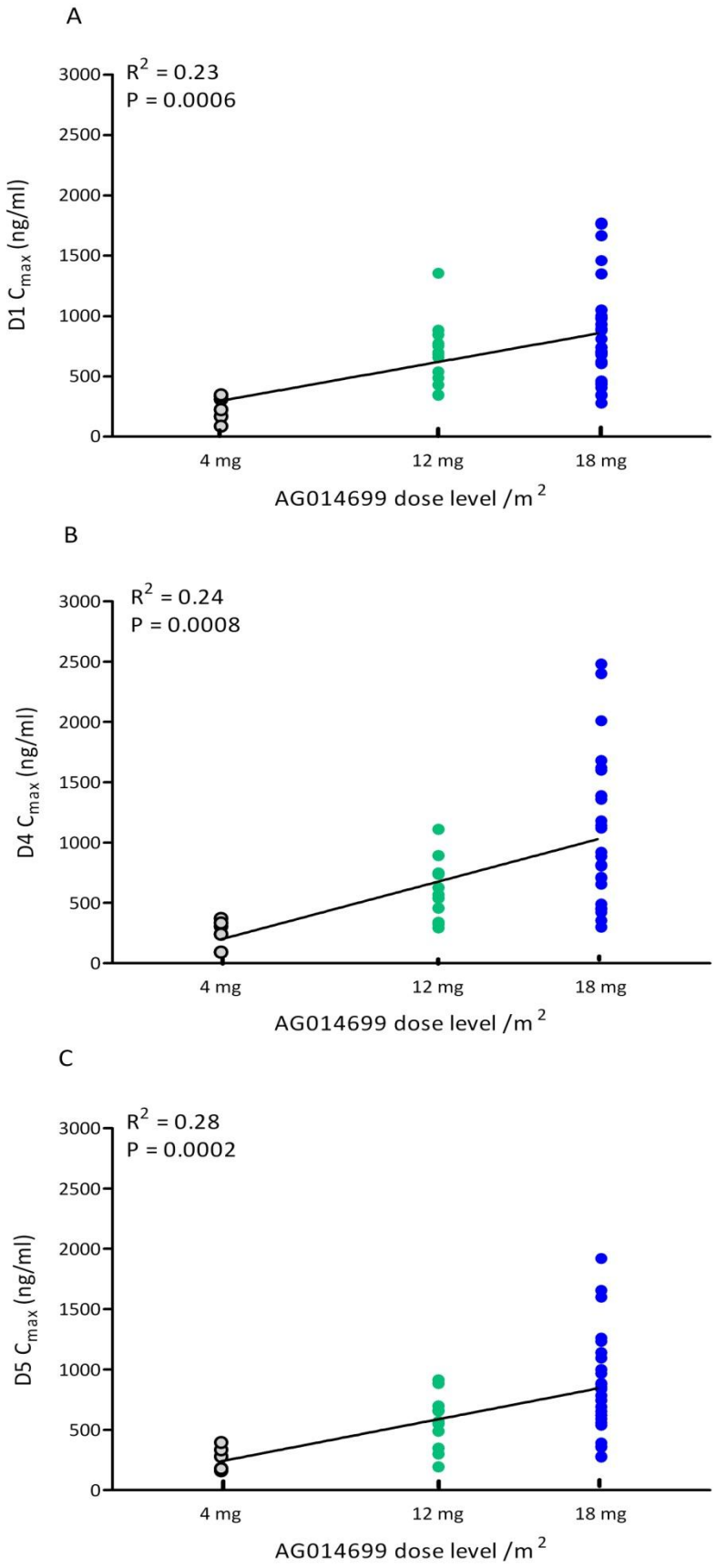

Figure 5.15: Linear regression analysis showing the relationship of AG014699 dose and C_{max} (ng/ml) on (A) D1, (B) D4 and (C) D5.

Patient study no.	Dose AG014699 (mg/m^2)	[AG014447] ng/ml								
		D1 pre-dose	D1 EOI	D1 1-3 hrs	D2 pre-dose	D4 pre-dose	D4 EOI	D4 1-3 hrs	D5 pre-dose	D5 EOI
40-001	4 12	0.00 0.00	168.00 844.00	7.98 22.70	0.25 2.06	2.60 4.05	91.90 627.00	29.90 77.20	1.52 4.37	161.00 569.00
40-002	4 12	0.00 0.00	311.00 658.00	21.20 83.50	4.32 11.80	5.77 21.20	305.00 538.00	58.10 182.00	6.95 22.00	280.00 301.00
40-003	4 12	0.00 0.00	222.60 883.0	37.90 121.60	9.75 39.80	17.70 78.10	370.00 *	97.40 *	19.90 *	334.00 *
40-004	4 12	0.00 0.00	89.30 488.00	20.00 83.50	6.09 26.40	10.60 27.30	242.00 748.00	63.10 224.00	10.90 35.90	176.00 *
40-005	4 12	0.00 0.00	335.00 1356.00	62.90 275.00	13.80 37.30	22.70 38.10	334.00 893.00	119.00 320.00	26.60 38.50	395.00 699.00
40-006	4 12	0.00 *	347.00 *	24.50 *	6.07 *	* *	* *	* *	14.90 *	180.00 *
40-007*	12	0.00	773.00	108.00	35.70	64.40	736.00	297.00	60.90	913.00
40-008	12 18	0.00 0.00	348.00 606.00	55.70 131.00	7.90 19.70	6.80 24.80	292.00 711.00	96.90 198.00	9.93 28.10	194.00 1655.00
20-009	12 18	0.00 0.00	430.00 708.00	226.00 368.00	27.20 25.80	33.40 60.40	340.00 886.00	272.00 328.00	35.10 45.90	488.00 1234.00
35-010	12 18	0.00 0.00	538.00 461.00	137.00 129.00	18.40 29.30	35.00 62.70	3410.00† 815.00	97.60 195.00	31.80 85.70	348.00 558.00

Patient study no.	Dose AG014699 (mg/m^2)	[AG014447] ng/ml								
		D1 pre-dose	D1 EOI	D1 1-3 hrs	D2 pre-dose	D4 pre-dose	D4 EOI	D4 1-3 hrs	D5 pre-dose	D5 EOI
35-011	12 18	0.00 0.00	754.00 342.00	86.20 109.00	24.50 24.40	33.80 68.20	325.00 706.00	83.50 156.00	38.80 36.40	549.00 1000.00
20-016	12 18	0.00 0.00	698.00 979.00	* 387.00	17.20 76.80	25.70 46.50	1110.00 2010.00	218.00 418.00	31.50 66.10	661.00 877.00
35-017	12 18	0.00 0.00	344.00 431.00	139.00 170.00	19.60 31.80	32.50 74.10	568.00 445.00	207.00 280.00	44.80 64.80	884.00 589.00
40-018	12 18	0.00 0.00	681.00 811.00	93.80 120.00	28.10 42.30	32.00 84.60	457.00 490.00	134.00 298.00	44.30 76.10	656.00 885.00
20-012	18	0.00	622.00	259.00	18.30	27.30	920.00	302.00	29.00	1095.00
35-013	18	0.00	894.00	307.00	61.70	70.90	1180.00	464.00	94.20	745.00
40-014	18	0.00	407.00	40.60	2.99	4.56	655.00	157.00	3.71	362.00
35-015	18	0.00	679.00	203.00	369.00	395.00	1385.00	675.00	434.00	1600.00
20-019	18	0.00	703.00	192.00	35.40	44.90	*	*	42.80	784.00
35-020	18	0.00	883.00	248.00	24.30	49.50	2400.00	441.00	69.80	967.00
35-021	18	0.00	985.00	158.00	27.40	65.70	455.00	222.00	56.10	653.00

Patient study no.	Dose AG014699 (mg/m^2)	[AG014447] ng/ml								
		D1 pre-dose	D1 EOI	D1 1-3 hrs	D2 pre-dose	D4 pre-dose	D4 EOI	D4 1-3 hrs	D5 pre-dose	D5 EOI
40-022	18	0.00	1460.00	173.00	53.30	85.90	1390.00	368.00	81.70	854.00
36-023	18	0.00	1760.00	624.00	62.60	91.40	1680.00	747.00	1780.00◊	*
35-024	18	0.00	444.00	102.00	5.55	3.96	300.00	100.00	3.18	276.00
36-025	18	0.00	1770.00	121.00	6.46	12.20	423.00	131.00	11.30	620.00
06-027	18	0.00	930.00	157.00	53.70	92.20	1360.00	348.00	81.00	538.00
52-028	18	0.00	279.00	92.30	17.70	34.80	298.00	213.00	41.10	355.00
40-029	18	0.00	1666.00	280.00	66.80	95.00	1600.00	645.00	108.00	1920.00
35-030	18	0.00	740.00	103.00	18.70	82.80	812.00	128.00	47.30	280.00
35-031	18	0.00	1050.00	273.00	88.10	118.00	2480.00	589.00	110.00	1260.00
52-032	18	0.00	1350.00	270.00	118.00	162.00	808.00	*	209.00	691.00
06-033	18	0.00	691.00	344.00	78.00	134.00	1140.00	586.00	74.30	837.00
35-035	18	0.00	700.00	191.00	83.00	83.50	1120.00	386.00	112.00	1140.00
35-037	18	0.00	1000.00	353.00	44.50	*	1620.00	48.30	143.00	877.00

Patient study no.	Dose AG014699 (mg/m^2)	[AG014447] ng/ml								
		D1 pre-dose	D1 EOI	D1 1-3 hrs	D2 pre-dose	D4 pre-dose	D4 EOI	D4 1-3 hrs	D5 pre-dose	D5 EOI
35-038	18	0.00	348.00	157.00	20.50	75.00	354.00	14.80	53.80	391.00

Table 5.6: Concentration of AG014447 (ng/ml) for the 35 patients in both Stage 1 and 2. * indicates that result unavailable due to sample not being taken or insufficient sample to do analysis †◊ Spurious results were confirmed in repeated assays but removed from further PK analysis

Dose level	No. Patients	Mean concentration AG014447 (ng/ml) ± SD (%CV)								
		D1 pre-dose	D1 EOI	D1 1-3h	D2 pre-dose	D4 pre-dose	D4 EOI	D4 1-3h	D5 pre-dose	D5 EOI
4 mg/m^2	6	0.00	246.10 103.30 (42)	29.08 19.14 (66)	6.71 4.64 (69)	11.87 8.31 (70)	268.60 109.30 (41)	73.50 34.96 (48)	13.46 9.03 (67)	254.30 97.12 (38)
12 mg/m^2	14	0.00	676.50 271.20 (40)	119.30 70.16 (59)	22.77 11.41 (50)	33.26 20.00 (60)	837.00 846.00 (101)	184.10 86.00 (47)	33.16 15.37 (46)	569.30 227.80 (40)
18 mg/m^2	28	0.00	846.40 423.30 (50)	216.50 122.80 (57)	53.79 68.04 (127)	79.63 73.19 (92)	1053.00 614.20 (58)	324.50 200.40 (62)	142.40 331.10 (232)	853.40 419.90 (49)

Table 5.7: Summary the PK AG014447 statistics for the three dose levels

5.4.5 Effects the of Pharmacokinetics of AG014699 on inhibition of PARP-1 activity

To determine whether any relationship exists between the PK of AG014699 and extent of PARP-1 enzyme inhibition paired sample sets of PK and PD (where available) for each patient treated within each dose level were investigated.

The results of PARP-1 enzyme inhibition at the D1 EOI and D1 24 hour time-points were analysed together with the D1 C_{max} (EOI) and D2 pre-dose plasma levels of AG014447 using Pearson correlation coefficients. The D1 EOI and D2 pre-dose data sets for PARP-1 activity were not normally distributed (positive skew) and therefore a log transformation was performed prior to application of the correlation.

In the 4 mg/m^2 cohort an inverse relationship was observed between the concentration of AG014447 and the levels of PARP-1 enzyme activity; with a trend towards higher levels of plasma concentration AG014447 being associated with lower PARP-1 activity. The strongest association was with the D1 C_{max} AG014447 and the D1 EOI PARP-1 activity ($R^2 = 0.62$, $P = 0.06$) and the D2 pre-dose concentration of AG014447 and the 24 hour PARP-1 activity levels ($R^2 = 0.63$, $P = 0.06$). These results, presented in figure 5.16, did not reach statistical significance but this may have been secondary to the small sample size. Not unexpectedly, the relationship between PARP-1 activity at D1 24 hours and the D1 C_{max} AG014447 showed the lowest correlation ($R^2 = 0.50$, $P = 0.12$).

In the 12 mg/m^2 cohort again a trend towards lower PARP-1 activity with higher plasma concentrations of AG014447 at the D2 pre-dose paired time-points was seen but any relationship was weak and not statistically significant ($R^2 = 0.34$, $P = 0.10$), see figure 5.17.

At the highest dose level 18 mg/m^2 cohort no significant relationship was observed between the degree of PARP-1 activity and the plasma concentration of AG014447 in any of the data sets, see Figure 5.18.

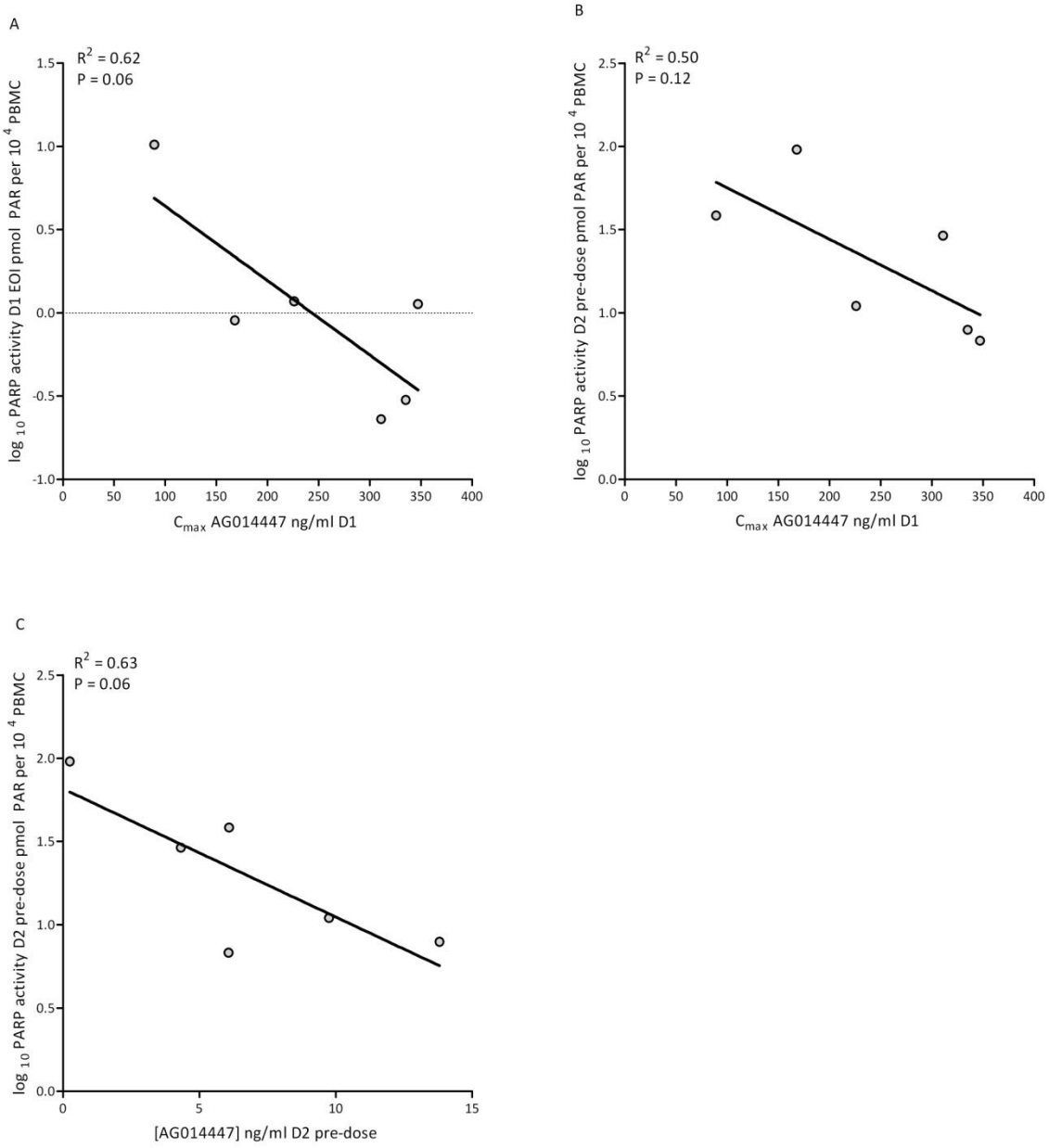

Figure 5.16: Relationship between concentration of AG014447 and PARP-1 enzyme activity for the 4 mg/m^2 cohort (**A)** $\log_{10}$ PARP-1 activity D1 *vs.* C_{max} AG014447 D1. (**B)** $\log_{10}$ PARP-1 activity D2 pre-dose *vs.* C_{max} AG014447 D1. **(C)** $\log_{10}$ PARP-1 activity D2 pre-dose *vs.* [AG014447] D2 pre-dose. R^2 and P values calculated using Pearson correlation coefficient.

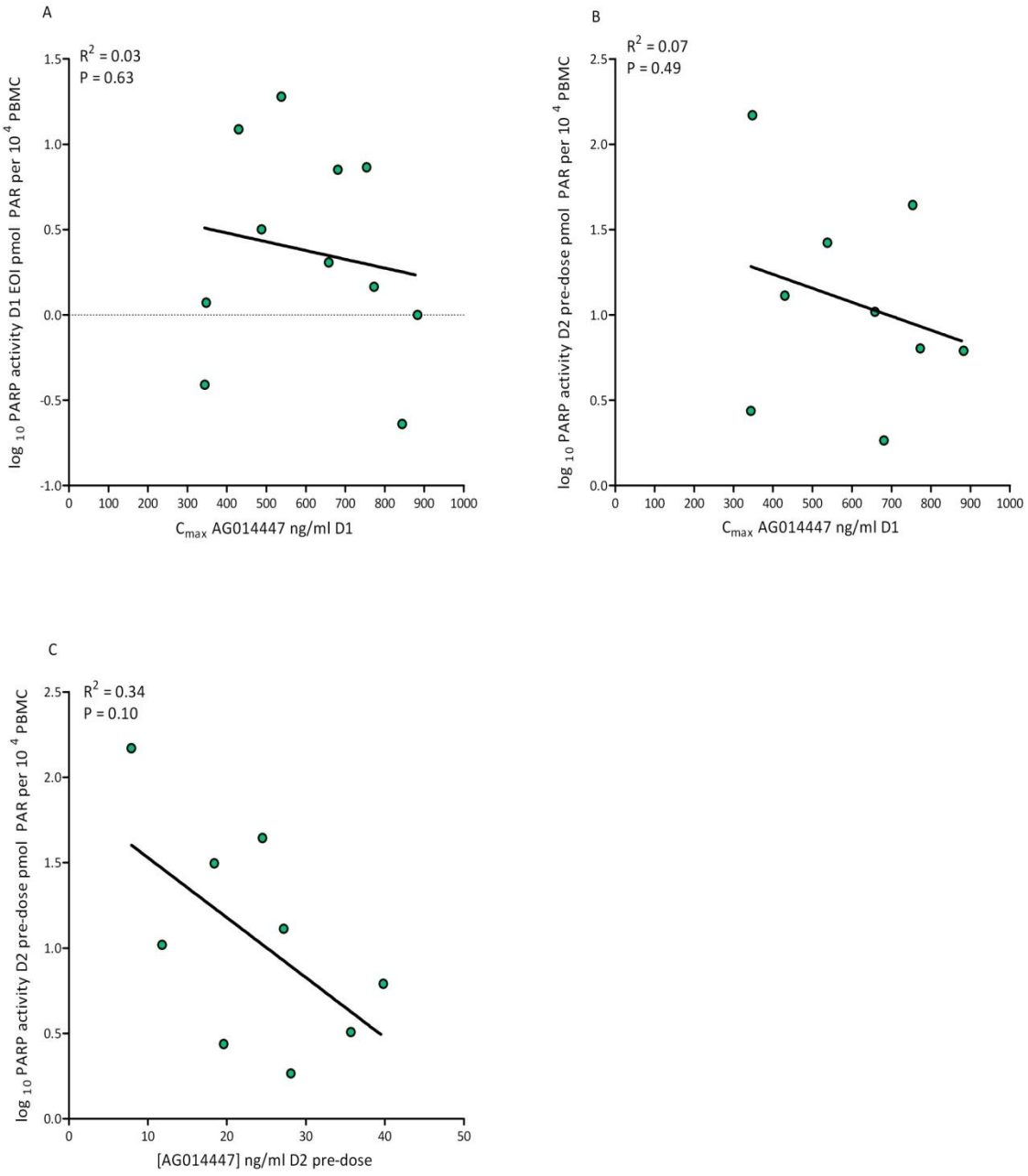

Figure 5.17: Relationship between concentration of AG014447 and PARP-1 enzyme activity for the 12 mg/m^2 cohort. **(A)** $\log_{10}$ PARP-1 activity D1 *vs.* C_{max} AG014447 D1. (**B)** $\log_{10}$ PARP-1 activity D2 pre-dose *vs.* C_{max} AG014447 D1.(**C)** $\log_{10}$ PARP-1 activity D2 pre-dose *vs.* [AG014447] D2 pre-dose. R^2 and P values calculated using Pearson correlation coefficient.

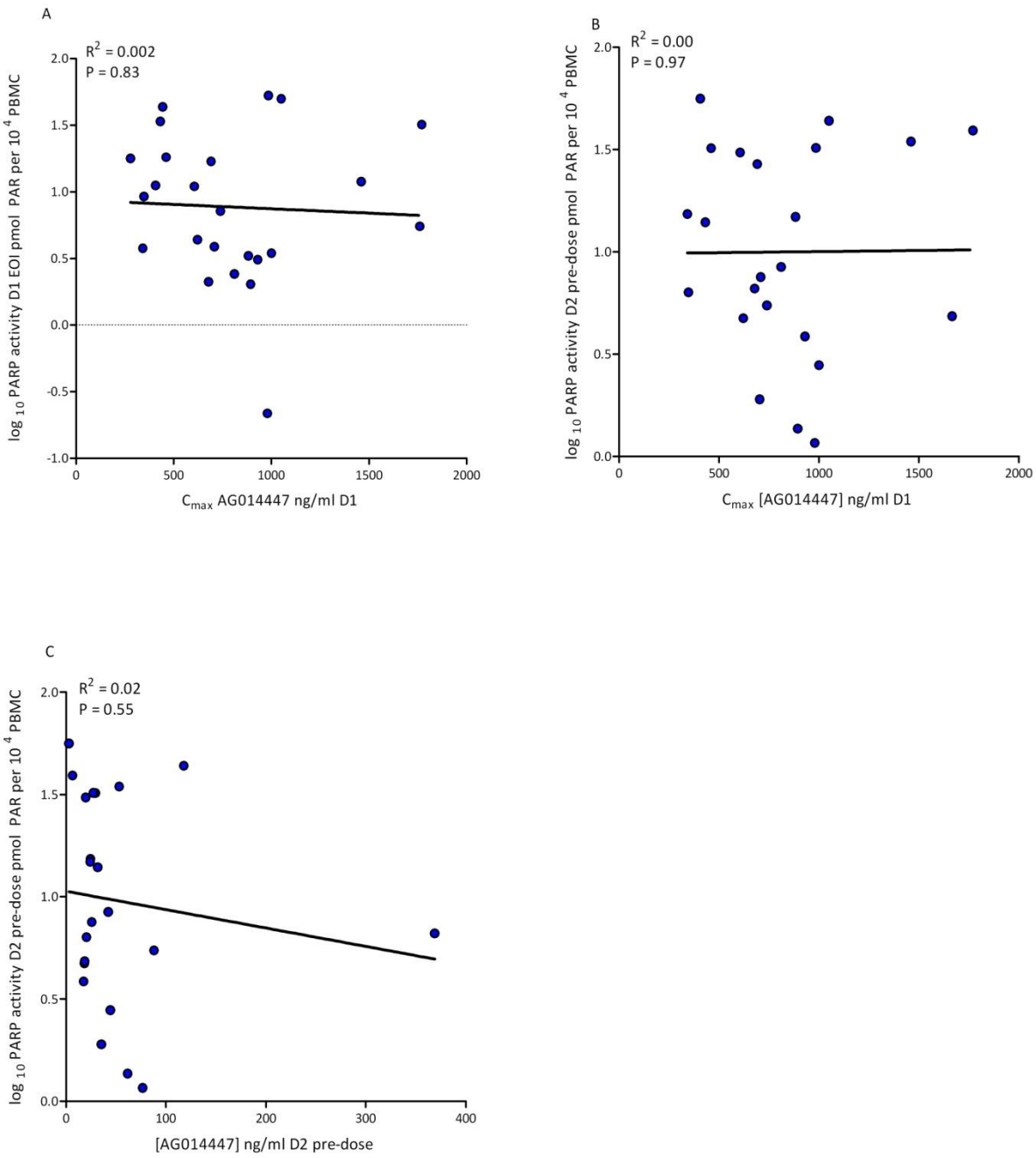

Figure 5.18: Relationship between concentration of AG014447 and PARP-1 enzyme activity for the 18 mg/m^2 cohort. **(A)** $\log_{10}$ PARP-1 activity D1 *vs.* C_{max} AG014447 D1. **(B)** $\log_{10}$ PARP-1 activity D2 pre-dose *vs.* C_{max} AG014447 D1. **(C)** $\log_{10}$ PARP-1 activity D2 pre-dose *vs.* [AG014447] D2 pre-dose. R^2 and P values calculated using Pearson correlation coefficient.

5.4.6 Pharmacokinetics of AG014699 in a tumour biopsy

As part of the Phase II PARP-BRCA study ethical approval to obtain single on-study tumour biopsies was obtained. Patient 40-014, with *BRCA*1 mutated ovarian cancer, had a vaginal vault recurrence at the time of study referral and consented to this additional biopsy. Patient 40-014 was treated within stage two of the trial and received all doses of AG014699 at a dose of 18 mg/m^2. Unfortunately, due to the availability of the gynae-oncology surgical team the biopsy could not be taken until the patient's second cycle of AG014699 treatment. The biopsy therefore did not coincide with the peripheral blood PK or PD sampling, which occurred, for this patient, in C1 only. The sample was taken 240 min following the start of the AG014699 infusion on C2 D4. The tumour was immediately snap frozen in liquid nitrogen and stored at -80^0 C until homogenisation and analysis using LC/MS/MS assay as described in chapter two, section 2.11. The concentrations of the analyte (AG014447) detected were multiplied by four to account for the dilution of the sample that occurred during the homogenisation step Results are shown in figure 5.19 together with the patient's plasma concentrations of AG014447 for C1. AG014447 was detectable in the tumour homogenate at a concentration of 692 ng/ml. This concentration compares to a plasma concentration of 157 ng/ml on the D4 + 92 min time-point in cycle 1 and demonstrates good tumour penetration and accumulation relative to plasma of AG014699 following intravenous administration.

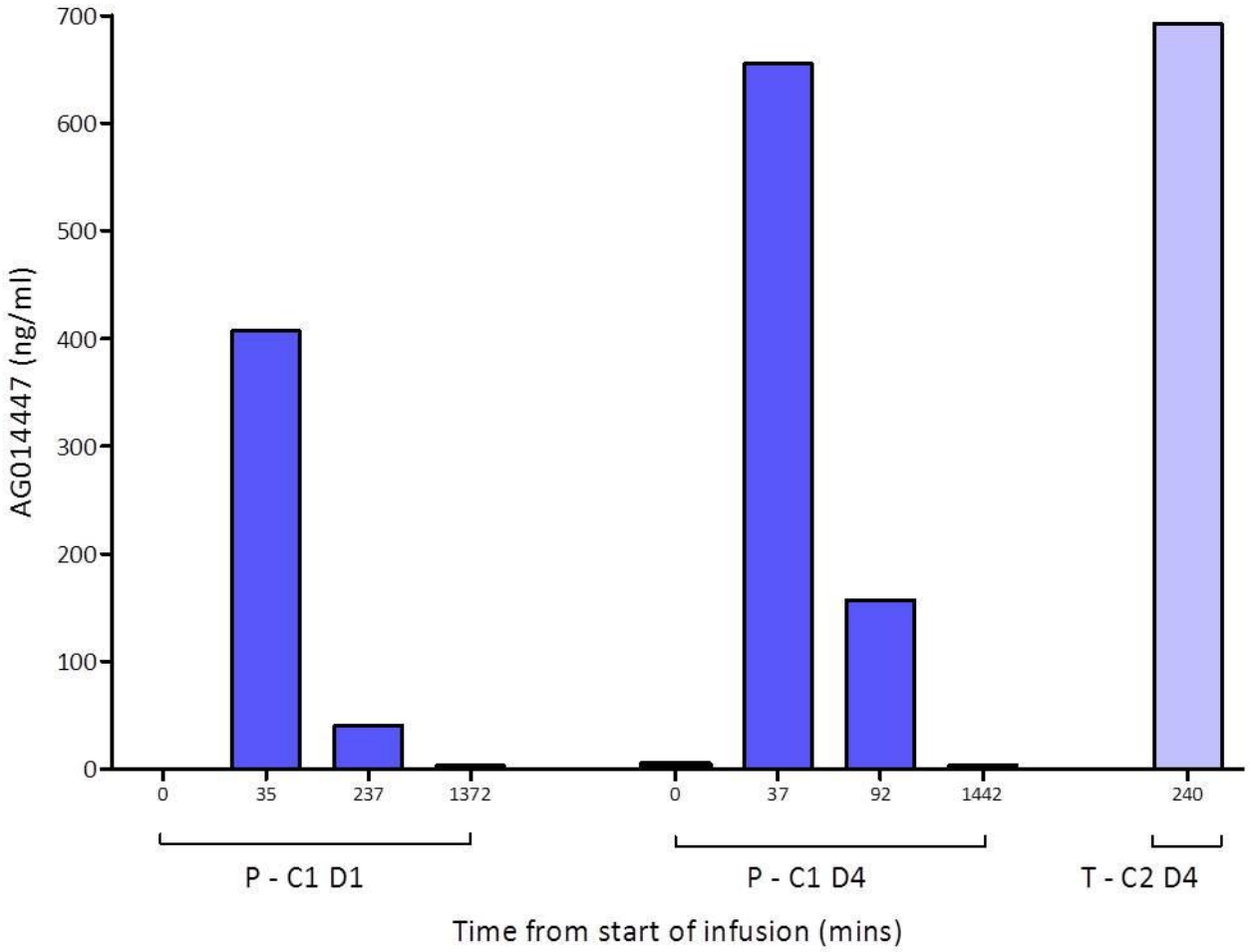

Figure 5.19: Concentration of AG014447 (ng/ml) in Patient 40-014 plasma (P) and tumour (T) samples following 18 mg/m^2 in cycle (C) one day (D) 1 and 4 for plasma and C2 D4 for the tumour homogenate.

5.4.7 Pharmacogenomics of AG014699 metabolism

A single whole blood sample was scheduled to be taken for each patient prior to commencing the first cycle of AG014699 for use in genotyping assays. DNA was extracted as described in section 5.3.3 and subsequently analysed using TaqMan Real-time PCR genotyping assay kits (Applied Biosystems, Warrington, UK) as described in chapter two, Materials and Methods, section 2.4.3. Whole blood samples for analysis of the CYP2D6 *2 and CYP2D6*4 SNP were received for 31 out of the 38 patients. The main reason for not obtaining a result for a given patient was that the blood sample was not taken at the treatment centre.

*5.4.7.1 CYP2D6*2*

Results for all 31 patients are shown in table 5.8 together with the corresponding PK results. The frequencies of the genotypes were as follows: major genotype (T/T) 12.9%, the heterozygote genotype (T/C) 38.7% and the minor variant genotype (C/C) 48.4%. The minor allele frequency of 68% is not in Hardy Weinberg Equilibrium (P = 0.52) and the frequency of the variant genotype higher than that reported in other Caucasian populations (20-35%), (Sistonen *et al*., 2007; Ramon y Cajal *et al*., 2010). However this result is difficult to interpret given the small sample size of this study. Figure 5.20 shows the D1 C_{max} (A) and D2 pre-dose concentrations of AG014447 (B) by CYP2D6*2 genotype result.

*5.4.7.2 CYP2D6*4*

CYP2D6*4 is the most common inactivating mutation found in Caucasian populations. It is reported to occur at a frequency of between 12 – 23% in European populations (Sistonen *et al*., 2007; Ramon y Cajal *et al*., 2010). Results for all 31 patients are shown in table 5.8 together with the corresponding PK results. The frequencies of the genotypes were similar to that reported in previous population studies (see above) and as follows: major genotype (G/G) 77.4%, the heterozygote genotype (G/A) 12.9% and the minor variant genotype (A/A) 9.7%. The minor allele frequency is 16% and consistent with Hardy Weinberg Equilibrium (P = 0.004). Figure 5.20 shows the D1 C_{max} (A) and D2 pre-dose concentrations of AG014447 (B) by CYP2D6*4 genotype result.

Patient no.	CYP2D6*2	CYP2D6*4	D1 Cmax [AG014447] ng/ml	D2 pre-dose[AG014447] ng/ml
40-001	C/C	G/A	844.00	2.06
40-002	T/T	G/G	658.00	11.80
40-003	T/C	G/G	883.00	39.80
40-004	C/C	A/A	488.00	26.40
40-005	T/C	G/G	1356.00	37.30
40-006	C/C	G/G	*	*
40-007	T/C	G/G	773.00	35.70
40-008	C/C	G/G	606.00	19.70
20-009	C/C	G/G	708.00	25.80
35-010	T/C	G/G	461.00	29.30
35-011	T/C	G/G	342.00	24.40
35-013	T/C	G/G	894.00	61.70
40-014	C/C	A/A	407.00	2.99
20-016	C/C	G/A	979.00	76.80
35-017	C/C	G/G	431.00	31.80
40-018	T/C	G/G	811.00	42.30
20-019	T/T	G/G	703.00	35.40
35-020	C/C	G/A	883.00	24.30
35-021	T/T	G/G	985.00	27.40
40-022	T/C	G/G	1460.00	53.30
36-023	T/C	G/G	1760.00	62.60
35-024	C/C	G/G	444.00	5.55
36-025	C/C	G/A	1770.00	6.46
52-028	T/T	G/G	279.00	17.70
40-029	C/C	G/G	1666.00	66.80
35-030	C/C	A/A	740.00	18.70
35-031	T/C	G/G	1050.00	88.10
52-032	T/C	G/G	1350.00	118.00
35-035	C/C	G/G	700.00	83.00
35-037	T/C	G/G	1000.00	44.50
35-038	C/C	G/G	348.00	20.50

Table 5.8: *CYP*2D6 genotyping results together with patients corresponding pharmacokinetic results.
* Sample not taken.

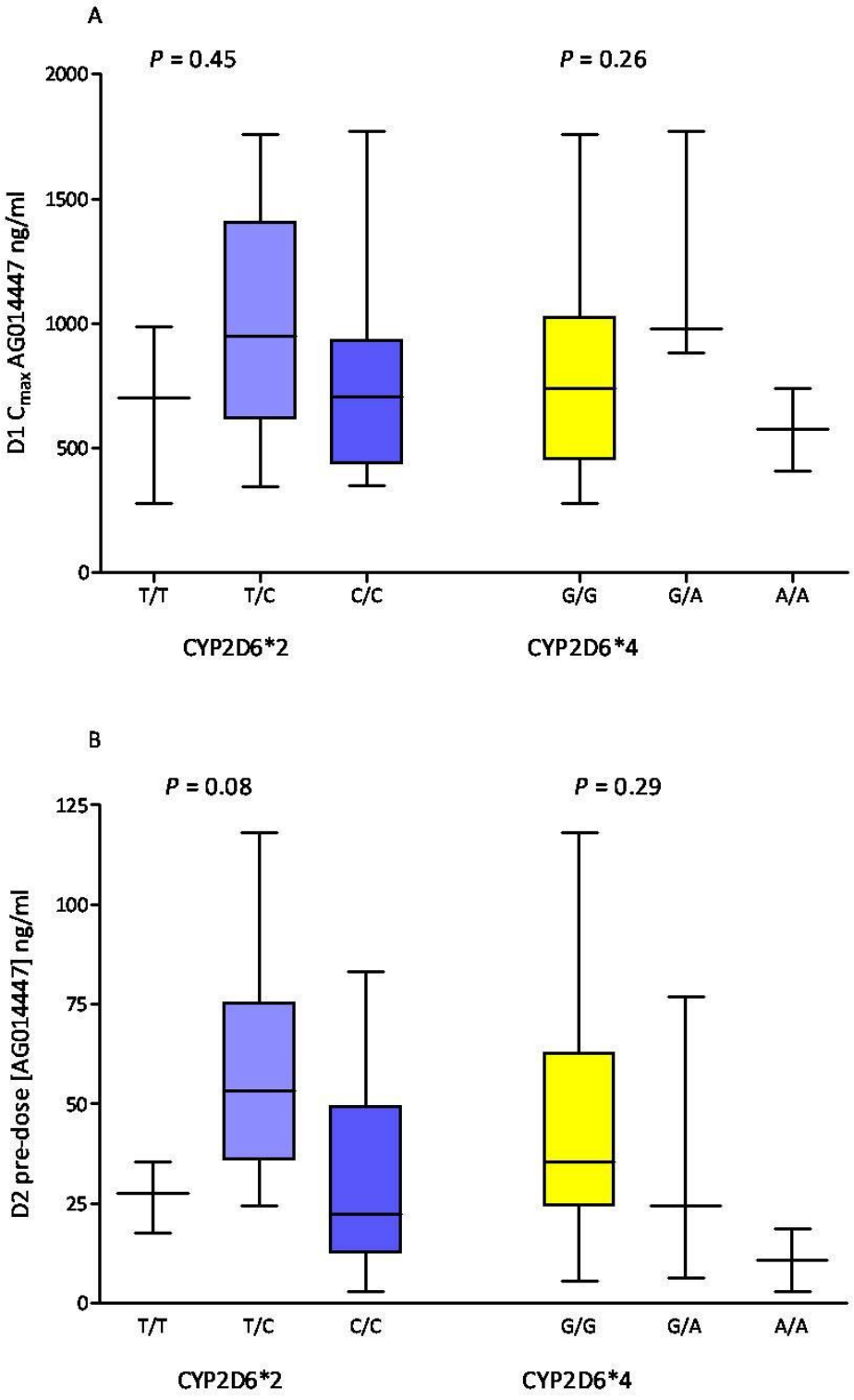

Figure 5.20: Box and whiskers plots showing concentration of AG014447 at D1 C_{max} (A) and D2 pre-dose (B) by CYP2D6 *2 and *4 genotype. P values are results of ANOVA comparing all three groups.

5.4.8 Clinical Outcomes of the Phase II trial

Between January 2007 and September 2010 38 patients were enrolled into the study and results for these patients are evaluated here. Final results of the completed study will be reported at a later date.

5.4.8.1 AG014699 administered

All 38 patients received at least one complete 21 day cycle of AG014699. In stage one of the study six patients received one cycle of AG014699 at the 4 mg/m^2 dose level and 14 patients (including the previous six) received a cycle at the 12 mg/m^2 level. In the second stage of the trial 31 patients (including seven from stage one cohort two) received at least one cycle of AG014699 at 18 mg/m^2. To the end of September 2010 a total of 201 AG014699 cycles were administered within the study. The median number of treatment cycles per patient was five (range = 1-21). Six patients were dose-escalated from 4 mg/m^2 to 12 mg/m^2 and seven patients were dose-escalated from 12 mg/m^2 to 18 mg/m^2 as per study protocol. No patients received a dose reduction. No treatment cycles were delayed due to AG014699-related toxicity.

5.4.8.2 Toxicity

All 38 patients received at least one dose of AG014699 and were therefore assessable for toxicity. Toxicity was categorised and coded by the CTCAE version 3.0. Over-all AG014699 was well tolerated in this patient population with no dose-limiting toxicities observed in any stage of the study. This adds to the findings of the phase I study of AG014699 in combination with temozolomide, in which no toxicity from test doses of single-agent AG014699 were reported (Plummer *et al.,* 2008).

AG014699 had an acceptable safety profile with drug-related toxicity mainly grade 1 and 2. The most commonly reported AG014699-related grade 1/2 non-haematological toxicities being: fatigue (16/38, 42.1% of patients), nausea (28.9%) and diarrhoea (21.1%). Haematological toxicities were not expected based on the previous studies of single doses of AG014699. However, possibly related grade 2 anaemia was reported in patient 40-007 during cycle one and possibly related grade 2 lymphopenia, grade 1 neutropenia and grade 1 thrombocytopenia were seen in patient 40-001 during C18. No patient withdrew from the study due to toxicity.

Two patients died within 28 days of last study drug treatment and both deaths were deemed to be unrelated to AG014699. Patient 40-007 died of disease progression on study and patient 52-032, with heavily pre-treated metastatic breast cancer, died of hepatic failure. All recorded adverse events (AEs) to date are listed in Table 5.9.

Body system	Adverse event CTCAE category	Number of episodes (Number of patients : % of total number of patients)		
		All AEs	Related AEs	Grade 3/4/5 Related AEs
Auditory/Ear	Auditory/Ear (other)	1 (1: 2.6%)	0 (0: 0%)	0 (0: 0%)
	Tinnitus	1 (1: 2.6%)	1 (1: 2.6%)	0 (0: 0%)
Blood/Bone marrow	Anaemia	1 (1: 2.6%)	1 (1: 2.6%)	0 (0: 0%)
	Lymphopenia	2 (2: 5.3%)	1 (1: 2.6%)	0 (0: 0%)
	Neutropenia	2 (2: 5.3%)	1 (1: 2.6%)	0 (0: 0%)
	Thrombocytopenia	1 (1: 2.6%)	1 (1: 2.6%)	0 (0: 0%)
Cardiac arrhythmia	Palpitations	1 (1: 2.6%)	1 (1: 2.6%)	0 (0: 0%)
	Sinus bradycardia	1 (1: 2.6%)	0 (0: 0%)	0 (0: 0%)
	Sinus tachycardia	1 (1: 2.6%)	0 (0: 0%)	0 (0: 0%)
	Vaso-vagal episode	1 (1: 2.6%)	0 (0: 0%)	0 (0: 0%)
Cardiac General	Hypertension	2 (1: 2.6%)	2 (1: 2.6%)	0 (0: 0%)
Constitutional Symptoms	Fatigue	36 (20: 52.6%)	31 (18: 47.3%)	3 (2: 5.3%)
	Fever	6 (5: 13.2%)	2 (2: 5.3%)	0 (0: 0%)
	Insomnia	3 (3: 7.9%)	0 (0: 0%)	0 (0: 0%)
	Rigors/chills	1 (1: 2.6%)	0 (0: 0%)	0 (0: 0%)
	Weight gain	1 (1: 2.6%)	0 (0: 0%)	0 (0: 0%)
	Weight loss	4 (4: 10.5%)	0 (0: 0%)	0 (0: 0%)
Death	Death-disease progression NOS	1 (1: 2.6%)	0 (0: 0%)	0 (0: 0%)

Body system	Adverse event CTCAE category	Number of episodes (Number of patients : % of total number of patients)		
		All AEs	Related AEs	Grade 3/4/5 Related AEs
Dermatology/Skin	Alopecia	3 (2: 5.3%)	3 (2: 5.3%)	0 (0: 0%)
	Bruising	3 (3: 7.9%)	0 (0: 0%)	0 (0: 0%)
	Dermatology-other	8 (5: 13.2%)	3 (2: 5.3%)	0 (0: 0%)
	Erythema multiforme	2 (2: 5.3%)	0 (0: 0%)	0 (0: 0%)
	Infection site reaction	13 (6: 15.8%)	8 (3: 7.9%)	0 (0: 0%)
	Pruritus	12 (3: 7.9%)	12 (3: 7.9%)	0 (0: 0%)
	Rash	2 (2: 5.3%)	0 (0: 0%)	0 (0: 0%)
Endocrine	Hot flashes	1 (1: 2.6%)	0 (0: 0%)	0 (0: 0%)
Gastrointestinal	Anorexia	8 (8: 21.1%)	4 (4: 10.5%)	0 (0: 0%)
	Constipation	16 (10: 26.3%)	2 (2: 5.3%)	0 (0: 0%)
	Dehydration	2 (1: 2.6%)	0 (0: 0%)	0 (0: 0%)
	Diarrhoea	25 (14: 36.8%)	15 (8: 21.1%)	0 (0: 0%)
	Distension	14 (11: 28.9%)	0 (0: 0%)	0 (0: 0%)
	Dry mouth	3 (3: 7.9%)	1 (1: 2.6%)	0 (0: 0%)
	Dysphagia	1 (1: 2.6%)	0 (0: 0%)	0 (0: 0%)
	Flatulence	1 (1: 2.6%)	0 (0: 0%)	0 (0: 0%)
	GI-other	4 (3: 7.9%)	2 (1: 2.6%)	0 (0: 0%)
	Heartburn	4 (4: 10.5%)	1 (1: 2.6%)	0 (0: 0%)

Body system	Adverse event CTCAE category	Number of episodes (Number of patients : % of total number of patients)		
		All AEs	Related AEs	Grade 3/4/5 Related AEs
Gastrointestinal	Mucositits	2 (1: 2.6%)	0 (0: 0%)	0 (0: 0%)
	Nausea	31 (18: 47.4%)	14 (11: 28.9%)	0 (0: 0%)
	Obstruction GI-Colon	2 (1: 2.6%)	0 (0: 0%)	0 (0: 0%)
	Obstruction GI-Small bowel	1 (1: 2.6%)	0 (0: 0%)	0 (0: 0%)
	Taste alteration	1 (1: 2.6%)	0 (0: 0%)	0 (0: 0%)
	Teeth	1 (1: 2.6%)	0 (0: 0%)	0 (0: 0%)
	Ulceration-stoma	1 (1: 2.6%)	0 (0: 0%)	0 (0: 0%)
	Vomiting	30 (14: 36.8%)	6 (5: 13.2%)	0 (0: 0%)
Haemorrhage/Bleeding	Haem GU-urinary	1 (1: 2.6%)	0 (0: 0%)	0 (0: 0%)
	Haem GU-vagina	8 (3: 7.9%)	1 (1: 2.6%)	0 (0: 0%)
	Haemorrhage-other	2 (2: 5.3%)	0 (0: 0%)	0 (0: 0%)
Hepatobiliary/Pancreas	Liver dysfunction	1 (1: 2.6%)	0 (0: 0%)	0 (0: 0%)
Infection	All systems	26 (19: 50.0%)	2 (2: 5.3%)	0 (0: 0%)
Lymphatics	Lymphatics-other	1 (1: 2.6%)	0 (0: 0%)	0 (0: 0%)
	Limb oedema	8 (6: 15.8%)	0 (0: 0%)	0 (0: 0%)
Metabolic/Laboratory	ALT	3 (3: 7.9%)	1 (1: 2.6%)	0 (0: 0%)
	ALP	3 (2: 5.3%)	2 (1: 2.6%)	0 (0: 0%)
	Creatinine	1 (1: 2.6%)	0 (0: 0%)	0 (0: 0%)

Body system	Adverse event CTCAE category	Number of episodes (Number of patients : % of total number of patients)		
		All AEs	Related AEs	Grade 3/4/5 Related AEs
Neurology	Dizziness	16 (10: 26.3%)	13 (7: 18.4%)	0 (0: 0%)
	Mood-Anxiety	3 (3: 7.9%)	0 (0: 0%)	0 (0: 0%)
	Mood-Depression	1 (1: 2.6%)	1 (1: 2.6%)	1 (1: 2.6%)
	Sensory neuropathy	9 (6: 15.8%)	4 (3: 7.9%)	0 (0: 0%)
Ocular/Visual	Dry eye	1 (1: 2.6%)	1 (1: 2.6%)	0 (0: 0%)
	Vitreous haemorrhage	1 (1: 2.6%)	0 (0: 0%)	0 (0: 0%)
Pain	Pain-Abdomen	26 (15: 39.5%)	3 (2: 5.3%)	0 (0: 0%)
Pulmonary/Upper respiratory	Cough	9 (8: 21.1%)	1 (1: 2.6%)	0 (0: 0%)
	Dyspnoea	8 (4: 10.5%)	0 (0: 0%)	0 (0: 0%)
	Pleural effusion	2 (2: 5.3%)	0 (0: 0%)	0 (0: 0%)
Renal/Genitourinary	Ureteric obstruction	3 (1: 2.6%)	0 (0: 0%)	0 (0: 0%)
	Urinary frequency	1 (1: 2.6%)	0 (0: 0%)	0 (0: 0%)
Syndromes	Flu-like symptoms	1 (2.6%)	0 (0: 0%)	0 (0: 0%)
Vascular	Phlebitis	1 (1: 2.6%)	1 (1: 2.6%)	0 (0: 0%)
	Thromboembolism	3 (2: 5.3%)	0 (0: 0%)	0 (0: 0%)

Table 5.9: Adverse events listings for the PARP-BRCA Phase II Trial

5.4.8.3 Response Rate

The primary end-point of the clinical trial was best objective response rate (ORR) as measured by the RECIST. At the time of writing this thesis, 35 of the 38 patients recruited had received two complete cycles of AG014699 and were eligible for a response evaluation. The three non-evaluable patients were: patient 40-007 who had clinical evidence of disease progression after C1; patient 20-026 who required ureteric stenting after C1 and patient 52-032 who withdrew their consent on C2 D3 of treatment. Therefore, for these 35 patients the ORR was 6% (2/35; patient 40-005 and 35-010). However, almost half the patients (49%, 17/35) achieved stable disease after two cycles, with 29% of all patients (10/35) achieving disease stabilisation for greater than four months and three patients remaining on study for over 54 weeks. This gives a clinical benefit response (CBR) rate of 34% (12/35). Interestingly this CBR rate was spread across all stages of the study and not limited to patients receiving the higher 18 mg/m^2 AG014699 doses. 16 patients had evidence of disease progression after two cycles of AG014699 and were withdrawn from the study. Data for the best overall response (expressed as % change in target lesions from pre-treatment values) was available in 33 of the 35 patients and is shown by waterfall plot in figure 5.21.

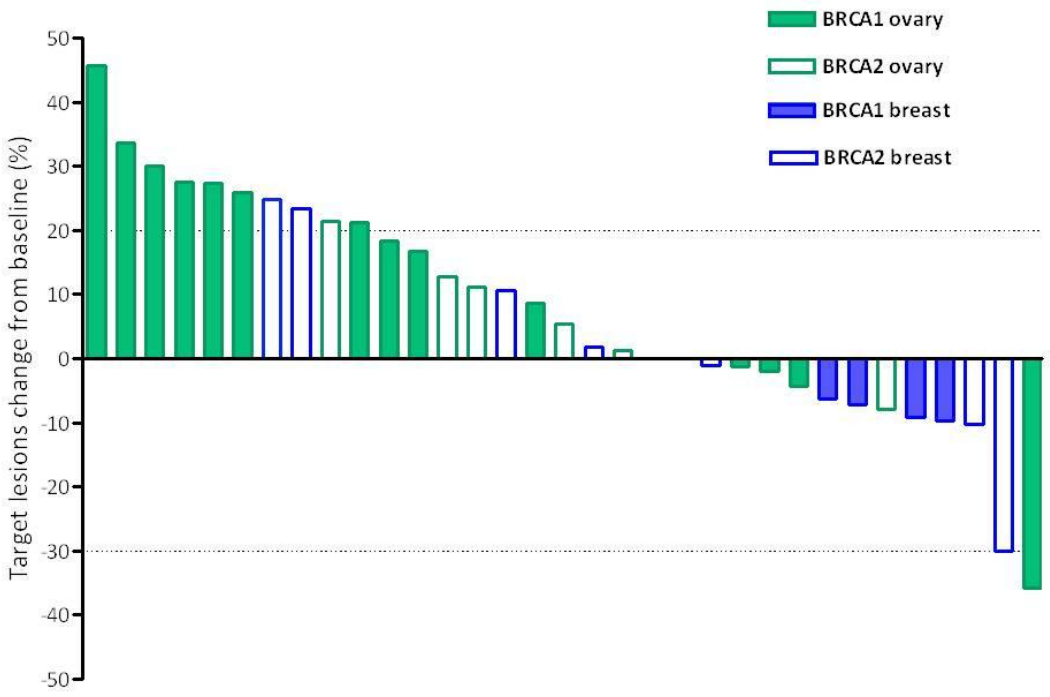

Figure 5.21: Waterfall plot showing best RECIST response to AG014699 expressed as % change in target lesions over baseline measurements. The grey bars represent patients with progressive disease, the white bars patients with stable disease and the yellow bars patients with a partial response. Data shown are results for 33 patients.

The two patients who had partial responses to AG014699 were patients 40-005 (BRCA2 breast) and 35-010 (BRCA1 ovary). Patient 40-005 had a partial response at C4 and a time to progression (TTP) of 173 days. She remained on study until radiological evidence of disease progression occurred shortly after C8. Patient 35-010 had a partial response at C8, a TTP of 421 days with evidence of disease progression after C20. The PD and PK data for these patients were subsequently reviewed and compared with the results for the rest of the study population. Patient 40-005 was found to have significantly higher endogenous PARP-1 activity (mean = 0.34 *vs*. 0.09 pmol PAR per 10^4 PBL; *P* = 0.0001, un-paired t-test with Welch correction) but significantly lower levels of PARP-1 protein expression (mean = 0.11 *vs.* 0.21 ng per μg total protein; *P* = 0.008, un-paired t-test with Welch correction). These data are difficult to interpret given that no differences were seen in PARP-1 activity or expression levels in the other partial responder patient 35-010.

To investigate whether the results of PD, PK end-points and baseline tumour characteristics differed between responders and non-responders in the whole study population, patients were divided into three outcome groups: those that had a partial response after 2 cycles and/or disease stabilisation for ≥ four months i.e. had a CBR (n=12); those who had SD after C2 but for less than four months (n=7) and finally those patients who developed PD after C2 i.e. at the first response assessment (n=16). Figure 5.22 shows the patients divided into these three groups, colour coded by dose level cohort.

5.4.8.4 Response to AG014699 and baseline PARP-1 characteristics

Results for baseline PARP-1 characteristics (endogenous i.e. un-stimulated, PARP-1 activity and baseline protein expression) by response to AG014699 are shown as box-plots in figure 5.23. Patients in the CBR group had a significantly higher pre-treatment baseline PARP-1 activity than those who failed to respond to AG014699 (mean $\log_{10}$ activity = 0.69 *vs*. 0.23 pmol PAR per 10^4 PBL, *P* = 0.03, un-paired t-test). However this difference was not seen with the endogenous PARP-1 activity levels (Figure 5.23B) PARP-1 protein levels were higher in the CBR group than the SD and PD groups (mean $\log_{10}$ expression = -0.66 *vs*. -0.74 *vs*. -0.89 ng per μg total protein) but there was no significant statistical difference between the groups (*P* = 0.06, using one way ANOVA) (figure 5.23C).

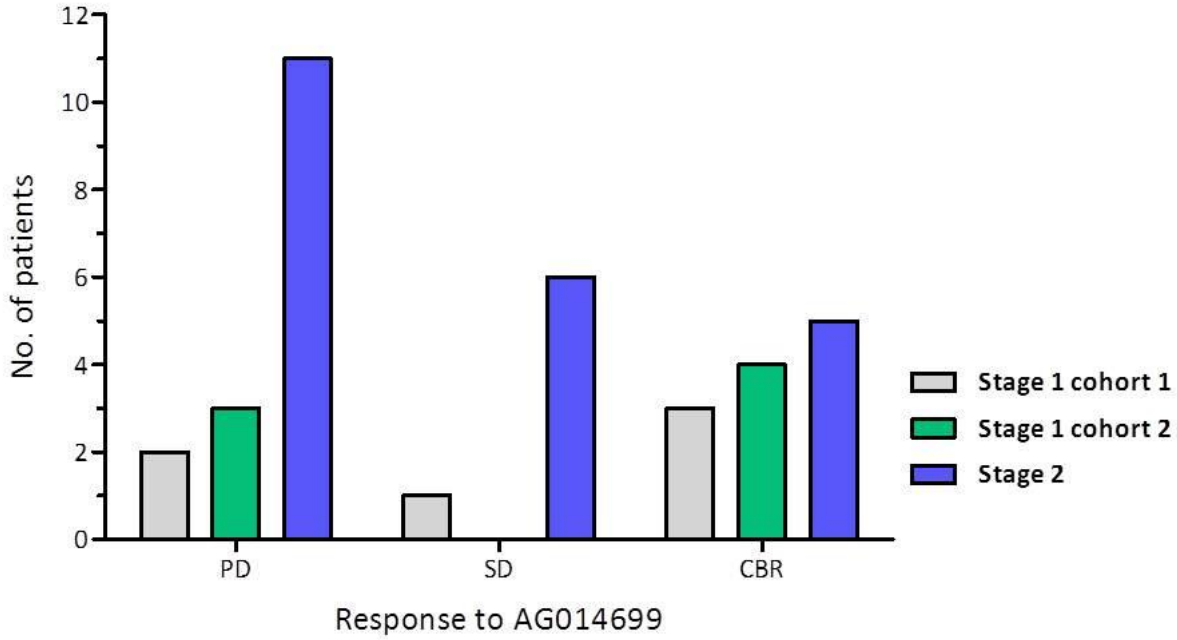

Figure 5.22: Response to AG014699 by dose cohort. Grey bars denote patients in cohort 1, stage 1; green bars patients in cohort 2, stage 1 and the blue bars represent stage 2 patients. PD = progressive disease after two cycles, SD = stable disease after two cycles but for < four months and CBR = partial response after C2 and/or disease stabilisation for ≥ four months.

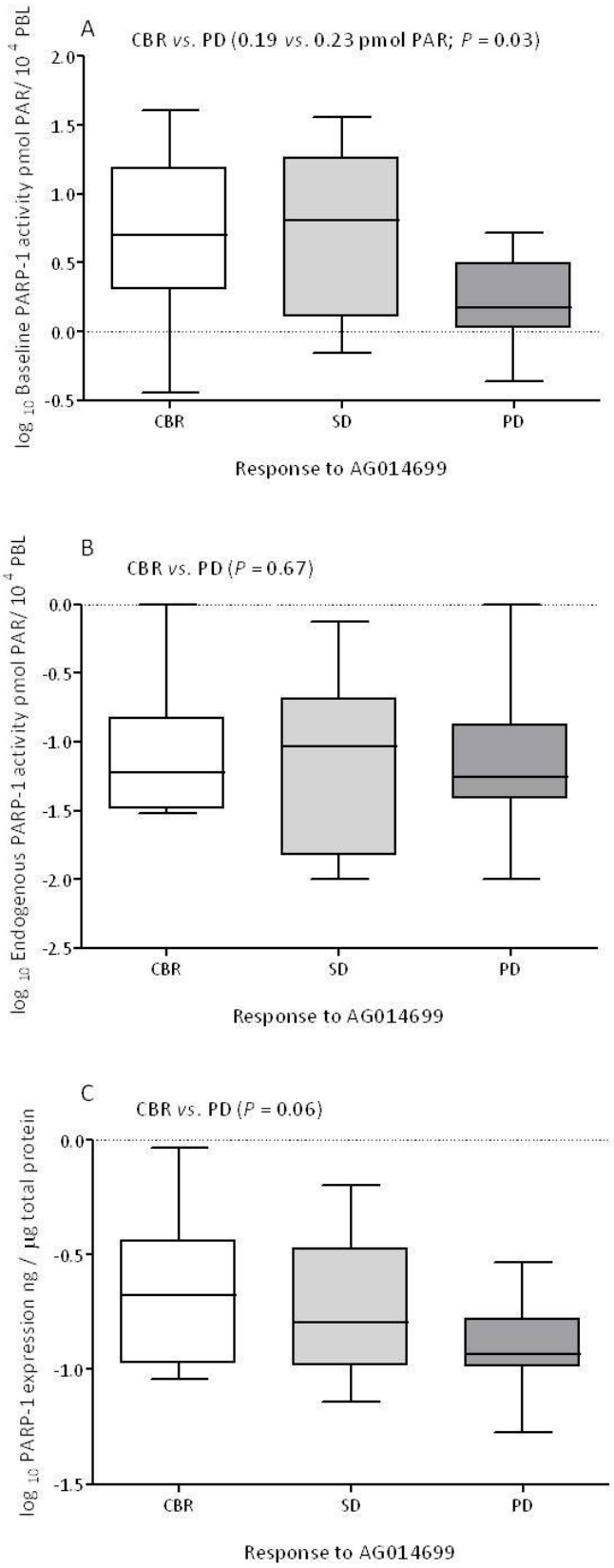

Figure 5.23: Box and whiskers plots showing (A) Pre-treatment PARP-1 levels, (B) Endogenous PARP-1 levels and (C) PARP-1 expression by clinical response to AG014699.

5.4.8.5 Clinical response to AG014699, PARP-1 inhibition and AG014699 PK

Results for PARP-1 activity at the D1 EOI and D2 pre-dose time-points together with their corresponding PK samples were grouped into the same three response outcomes: CBR, SD and PD. Box plots for each data set are shown in figure 5.24. Although the best responders (CBR group) had the lowest mean D1 EOI PARP-1 activity levels (0.67 pmol PAR per 10^4 PBL) this did not differ significantly from the other two groups (SD = 1.03 pmol PAR, PD = 0.68 pmol PAR; *P* = 0.47 1 way ANOVA).

A similar picture was seen at the D2 pre-dose PARP-1 activity levels (figure 5.24B) with no significant difference between the three groups. Analysis of the concentration of AG014699 at these time-points revealed no difference in the plasma concentrations between the clinical response groups (figure 5.24C+D). In fact the mean D1 C_{max} values were almost identical with CBR = 813.3 ng/ml, SD = 858.6 ng/ml and PD = 831.4; *P* = 0.97 1 way ANOVA).

Interestingly mean D2 pre-dose levels of AG014447 were lowest in the CBR group (32.11 ng/ml) but not significantly different from the SD (41.93 ng/ml) and PD (61.96 ng/ml) results.

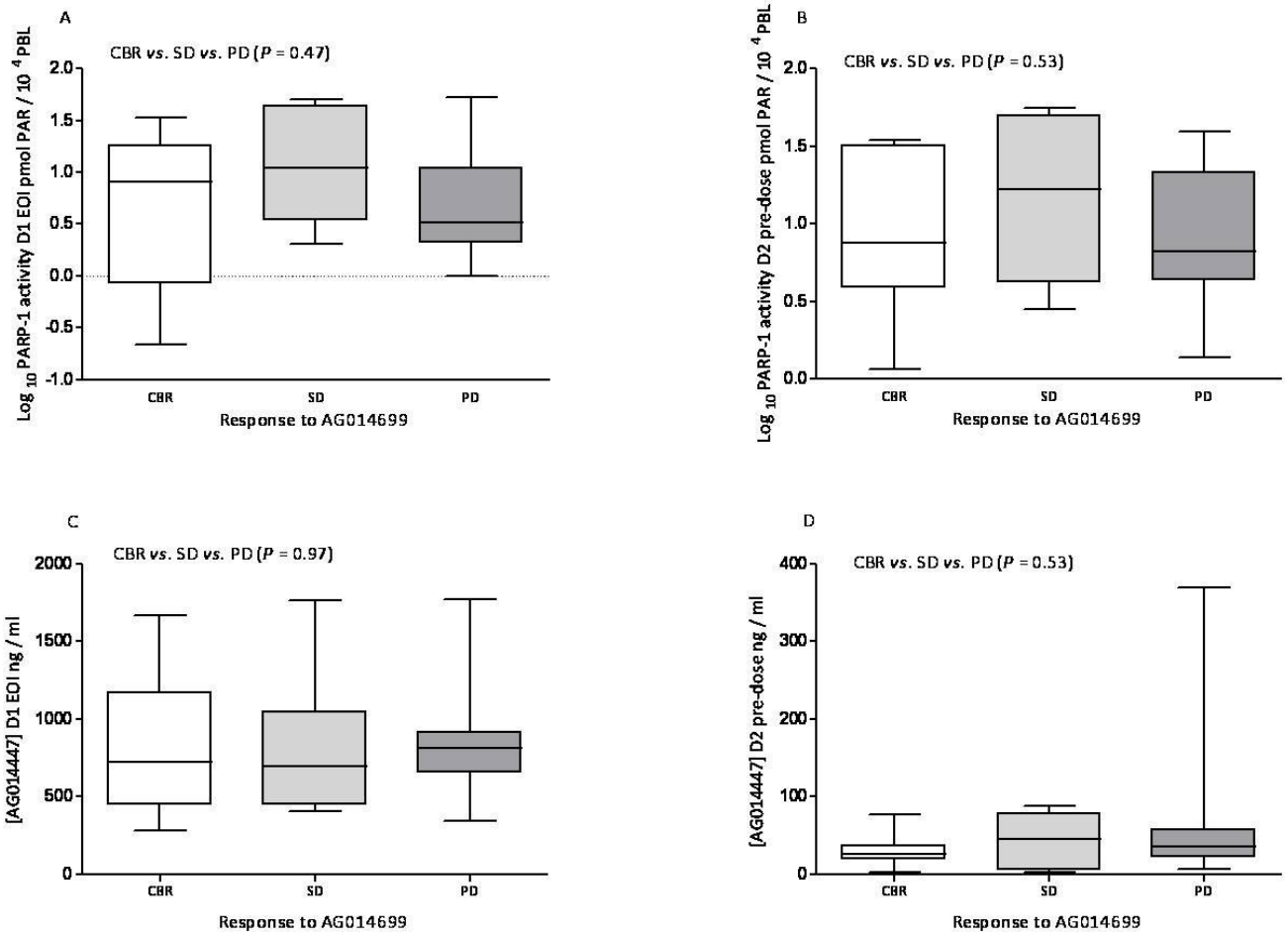

Figure 5.24: Box and whiskers plots of results of pharmacodynamic and kinetic assays by clinical outcome group. A: D1 EOI PARP-1 activity, B: D2 pre-dose PARP-1 activity, C: [AG014447] D1 EOI and D: D2-pre-dose AG014447 levels. P values calculated using 1 way ANOVA.

5.5 Discussion

The purpose of this study was to investigate the efficacy and toxicity of AG014699 in patients with advanced breast or ovarian cancer and known mutations within *BRCA1/2.* In addition, to evaluate pharmacodynamic, pharmacokinetic and pharmacogenomic endpoints and investigate their relationships, if any, to the clinical outcomes. And finally, to investigate whether using the data generated can more accurately predict which patients will respond to AG014699 and best apply this to future studies.

At the time of writing the phase II PARP-BRCA PH2/052 trial is still on-going. Data presented and discussed in this chapter are for the first 38 patients recruited and treated up to the 30th September 2010.

5.5.1. Patient recruitment and demographics

It was initially envisaged that accrual of the 56 required patients would take 24 months, with an average of 2-3 patients recruited per month. However recruitment has been slower than predicted; one possible reason for this is the restriction on the prior number of chemotherapies permitted in the metastatic breast cancer (MBC) patients. Oncologists treating MBC have an armamentarium of at least four systemic chemotherapies to use often before they will refer patients for early studies testing novel agents. This restriction on prior treatment has since been removed in a recent protocol amendment and hopefully will result in an increase in recruitment of MBC patients. Other possible reasons for the slow recruitment are: the presence of competing PARP inhibitor studies and the restriction of excluding non-UK residents, which of course reduces the pool of BRCA1/2 carrier patients. In contrast, the olaparib early phase studies recruited quickly and were conducted internationally including cancer centres specialising in the treatment of patients with familial cancers (Fong *et al*., 2009; Audeh *et al*., 2010; Tutt *et al*., 2010).

For the 38 patients discussed in this chapter all were female with 16 (42%) having breast cancer and 22 (58%) ovarian cancer. 21 (55%) of the patients had a *BRCA1* mutation and 17 (45%) carried a *BRCA2* mutation. The low number of *BRCA2* ovarian cancer patients (n=6) may reflect the lower risk of developing ovarian cancer in *BRCA2* mutation carriers (Ford *et al.,* 2004). Patients mean age was 51.4 years with a range of

28 to 72 years. This mean age is at least ten years lower than the reported average age at diagnosis of breast (61 years) and ovarian cancer (63 years) (www.cancerresearchuk.org/cancerstats) and not unexpected given that *BRCA* mutation carriers present at an earlier age with cancer (King *et al*., 2003).

Patients were all of a good performance status (WHO 0-1) and had received a mean number of two prior chemotherapies. All the ovarian cancer patients had received prior platinum therapy, either as carboplatin or cisplatin. The study excluded platinum refractory ovarian cancer patients at design because the investigators surmised that cancers resistant to the platinums may also be insensitive to PARP inhibitors. Since the study was designed this theory has been confirmed by reports of cisplatin therapy inducing secondary mutations in known BRCA2 mutation carriers resulting in restoration of BRCA2 protein function and platinum resistance (Sakai et al., 2009). In addition Fong *et al*. reported that there was a positive correlation between greatest response to the PARP inhibitor olaparib and the longer the patient's platinum-free interval (PFI) (Fong *et al*., 2010). Unfortunately information on the PFI of the 22 ovarian cancer patients in this study is not available but would be useful when discussing the individual's response to AG014699.

5.5.2. Baseline PARP-1 characteristics

The baseline PARP-1 activity was determined in the C1D1 pre-dose blood sample (obtained for 35 (92%) of patients) and enabled assessment of both endogenous PARP activity i.e. that which was not stimulated in the PARP activity assay by the addition of oligonucleotide and the substrate NAD^+ and the maximum stimulated PARP-1 activity in the PBL prior to addition of the PARP inhibitor.

Results for all 35 patients show low levels of endogenous PARP activity, with a mean value = 0.097 pmol PAR per 10^4 PBL and a large variation between patients (CV = 146.5%). The majority of results are read from the lower end of the standard curve which questions the accuracy of measuring such low LAU values. Loading more than 10,000 PBL into each well would result in a higher LAU signal and this could be considered for future work. As yet no published data are available for comparison of *endogenous* PBL PARP-1 activity in similar populations or even in non-*BRCA* cancer population or healthy volunteers using these methods.

For all patients the mean baseline maximum stimulated PARP activity was 6.80 pmol PAR per 10^4 PBL. Again a large variation in activity was seen between individuals; range 0.38 – 40.26 pmol PAR per 10^4 PBL and % CV = 145%.

Two other studies have measured baseline maximum stimulated PARP activity in cancer patients and healthy volunteers using the same PD assay (Jones, MD thesis 2006; Zaremba *et al*., 2011). Both these studies showed a large variation in baseline PARP activity levels between subjects. This may be because a true inter individual variation in PARP activity exists but the limitation of the immunoblot assay must also be considered. As discussed in chapter two: section 2.9, samples from individual patients were all analysed on the same blot to eliminate the known inter-assay variability and enable accurate comparisons of PARP activity levels in response to AG014699. However it was only possible to load a maximum of two patients' samples on any given blot. Therefore in comparing the PARP activity results for the whole study population multiple blots are being compared and although the inter-assay variability was well within the range (20-30%) considered acceptable for biological assays it may have contributed the large variation seen.

In addition data from Chris Jones (MD thesis, Newcastle University, UK) shows that activity levels vary up to 1.9-fold within the same subject in any given 72 hour period and this also has implications for this study where patients PARP activity in response to AG014699 is measured over a 24 hour period. Interestingly, a mean PARP activity in this PARP-BRCA PH2/052 study population of 6.80 pmol is almost double that reported in Zaremba's study of 118 cancer patients with unknown *BRCA* status (mean = 3.60 pmol). One could argue that this is simply a result of the inter-assay variability. However one possible explanation for this finding is that PARP is hyper-activated in patients with *BRCA* mutations, suggesting an up-regulation of the BER pathway to compensate for defective HR. This theory has also been proposed by Gottipati *et al* who demonstrated that PARP activity is increased in *BRCA2*-defective hamster cell lines (V-C8) compared to their *BRCA2*-complimented counter-parts (V-C8 + B2) (Gottipati *et al*., 2010). In addition, they showed that PAR was over-expressed in the *BRCA*- deficient human pancreatic cancer cell line, CAPAN-1, when compared to the *BRCA2*-proficient human pancreatic cancer cell line BXPC3. No increase in DNA single strand breaks were seen in these BRCA2-defective cell lines to account for this increase

in PARP activity. The authors speculated that this up-regulation of or over-dependence on PARP-1 could be the underlying mechanism behind the sensitivity of BRCA-defective cells to PARP inhibitors. But there are differences between the current study and that undertaken by Gottipati *et al.* For example, they measured un-stimulated activity as opposed to maximally stimulated PARP activity; they used *BRCA* defective cell lines instead of the surrogate tissues (PBL) and finally activity was determined through a different pharmacodynamic assay; therefore extrapolation to results presented here for this study is difficult.

Interestingly though in Gottipati's study increased levels of PARP activity (defined by PAR polymer quantification) correlated well with increased sensitivity to PARP-1 inhibition by 4 amino-1.8-naphthalimide (ANI) and they suggested that PAR levels could potentially be used as a biomarker to select out patients that might benefit from PARP inhibitor therapy. In a recent review of clinical biomarkers Redon *et al* also suggested as endogenous PARP activity levels vary between patients they may prove a useful biomarker to determine which patients will be sensitive to PARP inhibitors (Redon *et al*., 2010).

Review of the data presented in this chapter failed to show a link between endogenous PARP activity levels and clinical response to AG014699 (Figure 5.22A). However, the baseline mean *maximum stimulated* PARP-1 activity levels were significantly higher in those patients who responded to AG014699, defined by CBR, than those patients who had PD after two cycles (mean $\log_{10}$ activity = 0.69 *vs*. 0.23 pmol PAR per 10^4 PBL, P = 0.03, un-paired t-test). This might suggest that PARP enzyme dynamic function in response to DNA damage can be used as a predictor of PARP inhibitor response. However, this will, of course, require further investigation in larger studies. In addition the use of PARP activity as a marker of potential PARP inhibitor sensitivity in patients might be problematic given that it is reported that baseline PARP activity can vary within the same individual in any 72 hour period up to two-fold (Chris Jones, MD thesis, Newcastle University, UK, 2006).

Results for baseline PARP-1 protein expression were obtained for 30 (79%) patients and presented in section 5.4.2. Again as for PARP activity levels a large inter-patient variation was seen (% CV = 93%). Mean protein expression for the whole study population = 0.21 ng per μg and this was the same as that reported by Zaremba (mean

PARP-1 expression 0.21 ng per μg) suggesting that PARP-1 expression is not increased in *BRCA* defective populations.

One might speculate that higher PARP-1 protein expression would correlate with increased PARP-1 enzyme activity. The data in this chapter show a trend towards higher activity with increased protein expression but the correlation is weak and not statistically significant using Pearsons correlation coefficient ($R^2 = 0.14$, $P = 0.06$) (see figure 5.5).

The data from this study also failed to demonstrate a relationship between age and either PARP-1 activity or expression. This may be due to the small numbers of patients sampled in the clinical trial population. Other studies investigating this have reported conflicting results about the link between PARP-1 activity and age (Grube and Burkle, 1992; Muiras *et al*., 1998). More recently a negative correlation between increasing PARP activity and age in cancer patients was observed in Zaremba's study (Zaremba *et al*., 2011).

As discussed in section 5.1.2 lower PARP-1 activity is associated with the T2444C single nucleotide polymorphism within the PARP-1 gene. The amino acid substitution of valine to alanine in the catalytic domain of PARP-1 protein can result in an up to 40% reduction in PARP-1 activity (Lockett *et al*., 2004; Wang *et al*., 2007). Genotyping was performed on DNA extracted from 31 of the 38 study patients and only 1 patient (35-013) was homozygous for the variant SNP (C/C). This patient had the second lowest baseline PARP activity and as this was a single result further statistical analysis was not possible. The pooled data for the T/C and the C/C patients had a lower mean activity than that of the T/T group but this did not reach statistical significance. Again the small sample size may be impeding the statistical analysis of the results.

Interestingly, in terms of clinical response, patient 35-013 did not respond to AG014699 with disease progression after only two cycles.

5.5.3 PARP activity in response to AG014699

PARP activity following treatment with AG014699 was investigated in 33 of the 38 study patients. Six patients received a cycle of AG014699 at a dose of 4 mg/m^2; 13 received at least one cycle at 12 mg/m^2 and 24 patients were given at least one cycle of AG014699 at the 18 mg/m^2 dose level. 12 patients were dose-escalated either from

4 mg to 12 mg/m^2 or from 12 mg to 18 mg/m^2. This enabled assessment of the degree of PARP inhibition to different doses of AG014699 and the effect of intra-patient dose-escalation in *BRCA* patients to be investigated. Results, presented in section 5.4.3, show that AG014699 is a potent clinical inhibitor of PARP with a mean % inhibition over pre-treatment values at the end of the infusion being 97.6, 95.4 and 86.1% for the 4 mg/m^2, 12 mg/m^2 and 18 mg/m^2 dose levels respectively. The data also shows that 24 hours following a single dose of AG014699 PARP-1 activity remains well below 50% of baseline levels, even at the lowest dose cohort of 4 mg/m^2 with a mean inhibition of 69% seen.

However the most striking PD observation from these studies is that increasing the dose of AG014699 does not always result in a greater degree of PARP-1 enzyme inhibition. Reviewing the individual patient plots in Figures 5.8, 5.9, 5.11 and the summary data presented in Figure 5.13 it is clear that increasing the dose of AG014699 results in *not* greater but *prolonged* duration of PARP-1 inhibition. A clear dose-response is seen in the D2 pre-dose (24 hour) sample where the 18 mg/m^2 schedule results in lower recovery of PARP-1 activity than the lower dose levels. Given that the current schedule of AG014699 within this study is five days of treatment every 21 days the prolongation of inhibition may be as important as the degree of inhibition in order to illicit a clinical response.

Of note no correlation was seen between the degree of PARP-1 enzyme inhibition achieved at all three time-points post AG014699 and the baseline pre-treatment levels.

5.5.4 Pharmacokinetics of AG014699

Plasma samples to determine the PK of AG014447, the free base of AG014699, were received in 35 of the 38 patients. The results, presented in section 5.4.4, show that AG014699 displays linear pharmacokinetics with increasing dose. There was considerable inter-patient variability for each time-point, but the data set is comparable with the published results for the phase I study (Plummer *et al*., 2008). Interestingly, no statistically significant correlations were observed between the plasma concentration of AG014699 and the degree of PARP-1 enzyme inhibition and any dose level or time-point. A trend towards higher AG014699 concentration and lower PARP-1 activity was seen at the 4 mg/m^2 and 12 mg/m^2 dose levels, but not at

the highest dose 18 mg/m^2. This may suggest that above a certain concentration of AG014699 no further PARP-1 inhibition can be achieved and the dose dependent effect is lost.

The study protocol included the option of patients volunteering for an on-study tumour biopsy. This would enable the assessment of PARP-1 activity in the actual tumour as opposed to surrogate PBL and to measure the accumulation, if any, of AG014699 in tumour tissues. The common sites of metastatic disease in this cancer patient group potentially would mean biopsies of liver/lung or peritoneal deposits which are invasive and not without risk therefore the up-take for additional biopsy was low. In fact only one patient (40-014) who presented with a vaginal vault recurrence consented to biopsy, which was taken 240 minutes from the start of the AG014699 infusion on D2 of C2. PD analysis of PARP-1 activity levels was not performed as no pre-treatment sample was available to compare the result with. However, a high concentration of drug was measured within the tumour (692 ng/ml), demonstrating that AG014699 penetrates and accumulates in tumour cells following intravenous administration.

5.5.5 CYP2D6 genotyping

Results for the CYP2D6*2 and CYP2D6*4 are presented in section 5.4.7. At this stage in the trial it is difficult to draw firm conclusions about the effects of the SNPs on the pharmacokinetics of AG014699 given the small study population of 31 patients. Further analysis will need to be performed with the results of the whole study population.

5.5.6 Clinical outcomes

AG014699 was well tolerated in this patient population with no dose-limiting toxicities seen. At the time of study design it was not known whether inhibiting PARP-1 in *BRCA*1/2 mutation carriers would be toxic to normal tissues and these results are reassuring.

Perhaps the most disappointing finding of this study is the low objective response rate (6%) to AG014699. This is considerably lower than that reported in the phase II studies of olaparib in similar patient populations, where response rates of between 13 -41% were seen (Audeh *et al*., 2010; Tutt *et al*., 2010).

There are a number of possible explanations for this low response rate. Firstly, recent studies in cancer cell lines have demonstrated that second mutations in *BRCA1 or BRCA2* genes can lead to resistance to PARP inhibitors (Edwards *et al*., 2008; Sakai *et al*., 2008; Sakai *et al*., 2009). Secondary mutations restoring *BRCA* function and HR DNA repair in the face of PARP inhibition may arise in order to maintain genomic integrity. In one study, a model for drug resistance was first developed by producing cells from the *BRCA2*-deficient human pancreatic cancer cell line, CAPAN-1, that were insensitive to PARP inhibitors (Edwards *et al*., 2008). The PARP inhibitor–resistant (PIR) clones developed following exposure to the PARP inhibitor KU0058948 (Farmer *et al*., 2005) are highly resistant (>1,000-fold). PIR clones are also cross-resistant to the DNA cross-linking agent cisplatin, but not to the microtubule stabilizing drug docetaxel. KU0058948 and cisplatin both exert their effects on BRCA-deficient cells by increasing the frequency of un-repaired DSBs in the absence of effective HR, suggesting that the resistance of PIR clones to KU0058948 might be because of restored HR. cDNA and genomic DNA sequencing from PIR clones revealed the presence of novel *BRCA2* alleles with deletions surrounding and incorporating the c.6174delT mutation, leading to the restoration of an open reading frame and sufficient functional BRC repeats and C-terminal domains to restore HR repair functions.

Platinum chemotherapy is a well-established strategy in the treatment of ovarian cancer, including patients bearing *BRCA1* or *BRCA2* mutations. Clinical observations suggest that *BRCA1/2* mutation carriers with ovarian cancer tend to respond better to platinum therapy, in contrast to patients with no family history of the disease (Tan *et al*., 2008). Systemic chemotherapy with the platinum agents may exert *BRCA1/2*-selective effects through similar mechanisms to PARP inhibitors. To investigate this further, the *BRCA2* gene was sequenced in tumours from patients bearing the *BRCA2* c.6174delT mutation whose ovarian carcinomas had become resistant to carboplatin chemotherapy. These studies revealed deletions in the *BRCA2* gene, which restored the open reading frame; implying that a specific mutation (c.6174delT) in *BRCA2* and sensitivity to platinums in both cell lines and patients could potentially be reversed by an intragenic deletion (Edwards *et al*., 2008; Sakai *et al*., 2009). A similar phenomenon has also been reported in *BRCA1* mutated, cisplatin resistant ovarian cancers (Swisher *et al*., 2008).

In the current study population, 16 patients developed disease progression at the first assessment of response (after C2); suggesting primary PARP inhibitor resistance. Of these patients, 11 (69%) had platinum pre-treated ovarian cancer. Unfortunately, data is not available for their PFI and whether any of these patients would be defined as platinum resistant. However it is not yet clear if *BRCA1/2* mutations, other than those reported in the studies mentioned above, can be reverted by secondary intragenic mutation and whether secondary mutations resulting in PARP inhibitor resistance will be something we see in clinical practice. But it could explain why some patients failed to respond to AG014699 in this study.

Another possible explanation for the poor ORR is that these patients had unfavourable PARP-1 baseline characteristics or that the dose regimen did not result in optimum plasma levels of AG014699 or inhibition of PARP. Review of patients PARP baseline activity shows that patients who failed to respond i.e. the PD group had significantly lower PARP activity levels than those in the CBR group (0.23 vs. 0.69 pmol PAR per 10^4 PBL, $P = 0.03$).This may imply that these patients are less reliant on the BER pathway and less sensitive to PARP inhibitors. Of note, PARP-1 protein expression levels were not significantly different between the three response groups. There was also no significant difference between the degree of PARP-1 enzyme inhibition and the peak plasma or trough concentrations of AG014699 regardless of whether or not patients benefited from treatment. In fact, most patients had excellent inhibition of PARP activity as measured by the PD assay. However it is important to note again that these baseline PARP characteristics were determined from PBL and *not BRCA*-defective tumour samples.

The most likely explanation for the lack of clinical response to AG014699 seen in this study is the scheduling used. The drug is administered on days one to five of a 21 day cycle potentially allowing over two weeks for PARP-1 activity levels to be restored or even up-regulated as suggested in Figure 5.10. The *in vivo* data presented in chapter four adds weight to this this theory. In the UACC3199 xenografts experiment one, the anti-tumour effect of AG014699 was lost after ten days once the treatment was stopped, whereas greater tumour growth delay occurred in experiment two with a five day treatment repeated every seven days for six weeks. These data also fit with the more favourable response rates seen in olaparib studies where the drug is

administered on a continuous, oral basis (Fong *et al*., 2009; Audeh *et al*., 2010; Tutt et al., 2010). Informed by the preliminary trial data and the *in vivo* results, the PARP-BRCA clinical trial was amended to permit an additional PD PARP activity sampling time-point on D15. This additional sample would assess PARP activity during the non-treatment period (10 days after the last dose of AG014699). To date, four recently recruited patients (data not included in this thesis) have had this D15 sample taken. Results for these four patients' PARP activity, expressed as % of baseline levels, are shown in figure 5.25 (personal communication from James Murray, Newcastle University, UK). As the figure shows, in the majority of patients, by D15 PARP activity levels have almost fully recovered with the mean % activity of 77%. This suggests that once the five days of AG014699 treatment is complete, the PARP enzyme activity recovers and so any potential for synthetic lethality is lost; emphasising the point that for single agent activity, duration of PARP inhibition may be equally as important as the degree of inhibition.

The administration of an intravenous drug like AG014699 on a continuous basis to patients would be difficult, requiring the insertion of central venous catheters and a treatment commitment that may be unacceptable to many patients.

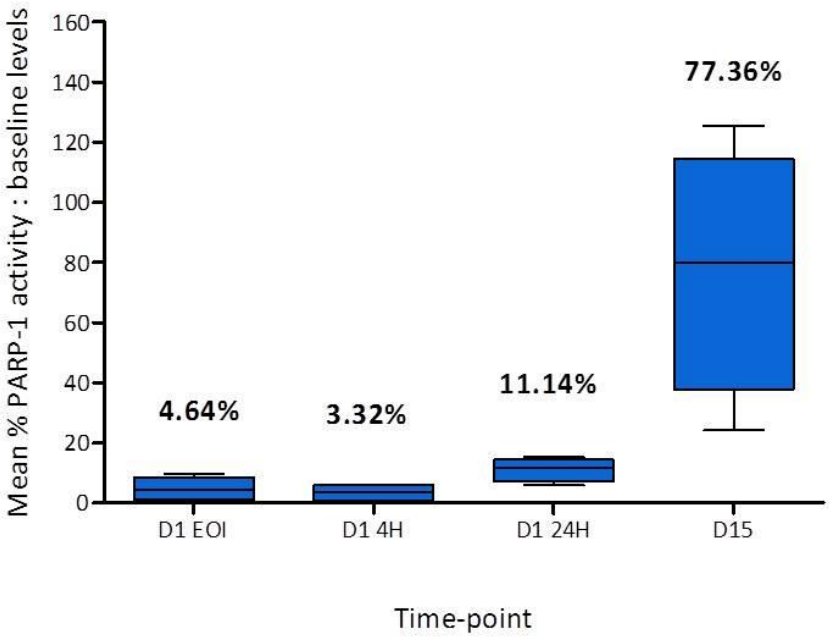

Figure 5.25: Mean % PARP activity in response to AG014699 over time for four patients. EOI = end of infusion, H = hours, D = day

However the recent development by Pfizer GRD of an oral formulation of AG014699 has allowed the protocol for the current study to be amended to test the safety and efficacy of a continuous dosing schedule. This will hopefully result in increased response rates and clinical benefit to patients.

5.5.7 Conclusions

In summary, this study has shown that AG014699 is a potent inhibitor of PARP-1 that is well tolerated in *BRCA*-mutation carriers with minimal normal tissue toxicity. Despite the poor ORR a considerable number of patients (34%) have derived a CBR from AG014699 even in its current intermittent schedule; with three patients remaining on treatment for greater than 12 months. Given the low reported toxicity rate of single agent AG014699 this could be considered an acceptable outcome in patients whose only alternative is likely to be systemic cytotoxic chemotherapy. Higher baseline PARP-1 activity levels were seen in the CBR group and this requires confirmation by testing the whole study population. Finally, results of the amended PARP-BRCA study, investigating the continuous scheduling of oral AG014699, are eagerly awaited.

Chapter Six

6. Summary and future directions

These studies represent the first comprehensive *in vitro*, *in vivo* and clinical investigation into the effects of the PARP-1 inhibitor, AG014699, in human cancers defective in homologous recombination DNA double strand break repair. The major findings of the preclinical experiments and the phase II clinical trial are summarised below.

6.1 Summary

Cell survival data presented in chapter three demonstrate that *BRCA* mutated human cancer cells are significantly more sensitive to AG014699 than human cell lines with wild type or heterozygote *BRCA* (mean LC_{50} = 3.96 ± 2.90 *vs*. mean LC_{50} = 25.09 ± 9.17; $P < 0.0001$). These results support the theory of PARP- BRCA synthetic lethality and confirm that AG014699 is active in *BRCA* deficient human cancer models. Interestingly, *BRCA*1 mutant human cells (MDA-MB-436) were more sensitive than the *BRCA*2 mutant (CAPAN-1) human cancer cell line (mean LC_{50} = 1.33 ± 0.59 *vs*. mean LC_{50} = 5.54 ± 2.51; $P = 0.03$). This difference is not explained by higher levels of PARP enzyme inhibition in the MDA-MB-436 cells following exposure to 10 μM AG014699. The MDA-MB-436 cells however did form the lowest numbers of Rad51 foci after AG014699 *and* were the most sensitive cell line to AG014699 of the whole panel; suggesting they harbour the most defective HR pathway. However, this observation is based on the comparison of only two human cell lines and it should be noted that the HCC1937 *BRCA*1 deficient breast cancer line, although not assessed by the same assay appear less sensitive than the CAPAN-1 cells. Furthermore, differences in patients' response to AG014699 by *BRCA* mutation have not been observed in the clinical trial data (see chapter five, section 5.4.8.3) and no difference in response rate by mutation status has been reported in any of the olaparib clinical trials (Fong *et al*., 2009; Audeh *et al*., 2010; Tutt *et al*., 2010). However, it is likely that a spectrum of HRD deficiency exists between BRCA mutant cancers; simply reflecting their genetic diversity.

The proposed mechanism for the synthetic lethality of PARP inhibitors in *BRCA* deficient cells is that PARP inhibition leads to the accumulation of DNA single-strand breaks which result in stalled replication forks and ultimately double-strand breaks. As DNA DSBs are normally repaired by the HR pathway, in HR-defective cells, these DSBs are left un-repaired or are repaired in an error-prone way by NHEJ. Both outcomes can result in genomic instability and ultimately cell death. To test this theory, immunofluoresence assays of γH2AX and Rad51 foci formation were undertaken in the panel of 11 cell lines. Results of these experiments support this hypothesis showing that following AG014699-induced PARP inhibition, all cell lines regardless of HR status accumulate DNA damage (γH2AX foci). But only the HR proficient cell lines are able to significantly increase nuclear Rad51 foci over baseline levels. The change in Rad51 numbers which discriminated the HR proficient cells from the HR deficient ones was found to be a ≥ 2-fold increase.

Both the *in vitro* and *in vivo* experiments described in chapters three and four respectively have shown that the *BRCA*1 methylated UACC3199 human breast cancer cell line is sensitive to PARP inhibition. The mean LC_{50} of 7.60 μM was significantly lower than in the HR proficient cell lines (mean LC_{50} = 29.68 μM; $P < 0.0001$). UACC3199 cells also failed to increase the number of Rad51 foci by ≥ 2-fold following AG014699. Furthermore, the UACC3199 xenografts responded to the prolonged i.p. AG014699 regimen, which delayed tumour growth by 9 days over un-treated controls. These data, together with the *in vitro* studies in XRCC3 deficient IRS-1SF cells presented in chapter thee, reinforce the theory proposed in other studies (McCabe *et al*., 2006) that it is HRD that confers sensitivity to PARP inhibition not simply germline *BRCA* mutation. The sensitivity of UACC3199 cells and xenografts to AG014699 is a major finding of this work as dysfunction of *BRCA*1, e.g. through epigenetic silencing, is known to occur commonly in high grade serous ovarian cancers (HGSOC) (Press *et al.,* 2008) and triple negative breast cancers (Turner *et al*., 2007). Recently reported phase II clinical trial data have shown that single agent olaparib has activity (24% response rate) in advanced non-germline BRCA mutated HGSOC (Gelmon *et al*., 2011). This together with the preliminary data, reported at ASCO 2011, showing that maintenance olaparib can delay disease progression in HGSOC with unknown *BRCA* mutation status (Ledermann *et al*., 2011) suggests that future studies of AG014699 should investigate

its activity in the HGSOC population. Interestingly, in the Gelmon study, no responses were seen in the triple negative breast cancer arm. This may be simply due to the small sample size (only 15 patients) or it could be that the degree of HRD in triple negative/basal-like breast cancers is not profound enough to result in PARP inhibitor-induced synthetic lethality. This highlights the need for biomarkers of HR function so that each cancer can be tested to see if the HRD is enough to warrant treatment with PARP inhibitors.

One such potential biomarker of HR function is the ability to form Rad51 foci following DNA damage. Data presented in chapter three, section 3.4.4 demonstrate that cells known to be HR deficient through *BRCA*1, *BRCA*2 or *XRCC3* deficiency do not significantly increase the number of nuclear Rad51 foci over baseline control values in response to AG014699-induced DNA damage. A major strength of this work was to propose that this method could be used to identify cancer cells with HRD and subsequent candidates for PARP inhibitor therapy. This idea was subsequently tested in ascitic fluid-derived primary ovarian cancer cell lines with unknown HR status (Mukhopadhyay *et al*., 2010). The results showed that a ≥ 2-fold increase in the number of Rad51 foci following *ex-vivo* treatment with AG014699 predicted with a 100% positive predictive value subsequent PARP inhibitor sensitivity. It is clear that this assay warrants further investigation. However, there are obvious weaknesses in using such approaches. Firstly, the difficulties in obtaining replicating viable cancer cells from patient sources such as ascites or pleural fluid. Also, many patients do not present with malignant effusions during the history of their cancer. In addition, there is a risk that in developing primary cultures one might exhibit selection pressure on the cell population which may result in a HR phenotype not reflective of the patients' primary tumour burden. There are also the technical difficulties of developing and establishing primary cultures and damaging DNA *ex vivo*. Another problem lies in the complexity of the HR pathway and that the lack of induction of Rad51 foci may not mean that HR is non-functional as other proteins may exist that may be able to perform similar functions as yet unknown. There may be no future in this assay outside of translational studies due to its technical difficulties. However, *even* if genome wide sequencing of all the HR genes was currently practical and affordable in normal clinical practice for every cancer patient, it would not be able to assess the actual function of the HR pathway.

Another challenge for the development of HRD biomarkers is the recent proposal that HRD can be 'contextual' (Chan et al., 2010). An example of this is seen hypoxia, which is a common feature of the tumour microenvironment. Chan and colleagues demonstrated that chronic hypoxia results in reduced synthesis of essential HR proteins with a three-fold reduction in HR capacity and increased sensitivity to DNA damaging chemotherapy agents and, in the more recent paper, sensitivity to PARP inhibition (Chan *et al.,* 2008; Chan *et al*., 2010). Another potential problem is the reported evolution of HRD tumours to HR proficient ones through, for example, secondary inter-genic mutations restoring BRCA function; which has been seen in both *BRCA1* and 2 mutant cancers (discussed in detail in section 1.9 of chapter one). It has also recently been reported that inactivation of NHEJ either through genetic loss or pharmacologic inhibition (Patel *et al*., 2011) and loss of 53BP1 (Bunting *et al*., 2010) can restore PARP inhibitor resistance in previously sensitive *BRCA*1 mutant models. 53BP1 is a human ortholog of the yeast DNA checkpoint proteins Rad9p/Crb2) which has a role in DNA damage response and checkpoint control (reviewed in Aly and Ganesan, 2011). In short, such phenomena would not necessarily be picked up by functional assays and therefore more research is needed to better select patients for PARP inhibitors in order to avoid non-responders and, pertinent to the current climate, to better allocate cancer drug resources.

There was a large variation in both the cell line and patient populations in the levels of baseline PARP activity. In the cell lines mean endogenous baseline PARP activity was 1.57 pmol PAR per 10^4 cells. This ranged from as low as 0.28 up to 5.95 pmol PAR per per 10^4 cells, with a CV of 101%. As expected the baseline (maximum stimulated) PARP activity levels were higher but there was less inter-cell variation with a mean of 45.07 pmol PAR per per 10^4 cells, range 8.82 to 87.60 pmol and CV of 42%. There was a trend towards higher baseline PARP activity (in both endogenous and maximum stimulated samples) in the HR deficient cell lines but the results did not meet statistical significance. For the clinical trial patient population the mean baseline (maximum stimulated) PARP activity was 6.80 pmol PAR per 10^4 PBL. This ranged from 0.38 up to 40.26 pmol PAR per 10^4 PBL with a CV of 145%. Comparing these findings to data from Zaremba *et al* using the same immunoblot technique in a cohort of 118 cancer patients with unknown BRCA status (Zaremba *et al*., 2011), PARP activity appears to be higher in *BRCA* mutation carriers. Although differences in these studies may be gender related

as 100% of this study subjects were women. Redon and colleagues also recently proposed that baseline PARP activity levels in patients could help predict which patients would respond to PARP inhibitors (Redon et al., 2010).

Reviewing the clinical PD data in chapter five, section 5.4.8.4, patients who responded to AG014699, i.e. had a clinical benefit response, had a significantly higher levels of mean pre-treatment (maximum stimulated) baseline PARP activity than the group of patients who failed to respond to AG014699 (evidence of disease progression after C2). This finding may be clinically as well as statistically significant; suggesting that a patient's baseline PARP activity level could determine whether or not they would respond to AG014699.

However, a weakness of this observation is that it represents the results of less than 40 patients and this analysis will need to be repeated with the larger complete study population. In addition, it should be noted that the results of both the cell lines and patients data suggesting that higher baseline levels of PARP activity is seen in the presence of HRD is influenced by the inter-assay variability of the PARP activity assay as these results are derived from the analysis and comparison of multiple immunoblots over several months of work.

Interestingly there was also a trend towards higher baseline PARP-1 protein expression in the clinical benefit responders (CBR) group compared to the non-responders but this did not reach levels of statistical significance.

Analysis of the *PARP-1* T2444C SNP did show a significantly lower baseline PARP activity with the homozygous variant but as this genotype (C/C) was only found in one patient (35-013) no further analysis as to whether this affected subsequent response to AG014699 could be made.

During the design of the phase II clinical trial, one of the major concerns of inhibiting PARP-1 in *BRCA* mutant carriers was the potential toxicity to normal tissues. This concern was not unwarranted given the results presented in chapter three demonstrating that DNA DSBs (represented by γH2AX foci) accumulated in cells lines continuously exposed to AG014699. This occurred in not just the *BRCA* mutant lines but in the heterozygote and wild type cells too. In fact, in most cell lines the numbers of γH2AX foci induced by AG014699 were similar to that seen after 2 Gy IR (see figure

3.13). The phase I study of olaparib also reported significant induction of γH2AX foci in normal tissue (eyebrow hair follicles), following PARP inhibition (Fong *et al*., 2009). The question then was if this DNA damage occurs continuously over time in patients' normal tissues, could it result in genomic instability and even secondary carcinomas? *In vivo* experiments by Tong *et al*. reported that deficiency of PARP-1 resulted in the development of mammary carcinoma in female mice, suggesting that PARP-1 dysfunction in humans may, in fact, be a risk factor for breast cancer (Tong *et al*., 2007). Reassuringly, the results of the xenograft studies, reported in chapter four, did not show that single agent AG014699 was toxic to mice with minimal weight loss seen and no evidence of secondary carcinomas. In addition, treating *BRCA*2 heterozygote and *BRCA*2 wild type mice with either AG014699 25 mg/kg D1-5 i.p. every 21 days for six cycles or saline control was shown to make no difference in the groups in terms of the animals weight loss or survival after a follow-up of 365 days (Drew *et al*., 2011b) This again suggests that intermittent scheduling of AG014699 is safe.

As patient safety is paramount in any clinical study the trial design included two safety cohorts (as discussed in chapter five, section 5.1.1.2) of 4 mg/m^2 and 12 mg/m^2 AG014699. The results show the intermittent schedule of AG014699 18 mg/m^2 (the highest dose level tested) to be safe and tolerable, at least in the short-term, in *BRCA* mutation carriers. Toxicity results for all 38 patients are presented in chapter five, section 5.4.8.2. To summarise, AG014699 had an acceptable safety profile with drug-related toxicity mainly grade 1 and 2. The most common being fatigue, nausea and diarrhoea. There were no DLTs at any dose level and no patients withdrew from the study due to drug-related toxicity. Whist these data are encouraging, it should be noted that to date no long term safety data about the use of PARP inhibitors in this cancer patient population are available; although three patients have so far received AG014699 within this study for over 54 weeks. More toxicity may manifest as the trial is amended and a more prolonged dosing schedule of the oral compound of AG014699 is investigated (discussed below).

The most disappointing result of the clinical study has been the low objective response rate (6%) to AG014699. This does not however down-play the CBR rate seen in 34% of patients; which for many patients is an acceptable outcome in the setting of minimal toxicity and limited treatment options. But it cannot be denied the response rate was

low and needs to be addressed. This low ORR is now less unexpected given the *in vivo* data presented in chapter four showing that a prolonged schedule of AG014699 resulted in greater anti-tumour activity. Although other reasons are postulated in the discussion of chapter five, the *in vivo* data suggest that the most likely explanation for the lack of responders in the clinical trial is the intermittent dosing schedule of AG014699. PD data from the patients show that the D1-5 dosing schedule results in profound PARP enzyme inhibition with very little recovery seen at 24 hours post dose. However once dosing has stopped after D5 it is likely that PARP activity will eventually recover. Additional data provided recently from the new D15 PD sampling time-point shows (figure 5.25) that PARP activity recovers on average to 77% over baseline pre-treatment levels by day 15. One of two conclusions can be drawn from this clinical response data: one that AG014699 in this patient population is inactive or two that it is active but anti-tumour effect through the mechanism of synthetic lethality is reduced or even lost during the non-treatment period. Given the PD data showing > 90 % PARP enzyme inhibition during the treatment period and the results of other classes of true PARP inhbitors (Fong *et al*., 2009; Audeh *et al*., 2010; Tutt *et al*., 2010) the second conclusion is most likely and continuous scheduling of AG014699 needs to be investigated.

In summary the major findings of these studies are:

1. AG014699 is selectively toxic to *BRCA* mutated human cancers.
2. AG014699 has anti-tumour activity in *BRCA*1 methylated models.
3. The ability of cells to increase nuclear Rad51 levels by ≥ 2-fold following AG014699 exposure was seen only in HR proficient cell lines.
4. There is a large variation in baseline PARP-1 activity levels in both cell lines and patients and activity appears to be higher in the presence of HRD.
5. AG014699 as a single agent in *BRCA* mutant cancer patients is well tolerated and appears to be safe in the short-term.
6. In *in vivo* experiments the more prolonged the exposure to AG014699-induced PARP inhibition the greater the anti-tumour activity suggesting that schedule matters in addition to the degree of PARP inhibition.

6.2 Future directions

One of the major strengths of this work is that it has influenced clinical practice. The *in vivo* data and the clinical response results presented and discussed in this thesis have recently led to a major amendment in the PARP-BRCA CRUK phase II clinical trial to investigate a more prolonged schedule of AG014699. Furthermore, continuous dosing of AG014699 is now theoretically possible and practical in patients with the recent development of an oral formulation of the compound. The amended trial will investigate continuous AG014699 in the same patient population as the original study (*BRCA*1/2 mutated advanced breast and ovarian cancer) with dosing cohorts of 7 days, 14 days and finally 21 days out of a 21 day cycle. The hope is that this will lead to increased response rates and meaningful clinical benefit to greater numbers of patients. Although it is almost certain that for single agent AG014699 use the more profound and the longer the duration of PARP enzyme inhibition the better, it is still not yet known to what extent and exactly for how long PARP-1 needs to be inhibited to achieve optimal activity. For these reasons the amended study must include more PD and PK sampling time-points following AG014699 dosing.

As already summarised data presented in this thesis suggest that AG014699 may have therapeutic potential in patients with non-*BRCA* germline mutated cancers such as those with epigenetically silenced *BRCA*1. In addition, data discussed in section 1.6.4 suggest that future target populations of single agent AG014699 should include: triple negative/basal-like breast cancers, high grade serous ovarian cancers and PTEN mutant endometrial cancers. Any such studies must include exploratory biomarkers of HRD and results of these assays should be correlated with clinical response in order to better select future patients for PARP inhibitor studies. Further investigation /development of the Rad51 assay should perhaps include looking for alternative sources of tumour cells such as that contained in FFPE tissue (something which almost all diagnosed cancer patients will have) and circulating tumour cells.

In early 2011 AG014699 was acquired by Clovis Oncology from Pfizer GRD. This sparked the end of AG014699 as we know it and the beginning of 'CO-338'. Fortunately the commitment to current AG014699 studies continues and the future development of the drug has been maintained.

The amended study is now open to recruitment with the first patient dosed on 25th October 2011. Whether patients can tolerate continuous dosing and whether it will result in greater efficacy will soon become apparent.

Finally, in 2003 when the first patient received the first ever dose of AG014699, a new class of drugs entered the stage of cancer treatment. Eight years on, there are at least eight other PARP inhibitors in clinical trial development. The demonstration of single-agent PARP inhibitor activity in *BRCA*-mutated ovarian and breast cancers, with a wider role being proposed in HR-defective sporadic tumours is probably the most exciting discovery to come of these studies. This selective targeting of cancer cells defective in one DNA repair pathway by inhibiting another is a major breakthrough in the treatment of cancer. As the clinical data mature and continuing clinical trials are reported, it is likely that PARP inhibitors, including CO-338, will become key players in the targeted treatment of cancer.

References

Ahmed, A. A., Etemadmoghadam, D., Temple, J., Lynch, A. G., Riad, M., Sharma, R., Stewart, C., Fereday, S., Caldas, C., deFazio, A., Bowtell, D. and Brenton, J. D. **(2010)** 'Driver mutations in TP53 are ubiquitous in high grade serous carcinoma of the ovary', *The Journal of Pathology,* 221, (1), pp. 49-56.

Alderson, T. **(1990)** 'New Targets for Cancer Chemotherapy – Poly(adpribosylation) processing and polyisoprene metabolism', *Biological Reviews,* 65, (4), pp. 623-641.

Aly, A. and Ganesan, S. **(2011)** 'BRCA1, PARP, and 53BP1: conditional synthetic lethality and synthetic viability', Journal of Molecular Cell Biology, 3, (1), pp. 66-74.

Ame, J. C., Rolli, V., Schreiber, V., Niedergang, C., Apiou, F., Decker, P., Muller, S., Hoger, T., Murcia, J. M. D. and de Murcia, G. **(1999)** 'PARP-2, a novel mammalian DNA damage-dependent poly(ADP-ribose) polymerase', *Journal of Biological Chemistry,* 274, (25), pp. 17860-17868.

Ame, J. C., Spenlehauer, C. and de Murcia, G. **(2004)** 'The PARP superfamily', *Bioessays,* 26, (8), pp. 882-893.

Aprelikova, O., Amy J. Pace, Bruno Fang, Beverly H. Koller, and Edison T. Liu and 25647-25650., J. B. C. **(2001)** 'BRCA1 Is a Selective Co-activator of 14-3-3 Gene Transcription in Mouse Embryonic Stem Cells' *Journal of Biological Chemistry,* 276, pp. 25647-25650.

Ashworth, A. **(2008)** 'A synthetic lethal therapeutic approach: Poly(ADP) ribose polymerase inhibitors for the treatment of cancers deficient in DNA double-strand break repair', *Journal of Clinical Oncology,* 26, (22), pp. 3785-3790.

Audebert, M., Salles, B., Weinfeld, M. and Calsou, P. **(2006)** 'Involvement of polynucleotide kinase in a poly(ADP-ribose) polymerase-1-dependent DNA, double-strand breaks rejoining pathway', *Journal of Molecular Biology,* 356, (2), pp. 257-265.

Audeh, M. W., Carmichael, J., Penson, R. T., Friedlander, M., Powell, B., Bell-McGuinn, K. M., Scott, C., Weitzel, J. N., Oaknin, A., Loman, N., Lu, K., Schmutzler, R. K., Matulonis, U., Wickens, M. and Tutt, A. **(2010)** 'Oral poly(ADP-ribose) polymerase inhibitor olaparib in patients with BRCA1 or BRCA2 mutations and recurrent ovarian cancer: a proof-of-concept trial', *Lancet,* 376, (9737), pp. 245-251.

Auer, B., Nagl, U., Herzog, H., Schneider, R. and Schweiger, M. **(1989)** 'Human Nuclear NAD+ ADP-Ribosyltransferase(polymerizing): Organization of the Gene', *DNA,* 8, (8), pp. 575-580.

Bakkenist, C. J. and Kastan, M. B. **(2004)** 'Phosphatases join kinases in DNA-damage response pathways', *Trends in Cell Biology,* 14, (7), pp. 339-341.

Bedikian, A. Y., Papadopoulos, N. E., Kim, K. B., Hwu, W.-J., Homsi, J., Glass, M. R., Cain, S., Rudewicz, P., Vernillet, L. and Hwu, P**. (2009)** 'A Phase IB Trial of Intravenous INO-1001 Plus Oral Temozolomide in Subjects with Unresectable Stage-III or IV Melanoma', *Cancer Investigation,* 27, (7), pp. 756-763.

Bell, D. A. **(2005)** 'Origins and molecular pathology of ovarian cancer', *Modern Pathology,* 18, (S2), pp. S19-S32.

Beneke, S., Scherr, A. L., Ponath, V., Popp, O. and Burkle, A. **(2010)** 'Enzyme characteristics of recombinant poly(ADP-ribose) polymerases-1 of rat and human origin mirror the correlation between cellular poly(ADP-ribosyl)ation capacity and species-specific life span', *Mechanisms of Ageing and Development,* 131, (5), pp. 366-369.

Ben-Hur, E., Chen, C.-C. and Elkind, M. M. **(1985)** 'Inhibitors of Poly(adenosine Diphosphoribose) Synthetase, Examination of Metabolic Perturbations, and Enhancement of Radiation Response in Chinese Hamster Cells', *Cancer Research,* 45, (5), pp. 2123-2127.

Benjamin, R. C. and Gill, D. M. **(1980)** 'ADP-ribosylation in mammalian cell ghosts. Dependence of poly(ADP-ribose) synthesis on strand breakage in DNA', *The Journal of Biological Chemistry,* 255, (21), pp. 10493-10501.

Bennett, L. M., McAllister, K. A., Malphurs, J., Ward, T., Collins, N. K., Seely, J. C., Gowen, L. C., Koller, B. H., Davis, B. J. and Wiseman, R. W. **(2000)** 'Mice Heterozygous for a Brca1 or Brca2 Mutation Display Distinct Mammary Gland and Ovarian Phenotypes in Response to Diethylstilbestrol', *Cancer Research,* 60, (13), pp. 3461-3469.

Bernges, F. and Zeller, W. J. **(1996)** 'Combination effects of poly(ADP-ribose) polymerase inhibitors and DNA-damaging agents in ovarian tumor cell lines with special reference to cisplatin', *Journal of Cancer Research and Clinical Oncology,* 122, (11), pp. 665-670.

Bernstein, C., Bernstein, H., Payne, C. M. and Garewal, H. **(2002)** 'DNA repair/pro-apoptotic dual-role proteins in five major DNA repair pathways: fail-safe protection against carcinogenesis', *Mutation Research-Reviews in Mutation Research,* 511, (2), pp. 145-178.

Bertwistle, D. and Ashworth, A. **(1998)** 'Functions of the BRCA1 and BRCA2 genes', *Current Opinion in Genetics & Development,* 8, (1), pp. 14-20.

Bhattacharyya, A., Ear, U. S., Koller, B. H., Weichselbaum, R. R. and Bishop, D. K. **(2000)** 'The breast cancer susceptibility gene BRCA1 is required for subnuclear assembly of Rad51 and survival following treatment with the DNA cross-linking agent cisplatin', *Journal of Biological Chemistry,* 275, (31), pp. 23899-23903.

Bindra, R. S., Schaffer, P. J., Meng, A., Woo, J., MÅSeide, K., Roth, M. E., Lizardi, P., Hedley, D. W., Bristow, R. G. and Glazer, P. M. **(2005)** 'Alterations in DNA Repair Gene Expression under Hypoxia: Elucidating the Mechanisms of Hypoxia-Induced Genetic Instability', *Annals of the New York Academy of Sciences,* 1059, (1), pp. 184-195.

Bowman, K. J., White, A., Golding, B. T., Griffin, R. J. and Curtin, N. J. **(1998)** 'Potentiation of anti-cancer agent cytotoxicity by the potent poly(ADP-ribose) polymerase inhibitors NU1025 and NU1064', *British Journal of Cancer,* 78, (10), pp. 1269-1277.

Brohet, R. M., Goldgar, D. E., Easton, D. F., Antoniou, A. C., Andrieu, N., Chang-Claude, J., Peock, S., Eeles, R. A., Cook, M., Chu, C., NoguÃ¨s, C., Lasset, C., Berthet, P., Meijers-Heijboer, H., Gerdes, A.-M., Olsson, H. k., Caldes, T., van Leeuwen, F. E. and Rookus, M. A. **(2007)** 'Oral Contraceptives and Breast Cancer Risk in the International BRCA1/2 Carrier Cohort Study: A Report From EMBRACE, GENEPSO, GEO-HEBON, and the IBCCS Collaborating Group', *Journal of Clinical Oncology,* 25, (25), pp. 3831-3836.

Brose, M. S., Rebbeck, T. R., Calzone, K. A., Stopfer, J. E., Nathanson, K. L. and Weber, B. L. **(2002)** 'Cancer risk estimates for BRCA1 mutation carriers identified in a risk evaluation program', *Journal of the National Cancer Institute,* 94, (18), pp. 1365-1372.

Bryant, H. E., Petermann, E., Schultz, N., Jemth, A.-s., Loseva, O., Issaeva, N., Johansson, F., Fernandez, S., McGlynn, P. and Helleday, T. **(2009)** 'PARP is activated at stalled forks to mediate Mre11-dependent replication restart and recombination', *EMBO Journal,* 28, (17), pp. 2601-2615.

Bryant, H. E., Schultz, N., Thomas, H. D., Parker, K. M., Flower, D., Lopez, E., Kyle, S., Meuth, M., Curtin, N. J. and Helleday, T. **(2005)** 'Specific killing of BRCA2-deficient tumours with inhibitors of poly(ADP-ribose) polymerase', *Nature,* 434, (7035), pp. 913-917.

Bunting, S. F., Callen, E., Wong, N., Chen, H. T., Polato, F., Gunn, A., Bothmer, A., Feldhahn, N., Fernandez-Capetillo, O., Cao, L., Xu, X. L., Deng, C. X., Finkel, T., Nussenzweig, M., Stark, J. M. and Nussenzweig, A. **(2010)** '53BP1 Inhibits Homologous Recombination in Brca1-Deficient Cells by Blocking Resection of DNA Breaks', *Cell,* 141, (2), pp. 243-254.

Burkart, V., Wang, Z.-Q., Radons, J., Heller, B., Herceg, Z., Stingl, L., Wagner, E. F. and Kolb, H. **(1999)** 'Mice lacking the poly(ADP-ribose) polymerase gene are resistant to pancreatic beta-cell destruction and diabetes development induced by streptozocin', *Nature Medicine,* 5, (3), pp. 314-319.

Byrski, T., Gronwald, J., Huzarski, T., Grzybowska, E., Budryk, M., Stawicka, M., Mierzwa, T., Szwiec, M., Wianiowski, R., Siolek, M., Dent, R., Lubinski, J. and Narod, S. **(2009)** 'Pathologic Complete Response Rates in Young Women With BRCA1-Positive Breast Cancers After Neoadjuvant Chemotherapy', *Journal of Clinical Oncology,* 28, (3), pp. 375-379.

Calabrese, C. R., Almassy, R., Barton, S., Batey, M. A., Calvert, A. H., Canan-Koch, S., Durkacz, B. W., Hostomsky, Z., Kumpf, R. A., Kyle, S., Li, J., Maegley, K., Newell, D. R., Notarianni, E., Stratford, I. J., Skalitzky, D., Thomas, H. D., Wang, L. Z., Webber, S. E., Williams, K. J. and Curtin, N. J. **(2004)** 'Anticancer chemosensitization and radiosensitization by the novel poly(ADP-ribose) polymerase-1 inhibitor AG14361', *Journal of the National Cancer Institute,* 96, (1), pp. 56-67.

Caldecott K. and Jeggo PP, **(1991)** 'Cross-sensitivity of γ-ray-sensitive hamster mutants to cross-linking agents. ', *DNA Repair,* 255, pp. 111-121.

Casey, M. J., Synder, C., Bewtra, C., Narod, S. A., Watson, P. and Lynch, H. T. **(2005)** 'Intra-abdominal carcinomatosis after prophylactic oophorectomy in women of hereditary breast ovarian cancer syndrome kindreds associated with BRCA1 and BRCA2 mutations', *Gynecologic Oncology,* 97, (2), pp. 457-467.

Chai, Y. L., Cui, J. Q., Shao, N. S., Reddy, E. S. P. and Rao, V. N. **(1999)** 'The second BRCT domain of BRCA-1 proteins interacts with p53 and stimulates transcription from the p21(WAF1/CIP1) promoter', *Oncogene,* 18, (1), pp. 263-268.

Chambon, P., Weill, J. D., Doly, J., Strosser, M. T. and Mandel, P. **(1966)** 'On the formation of a novel adenylic compound by enzymatic extracts of liver nuclei', *Biochemical and Biophysical Research Communications,* 25, (6), pp. 638-643.

Chambon, P., Weill, J. D. and Mandel, P. **(1963)** 'Nicotinamide mononucleotide activation of new DNA-dependent polyadenylic acid synthesizing nuclear enzyme', *Biochem Biophysical Research Communications,* 11, pp. 39-43.

Chan, N., Koritzinsky, M., Zhao, H., Bindra, R., Glazer, P. M., Powell, S., Belmaaza, A., Wouters, B. and Bristow, R. G. **(2008)** 'Chronic Hypoxia Decreases Synthesis of Homologous Recombination Proteins to Offset Chemoresistance and Radioresistance', *Cancer Research,* 68, (2), pp. 605-614.

Chan, N., Pires, I. M., Bencokova, Z., Coackley, C., Luoto, K. R., Bhogal, N., Lakshman, M., Gottipati, P., Oliver, F. J., Helleday, T., Hammond, E. M. and Bristow, R. G. **(2010)** 'Contextual Synthetic Lethality of Cancer Cell Kill Based on the Tumor Microenvironment', *Cancer Research,* 70, (20), pp. 8045-8054.

Chiang, F. Y., Wu, C. W., Hsiao, P. J., Kuo, W. R., Lee, K. W., Lin, J. C., Liao, Y. C. and Juo, S. H. H. **(2008)** 'Association between polymorphisms in DNA base excision repair genes XRCC1, APE1, and ADPRT and differentiated thyroid carcinoma', *Clinical Cancer Research,* 14, (18), pp. 5919-5924.

Christmann, M., Tomicic, M. T., Roos, W. P. and Kaina, B. **(2003)** 'Mechanisms of human DNA repair: an update', *Toxicology,* 193, (1-2), pp. 3-34.

Chu, G. **(1997)** 'Double Strand Break Repair', *Journal of Biological Chemistry,* 272, (39), pp. 24097-24100.

Cleator, S., Heller, W. and Coombes, R. C. **(2007)** 'Triple-negative breast cancer: therapeutic options', *Lancet Oncology,* 8, (3), pp. 235-244.

Collis, S. J., DeWeese, T. L., Jeggo, P. A. and Parker, A. R. **(2005)** 'The life and death of DNA-PK', *Oncogene,* 24, (6), pp. 949-961.

The CHEK2 Breast Cancer Consortium, **(2004)** 'CHEK2*1100delC and Susceptibility to Breast Cancer: A Collaborative Analysis Involving 10,860 Breast Cancer Cases and 9,065 Controls from 10 Studies', *American journal of human genetics,* 74, (6), pp. 1175-1182.

Constantinou, A., Davies, A. A. and West, S. C. **(2001)** 'Branch Migration and Holliday Junction Resolution Catalyzed by Activities from Mammalian Cells', *Cell,* 104, (2), pp. 259-268.

Cottet, F., Blanche, H., Verasdonck, P., Le Gall, I., Schachter, F., Burkle, A. and Muiras, M. L. **(2000)** 'New polymorphisms in the human poly(ADP-ribose) polymerase-1 coding sequence: lack of association with longevity or with increased cellular poly(ADP-ribosyl)ation capacity', *Journal of Molecular Medicine,* 78, (8), pp. 431-440.

Davies, A. A., Masson, J. Y., McLlwraith, M. J., Stasiak, A. Z., Stasiak, A., Venkitaraman, A. R. and West, S. C. **(2001)** 'Role of BRCA2 in control of the RAD51 recombination and DNA repair protein', *Molecular Cell,* 7, (2), pp. 273-282.

Davies, B. R., Steele, I. A., Edmondson, R. J., Zwolinski, S. A., Saretzki, G., von Zglinicki, T. and O'Hare, M. J. **(2003)** 'Immortalisation of human ovarian surface epithelium with telomerase and temperature-senstitive SV40 large T antigen', *Experimental Cell Research,* 288, (2), pp. 390-402.

De Bont, R. and van Larebeke, N. **(2004)** 'Endogenous DNA damage in humans: a review of quantitative data', *Mutagenesis,* 19, (3), pp. 169-185.

de Murcia, G. and de Murcia, J. M. **(1994)** 'Poly(ADP-ribose) polymerase: a molecular nick-sensor', *Trends in biochemical sciences,* 19, (4), pp. 172-173.

De Soto, J. A., Wang, X., Tominaga, Y., Wang, R.-H., Cao, L., Qiao, W., Li, C., Xu, X., Skoumbourdis, A. P., Prindiville, S. A., Thomas, C. J. and Deng, C.-X. **(2006)** 'The inhibition and treatment of breast cancer with poly (ADP-ribose) polymerase (PARP-1) inhibitors', *International Journal of Biological Science,* 2, (4), pp. 179-85.

Delaney, C. A., Wang, L. Z., Kyle, S., White, A. W., Calvert, A. H., Curtin, N. J., Durkacz, B. W., Hostomsky, Z. and Newell, D. R. **(2000)** 'Potentiation of temozolomide and topotecan growth inhibition and cytotoxicity by novel poly(adenosine diphosphoribose) polymerase inhibitors in a panel of human tumor cell lines', *Clinical Cancer Research,* 6, (7), pp. 2860-2867.

Demuth, I. and Digweed, M. **(2007)** 'The clinical manifestation of a defective response to DNA double-strand breaks as exemplified by Nijmegen breakage syndrome', *Oncogene,* 26, (56), pp. 7792-7792-8.

Denny, B. J., Wheelhouse, R. T., Stevens, M. F. G., Tsang, L. L. H. and Slack, J. A. **(1994)** 'NMR and Molecular Modeling Investigation of the Mechanism of Activation of the Antitumor Drug Temozolomide and Its Interaction with DNA', *Biochemistry,* 33, (31), pp. 9045-9051.

DeVita VT, L. T., Rosenberg SA, DePinho RA, Weinberg RA. **(2010)** *DeVita, Hellman and Rosenberg's Cancer Principles and Practice of Oncology.* Lippincott Williams and Wilkins.

Domchek, S. M., Friebel, T. M., Neuhausen, S. L., Wagner, T., Evans, G., Isaacs, C., Garber, J. E., Daly, M. B., Eeles, R., Matloff, E., Tomlinson, G. E., Van't Veer, L., Lynch, H. T., Olopade, O. I., Weber, B. L. and Rebbeck, T. R. **(2006)** 'Mortality after bilateral salpingo-oophorectomy in BRCA1 and BRCA2 mutation carriers: a prospective cohort study', *Lancet Oncology,* 7, (3), pp. 223-229.

Domchek, S. M. and Weber, B. L. **(2006)** 'Clinical management of BRCA1 and BRCA2 mutation carriers', *Oncogene,* 25, (43), pp. 5825-5831.

Donawho, C. K., Luo, Y., Luo, Y., Penning, T. D., Bauch, J. L., Bouska, J. J., Bontcheva-Diaz, V. D., Cox, B. F., DeWeese, T. L., Dillehay, L. E., Ferguson, D. C., Ghoreishi-Haack, N. S., Grimm, D. R., Guan, R., Han, E. K., Holley-Shanks, R. R., Hristov, B., Idler, K. B., Jarvis, K., Johnson, E. F., Kleinberg, L. R., Klinghofer, V., Lasko, L. M., Liu, X., Marsh, K. C., McGonigal, T. P., Meulbroek, J. A., Olson, A. M., Palma, J. P., Rodriguez, L. E., Shi, Y., Stavropoulos, J. A., Tsurutani, A. C., Zhu, G.-D., Rosenberg, S. H., Giranda, V. L. and Frost, D. J. **(2007)** 'ABT-888, an Orally Active Poly(ADP-Ribose) Polymerase Inhibitor that Potentiates DNA-Damaging Agents in Preclinical Tumor Models', *Clinical Cancer Research,* 13, (9), pp. 2728-2737.

Drew, Y. and Calvert, H. **(2008)** 'The Potential of PARP Inhibitors in Genetic Breast and Ovarian Cancers', *Recent Advances in Clinical Oncology.* Vol. 1138 Oxford: Blackwell Publishing, pp. 136-145.

Drew, Y., Ledermann, J. A., Jones, A., Hall, G., Jayson, G. C., Highley, M., Rea, D., Glasspool, R. M., Halford, S. E. R., Crosswell, G., Colebrook, S., Boddy, A. V., Curtin, N. J. and Plummer, E. R. **(2011a)** 'Phase II trial of the poly(ADP-ribose) polymerase (PARP) inhibitor AG-014699 in BRCA 1 and 2-mutated, advanced ovarian and/or locally advanced or metastatic breast cancer', *Journal of Clinical Oncology,* 29, (15_suppl), pp. 3104.

Drew, Y., Mulligan, E. A., Vong, W.-T., Thomas, H. D., Kahn, S., Kyle, S., Mukhopadhyay, A., Los, G., Hostomsky, Z., Plummer, E. R., Edmondson, R. J. and Curtin, N. J. **(2011b)** 'Therapeutic Potential of Poly(ADP-ribose) Polymerase Inhibitor AG014699 in Human Cancers With Mutated or Methylated BRCA1 or BRCA2', *Journal of the National Cancer Institute,* 103, (4), pp. 334.

Duffy, S. W., Tabar, L., Olsen, A. H., Vitak, B., Allgood, P. C., Chen, T. H. H., Yen, A. M. F. and Smith, R. A. **(2010)** 'Absolute numbers of lives saved and overdiagnosis in breast cancer screening, from a randomized trial and from the Breast Screening Programme in England', *Journal of Medical Screening,* 17, (1), pp. 25-30.

Dungey, F. A., Caldecott, K. W. and Chalmers, A. J. **(2009)** 'Enhanced radiosensitization of human glioma cells by combining inhibition of poly(ADP-ribose) polymerase with inhibition of heat shock protein 90', *Molecular Cancer Therapeutics,* 8, (8), pp. 2243-2254.

Durant, S. T. and Nickoloff, J. A. **(2005)** 'Good Timing in the Cell Cycle for Precise DNA Repair by BRCA1', *Cell Cycle,* 4, (9), pp. 1216-1222.

Durkacz, B. W., Omidiji, O., Gray, D. A. and Shall, S. **(1980)** '(ADP-ribose)n participates in DNA excision repair', *Nature,* 283, (5747), pp. 593-596.

Edwards, S. L., Brough, R., Lord, C. J., Natrajan, R., Vatcheva, R., Levine, D. A., Boyd, J., Reis, J. S. and Ashworth, A. **(2008)** 'Resistance to therapy caused by intragenic deletion in BRCA2', *Nature,* 451, (7182), pp. 1111-U8.

Eisenhauer, E. A., Therasse, P., Bogaerts, J., Schwartz, L. H., Sargent, D., Ford, R., Dancey, J., Arbuck, S., Gwyther, S., Mooney, M., Rubinstein, L., Shankar, L., Dodd, L., Kaplan, R., Lacombe, D. and Verweij, J. **(2009)** 'New response evaluation criteria in solid tumours: Revised RECIST guideline (version 1.1)', *European Journal of Cancer,* 45, (2), pp. 228-247.

Elledge, S. J. and Amon, A. **(2002)** 'The BRCA1 suppressor hypothesis: An explanation for the tissue-specific tumor development in BRCA1 patients', *Cancer cell,* 1, (2), pp. 129-132.

Elstrodt, F., Hollestelle, A., Nagel, J. H. A., Gorin, M., Wasielewski, M., van den Ouweland, A., Merajver, S. D., Ethier, S. P. and Schutte, M. **(2006)** 'BRCA1 mutation analysis of 41 human breast cancer cell lines reveals three new deleterious mutants', *Cancer Research,* 66, (1), pp. 41-45.

Esashi, F., Galkin, V. E., Yu, X., Egelman, E. H. and West, S. C. **(2007)** 'Stabilization of RAD51 nucleoprotein filaments by the C-terminal region of BRCA2', *Nature Structrual and Molecular Biology,* 14, (6), pp. 468-474.

Evers, B., Drost, R., Schut, E., de Bruin, M., van der Burg, E., Derksen, P. W. B., Holstege, H., Liu, X., van Drunen, E., Beverloo, H. B., Smith, G. C. M., Martin, N. M. B., Lau, A., O'Connor, M. J. and Jonkers, J. **(2008)** 'Selective Inhibition of BRCA2-Deficient Mammary Tumor Cell Growth by AZD2281 and Cisplatin', *Clinical Cancer Research,* 14, (12), pp. 3916-3925.

Falck, J., Coates, J. and Jackson, S. P. **(2005)** 'Conserved modes of recruitment of ATM, ATR and DNA-PKcs to sites of DNA damage', *Nature,* 434, (7033), pp. 605-611.

Fan, S., Wang, J. A., Yuan, R., Ma, Y., Meng, Q., Erdos, M. R., Pestell, R. G., Yuan, F., Auborn, K. J., Goldberg, I. D. and Rosen, E. M. **(1999)** 'BRCA1 Inhibition of Estrogen Receptor Signaling in Transfected Cells', *Science,* 284, (5418), pp. 1354-1356.

Farmer, H., McCabe, N., Lord, C. J., Tutt, A. N. J., Johnson, D. A., Richardson, T. B., Santarosa, M., Dillon, K. J., Hickson, I., Knights, C., Martin, N. M. B., Jackson, S. P., Smith, G. C. M. and Ashworth, A. **(2005)** 'Targeting the DNA repair defect in BRCA mutant cells as a therapeutic strategy', *Nature,* 434, (7035), pp. 917-921.

Ferraris, D. V. **(2010)** 'Evolution of Poly(ADP-ribose) Polymerase-1 (PARP-1) Inhibitors. From Concept to Clinic', *Journal of Medicinal Chemistry,* 53, (12), pp. 4561-4584.

Fong, P. C., Boss, D. S., Yap, T. A., Tutt, A., Wu, P. J., Mergui-Roelvink, M., Mortimer, P., Swaisland, H., Lau, A., O'Connor, M. J., Ashworth, A., Carmichael, J., Kaye, S. B., Schellens, J. H. M. and de Bono, J. S. **(2009)** 'Inhibition of Poly(ADP-Ribose) Polymerase in Tumors from BRCA Mutation Carriers', *New England Journal of Medicine,* 361, (2), pp. 123-134.

Fong, P. C., Yap, T. A., Boss, D. S., Carden, C. P., Mergui-Roelvink, M., Gourley, C., De Greve, J., Lubinski, J., Shanley, S., Messiou, C., A'Hern, R., Tutt, A., Ashworth, A., Stone, J., Carmichael, J., Schellens, J. H. M., de Bono, J. S. and Kaye, S. B. **(2010)** 'Poly(ADP)-Ribose Polymerase Inhibition: Frequent Durable Responses in BRCA Carrier Ovarian Cancer Correlating With Platinum-Free Interval', *Journal of Clinical Oncology,* 28, (15), pp. 2512-2519.

Ford, D., Easton, D. F., Bishop, D. T., Narod, S. A., Goldgar, D. E., Haites, N., Milner, B., Allan, L., Ponder, B. A. J., Peto, J., Smith, S., Stratton, M., Lenoir, G. M., Feunteun, J., Lynch, H., Arason, A., Barkardottir, R., Egilsson, V., Black, D. M., Kelsell, D., Spurr, N., Devilee, P., Cornelisse, C. J., Varsen, H., Birch, J. M., Skolnick, M., Santibanezkoref, M. S., Teare, D., Steel, M., Porter, D., Cohen, B. B., Carothers, A., Smyth, E., Weber, B., Newbold, B., Boehnke, M., Collins, F. S., Cannonalbright, L. A. and Goldgar, D. **(1994)** 'Risks of Cancer in Brca1-Mutation Carriers', *Lancet,* 343, (8899), pp. 692-695.

Fougerousse, F., Meloni, R., Roudaut, C. and Beckmann, J. S. **(1992)** 'Dinucleotide repeat polymorphism at the human Poly (ADP-Ribose) polymerase gene (PPOL)', *Nucleic Acids Research,* 20, (5), pp. 1166.

Friend, S. H. and Oliff, A. **(1998)** 'Emerging Uses for Genomic Information in Drug Discovery', *New England Journal of Medicine,* 338, (2), pp. 125-126.

Frizzell, K. M., Gamble, M. J., Berrocal, J. G., Zhang, T., Krishnakumar, R., Cen, Y., Sauve, A. A. and Kraus, W. L. **(2009)** 'Global Analysis of Transcriptional Regulation by Poly(ADP-ribose) Polymerase-1 and Poly(ADP-ribose) Glycohydrolase in MCF-7 Human Breast Cancer Cells', *Journal of Biological Chemistry,* 284, (49), pp. 33926-33938.

Gallmeier, E. and Kern, S. E. **(2005)** 'Absence of specific cell killing of the BRCA2-deficient human cancer cell line CAPAN1 by poly(ADP-ribose) polymerase inhibition', *Cancer Biology & Therapy,* 4, (7), pp. 703-706.

Gaymes, T. J., Shall, S., MacPherson, L. J., Twine, N. A., Lea, N. C., Farzaneh, F. and Mufti, G. J. **(2009)** 'Inhibitors of poly ADP-ribose polymerase (PARP) induce apoptosis of myeloid leukemic cells: potential for therapy of myeloid leukemia and myelodysplastic syndromes', *Haematologica-the Hematology Journal,* 94, (5), pp. 638-646.

Gelmon, K. A., Hirte, H. W., Robidoux, A., Tonkin, K. S., Tischkowitz, M., Swenerton, K., Huntsman, D., Carmichael, J., Macpherson, E. and Oza, A. M. **(2010)** 'Can we define tumors that will respond to PARP inhibitors? A phase II correlative study of olaparib in advanced serous ovarian cancer and triple-negative breast cancer', *Journal of Clinical Oncology,* 28, (15_suppl), pp. 3002.

Gelmon, K. A., Tischkowitz, M., Mackay, H., Swenerton, K., Robidoux, A., Tonkin, K., Hirte, H., Huntsman, D., Clemons, M., Gilks, B., Yerushalmi, R., Macpherson, E., Carmichael, J. and Oza, A. **(2011)** 'Olaparib in patients with recurrent high-grade serous or poorly differentiated ovarian carcinoma or triple-negative breast cancer: a phase 2, multicentre, open-label, non-randomised study', *Lancet Oncology,* 12, (9), pp. 852-861.

Giaccone, G., Rajan, A., Kelly, R. J., Gutierrez, M., Kummar, S., Yancey, M., Ji, J. J., Zhang, Y., Parchment, R. E. and Doroshow, J. H. **(2010)** 'A phase I combination study of olaparib (AZD2281; KU-0059436) and cisplatin (C) plus gemcitabine (G) in adults with solid tumors', *Journal of Clinical Oncology,* 28, (15_suppl), pp. 3027.

Goggins, M., Schutte, M., Lu, J., Moskaluk, C. A., Weinstein, C. L., Petersen, G. M., Yeo, C. J., Jackson, C. E., Lynch, H. T., Hruban, R. H. and Kern, S. E. **(1996)** 'Germline BRCA2 Gene Mutations in Patients with Apparently Sporadic Pancreatic Carcinomas', *Cancer Research,* 56, (23), pp. 5360-5364.

Gorski, J. J., Kennedy, R. D., Hosey, A. M. and Harkin, D. P. **(2009)** 'The Complex Relationship between BRCA1 and ERα in Hereditary Breast Cancer', *Clinical Cancer Research,* 15, (5), pp. 1514-1518.

Gottipati, P., Vischioni, B., Schultz, N., Solomons, J., Bryant, H. E., Djureinovic, T., Issaeva, N., Sleeth, K., Sharma, R. A. and Helleday, T. **(2010)** 'Poly(ADP-Ribose) Polymerase Is Hyperactivated in Homologous Recombination-Defective Cells', *Cancer Research,* 70, (13), pp. 5389-5398.

Graeser, M., McCarthy, A., Lord, C. J., Savage, K., Hills, M., Salter, J., Orr, N., Parton, M., Smith, I. E., Reis-Filho, J. S., Dowsett, M., Ashworth, A. and Turner, N. C. **(2010)** 'A Marker of Homologous Recombination Predicts Pathologic Complete Response to Neoadjuvant Chemotherapy in Primary Breast Cancer', *Clinical Cancer Research,* 16, (24), pp. 6159-6168.

The MARIBS study group, **(2005)** 'Screening with magnetic resonance imaging and mammography of a UK population at high familial risk of breast cancer: a prospective multicentre cohort study (MARIBS)', *The Lancet,* 365, (9473), pp. 1769-1778.

Grube, K. and Burkle, A. **(1992)** 'Poly(Adp-Ribose) Polymerase-Activity in Mononuclear Leukocytes of 13 Mammalian-Species Correlates with Species-Specific Life-Span', *Proceedings of the National Academy of Sciences of the United States of America,* 89, (24), pp. 11759-11763.

Gudmundsdottir, K. and Ashworth, A. **(2006)** 'The roles of BRCA1 and BRCA2 and associated proteins in the maintenance of genomic stability', *Oncogene,* 25, (43), pp. 5864-5874.

Haince, J.F., Kozlov, S., Dawson, V. L., Dawson, T. M., Hendzel, M. J., Lavin, M. F. and Poirier, G. G. **(2007)** 'Ataxia Telangiectasia Mutated (ATM) Signaling Network Is Modulated by a Novel Poly(ADP-ribose)-dependent Pathway in the Early Response to DNA-damaging Agents', *Journal of Biological Chemistry,* 282, (22), pp. 16441-16453.

Haince, J.F., McDonald, D., Rodrigue, A. l., Dery, U., Masson, J.-Y., Hendzel, M. J. and Poirier, G. G. **(2008)** 'PARP1-dependent Kinetics of Recruitment of MRE11 and NBS1 Proteins to Multiple DNA Damage Sites', *The Journal of biological chemistry,* 283, (2), pp. 1197-1208.

Hall, J. M., Lee, M. K., Newman, B., Morrow, J. E., Anderson, L. A., Huey, B. and King, M. C. **(1990)** 'Linkage of early-onset familial breast cancer to chromosome 17q21', *Science,* 250, (4988), pp. 1684-1689.

Hanahan, D. and Weinberg, Robert A. **(2011)** 'Hallmarks of Cancer: The Next Generation', *Cell,* 144, (5), pp. 646-674.

Hao, B. T., Wang, H. J., Zhou, K. X., Li, Y., Chen, X. P., Zhou, G. Q., Zhu, Y. P., Miao, X. P., Tan, W., Wei, Q. Y., Lin, D. X. and He, F. C**. (2004)** 'Identification of genetic variants in base excision repair pathway and their associations with risk of oesophageal squamous cell carcinoma', *Cancer Research,* 64, (12), pp. 4378-4384.

Harper, J. V., Anderson, J. A. and O'Neill, P. **(2010)** 'Radiation induced DNA DSBs: Contribution from stalled replication forks?', *DNA Repair,* 9, (8), pp. 907-913.

Harrap, K. **(1985)** 'Preclinical studies identifying carboplatin as a viable cisplatin alternative', *Cancer Treatment Reviews,* 12, pp. 21-33.

Hartman, A.R. and Ford, J. M. **(2002)** 'BRCA1 induces DNA damage recognition factors and enhances nucleotide excision repair', *Nature Genetics,* 32, (1), pp. 180-184.

Hassa, P. O., Buerki, C., Lombardi, C., Imhof, R. and Hottiger, M. O. **(2003)** 'Transcriptional Coactivation of Nuclear Factor-ÎºB-dependent Gene Expression by p300 Is Regulated by Poly(ADP)-ribose Polymerase-1', *Journal of Biological Chemistry,* 278, (46), pp. 45145-45153.

Hastak, K., Alli, E. and Ford, J. M. **(2010)** 'Synergistic Chemosensitivity of Triple-Negative Breast Cancer Cell Lines to Poly(ADP-Ribose) Polymerase Inhibition, Gemcitabine, and Cisplatin', *Cancer Research,* 70, (20), pp. 7970-7980.

Hay, T., Matthews, J. R., Pietzka, L., Lau, A., Cranston, A., Nygren, A. O. H., Douglas-Jones, A., Smith, G. C. M., Martin, N. M. B., O'Connor, M. and Clarke, A. R. **(2009)** 'Poly(ADP-Ribose) Polymerase-1 Inhibitor Treatment Regresses Autochthonous Brca2/p53-Mutant Mammary Tumors In vivo and Delays Tumor Relapse in Combination with Carboplatin', *Cancer Research,* 69, (9), pp. 3850-3855.

Helleday, T., Lo, J., van Gent, D. C. and Engelward, B. P. **(2007)** 'DNA double-strand break repair: From mechanistic understanding to cancer treatment', *DNA Repair,* 6, (7), pp. 923-935.

Helleday, T., Petermann, E., Lundin, C., Hodgson, B. and Sharma, R. A. **(2008)** 'DNA repair pathways as targets for cancer therapy', *Nature Reviews: Cancer,* 8, (3), pp. 193-193-204.

Hennessy, B. T. J., Timms, K. M., Carey, M. S., Gutin, A., Meyer, L. A., Flake, D. D., Abkevich, V., Potter, J., Pruss, D., Glenn, P., Li, Y., Li, J., Gonzalez-Angulo, A. M., McCune, K. S., Markman, M., Broaddus, R. R., Lanchbury, J. S., Lu, K. H. and Mills, G. B. **(2010)** 'Somatic Mutations in BRCA1 and BRCA2 Could Expand the Number of Patients That Benefit From Poly (ADP Ribose) Polymerase Inhibitors in Ovarian Cancer', *Journal of Clinical Oncology,* 28, (22), pp. 3570-3576.

Henry-Mowatt, J., Jackson, D., Masson, J. Y., Johnson, P. A., Clements, P. M., Benson, F. E., Thompson, L. H., Takeda, S., West, S. C. and Caldecott, K. W. **(2003)** 'XRCC3 and Rad51 modulate replication fork progression on damaged vertebrate chromosomes', *Molecular Cell,* 11, (4), pp. 1109-1117.

Hickson, I. D. **(2003)** 'RecQ helicases: caretakers of the genome', *Nature Reviews. Cancer,* 3, (3), pp. 169-169-78.

Hoeijmakers, J. H. J. **(2001)** 'Genome maintenance mechanisms for preventing cancer', *Nature,* 411, (6835), pp. 366-374.

Hoeijmakers, J. H. J. **(2009)** 'DNA Damage, Aging, and Cancer', *New England Journal of Medicine,* 361, (15), pp. 1475-1485.

Hughes-Davies, L., Huntsman, D., Ruas, M., Fuks, F., Bye, J., Chin, S.-F., Milner, J., Brown, L. A., Hsu, F., Gilks, B., Nielsen, T., Schulzer, M., Chia, S., Ragaz, J., Cahn, A., Linger, L., Ozdag, H., Cattaneo, E., Jordanova, E. S., Schuuring, E., Yu, D. S., Venkitaraman, A., Ponder, B., Doherty, A., Aparicio, S., Bentley, D., Theillet, C., Ponting, C. P., Caldas, C. and Kouzarides, T. **(2003)** 'EMSY Links the BRCA2 Pathway to Sporadic Breast and Ovarian Cancer', *Cell,* 115, (5), pp. 523-535.

Irminger-Finger, I., Siegel, B. D. and Leung, W. C. **(1999)** 'The Functions of Breast Cancer Susceptibility Gene 1 (BRCA1) Product and Its Associated Proteins', *Biological Chemistry,* 380, (2), pp. 117-128.

Isakoff, S. J., Overmoyer, B., Tung, N. M., Gelman, R. S., Giranda, V. L., Bernhard, K. M., Habin, K. R., Ellisen, L. W., Winer, E. P. and Goss, P. E. **(2010)** 'A phase II trial of the PARP inhibitor veliparib (ABT888) and temozolomide for metastatic breast cancer', *Journal of Clinical Oncology,* 28, (15_suppl), pp. 1019.

Jazayeri, A., Balestrini, A., Garner, E., Haber, J. E. and Costanzo, V. (2008) 'Mre11-Rad50-Nbs1-dependent processing of DNA breaks generates oligonucleotides that stimulate ATM activity', *EMBO Journal,* 27, (14), pp. 1953-1953-62.

Jazayeri, A., Falck, J., Lukas, C., Bartek, J., Smith, G. C. M., Lukas, J. and Jackson, S. P. **(2006)** 'ATM- and cell cycle-dependent regulation of ATR in response to DNA double-strand breaks', *Nature Cell Biology,* 8, (1), pp. 37-37-45.

Jensen, R. B., Carreira, A. and Kowalczykowski, S. C. **(2010)** 'Purified human BRCA2 stimulates RAD51-mediated recombination', *Nature,* 467, (7316), pp. 678-683.

Ji, J. J., Kummar, S., Chen, A. P., Zhang, Y., Putvtana, R., Kinders, R. J., Rubinstein, L., Parchment, R. E., Tomaszewski, J. E. and Doroshow, J. H**. (2010)** 'Pharmacodynamic response in phase I combination study of ABT-888 and topotecan in adults with refractory solid tumors and lymphomas', *Journal of Clinical Oncology,* 28, (15_suppl), pp. 2514.

Johnson, N., Li, Y.-C., Walton, Z.E., Cheng, K.A., Li, D., Rodig, S.J., Moreau, L.A., Unitt, C., Bronson, R.T., Thomas, H.D., Newell, D.R., D'Andrea, A.D., Curtin, N.J., Wong, K.-K., Shapiro, G.I. **(2011)** 'Compromised CDK1 activity sensitizes BRCA-proficient cancers to PARP inhibition', *Nature Medicine*, 17, pp. 875-882.

Kaelin, W. G. **(2005)** 'The concept of synthetic lethality in the context of anticancer therapy', *Nature Reviews Cancer,* 5, (9), pp. 689-698.

Kawai, H., Li, H. C., Chun, P., Avraham, S. and Avraham, H. K. **(2002)** 'Direct interaction between BRCA1 and the estrogen receptor regulates vascular endothelial growth factor (VEGF) transcription and secretion in breast cancer cells', *Oncogene,* 21, (50), pp. 7730-7739.

Kennedy, R. D. and D'Andrea, A. D. **(2006)** 'DNA repair pathways in clinical practice: Lessons from pediatric cancer susceptibility syndromes', *Journal of Clinical Oncology,* 24, (23), pp. 3799-3808.

Kennedy, R. D., Quinn, J. E., Johnston, P. G. and Harkin, D. P. **(2002)** 'BRCA1: Mechanisms of inactivation and implications for management of patients', *Lancet,* 360, (9338), pp. 1007-1014.

Khan, O. A., Gore, M., Lorigan, P., Stone, J., Greystoke, A., Burke, W., Carmichael, J., Watson, A. J., McGown, G., Thorncroft, M., Margison, G. P., Califano, R., Larkin, J., Wellman, S. and Middleton, M. R. **(2011)** 'A phase I study of the safety and tolerability of olaparib (AZD2281, KU0059436) and dacarbazine in patients with advanced solid tumours', *British Journal of Cancer,* 104, (5), pp. 750-755.

King, M. C., Marks, J. H. and Mandell, J. B. **(2003)** 'Breast and ovarian cancer risks due to inherited mutations in BRCA1 and BRCA2', *Science,* 302, (5645), pp. 643-646.

Knudson, A. G. (1971) 'Mutation and Cancer - Statistical Study of Retinoblastoma', *Proceedings of the National Academy of Sciences of the United States of America,* 68, (4), pp. 820-25.

Konstantinopoulos, P. A., Spentzos, D., Karlan, B. Y., Taniguchi, T., Fountzilas, E., Francoeur, N., Levine, D. A. and Cannistra, S. A. **(2010)** 'Gene Expression Profile of BRCAness That Correlates With Responsiveness to Chemotherapy and With Outcome in Patients With Epithelial Ovarian Cancer', *Journal of Clinical Oncology,* 28, (22), pp. 3555-3561.

Krupitza, G. and Cerutti, P. (1989) 'ADP-ribosylation of ADPR-transferase and topoisomerase I in intact mouse epidermal cells JB6', *Biochemistry,* 28, (5), pp. 2034-2040.

Kummar, S., Chen, A. P., Ji, J. J., Allen, D., Egorin, M. J., Gandara, D. R., Lenz, H., Morgan, R., Newman, E. M. and Doroshow, J. H. **(2010)** 'A phase I study of ABT-888 (A) in combination with metronomic cyclophosphamide (C) in adults with refractory solid tumors and lymphomas', *Journal of Clinical Oncology,* 28, (15_suppl), pp. 2605.

Kurosaki, T., Ushiro, H., Mitsuuchi, Y., Suzuki, S., Matsuda, M., Matsuda, Y., Katunuma, N., Kangawa, K., Matsuo, H. and Hirose, T. **(1987)** 'Primary structure of human poly(ADP-ribose) synthetase as deduced from cDNA sequence', *Journal of Biological Chemistry,* 262, (33), pp. 15990-15997.

Langelier, M.-F., Servent, K. M., Rogers, E. E. and Pascal, J. M. **(2008)** 'A Third Zinc-binding Domain of Human Poly(ADP-ribose) Polymerase-1 Coordinates DNA-dependent Enzyme Activation', *The Journal of biological chemistry,* 283, (7), pp. 4105-4114.

Leavy, O**. (2010)** 'V(D)J recombination: RAG recombination centres', *Nature Reviews Immunology,* 10, (6), pp. 383-383.

Ledermann, J. A., Harter, P., Gourley, C., Friedlander, M., Vergote, I. B., Rustin, G. J. S., Scott, C., Meier, W., Shapira-Frommer, R., Safra, T., Matei, D., Macpherson, E., Watkins, C., Carmichael, J. and Matulonis, U. **(2011)** 'Phase II randomized placebo-controlled study of olaparib (AZD2281) in patients with platinum-sensitive relapsed serous ovarian cancer (PSR SOC)', *Journal of Clinical Oncology,* 29, (15_suppl), pp. 5003.

Lee, E., McKean-Cowdin, R., Ma, H., Spicer, D. V., Van Den Berg, D., Bernstein, L. and Ursin, G. **(2011)** 'Characteristics of Triple-Negative Breast Cancer in Patients With a BRCA1 Mutation: Results From a Population-Based Study of Young Women', *Journal of Clinical Oncology,* 29, (33), pp. 4373-4380.

Liede, A., Karlan, B. Y. and Narod, S. A. **(2004)** 'Cancer risks for male carriers of germline mutations in BRCA1 or BRCA2: A review of the literature', *Journal of Clinical Oncology,* 22, (4), pp. 735-742.

Lindahl, T. **(1993)** 'Instability and decay of the primary structure of DNA', *Nature,* 362, (6422), pp. 709-715.

Lindahl, T. and Wood, R. D. **(1999)** 'Quality control by DNA repair', *Science,* 286, (5446), pp. 1897-1905.

Lockett, K. L., Hall, M. C., Xu, J. F., Zheng, S. L., Berwick, M., Chuang, S. C., Clark, P. E., Cramer, S. D., Lohman, K. and Hu, J. J. **(2004)** 'The ADPRT V762A genetic variant contributes to prostate cancer susceptibility and deficient enzyme function', *Cancer Research,* 64, (17), pp. 6344-6348.

Lord, C. J., Garrett, M. D. and Ashworth, A. **(2006)** 'Targeting the Double-Strand DNA Break Repair Pathway as a Therapeutic Strategy', *Clinical Cancer Research,* 12, (15), pp. 4463-4468.

LoRusso, P., Ji, J. J., Li, J., Heilbrun, L. K., Shapiro, G., Sausville, E. A., Boerner, S. A., Smith, D. W., Pilat, M. J., Zhang, J., Chen, A. P., Nechiporchik, N. and Parchment, R. E. **(2011)** 'Phase I study of the safety, pharmacokinetics (PK), and pharmacodynamics (PD) of the poly(ADP-ribose) polymerase (PARP) inhibitor veliparib (ABT-888; V) in combination with irinotecan (CPT-11; Ir) in patients (pts) with advanced solid tumors', *Journal of Clinical Oncology,* 29, (15_suppl), pp. 3000.

Loser, D. A., Shibata, A., Shibata, A. K., Woodbine, L. J., Jeggo, P. A. and Chalmers, A. J. **(2010)** 'Sensitization to Radiation and Alkylating Agents by Inhibitors of Poly(ADP-ribose) Polymerase Is Enhanced in Cells Deficient in DNA Double-Strand Break Repair', *Molecular Cancer Therapeutics,* 9, (6), pp. 1775-1787.

Loveday, C., Turnbull, C., Ramsay, E., Hughes, D., Ruark, E., Frankum, J. R., Bowden, G., Kalmyrzaev, B., Warren-Perry, M., Snape, K., Adlard, J. W., Barwell, J., Berg, J., Brady, A. F., Brewer, C., Brice, G., Chapman, C., Cook, J., Davidson, R., Donaldson, A., Douglas, F., Greenhalgh, L., Henderson, A., Izatt, L., Kumar, A., Lalloo, F., Miedzybrodzka, Z., Morrison, P. J., Paterson, J., Porteous, M., Rogers,

M. T., Shanley, S., Walker, L., Eccles, D., Evans, D. G., Renwick, A., Seal, S., Lord, C. J., Ashworth, A., Reis-Filho, J. S., Antoniou, A. C. and Rahman, N. **(2011)** 'Germline mutations in RAD51D confer susceptibility to ovarian cancer', *Nature Genetics,* 43, (9), pp. 879-882.

Lynch, E. D., Ostermeyer, E. A., Lee, M. K., Arena, J. F., Ji, H., Dann, J., Swisshelm, K., Suchard, D., MacLeod, P. M., Kvinnsland, S., Gjertsen, B. T., Heimdal, K., Lubs, H., Møller, P. and King, M.-C. **(1997)** 'Inherited Mutations in PTEN That Are Associated with Breast Cancer, Cowden Disease, and Juvenile Polyposis', *American journal of human genetics,* 61, (6), pp. 1254-1260.

Maegley, K. A., Bingham, P., Tatlock, J. H. and Thomas, H. D. **(2011)** 'All PARP inhibitors are not equal: An in vitro mechanistic comparison of PF-01367338 to iniparib', *Journal of Clinical Oncology,* 29, (15_suppl), pp. e13576.

Marmorstein, L. Y., Kinev, A. V., Chan, G. K. T., Bochar, D. A., Beniya, H., Epstein, J. A., Yen, T. J. and Shiekhattar, R. **(2001)** 'A human BRCA2 complex containing a structural DNA binding component influences cell cycle progression', *Cell,* 104, (2), pp. 247-257.

Masutani M, N. T., Nakamoto K, Nakagama H, Suzuki H, Kusuoka O, Tsutsumi M, Sugimura T. **(2000)** 'The response of Parp knockout mice against DNA damaging agents', *Mutation Research,* 462, pp. 159-66.

Mattern, M. R., Mong, S.-M., Bartus, H. F., Mirabelli, C. K., Crooke, S. T. and Johnson, R. K. **(1987)** 'Relationship between the Intracellular Effects of Camptothecin and the Inhibition of DNA Topoisomerase I in Cultured L1210 Cells', *Cancer Research,* 47, (7), pp. 1793-1798.

McCabe, N., Lord, C. J., Tutt, A. N. J., Martin, N. M. B., Smith, G. C. M. and Ashworth, A. **(2005)** 'BRCA2-deficient CAPAN-1 cells are extremely sensitive to the inhibition of poly (ADP-Ribose) polymerase', *Cancer Biology & Therapy,* 4, (9), pp. 934-936.

McCabe, N., Turner, N. C., Lord, C. J., Kluzek, K., Bialkowska, A., Swift, S., Giavara, S., O'Connor, M. J., Tutt, A. N., Zdzienicka, M. g. Z., Smith, G. C. M. and Ashworth, A. **(2006)** 'Deficiency in the Repair of DNA Damage by Homologous Recombination and Sensitivity to Poly(ADP-Ribose) Polymerase Inhibition', *Cancer Research,* 66, (16), pp. 8109-8115.

Mendes-Pereira, A. M., Martin, S. A., Brough, R., McCarthy, A., Taylor, J. R., Kim, J. S., Waldman, T., Lord, C. J. and Ashworth, A. **(2009)** 'Synthetic lethal targeting of PTEN mutant cells with PARP inhibitors', *Embo Molecular Medicine,* 1, (6-7), pp. 315-322.

Menissier-de Murcia, J., Molinete, M., Gradwohl, G. r., Simonin, F. d. r. and de Murcia, G. **(1989)** 'Zinc-binding domain of poly(ADP-ribose)polymerase participates in the recognition of single strand breaks on DNA', *Journal of Molecular Biology,* 210, (1), pp. 229-233.

Miki, Y., Swensen, J., Shattuck-Eidens, D., Futreal, P. A., Harshman, K., Tavtigian, S., Liu, Q., Cochran, C., Bennett, L. M., Ding, W. **(1994)** 'A strong candidate for the breast and ovarian cancer susceptibility gene BRCA1', *Science,* 266, (5182), pp. 66-71.

Milam, K. M. and Cleaver, J. E. **(1984)** 'Inhibitors of poly(adenosine diphosphate-ribose) synthesis: effect on other metabolic processes', *Science,* 223, (4636), pp. 589-591.

Miller, C. W., Ikezoe, T., Krug, U., Hofmann, W.-K., Tavor, S., Vegesna, V., Tsukasaki, K., Takeuchi, S. and Koeffler, H. P. **(2002)** 'Mutations of the CHK2 gene are found in some osteosarcomas, but are rare in breast, lung, and ovarian tumors', *Genes, Chromosomes and Cancer,* 33, (1), pp. 17-21.

Mitchell, J., Smith, G. C. M. and Curtin, N. J. **(2009)** 'Poly(ADP-Ribose) Polymerase-1 and DNA-Dependent Protein Kinase Have Equivalent Roles in Double Strand Break Repair Following Ionizing Radiation', *International Journal of Radiation Oncology, Biology Physics,* 75, (5), pp. 1520-1527.

Muiras, M. L., Muller, M., Schachter, F. and Burkle, A. **(1998)** 'Increased poly(ADP-ribose) polymerase activity in lymphoblastoid cell lines from centenarians', *Journal of Molecular Medicine,* 76, (5), pp. 346-354.

Mukhopadhyay, A., Elattar, A., Cerbinskaite, A., Wilkinson, S. J., Drew, Y., Kyle, S., Los, G., Hostomsky, Z., Edmondson, R. J. and Curtin, N. J. **(2010)** 'Development of a Functional Assay for Homologous Recombination Status in Primary Cultures of Epithelial Ovarian Tumor and Correlation with Sensitivity to Poly(ADP-Ribose) Polymerase Inhibitors', *Clinical Cancer Research,* 16, (8), pp. 2344-2351.

Mullan, P. B., Quinn, J. E., Gilmore, P. M., McWilliams, S., Andrews, H., Gervin, C., McCabe, N., McKenna, S., White, P., Song, Y. H., Maheswaran, S., Liu, E., Haber, D. A., Johnston, P. G. and Harkin, D. P. **(2001)** 'BRCA1 and GADD45 mediated G2/M cell cycle arrest in response to antimicrotubule agents', *Oncogene,* 20, (43), pp. 6123-6131.

Mulligan, J.M., Hill, L.A., Deharo, S., McDyer, F.A., Davison, T.S., Bylesjo, M., Lindor, N.M., Galligan, L., Delaney, T., Halfpenny, I.A., Farztdinov, V., Goffard, N., Proutski, V., Keating, K.E., Mullan, P.B., Quinn, J.E., Johnston, P.G., Couch, F.J., Harkin, D.P., Kennedy, R.D. **(2011)** 'Identification of a novel breast cancer molecular subgroup associated with a deficiency in DNA-damage response', *Journal of Clinical Oncology,* 29, (15_suppl), pp. 10511.

Narod, S. A., Risch, H., Moslehi, R., Darum, A., Neuhausen, S., Olsson, H., Provencher, D., Radice, P., Evans, G., Bishop, S., Brunet, J.-S. b., Ponder, B. A. J. and Klijn, J. G. M. **(1998)** 'Oral Contraceptives and the Risk of Hereditary Ovarian Cancer', *New England Journal of Medicine,* 339, (7), pp. 424-428.

Neale, M. J. and Keeney, S. **(2006)** 'Clarifying the mechanics of DNA strand exchange in meiotic recombination', *Nature,* 442, (7099), pp. 153-153-8.

Nguewa PA, F. M., Cepeda V, Alonso C, Quevedo C, Soto M and Perez JM. **(2006)** 'Poly(ADP-ribose) polymerase-1 inhibitor 3-aminobenzamide enhances apoptosis induction by platinum complexes in cisplatin-resistant tumour cells. Med Chem:2:47-53', *Medicinal Chemistry*, 2, pp. 47-53.

Nishizuka, Y., Ueda, K., Nakazawa, K. and Hayaishi, O. **(1967)** 'Studies on the Polymer of Adenosine Diphosphate Ribose', *The Journal of biological chemistry,* 242, (13), pp. 3164-3171.

Nosho K, Y. H., Mikami M, Taniguchi H, Takahashi T, Adachi Y, Imamura A, Imai K, Shinomura Y. **(2006)** 'Overexpression of poly(ADP-ribose) polymerase-1 (PARP-1) in the early stage of colorectal carcinogenesis', *European Journal of Cancer,* 42, (14), pp. 2374-81.

O'Driscoll, M. and Jeggo, P. A. **(2006)** 'The role of double-strand break repair - insights from human genetics', *Nature Reviews Genetics,* 7, (1), pp. 45-54.

Oei, S. L., Herzog, H., Hirschkauffmann, M., Schneider, R., Auer, B. and Schweiger, M. **(1994)** 'Transcriptional Regulation and Autoregulation of the Human Gene for Adp-Ribosyltransferase', *Molecular and Cellular Biochemistry,* 138, (1-2), pp. 99-104.

Oei, S. L. and Shi, Y. **(2001)** 'Poly(ADP-Ribosyl)ation of Transcription Factor Yin Yang 1 under Conditions of DNA Damage', *Biochemical and Biophysical Research Communications,* 285, (1), pp. 27-31.

Okayama, H., Edson, C. M., Fukushima, M., Ueda, K. and Hayaishi, O. **(1977)** 'Purification and Properties of Poly(Adenosine Diphosphate Ribose) Synthetase - Role of Histone in Poly(Adp-Ribose) Synthesis', *Journal of Biological Chemistry,* 252, (20), pp. 7000-7005.

Oliver, F. J., Menissier-de Murcia, J. and de Murcia, G. **(1999)** 'Poly(ADP-Ribose) Polymerase in the Cellular Response to DNA Damage, Apoptosis, and Disease', *The American Journal of Human Genetics,* 64, (5), pp. 1282-1288.

O'Shaughnessy, J., Osborne, C., Pippen, J. E., Yoffe, M., Patt, D., Rocha, C., Koo, I. C., Sherman, B. M. and Bradley, C. **(2011)** 'Iniparib plus Chemotherapy in Metastatic Triple-Negative Breast Cancer', *New England Journal of Medicine,* 364, (3), pp. 205-214.

O'Shaughnessy, J., Schwartzberg, L. S., Danso, M. A., Rugo, H. S., Miller, K., Yardley, D. A., Carlson, R. W., Finn, R. S., Charpentier, E., Freese, M., Gupta, S., Blackwood-Chirchir, A. and Winer, E. P. **(2009)** 'A randomized phase III study of iniparib (BSI-201) in combination with gemcitabine/carboplatin (G/C) in metastatic triple-negative breast cancer (TNBC)', *Journal of Clinical Oncology,* 29, (15_suppl), pp. 1007.

Palma, J. P., Wang, Y.-C., Rodriguez, L. E., Montgomery, D., Ellis, P. A., Bukofzer, G., Niquette, A., Liu, X., Shi, Y., Lasko, L., Zhu, G.-D., Penning, T. D., Giranda, V. L.,

Rosenberg, S. H., Frost, D. J. and Donawho, C. K. **(2009)** 'ABT-888 Confers Broad In vivo Activity in Combination with Temozolomide in Diverse Tumors', *Clinical Cancer Research,* 15, (23), pp. 7277-7290.

Parant, J. M. and Lozano, G. **(2003)** 'Disrupting TP53 in mouse models of human cancers', *Human Mutation,* 21, (3), pp. 321-326.

Patel, A. G., Sarkaria, J. N. and Kaufmann, S. H. **(2011)** 'Nonhomologous end joining drives poly(ADP-ribose) polymerase (PARP) inhibitor lethality in homologous recombination-deficient cells', *Proceedings of the National Academy of Sciences of the United States of America,* 108, (8), pp. 3406-3411.

Paull, T. T., Rogakou, E. P., Yamazaki, V., Kirchgessner, C. U., Gellert, M. and Bonner, W. M. **(2000)** 'A critical role for histone H2AX in recruitment of repair factors to nuclear foci after DNA damage', *Current Biology,* 10, (15), pp. 886-895.

Perou, C. M., Sorlie, T., Eisen, M. B., van de Rijn, M., Jeffrey, S. S., Rees, C. A., Pollack, J. R., Ross, D. T., Johnsen, H., Akslen, L. A., Fluge, O., Pergamenschikov, A., Williams, C., Zhu, S. X., Lonning, P. E., Borresen-Dale, A. L., Brown, P. O. and Botstein, D. **(2000)** 'Molecular portraits of human breast tumours', *Nature,* 406, (6797), pp. 747-752.

Petermann, E., Orta, M. L., Issaeva, N., Schultz, N. and Helleday, T. **(2010)** 'Hydroxyurea-Stalled Replication Forks Become Progressively Inactivated and Require Two Different RAD51-Mediated Pathways for Restart and Repair', *Molecular Cell,* 37, (4), pp. 492-502.

Pierce, A. J., Johnson, R. D., Thompson, L. H. and Jasin, M. **(1999)** 'XRCC3 promotes homology-directed repair of DNA damage in mammalian cells', *Genes & Development,* 13, (20), pp. 2633-2638.

Plummer, R., Jones, C., Middleton, M., Wilson, R., Evans, J., Olsen, A., Curtin, N., Boddy, A., McHugh, P., Newell, D., Harris, A., Johnson, P., Steinfeldt, H., Dewji, R., Wang, D., Robson, L. and Calvert, H. **(2008)** 'Phase I Study of the Poly (ADP-Ribose) Polymerase Inhibitor, AG014699, in Combination with Temozolomide in Patients with Advanced Solid Tumors', *Clinical Cancer Research,* 14, (23), pp. 7917-7923.

Plummer, R., Lorigan, P., Evans, J., Steven, N., Middleton, M., Wilson, R., Snow, K., Dewji, R. and Calvert, H. **(2006)** 'First and final report of a phase II study of the poly(ADP-ribose) polymerase (PARP) inhibitor, AGO14699, in combination with temozolomide (TMZ) in patients with metastatic malignant melanoma (MM)', *Journal of Clinical Oncology,* 24, (18), pp. 456S-456S.

Pommier, Y. **(2006)** 'Topoisomerase I inhibitors: camptothecins and beyond', *Nature Reviews Cancer,* 6, (10), pp. 789-802.

Powell, C., Mikropoulos, C., Kaye, S. B., Nutting, C. M., Bhide, S. A., Newbold, K. and Harrington, K. J. **(2010)** 'Pre-clinical and clinical evaluation of PARP inhibitors as tumour-specific radiosensitisers', *Cancer treatment reviews,* 36, (7), pp. 566-575.

Press, J. Z., De Luca, A., Boyd, N., Young, S., Troussard, A., Ridge, Y., Kaurah, P., Kalloger, S. E., Blood, K. A., Smith, M., Spellman, P. T., Wang, Y., Miller, D. M., Horsman, D., Faham, M., Gilks, C. B., Gray, J. and Huntsman, D. G. **(2008)** 'Ovarian carcinomas with genetic and epigenetic BRCA1 loss have distinct molecular abnormalities', *BMC Cancer,* 8, pp. 12.

Purnell, M. R. and Whish, W. J. **(1980)** 'Novel inhibitors of poly(ADP-ribose) synthetase', *Biochemical Journal,* 185, (3), pp. 775-777.

Quinn, J. E., James, C. R., Stewart, G. E., Mulligan, J. M., White, P., Chang, G. K. F., Mullan, P. B., Johnston, P. G., Wilson, R. H. and Harkin, D. P. **(2007)** 'BRCA1 mRNA Expression Levels Predict for Overall Survival in Ovarian Cancer after Chemotherapy', *Clinical Cancer Research,* 13, (24), pp. 7413-7420.

Ramon y Cajal, T., Altes, A., Pare, L., del Rio, E., Alonso, C., Barnadas, A. and Baiget, M. **(2009)** 'Impact of CYP2D6 polymorphisms in tamoxifen adjuvant breast cancer treatment', *Breast Cancer Res Treat,* 119, (1), pp. 33-8.

Redon, C. E., Nakamura, A. J., Zhang, Y. W., Ji, J. P., Bonner, W. M., Kinders, R. J., Parchment, R. E., Doroshow, J. H. and Pommier, Y. **(2010)** 'Histone yH2AX and Poly(ADP-Ribose) as Clinical Pharmacodynamic Biomarkers', *Clinical Cancer Research,* 16, (18), pp. 4532-4542.

Risch, H. A., McLaughlin, J. R., Cole, D. E. C., Rosen, B., Bradley, L., Fan, I., Tang, J., Li, S., Zhang, S. Y., Shaw, P. A. and Narod, S. A. **(2006)** 'Population BRCA1 and BRCA2 mutation frequencies and cancer penetrances: A kin-cohort study in Ontario, Canada', *Journal of the National Cancer Institute,* 98, (23), pp. 1694-1706.

Rogakou, E. P., Boon, C., Redon, C. and Bonner, W. M. **(1999)** 'Megabase Chromatin Domains Involved in DNA Double-Strand Breaks in Vivo', *The Journal of Cell Biology,* 146, (5), pp. 905-916.

Rogakou, E. P., Pilch, D. R., Orr, A. H., Ivanova, V. S. and Bonner, W. M. **(1998)** 'DNA Double-stranded Breaks Induce Histone H2AX Phosphorylation on Serine 139', *Journal of Biological Chemistry,* 273, (10), pp. 5858-5868.

Rottenberg, S., Jaspers, J. E., Kersbergen, A., van der Burg, E., Nygren, A. O. H., Zander, S. A. L., Derksen, P. W. B., de Bruin, M., Zevenhoven, J., Lau, A., Boulter, R., Cranston, A., O'Connor, M. J., Martin, N. M. B., Borst, P. and Jonkers, J. **(2008)** 'High sensitivity of BRCA1-deficient mammary tumors to the PARP inhibitor AZD2281 alone and in combination with platinum drugs', *Proceedings of the National Academy of Sciences of the United States of America,* 105, (44), pp. 17079-17084.

Rouleau, M., Patel, A., Hendzel, M. J., Kaufmann, S. H. and Poirier, G. G. **(2010)** 'PARP inhibition: PARP1 and beyond', *Nature Reviews Cancer,* 10, (4), pp. 293-301.

Ruscetti, T., Lehnert, B. E., Halbrook, J., Le Trong, H., Hoekstra, M. F., Chen, D. J. and Peterson, S. R. **(1998)** 'Stimulation of the DNA-dependent Protein Kinase by Poly(ADP-Ribose) Polymerase', *The Journal of biological chemistry,* 273, (23), pp. 14461-14467.

Russo, A. L., Kwon, H.-C., Burgan, W. E., Carter, D., Beam, K., Weizheng, X., Zhang, J., Slusher, B. S., Chakravarti, A., Tofilon, P. J. and Camphausen, K. **(2009)** 'In vitro and In vivo Radiosensitization of Glioblastoma Cells by the Poly (ADP-Ribose) Polymerase Inhibitor E7016', *Clinical Cancer Research,* 15, (2), pp. 607-612.

Sakai, W., Swisher, E. M., Jacquemont, C., Chandramohan, K. V., Couch, F. J., Langdon, S. P., Wurz, K., Higgins, J., Villegas, E. and Taniguchi, T. **(2009)** 'Functional Restoration of BRCA2 Protein by Secondary BRCA2 Mutations in BRCA2-Mutated Ovarian Carcinoma', *Cancer Research,* 69, (16), pp. 6381-6386.

Sakai, W., Swisher, E. M., Karlan, B. Y., Agarwal, M. K., Higgins, J., Friedman, C., Villegas, E., Jacquemont, C., Farrugia, D. J., Couch, F. J., Urban, N. and Taniguchi, T. (2008) 'Secondary mutations as a mechanism of cisplatin resistance in BRCA2-mutated cancers', *Nature,* 451, (7182), pp. 1116-U9.

Salmena, L., Carracedo, A. and Pandolfi, P. P. **(2008)** 'Tenets of PTEN tumor suppression', *Cell,* 133, (3), pp. 403-414.

Samol, J., Ranson, M., Scott, E., Macpherson, E., Carmichael, J., Thomas, A. and Cassidy, J. **(2011)** 'Safety and tolerability of the poly(ADP-ribose) polymerase (PARP) inhibitor, olaparib (AZD2281) in combination with topotecan for the treatment of patients with advanced solid tumors: a phase I study', *Investigational New Drugs*, pp. 1-8.

Schilsky, R. L. **(2010)** 'OPINION Personalized medicine in oncology: the future is now', *Nature Reviews Drug Discovery,* 9, (5), pp. 363-366.

Schreiber, V., Ame, J. C., Dolle, P., Schultz, I., Rinaldi, B., Fraulob, V., Menissier-de Murcia, J. and de Murcia, G. **(2002)** 'Poly(ADP-ribose) polymerase-2 (PARP-2) is required for efficient base excision DNA repair in association with PARP-1 and XRCC1', *Journal of Biological Chemistry,* 277, (25), pp. 23028-23036.

Schreiber, V., Dantzer, F., Ame, J. C. and de Murcia, G. **(2006)** 'Poly(ADP-ribose): novel functions for an old molecule', *Nature Reviews Molecular Cell Biology,* 7, (7), pp. 517-528.

Schultz, N., Lopez, E., Saleh-Gohari, N. and Helleday, T. **(2003)** 'Poly(ADP-ribose) polymerase (PARP-1) has a controlling role in homologous recombination', *Nucleic Acids Research,* 31, (17), pp. 4959-4959-64.

Scully, R., Chen, J. J., Plug, A., Xiao, Y. H., Weaver, D., Feunteun, J., Ashley, T. and Livingston, D. M. **(1997)** 'Association of BRCA1 with Rad51 in mitotic and meiotic cells', *Cell,* 88, (2), pp. 265-275.

Shimizu, S., Nomura, F., Tomonaga, T., Sunaga, M., Noda, M., Ebara, M. and Saisho, H**. (2004)** 'Expression of poly(ADP-ribose) polymerase in human hepatocellular carcinoma and analysis of biopsy specimens obtained under sonographic guidance', *Oncology Reports,* 12, (4), pp. 821-825.

Shinohara, A., Ogawa, H. and Ogawa, T. **(1992)** 'Rad51 Protein Involved in Repair and Recombination in Saccharomyces-Cerevisiae Is a Reca-Like Protein', *Cell,* 69, (3), pp. 457-470.

Simbulan-Rosenthal, C. M., Ly, D. H., Rosenthal, D. S., Konopka, G., Luo, R., Wang, Z.-Q., Schultz, P. G. and Smulson, M. E. **(2000)** 'Misregulation of gene expression in primary fibroblasts lacking poly(ADP-ribose) polymerase', *Proceedings of the National Academy of Sciences of the United States of America,* 97, (21), pp. 11274-11279.

Simonin, F., Menissier-de Murcia, J., Poch, O., Muller, S., Gradwohl, G., Molinete, M., Penning, C., Keith, G. and de Murcia, G. **(1990)** 'Expression and site-directed mutagenesis of the catalytic domain of human poly(ADP-ribose)polymerase in Escherichia coli. Lysine 893 is critical for activity', *The Journal of biological chemistry,* 265, (31), pp. 19249-56.

Sistonen, J., Sajantila, A., Lao, O., Corander, J., Barbujani, G. and Fuselli, S. **(2007)** 'CYP2D6 worldwide genetic variation shows high frequency of altered activity variants and no continental structure', *Pharmacogenetics and Genomics,* 17, (2), pp. 93-101.

Skalitzky, D. J., Marakovits, J. T., Maegley, K. A., Ekker, A., Yu, X.-H., Hostomsky, Z., Webber, S. E., Eastman, B. W., Almassy, R., Li, J., Curtin, N. J., Newell, D. R., Calvert, A. H., Griffin, R. J. and Golding, B. T. **(2002)** 'Tricyclic Benzimidazoles as Potent Poly(ADP-ribose) Polymerase-1 Inhibitors', *Journal of Medicinal Chemistry,* 46, (2), pp. 210-213.

Smith, L. M., Willmore, E., Austin, C. A. and Curtin, N. J. **(2005)** 'The Novel Poly(ADP-Ribose) Polymerase Inhibitor, AG14361, Sensitizes Cells to Topoisomerase I Poisons by Increasing the Persistence of DNA Strand Breaks', *Clinical Cancer Research,* 11, (23), pp. 8449-8457.

Stoehlmacher, J., Ghaderi, V., Iqbal, S., Groshen, S., Tsao-Wei, D., Park, D. and Lenz, H. J. **(2001)** 'A polymorphism of the XRCC1 gene predicts for response to platinum based treatment in advanced colorectal cancer', *Anticancer Research,* 21, (4B), pp. 3075-3079.

Stratton, J., Gayther, SA, Russell, P, **(1997)** 'Contribution of BRCA1 mutations to ovarian cancer', *New England Journal of Medicine,* 336, (16), pp. 1125.

Struewing, J. P., Hartge, P., Wacholder, S., Baker, S. M., Berlin, M., McAdams, M., Timmerman, M. M., Brody, L. C. and Tucker, M. A. **(1997)** 'The Risk of Cancer Associated with Specific Mutations of BRCA1 and BRCA2 among Ashkenazi Jews', *New England Journal of Medicine,* 336, (20), pp. 1401-1408.

Sugimura, T., Fujimura, S., Hasegawa, S. and Kawamura, Y. **(1967)** 'Polymerization of the adenosine 5'-diphosphate ribose moiety of NAD by rat liver nuclear enzyme', *Biochimica et biophysica acta,* 138, (2), pp. 438-41.

Sung, P. and Klein, H. **(2006)** 'Mechanism of homologous recombination: mediators and helicases take on regulatory functions', *Nature Reviews Molecular Cell Biology,* 7, (10), pp. 739-750.

Swift, M., Morrell, D., Massey, R. B. and Chase, C. L. **(1991)** 'Incidence of Cancer in 161 Families Affected by Ataxiaâ€"Telangiectasia', *New England Journal of Medicine,* 325, (26), pp. 1831-1836.

Swisher, E. M., Sakai, W., Karlan, B. Y., Wurz, K., Urban, N. and Taniguchi, T. **(2008)** 'Secondary BRCA1 mutations in BRCA1-mutated ovarian carcinomas with platinum resistance', *Cancer Research,* 68, (8), pp. 2581-2586.

Szabo, C. and Dawson, V. L. **(1998)** 'Role of poly(ADP-ribose) synthetase in inflammation and ischaemia-reperfusion', *Trends in Pharmacological Sciences,* 19, (7), pp. 287-298.

Takata, M., Sasaki, M. S., Sonoda, E., Morrison, C., Hashimoto, M., Utsumi, H., Yamaguchi-Iwai, Y., Shinohara, A. and Takeda, S. **(1998)** 'Homologous recombination and non-homologous end-joining pathways of DNA double-strand break repair have overlapping roles in the maintenance of chromosomal integrity in vertebrate cells', *EMBO J,* 17, (18), pp. 5497-5508.

Tan, D. S. P., Rothermundt, C., Thomas, K., Bancroft, E., Eeles, R., Shanley, S., Ardern-Jones, A., Norman, A., Kaye, S. B. and Gore, M. E. **(2008)** ''BRCAness" Syndrome in Ovarian Cancer: A Case-Control Study Describing the Clinical Features and Outcome of Patients With Epithelial Ovarian Cancer Associated With BRCA1 and BRCA2 Mutations', *Journal of Clinical Oncology,* 26, (34), pp. 5530-5536.

Tao, Z., Gao, P. and Liu, H.-w. **(2009)** 'Identification of the ADP-Ribosylation Sites in the PARP-1 Automodification Domain: Analysis and Implications', *Journal of the American Chemical Society,* 131, (40), pp. 14258-14260.

Tarsounas, M., Davies, D. and West, S. C. **(2003)** 'BRCA2-dependent and independent formation of RAD51 nuclear foci', *Oncogene,* 22, (8), pp. 1115-1123.

Tassone, P., Tagliaferri, P., Perricelli, A., Blotta, S., Quaresima, B., Martelli, M. L., Goel, A., Barbieri, V., Costanzo, F., Boland, C. R. and Venuta, S. **(2003)** 'BRCA I expression modulates chemosensitivity of BRCA I-defective HCC1937 human breast cancer cells', *British Journal of Cancer,* 88, (8), pp. 1285-1291.

Tavecchio, M., Munck, J., Cano, C., Newell, D. and Curtin, N. **(2011)** 'Further characterisation of the cellular activity of the DNA-PK inhibitor, NU7441, reveals potential cross-talk with homologous recombination', *Cancer Chemotherapy and Pharmacology*, pp. 1-10.

Tentori, L., Leonetti, C., Scarsella, M., Muzi, A., Mazzon, E., Vergati, M., Forini, O., Lapidus, R., Xu, W., Dorio, A. S., Zhang, J., Cuzzocrea, S. and Graziani, G. **(2006)** 'Inhibition of poly(ADP-ribose) polymerase prevents irinotecan-induced intestinal damage and enhances irinotecan/temozolomide efficacy against colon carcinoma', *The FASEB journal,* 20, (10), pp. 1709-1711.

Tentori, L., Muzi, A., Dorio, A. S., Bultrini, S., Mazzon, E., Lacal, P. M., Shah, G. M., Zhang, J., Navarra, P., Nocentini, G., Cuzzocrea, S. and Graziani, G. **(2008)** 'Stable depletion of poly (ADP-ribose) polymerase-1 reduces in vivo melanoma growth and increases chemosensitivity', *European Journal of Cancer,* 44, (9), pp. 1302-1314.

Tentori L, M. A., Dorio AS, Scarsella M, Leonetti C, Shah GM, Xu W, Camaioni E, Gold B, Pellicciari R, Dantzer F, Zhang J, Graziani G. . **(2010)** 'Pharmacological inhibition of poly(ADP-ribose) polymerase (PARP) activity in PARP-1 silenced tumour cells increases chemosensitivity to temozolomide and to a N3-adenine selective methylating agent. ', *Current Cancer Drug Targets,* 10, (4), pp. 368-383.

The Breast Cancer Linkage Consortium. **(1999)** 'Cancer Risks in BRCA2 Mutation Carriers', *Journal of the National Cancer Institute,* 91, (15), pp. 1310-1316.

Thomas, H. D., Calabrese, C. R., Batey, M. A., Canan, S., Hostomsky, Z., Kyle, S., Maegley, K. A., Newell, D. R., Skalitzky, D., Wang, L.-Z., Webber, S. E. and Curtin, N. J. **(2007)** 'Preclinical selection of a novel poly(ADP-ribose) polymerase inhibitor for clinical trial', *Molecular Cancer Therapeutics,* 6, (3), pp. 945-956.

Thompson, D. and Easton, D. F. (2002) 'Cancer incidence in BRCA1 mutation carriers', *Journal of the National Cancer Institute,* 94, (18), pp. 1358-1365.

Tibbetts, R. S., Cortez, D., Brumbaugh, K. M., Scully, R., Livingston, D., Elledge, S. J. and Abraham, R. T. **(2000)** 'Functional interactions between BRCA1 and the checkpoint kinase ATR during genotoxic stress', *Genes & Development,* 14, (23), pp. 2989-3002.

Tomlinson, G. E., Chen, T. T. L., Stastny, V. A., Virmani, A. K., Spillman, M. A., Tonk, V., Blum, J. L., Schneider, N. R., Wistuba, I. I., Shay, J. W., Minna, J. D. and Gazdar, A. F. **(1998)** 'Characterization of a Breast Cancer Cell Line Derived from a Germ-Line BRCA1 Mutation Carrier', *Cancer Research,* 58, (15), pp. 3237-3242.

Tong, W. M., Yang, Y. G., Cao, W. H., Galendo, D., Frappart, L., Shen, Y. and Wang, Z. Q. **(2007)** 'Poly(ADP-ribose) polymerase-1 plays a role in suppressing mammary tumourigenesis in mice', *Oncogene,* 26, (26), pp. 3857-3867.

Turner, N. C., Reis, J. S., Russell, A. M., Springall, R. J., Ryder, K., Steele, D., Savage, K., Gillett, C. E., Schmitt, F. C., Ashworth, A. and Tutt, A. N. **(2007)** 'BRCA1 dysfunction in sporadic basal-like breast cancer', *Oncogene,* 26, (14), pp. 2126-2132.

Tutt, A., Bertwistle, D., Valentine, J., Gabriel, A., Swift, S., Ross, G., Griffin, C., Thacker, J. and Ashworth, A. **(2001)** 'Mutation in Brca2 stimulates error-prone homology-directed repair of DNA double-strand breaks occurring between repeated sequences', *EMBO J,* 20, (17), pp. 4704-4716.

Tutt, A., Robson, M., Garber, J. E., Domchek, S. M., Audeh, M. W., Weitzel, J. N., Friedlander, M., Arun, B., Loman, N., Schmutzler, R. K., Wardley, A., Mitchell, G., Earl, H., Wickens, M. and Carmichael, J. **(2010)** 'Oral poly(ADP-ribose) polymerase inhibitor olaparib in patients with BRCA1 or BRCA2 mutations and advanced breast cancer: a proof-of-concept trial', *Lancet,* 376, (9737), pp. 235-244.

van der Heijden, M. S., Brody, J. R., Dezentje, D. A., Gallmeier, E., Cunningham, S. C., Swartz, M. J., DeMarzo, A. M., Offerhaus, G. J. A., Isacoff, W. H., Hruban, R. H. and Kern, S. E. **(2005)** 'In vivo therapeutic responses contingent on Fanconi anemia/BRCA2 status of the tumor', *Clinical Cancer Research,* 11, (20), pp. 7508-7515.

Venkitaraman, A. R. **(2002)** 'Cancer susceptibility and the functions of BRCA1 and BRCA2', *Cell,* 108, (2), pp. 171-182.

Venkitaraman, A. R. **(2009)** 'Linking the Cellular Functions of BRCA Genes to Cancer Pathogenesis and Treatment', *Annual Reviews of Pathology,* 4, (1), pp. 461-487.

Veuger, S. J., Curtin, N. J., Richardson, C. J., Smith, G. C. M. and Durkacz, B. W. **(2003)** 'Radiosensitization and DNA Repair Inhibition by the Combined Use of Novel Inhibitors of DNA-dependent Protein Kinase and Poly(ADP-Ribose) Polymerase-1', *Cancer Research,* 63, (18), pp. 6008-6015.

Veuger, S. J., Curtin, N. J., Smith, G. C. M. and Durkacz, B. W. **(2004)** 'Effects of novel inhibitors of poly(ADP-ribose) polymerase-1 and the DNA-dependent protein kinase on enzyme activities and DNA repair', *Oncogene,* 23, (44), pp. 7322-7329.

Vichai, V. and Kirtikara, K. **(2006)** 'Sulforhodamine B colorimetric assay for cytotoxicity screening', *Nature Protocols,* 1, (3), pp. 1112-1116.

Virag, L. and Szabo, C. **(2002)** 'The therapeutic potential of poly(ADP-ribose) polymerase inhibitors', *Pharmacological Reviews,* 54, (3), pp. 375-429.

W.Neal, B. **(1981)** '"Western Blotting": Electrophoretic transfer of proteins from sodium dodecyl sulfate-polyacrylamide gels to unmodified nitrocellulose and radiographic detection with antibody and radioiodinated protein A', *Analytical Biochemistry,* 112, (2), pp. 195-203.

Wang, M., Wu, W., Wu, W., Rosidi, B., Zhang, L., Wang, H. and Iliakis, G. **(2006)** 'PARP-1 and Ku compete for repair of DNA double strand breaks by distinct NHEJ pathways', *Nucleic Acids Research,* 34, (21), pp. 6170-6182.

Wang, X. G., Wang, Z. Q., Tong, W. M. and Shen, Y**. (2007)** 'PARP1 Val762Ala polymorphism reduces enzymatic activity', *Biochemical and Biophysical Research Communications,* 354, (1), pp. 122-126.

Wang, L.H., Pfister, T.D., Parchment, R.E., Kummar, S., Rubinstein, L., Evrard, Y.A., Gutierrez, M.E., Murgo, A.J., Tomaszewski, J.E., Doroshow, J.H., Kinders, R.J., **(2010) '**Monitoring Drug-Induced gamma H2AX as a Pharmacodynamic Biomarker in Individual Circulating Tumor Cells*'*, *Clinical Cancer Research*, 16, (3), pp.1073-1084.

Wei, M., Grushko, T. A., Dignam, J., Hagos, F., Nanda, R., Sveen, L., Xu, J., Fackenthal, J., Tretiakova, M., Das, S. and Olopade, O. I. **(2005)** 'BRCA1 Promoter Methylation in Sporadic Breast Cancer Is Associated with Reduced BRCA1 Copy Number and Chromosome 17 Aneusomy', *Cancer Research,* 65, (23), pp. 10692-10699.

Willers, H., Taghian, A. G., Luo, C.-M., Treszezamsky, A., Sgroi, D. C. and Powell, S. N. **(2009)** 'Utility of DNA Repair Protein Foci for the Detection of Putative BRCA1 Pathway Defects in Breast Cancer Biopsies', *Molecular Cancer Research,* 7, (8), pp. 1304-1309.

Williamson, E. A., Dadmanesh, F. and Koeffler, H. P**. (2002)** 'BRCA1 transactivates the cyclin-dependent kinase inhibitor p27 (Kip1)', *Oncogene,* 21, (20), pp. 3199-3206.

Wooster, R., Neuhausen, S. L., Mangion, J., Quirk, Y., Ford, D., Collins, N., Nguyen, K., Seal, S., Tran, T., Averill, D. **(1994)** 'Localization of a breast cancer susceptibility gene, BRCA2, to chromosome 13q12-13', *Science,* 265, (5181), pp. 2088-2090.

Xu, J. W., Fan, S. J. and Rosen, E. M. **(2005)** 'Regulation of the estrogen-inducible gene expression profile by the breast cancer susceptibility gene BRCA1', *Endocrinology,* 146, (4), pp. 2031-2047.

Xu, X., Wagner, K.-U., Larson, D., Weaver, Z., Li, C., Ried, T., Hennighausen, L., Wynshaw-Boris, A. and Deng, C.-X. **(1999)** 'Conditional mutation of Brca1 in mammary epithelial cells results in blunted ductal morphogenesis and tumour formation', *Nat Genet,* 22, (1), pp. 37-43.

Yang, H. J., Jeffrey, P. D., Miller, J., Kinnucan, E., Sun, Y. T., Thoma, N. H., Zheng, N., Chen, P. L., Lee, W. H. and Pavletich, N. P. **(2002)** 'BRCA2 function in DNA binding and recombination from a BRCA2-DSS1-ssDNA structure', *Science,* 297, (5588), pp. 1837-1848.

Yuan, S.-S. F., Lee, S.-Y., Chen, G., Song, M., Tomlinson, G. E. and Lee, E. Y. H. P. **(1999)** 'BRCA2 Is Required for Ionizing Radiation-induced Assembly of Rad51 Complex in Vivo', *Cancer Research,* 59, (15), pp. 3547-3551.

Yung, T. M. C., Sato, S. and Satoh, M. S. **(2004)** 'Poly(ADP-ribosyl)ation as a DNA Damage-induced Post-translational Modification Regulating Poly(ADP-ribose) Polymerase-1-Topoisomerase I Interaction', *The Journal of biological chemistry,* 279, (38), pp. 39686-39696.

Zaremba, T., Ketzer, P., Cole, M., Coulthard, S., Plummer, E. R. and Curtin, N. J. **(2009)** 'Poly(ADP-ribose) polymerase-1 polymorphisms, expression and activity in selected human tumour cell lines', *British Journal of Cancer,* 101, (2), pp. 256-262.

Zaremba, T., Thomas, H. D., Cole, M., Coulthard, S. A., Plummer, E. R. and Curtin, N. J. **(2011)** 'Poly(ADP-ribose) polymerase-1 (PARP-1) pharmacogenetics, activity and expression analysis in cancer patients and healthy volunteers', *Biochemical Journal,* 436, (3), pp. 671-679.

Zhang, X. M., Miao, X. P., Liang, G., Hao, B. T., Wang, Y. G., Tan, W., Li, Y., Guo, Y. L., He, F. C., Wei, Q. Y. and Lin, D. X. **(2005)** 'Polymorphisms in DNA base excision repair genes ADPRT and XRCC1 and risk of lung cancer', *Cancer Research,* 65, (3), pp. 722-726.

Zhao, Y., Thomas, H. D., Batey, M. A., Cowell, I. G., Richardson, C. J., Griffin, R. J., Calvert, A. H., Newell, D. R., Smith, G. C. M. and Curtin, N. J. **(2006)** 'Preclinical evaluation of a potent novel DNA-dependent protein kinase inhibitor NU7441', *Cancer Research,* 66, (10), pp. 5354-5362.

Zhong, Q., Chen, C. F., Li, S., Chen, Y. M., Wang, C. C., Xiao, J., Chen, P. L., Sharp, Z. D. and Lee, W. H. **(1999)** 'Association of BRCA1 with the hRad50-hMre11-p95 complex and the DNA damage response', *Science,* 285, (5428), pp. 747-750.

Zhou, B. S. and Bartek, J. **(2004)** 'Targeting the checkpoint kinases: chemosensitization versus chemoprotection', *Nature Reviews. Cancer,* 4, (3), pp. 216-216-25.

Zhu, G., Chang, P. and Lippard, S. J. **(2010)** 'Recognition of Platinum DNA Damage by Poly(ADP-ribose) Polymerase-1', *Biochemistry,* 49, (29), pp. 6177-6183.

Zhuang, J., Zhang, J. R., Willers, H., Wang, H., Chung, J. H., van Gent, D. C., Hallahan, D. E., Powell, S. N. and Xia, F. **(2006)** 'Checkpoint kinase 2-mediated phosphorylation of BRCA1 regulates the fidelity of non-homologous end-joining', *Cancer Research,* 66, (3), pp. 1401-1408.

Appendix

Selected publications:

1. **Y Drew**, E Mulligan, W Vong, H Thomas, S Kahn, S Kyle, A Mukhopadhyay, ER Plummer, RJ Edmondson, NJ Curtin 'Therapeutic potential of the PARP inhibitor AG014699 in human cancer with mutated or epigenetically silenced *BRCA*1 and 2'. **(2011)** *Journal of the National Cancer Institute,* 16: 103 (4) 334-46

2**. Y Drew**, ER Plummer. 'PARP inhibitors in cancer therapy: two modes of attack on the cancer cell widening the clinical applications' **(2009)**. *Drug Resistance Updates, 12(6):153-6.*

3. **Y Drew**, JA Ledermann, A Jones, G Hall, GC Jayson, M Highley, D Rea, R Glasspool, SER Halford, G Crosswell, S Colebrook, AV Boddy, NJ Curtin, ER Plummer, E. R. 'Phase II trial of the poly(ADP-ribose) polymerase (PARP) inhibitor AG-014699 in BRCA 1 and 2-mutated, advanced ovarian and/or locally advanced or metastatic breast cancer' **(2011)** *Journal of Clinical Oncology*, 29, (15_suppl), pp. 3104.